Electrophysiological Indices of Graded Attentional and Decision-Making Processes

Ian C. Gould

A dissertation submitted in partial fulfilment of the requirements for the degree of Doctor of Philosophy in the University of Oxford

Merton College **Michaelmas Term 2011**

Electrophysiological Indices of Graded Attentional and Decision-Making Processes

Ian C. Gould

Merton College, Oxford **Michaelmas Term 2011**

A dissertation submitted in partial fulfilment of the requirements for the degree of Doctor of Philosophy in the University of Oxford

ABSTRACT

In everyday life we regularly update our expectations about the locations at which sensory events may occur, and about the motor responses that are appropriate in a given situation. The experiments in this thesis investigated the neural correlates of perceptual processes and motor preparation during human decision making, and the regions that causally contribute to decision making in the human brain. In Chapter 3, I used electroencephalography (EEG) to investigate whether alpha-band (~8-14 Hz) oscillations provide a graded index of participants' preparatory attentional states. Time-frequency analysis revealed that manipulating spatial certainty regarding the location of an upcoming visual target led to parametric changes in the lateralization of preparatory occipito-parietal alpha oscillations, and to parametric modulation of parieto-central beta-band (~15-25 Hz) power typically associated with response preparation. In Chapter 4, I used EEG to investigate whether evolution of lateralization of sensorimotor alpha- and beta-band activity reflected participants' evolving expectations about an upcoming motor response. Lateralization of activity in both frequency bands varied parametrically with the available evidence, suggesting such lateralized activity correlates with participants' internal decision variables. Further analysis identified unique contributions to lateralized and non-lateralized oscillatory activity due to the prior evidence, evidence update, and surprise related to the observed information at each stage of the task. In Chapter 5, I extended the paradigm developed in Chapter 4 for use with online repetitive transcranial magnetic stimulation (TMS) and concurrent EEG recording. Delivery of TMS during decision making allowed investigation of the causal role played by a left hemisphere medial intraparietal region that is the putative human homologue of the macaque medial intraparietal cortex (MIP). MIP stimulation disrupted decision-making behaviour by biasing participants' decisions against contralateral-to-stimulation (i.e., right-handed) responses. Comparison of the magnitude of TMS-induced changes in behaviour and beta-band activity demonstrated that the intraparietal cortex plays a causal role both in decision making and in the appearance of beta-band activity over the motor cortex. In Chapter 6, the broader consequences of the experimental work presented in this thesis are discussed, in addition to promising directions for future research.

This work was funded by a 4-year Wellcome Trust studentship.

Approximate word count: 50,000 words.

ACKNOWLEDGEMENTS

First and foremost I'd like to thank my two dedicated supervisors, Matthew Rushworth and Kia Nobre. Their endless passion for science, constant support, and occasional lessons in the way of the samurai have been major inspirations throughout my DPhil. They have constantly surpassed my expectations as supervisors, and I could not have asked for more.

I'd also like to thank the lab mates I was so incredibly lucky to find myself in an office with. Many of the highs and lows of the last few years were shared in the open confines of C100 with Alexandra, Riam and Zita; from working out how to tell ERPs from blinks, to late night drinks when they were really needed. Gustavo is also an important member of this list, who must be thanked for keeping the office completely clear of imaginary flies in the first year of my DPhil. Though not a member of my immediate office, I've also enjoyed the many hours of sitting and whispering in dark testing rooms as the TMS clicks away with Vanessa, who I'd also like to thank for being on-call as a late night drinking buddy.

Beyond my immediate supervisors, a few people in particular stand out as having helped shaped the ideas in this thesis. Valentin, Gustavo, Mark, Andre, Vincent, Chris, and Bo. I'd also like to thank all my other lab mates and friends in E.P., who have made the last few years as enjoyable as they've been.

Though physically far away most of the DPhil, I have also really appreciated the on-going support and advice of my mum and dad. This has been crucial from the day I was offered an interview at Oxford until the day I submitted.

Finally, one of the most important figures throughout my DPhil has of course been Ruth. I'm not sure how I would have gotten through this without your love, patience, and knack of knowing when it was one of those occasional nights where I just needed to be left alone. I hope you know how much it helped and how much it meant to me, and that I'll be able to provide the same for you in the upcoming year.

Table of Contents

LONG ABSTRACT VII

LIST OF ABBREVIATIONS X

CHAPTER 1 - GENERAL INTRODUCTION 1

1.1. Perceptual Decision Making Towards Actions 1

1.2. Overview 6

1.3. Sensory Regions Can Provide Inputs to Decisions But Do Not Compute Decision Variables 7

1.4. Integration of Evidence in the Monkey Brain 14

1.4.1. Macaque Parietal Lobe Anatomy and Subdivisions 15

1.4.2. Decision Integration by LIP Neurons 16

1.4.3. LIP is Not the Final Stage in Response Selection 23

1.4.4. Is LIP an Attentional or Intentional Structure? 23

1.4.5. Function of Neurons in the Parietal Reach Region (PRR) and Area 5 26

1.4.6. Decision Integration Neurons beyond the Parietal Lobe 29

1.5. Integration of Evidence in the Human Parietal and Prefrontal Lobes 38

1.6. Neural Oscillations 52

1.6.1. Alpha-Band Oscillations and Visual Attention 54

1.6.2. Alpha-Band Oscillations – From Visual Attention to Motor Preparation 57

1.6.3. Beta-Band Oscillations and Motor Preparation 58

1.6.4. Oscillatory Correlates of Decision Processes 61

1.7. Thesis Experiments 64

CHAPTER 2 - METHODS 67

2.1. Transcranial Magnetic Stimulation (TMS) 67

2.2. Electroencephalography 74

2.2.1. Measurement and Biophysical Origins of EEG signals 75

2.2.2. Recording, Preprocessing and Analysis of EEG signals 77

2.2.3. Relationship Between Oscillatory EEG Activity and Neural Activity 80

2.2.4. Concurrent EEG and TMS 82

2.3. Methodological Rationale 83

CHAPTER 3 - INDEXING THE GRADED ALLOCATION OF VISUOSPATIAL ATTENTION USING ANTICIPATORY ALPHA OSCILLATIONS 85

3.1. Introduction 85

3.2. Materials and Methods 88

3.2.1. Participants 88

3.2.2. Task and Stimuli 88

3.2.3. Electroencephalography (EEG) Recording and Pre-Processing 90

3.2.4. Determination of Individual Alpha Frequency Bands 91

3.2.5. Time-Frequency Analysis 92

3.2.6. Event-Related Potential (ERP) Analysis 93

3.3. Results 94

3.3.1. Behavioral Results 94

3.3.2. Alpha Power 97

3.3.3. Beta Power 99

3.3.4. Visual Potentials 100

3.3.5. Correlation Between Behavioral and Neural Results 101

3.4. Discussion 103

CHAPTER 4 - OSCILLATORY CORRELATES OF MOTOR-RELATED DECISION MAKING IN THE HUMAN BRAIN 107

4.1. Introduction 107

4.2. Materials and Methods 109

4.2.1. Participants 109

4.2.2. Probabilistic Categorization Task 109

4.2.3. Procedure – EEG Session 115

4.2.4. Procedure - Training Session 116

4.2.5. Visual Stimuli 117

4.2.6. Data Analysis Software 118

4.2.7. Behavioural Data Analysis 118

4.2.8. EEG Recording and Pre-Processing 119

4.2.9. Spectral Analysis 120

4.2.10. Region of Interest Selection and Beta Rebound 121

4.2.11. Statistical Analysis of Spectral Data 121

4.3. Results 125

4.3.1. Behavioural Data 125

4.3.2. EEG Results 128

4.4. Discussion 141

CHAPTER 5 - INVESTIGATION OF THE CAUSAL ROLE OF INTRAPARIETAL CORTEX IN MOTOR-RELATED DECISION-MAKING 154

5.1. Introduction 154

5.2. Materials and Methods 159

5.2.1. Participants 159
5.2.2. TMS-EEG Procedure 159
5.2.3. TMS Site Localisation 162
5.2.4. EEG Recording, Pre-Processing and Spectral Analysis 163
5.2.5. Region of Interest Selection and Beta Rebound 164
5.2.6. Visual Stimuli 165
5.2.7. Behavioural Effects of TMS 165
5.2.8. Validation of EEG data - Analysis of Spectral Data from no-TMS Trials 167
5.2.9. Analysis of TMS Effects on EEG and their Relation to Behavioural TMS Effects 170
5.3. Results 172
5.3.1. Behavioural Consequences of TMS 172
5.3.2. EEG Results from no-TMS Trials 174
5.3.3. EEG Effects of TMS 182
5.4. Discussion 186
CHAPTER 6 - GENERAL DISCUSSION 191
6.1. Alpha- and Beta-Band Neural Oscillations Provide an Ongoing Index of Attentional and Intentional States 191
6.2. Do Neural Oscillations Causally Shape Attention and Decision Making? 196
6.3. What Can We Conclude About How Decisions Evolve in the Human Brain? 199
BIBLIOGRAPHY 205

Long Abstract

In everyday life we regularly update our expectations about the locations at which sensory events may occur, and about the motor responses that are appropriate in a given situation. Electrophysiological recordings involving non-human primates have provided considerable insights into the neural processes by which incoming sensory signals may be selected and integrated towards a decision. Many of these insights have relied on the high spatial and temporal resolution provided by single-unit recordings, and relate to fine-grained properties of how neural activity evolves over the time-course of a decision. In Chapter 1 of this thesis, human and monkey neural data from decision-making tasks are discussed, and it is suggested why, at present, key findings from the monkey decision literature have not been clearly replicated in human neuroimaging recordings. In Chapters 3 to 5, three experiments are presented which aimed to elucidate the neural mechanisms by which the human brain may flexibly select and transform perceptual information in order to update the selection of appropriate motor responses. A primary aim was to explore whether characterization of electroencephalographic (EEG) oscillations from healthy human participants may provide evidence for similar decision-making processes as those described in the animal literature, and to identify brain regions that causally contribute to decision making. Methodological aspects of the experimental techniques used are discussed in Chapter 2.

Fine-grained differences in oscillatory power have previously been related to behavioural differences in choice and performance. It was unclear, however, whether such effects reflected random fluctuations in neural activity or are under top-down control. In Chapter 3, results are presented from an experiment that validated the use of oscillations as a parametric index of participants' preparatory attentional states. Specifically, we investigated

whether parametric variations in the lateralization of alpha (~8-14 Hz) oscillations recorded over occipito-parietal cortex could be related to graded differences in top-down attentional goals. Time-frequency analysis of EEG data demonstrated that manipulating spatial certainty about the location of an upcoming visual target led to parametric changes in the lateralization of alpha oscillations during the cue-target interval, and to modulation of parieto-central beta-band (~15-25 Hz) power typically associated with response preparation. Individual differences in alpha desynchronization contralateral to attention predicted reaction times, event-related potential measures of perceptual processing of targets, and beta-band power. These results support the hypothesis that anticipatory alpha modulation is a plausible neural mechanism underlying the allocation of visuospatial attention, and is under flexible top-down control. Results further suggest that graded modulation of somatomotor beta-band activity reflects participants' expectations about upcoming responses.

In Chapter 4, data are presented from a novel decision-making task that required human participants to integrate multiple pieces of sequentially presented evidence towards a manual motor response. We investigated whether evolution of lateralization of alpha- and beta-band oscillatory activity over motor planning regions flexibly reflected participants' evolving expectations about the motor response that was to be made at the end of the trial. Results confirmed this hypothesis, demonstrating that lateralization of activity in both frequency bands varied parametrically with the available evidence in favour of left- versus right-hand responses at each stage of the task. Control analyses demonstrated these effects could not be ascribed to categorical response-preparation processes. These results thus provide evidence of a neural correlate of participants' internal decision variables as they completed the task. Further analysis identified unique contributions to lateralized and non-lateralized oscillatory activity due to the prior evidence, evidence update, and surprise at the

observed information at each stage of the task. Subtle qualitative differences in the nature of alpha- and beta-band effects in these analyses are discussed in light of recent theories about the functional role of activity and inter-regional neural synchrony in these frequency bands.

For the study described in Chapter 5, the experimental task utilised in Chapter 4 was adapted for use with concurrent TMS-EEG. Delivery of TMS during the decision-integration task allowed investigation of the causal role a left hemisphere medial intraparietal region considered to be the putative human homologue of the macaque medial intraparietal cortex (MIP). Compared with an active lateralized control site (left V5/MT+), MIP stimulation disrupted decision-making behaviour by biasing participants' decisions against contralateral-to-stimulation (i.e., right-handed) responses. Comparison of the magnitude of TMS-induced changes in behaviour and beta-band activity demonstrated that the intraparietal cortex plays a causal role both in decision making and in the appearance of beta band activity over the motor cortex

In Chapter 6, the broader consequences of the experimental work presented in this thesis are discussed, in addition to promising directions for future research.

List of Abbreviations

ACC – anterior cingulate cortex

AIP – anterior intraparietal area

ANOVA – analysis of variance

dB – decibel

CIP – caudal intraparietal area

CNV – contingent negative variation

BOLD – blood-oxygen-level-dependent

DLPFC – dorsolateral prefrontal cortex

DPC – dorsal premotor cortex

DV – decision variable

ECoG – electrocorticography

EEG – electroencephalography

EMG – electromyogram

EOG – electrooculogram

ERP – event related potential

FEF – frontal eye fields

fMRI – functional magnetic resonance imaging

IAF – individual alpha frequency

IFJ – inferior frontal junction

IPL – inferior parietal lobule

IPS – intraparietal sulcus

ISI – inter-stimulus interval

IT – inferior temporal

ITI – inter-trial interval

LFP – local field potential

LI – lateralization index

LIP – lateral intraparietal area

LIPd – dorsal lateral intraparietal area

LIPv – ventral lateral intraparietal area

LLR – log-likelihood ratio

LRP – lateralized readiness potential

M1 – primary motor cortex

MEG – magnetoencephalography

MEP – motor-evoked potential

MIP – medial intraparietal area

MPC – medial prefrontal cortex

PFC – prefrontal cortex

PET – positron emission tomography

PMd – dorsal premotor cortex

PPC – posterior parietal cortex

pre-SMA – pre-supplemental motor area

PRR – parietal reach region

PSP – post-synaptic potential

RDM – random dot motion

ROI – region of interest

RT – reaction time

rTMS – repetitive transcranial magnetic stimulation

S1 – primary somatosensory cortex

S2 – secondary somatosensory cortex

SC – superior colliculus

SEF – supplemental eye fields

SFS – superior frontal sulcus

SMA – supplemental motor area

SPL – superior parietal lobule

SWOE – subjective weight of evidence

tACS – transcranial alternating current stimulation

T_{in} – a target inside a neuron's response field

T_{out} – a target outside a neuron's response field

TMS – transcranial magnetic stimulation

VPC – ventral prefrontal cortex

WOE – weight of evidence

Chapter 1 - General Introduction

1.1. Perceptual Decision Making Towards Actions

Perceptual decision making describes the process by which sensory information transduced from the external world is used to guide decision making, the results of which are often expressed via an action. Understanding how such processes are carried out in the human brain is of pivotal importance in understanding how perception, cognition and action are linked, underlying the flexibility with which we can make appropriate behavioural responses to changes in our external environment (Gold & Shadlen, 2007; Gottlieb, 2007; Heekeren et al., 2008; Kable & Glimcher, 2009; Platt et al., 2008; Smith & Ratcliff, 2004).

Perceptual decision making can vary greatly in its difficulty, and depends on the quality of the information available to guide it. For example, detecting a salient change in our visual environment, like a change in the colour of a traffic light from green to red, is often relatively easy. In contrast, searching for a friend at a crowded party may be perceptually difficult at a number of levels. First, the visual information that needs to be processed can be degraded due to environmental factors such as poor lighting. Second, the temporal duration over which information about any single person is available may be short, as people emerge from the crowd then disappear back into it.

A rich tradition of psychological research has been devoted to characterizing how these sorts of perceptual decisions are made. Historically, one of the longest traditions in this field has assumed that sensory encoding, decision making and motor execution processing

stages occurring serially and independently (Ashby & Townsend, 1980; Donders, 1969; Stanford et al., 2010; Sternberg, 1969). However, the last 50 years have seen a rise in the use of sequential sampling models to describe decision-making processes (Brown & Heathcote, 2005; Laming, 1968; Link & Heath, 1975; Luce, 1991; Ratcliff, 1978; Stone, 1960; Townsend & Ashby, 1983; Vickers, 1979). Like signal detection theory (Green & Swets, 1974; Macmillan & Creelman, 2005), sequential sampling models assume that sensory representations of perceptual information are inherently variable due to both external noise in inputs and internal noise in neural processing. However, while signal detection theory assumes that decisions are made using a single sample of noisy information, sequential sampling models assume that multiple samples of noisy perceptual information are accumulated over time. Sensory accumulation continues until a 'threshold' amount of evidence is reached favouring one decision outcome, at which point the decision process is terminated and expressed via a response. Reaction times (RTs) reflect the number of samples required for a response, which depend on model parameters reflecting several factors including the starting point (or 'prior bias') for the accumulation process, the quality of information sampled, decision threshold levels, and non-decisional times associated with sensory encoding, initiation of decision-making processes, and carrying out a response (Figure 1-1). Allowing these parameters to vary systematically with task demands and randomly between trials allows prediction of major qualitative aspects of accuracy and RT data in simple two-alternative forced-choice decisions, such as positively skewed RT distributions, speed-accuracy trade-offs, effects of task difficulty on accuracy and RT distributions, and differences in the speeds of correct and error responses (Ratcliff & Rouder, 1998; Ratcliff & Smith, 2004).

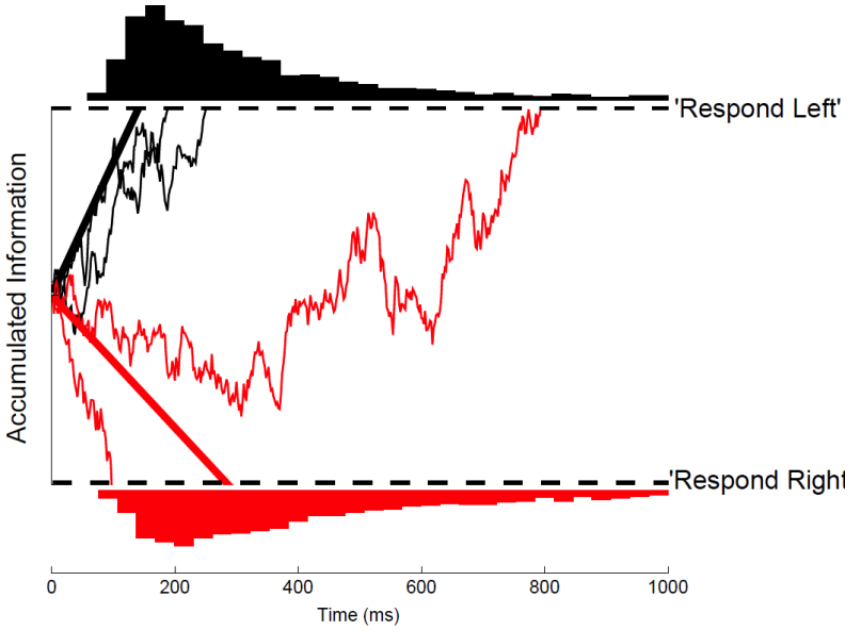


Figure 1-1. Schematic of a drift-diffusion decision process. Information accumulates proportional to the quality of available decision information but varies due to stochastic noise in encoding and decision-making processes. Red and black lines indicate decision paths where the stimulus favoured left and right responses, respectively. Thick black and red lines show the average drift over many trials for an easy and a moderately difficult decision, respectively, and are unaffected by noise. Thin lines show example trajectories of the decision variable for several trials. Some decisions result in incorrect responses due to noise accumulation, as in the case of the red line hitting the 'left response' bound. The histograms show the times of the end-points of decisions, where the decision paths hit one of the bounds. Data are from 10,000 simulated decision processes. The shapes of such reaction time distributions are predictable given changes in the drift rate, and how it randomly fluctuates between trials. Decisions may also be biased by vertical changes in the starting point of the decision process (not shown here). Behavioural reaction times also include non-decisional times associated with stimulus encoding and motor execution, also not shown here.

The popularity of sequential sampling models, most prominently the drift-diffusion model (Ratcliff, 1978; Ratcliff & McKoon, 2008; Ratcliff & Smith, 2004), reflects a number of factors. First, compared with more traditional analysis of mean or median accuracy and RT data, these models have a remarkable capacity to explain complex changes in behavioural performance as a result of changes in a relatively small number of model parameters with psychologically intuitive interpretations (Ratcliff & Rouder, 1998; Ratcliff et al., 1999). Second, the models' explanatory power applies to a wide range of tasks, including perceptual

detection and discrimination (Palmer et al., 2005; Ratcliff & Rouder, 1998; Ratcliff & Smith, 2004), attentional cuing (Smith & Ratcliff, 2009; Smith et al., 2004), lexical discrimination (Ratcliff et al., 2004), recognition memory (Ratcliff, 1978), go/no-go tasks (Verbruggen & Logan, 2009), and value-based choices (Krajbich et al., 2010; Milosavljevic et al., 2010). Although initially limited to explaining data from two-alternative forced-choice tasks, recent advances have begun to bridge this gap (Beck et al., 2008; Brown et al., 2009; Krajbich & Rangel, 2011; Leite & Ratcliff, 2010; Tsetsos et al., 2011). Working from the assumption that changes in model parameters reflect meaningful changes in latent psychological variables, sequential sampling models also offer a promising means of characterising between-group differences in cognitive processing components such as those associated with age (Ratcliff et al., 2001, 2003c) and clinical disorders (White et al., 2010). Third, accumulator models have been highly successful in providing an integrated theoretical framework for understanding behavioural and neural recordings from the same tasks (Ditterich, 2006; Hanes & Schall, 1996; Heekeren et al., 2008; Huk & Shadlen, 2005; Mazurek et al., 2003; Smith & Ratcliff, 2004). As discussed in detail in Sections 1.4 to 1.6, such neural effects have been most frequently reported in sensorimotor integration and motor areas involved in preparation for an upcoming response.

Despite their explanatory power and intuitive appeal, sequential sampling models have been criticised because they have been developed from a statistical framework describing the process of making optimal decisions, and lack transparency about the neural circuitry that may underpin decision making (Wang, 2002). Other models, primarily neural network and attractor models, have attempted to account for the same behavioural and neural datasets using models constrained by biophysically plausible assumptions (Albantakis & Deco, 2009; Furman & Wang, 2008; Lo & Wang, 2006; Martínez-García et al., 2011; Soltani

& Wang, 2010; Usher & McClelland, 2001; Wang, 2002; Wong et al., 2007; Wong & Wang, 2006). Indeed, neuroscientists aiming to elucidate the neural basis of decision making are becoming increasingly interested in discriminating between different model classes by considering how well each model's predictions accord with neural recordings as well as behavioural accuracy and reaction times (Churchland et al., 2011; Cisek et al., 2009; Ditterich, 2006; Hanes & Schall, 1996; Kiani et al., 2008; Niwa & Ditterich, 2008; Purcell et al., 2010; Ratcliff et al., 2003a; Smith & Ratcliff, 2004). Despite the rise of neurally inspired decision models, more recent diffusion-style models and cortico-basal ganglia network models have also, however, begun to describe more directly how the statistical properties of drift-diffusion decision-making processes might map onto neural signals and neurally plausible mechanisms (Beck et al., 2008; Bogacz & Gurney, 2007; Smith, 2010; Smith & Ratcliff, 2009). It should also be noted that while some models may appear more plausible given their derivation from neurally plausible assumptions, different models may also be viewed as describing the same processes but at different levels of abstraction. Indeed, most models mimic each other in their behavioural predictions (Leite & Ratcliff, 2010; Ratcliff & Smith, 2004; Ratcliff et al., 1999), and under plausible assumptions most models mathematically reduce to either a drift-diffusion model or a race model between independent accumulators (Bogacz, 2007; Smith, 2010). These two model classes cannot mimic each other entirely, because strict race models do not allow coupling between activity in different accumulator processes. In recent years, strict race models have been criticised as being sub-optimally slow in their reaction times, and for failing to describe behavioural and neural empirical results as well as diffusion models (Bogacz, 2007; Ratcliff et al., 2003a; Ratcliff & Smith, 2004) (though see Brown & Heathcote, 2005).

1.2. Overview

The main aim of the experimental work presented in this thesis is to elucidate neural signals reflecting integration of evidence towards decisions in the human brain, and to investigate which brain regions causally underpin decision processes. To provide background for this goal, I describe below empirical findings involving humans and monkeys that have contributed to our understanding of how neural data accords with the basic qualitative predictions of sequential sampling decision-making models. Given the similarity in the predictions of many decision models, the goal of this review is deliberately crude from a model-based point of view, largely ignoring model-specific subtleties. Instead, the main aim is to identify the key nodes of cortical networks exhibiting general properties that suggest their involvement in perceptual decision-making processes. It will be argued that whilst major advances in understanding perceptual decision making have resulted from analysing the temporal evolution of neural activity from electrophysiological recordings with monkeys, a remaining challenge is to differentiate the causal role of qualitatively similar decision-related neural activity across multiple brain regions. Although data from recent human decision-making studies are broadly concordant with monkey data, few of the key electrophysiological findings from monkey decision-making studies have been directly demonstrated in the human brain. Methodological challenges in obtaining the temporal resolution necessary for identifying decision-related activity in the human brain are discussed, and potential solutions raised.

1.3. Sensory Regions Can Provide Inputs to Decisions But Do Not Compute Decision Variables

Sequential decision models posit that many decisions involve integration of multiple samples of evidence towards a decision outcome. This leads to several simple and testable predictions. If true, then the brain must represent the evidence that provides input to a decision process, and consideration of how these evidence signals vary over time should allow prediction of changes in a participant's internal 'decision variable' (DV), which reflects the total evidence accumulated towards specific decision outcomes. Note that the general idea of a DV is abstract in that it is not tied to any specific decision-making model, though DVs should allow accurate prediction of the outcome of participants' decisions, and thus their behavioural responses on decision-making tasks.

Consistent with these predictions, a great deal of evidence suggests that when humans and monkeys perform perceptual decisions, decision-relevant sensory evidence is encoded in functionally specialised sensory processing brain regions. This has been most clearly demonstrated by characterisation of single-neuron responses when monkeys make detection or discrimination judgements about noisy perceptual stimuli such as random-dot motion (RDM) stereograms, which lesion studies show rely on extrastriate visual area MT (Newsome & Pare, 1988; Newsome et al., 1985). Some of the most informative studies simultaneously measured behavioural and neural responses as monkeys discriminated RDM stimuli matched to the size, location and directional tuning of MT neurons being recorded from. These demonstrated that presenting RDM stimuli within the receptive field of MT neurons elicits firing rates proportional to the motion coherence in the neuron's preferred direction (Newsome et al., 1989). Construction of 'neurometric functions' describing the optimal choice based on differences between neural responses to preferred and anti-preferred

motion directions are on average indistinguishable from curves describing the monkey's psychophysical performance (Britten et al., 1992; Newsome et al., 1989). Sensitivity of individual neurons can greatly exceed psychophysical performance, suggesting that monkeys were unable to attend selectively to the optimal perceptual channels; instead basing their decisions according to pooled responses across a large number of MT neurons. This has the advantage of allowing reliable perceptual estimates from neural responses over reasonably short intervals (< 50ms) (Shadlen & Newsome, 1998). The need for pooling activity over multiple neurons in decision making is also supported by recent data suggesting that the visual sensitivity and impact on decisions of individual neurons may be much smaller than early studies suggested (Cook & Maunsell, 2002), partly due to mistaken assumptions regarding the nature of noise correlations in sensory regions (Cohen & Maunsell, 2010). Still, trial-to-trial variations in responses of MT neurons are weakly but significantly predictive of behavioural choices, even for RDM stimuli with 0% coherence (Britten et al., 1996), suggesting a link between MT neuron activity and subjective perception.

Importantly, the effects of sensory cortex activity are not just correlational, but causally influence choice behaviour. Micro-stimulation of MT and nearby MST neurons (which have similar motion sensitivity to MT but larger receptive fields) consistently biases choice behaviour in favour of the motion direction coded by the stimulated neuron (Celebrini & Newsome, 1995; Salzman et al., 1992; Salzman et al., 1990; Seidemann et al., 1998). Micro-stimulation does not always determine a monkey's decision, but does typically reduce RTs for behavioural responses consistent with the stimulated neuron's preferred motion direction, and increases RTs for responses indicating the monkey thought the motion was in the opposite direction. These effects are consistent with the notion that micro-stimulation adds a discrete quantity of sensory evidence to decision processes (Ditterich et al., 2003).

Although MT neurons clearly represent sensory evidence, a number of findings suggest they do not represent subsequent motor response planning. Lesions to MT do not impair the ability to make saccadic eye movements (Newsome et al., 1985), MT micro-stimulation does not induce short-latency saccades (Salzman et al., 1992), and single-unit recordings have not found evidence of motor signals in MT (Newsome et al., 1988). More importantly, nor do MT neurons appear to reflect DVs. For example, firing changes in MT neurons are proportional to RDM coherence and remain reasonably constant over time, whereas accumulator neurons would be expected to encode their integral (Cook & Maunsell, 2002; Gold & Shadlen, 2007). The time course of MT micro-stimulation effects further suggests these signals are integrated elsewhere, as micro-stimulation-induced biases most strongly influence behaviour at earlier times in a decision period, consistent with MT readout only affecting decisions during the limited time frame over which integrated information has not yet reached a threshold level (Huk & Shadlen, 2005). Furthermore, perceptual learning improves the motion discrimination sensitivity of monkeys without major changes in firing properties of MT neurons. Instead, modelling results suggest learning reflects changes in the weights of these inputs on downstream accumulation regions (Gold et al., 2010; Law & Gold, 2008). Similarly, task switching does not impact on MT responses to RDM stimuli, but does change how MT responses co-vary with behaviour (Sasaki & Uka, 2009).

Importantly, similar results to those described for area MT have been reported for regions specialised in processing of other tasks and stimulus types. For example, when monkeys perform a vibrotactile frequency discrimination task, firing rates of neurons in primary somatosensory cortex (S1) tend to increase monotonically with the frequency of stimulation (Romo et al., 2002; Salinas et al., 2000). Interestingly, neurometric curves based on S1 firing rates (i.e. ideal-observer decisions based on observed firing rate data) closely

match monkeys' psychophysical performance, whereas neurometric functions based on S1 perdiodicity - rhythmic fluctuations in S1 activity that follow the frequency of vibrotactile stimulation - vastly outperform monkeys' behavioural discrimination performance (de Lafuente & Romo, 2005; Hernández et al., 2000). This provides compelling evidence that vibrotactile stimulus processing is based on a firing rate code. S1 neuron firing rates during vibrotactile discrimination can also provide weak but significant predictions about monkeys' behavioural choices (Salinas et al., 2000). However, perceptual reports for near-threshold yes/no vibrotactile detection judgements are not predicted by variability in S1 firing rates (de Lafuente & Romo, 2005), suggesting these decisions are based on a processed version of this activity in downstream regions. S1 activity does causally influence behaviour though - remarkably, monkeys are highly accurate at the frequency discrimination task regardless of whether one or both stimuli are mechanical vibrotactile stimulation of the fingertips, or artificial vibrotactile stimuli delivered to area 3b of S1 that consist of period current bursts designed to match the normal cortical responses to a stimulation frequency (Romo et al., 2000; Romo et al., 1998). Finally, like in MT, S1 neurons do not seem to encode DVs. S1 neurons fire only transiently in response to vibrotactile stimulation, and do not seem to encode a combination of the stimuli as would expected for a decision comparison process (Hernández et al., 2010; Romo et al., 2002).

For many higher-level stimuli, the above principles are thought to generalise to other task-relevant brain regions. For example, some inferior temporal (IT) cortex neurons fire transiently to presentation of visual objects, and their firing rates increase monotonically with visual similarity of stimuli to high level categories such as 'cats' and 'dogs' (Freedman et al., 2003). These effects again seem to be causal. When monkeys categorise noisy visual stimuli as being faces or non-faces, micro-stimulation of IT neuron clusters responding to faces

biases decisions towards face responses (Afraz et al., 2006). These effects increase in magnitude with the face-selectivity and size of the stimulated cluster, and only significantly affect behaviour when stimulation is delivered at a task-relevant time more than 50 ms after presentation of a visual stimulus. At a higher level than object categorisation, decisions based on past events are likely to be guided by memory traces. It should be noted, however, that once information enters persistent working-memory representations, it may become difficult to distinguish between processes involved in maintaining representations of information guiding decisions and processes mediating temporal integration of evidence towards a decision (Curtis & Lee, 2010; Machens et al., 2005).

Although still under active investigation, affective and value-guided judgements may similarly involve a multi-stage process whereby evidence is encoded, then integrated towards a decision. However, the relevant decision evidence in these contexts is not simply encoded by primary sensory cortices. Instead, evidence representations in these contexts may emerge from a pre-decision valuation stage involving structures such as the striatum, amygdala, and medial orbitofrontal and ventromedial prefrontal cortices, yielding a representation of the reward or subjective value of stimuli that may be used to guide actions elsewhere in the brain (Basten et al., 2010; Boorman et al., 2009; Noonan et al., 2010; Padoa-Schioppa & Assad, 2006; Philiastides et al., 2010; Wunderlich et al., 2009). Discussion of current understanding of this valuation stage are beyond the scope of this review, and have been reviewed in detail elsewhere (Kable & Glimcher, 2009; Platt et al., 2008; Rushworth et al., 2011; Salzman et al., 2007; Sugrue et al., 2005).

Human neuroimaging data suggest human and monkey brains show strong homologies in the encoding of sensory evidence, and in how these signals relate to decision-making behaviour. I briefly review some of these findings, focussing on experiments using

the RDM task most commonly used in monkey studies, though I note that recent studies using other tasks have similarly demonstrated both correlative and causal relationships between sensory activity and perceptual judgements (Bankó et al., 2011; Binder et al., 2004; Feurra et al., 2011b; Harris et al., 2002; Philiastides et al., 2010; Philiastides et al., 2006; Philiastides & Sajda, 2006, 2007; Pleger et al., 2006; Quian Quiroga et al., 2009; Quiroga et al., 2005; Rahnev et al., 2011; Ratcliff et al., 2009; Spitzer et al., 2010; Tegenthoff et al., 2005). Magnetoencephalographic recordings of humans performing RDM discriminations have isolated stimulus-related 60-100 Hz gamma-band activity that seems to reflect the strength of motion processing. This activity increases monotonically in amplitude with RDM stimulus coherence, and source reconstruction attributes it to a lateral occipito-temporal region likely to be MT+, the human homologue of macaque area MT (Siegel et al., 2007). The integral of RDM-induced gamma-band activity in MT+ over a decision period was also shown to predict human participants' behavioural choices on a yes/no RDM detection task when motion coherence was 0% (Donner et al., 2009). Blood-oxygen-level-dependent (BOLD) signal data from functional magnetic resonance imaging (fMRI) of humans performing a RDM task have also demonstrated elevated overall responses in MT+ when decisions were difficult (Ho et al., 2009). Although fMRI could not resolve the time course of this activity in detail, this effect may have reflected that MT+ was active for longer during difficult decisions. Alternatively, low coherence motion stimuli may have activated a wide range of directionally tuned MT+ channels to a small extent, resulting in net population activity that exceeded the stronger responses that would have been elicited in a smaller number of cells when coherence was higher (Britten et al., 1993; Kayser et al., 2010a; Kayser et al., 2010b).

The causal role of V1, V2 and MT+ in motion perception has been robustly demonstrated by transcranial magnetic stimulation (TMS) studies. These have shown that TMS to MT+/V5 can induce perception of moving phosphenes and modulate detection and discrimination of motion processing, with consequences that depend on the task, TMS stimulation paradigm and physical configuration of stimuli (Boroojerdi et al., 2000; Burton et al., 2009; Campana et al., 2002; Cowey & Walsh, 2000; McKeefry et al., 2008; Pascual-Leone & Walsh, 2001; Ruzzoli et al., 2011; Sack et al., 2006; Silvanto et al., 2008; Silvanto et al., 2005; Stevens et al., 2009; Tadin et al., 2011; Thakral & Slotnick, 2011).

Although, in humans, sensory cortex activity is clearly a determinant of decisions, dissociations between sensory cortex activity and behavioural choice have also been documented (Crick & Koch, 1995; Leopold & Logothetis, 1999; Meyer, 2011; Tong, 2003). Although some studies have reported early sensory cortex activity that was predictive of perceptual judgements, such relationships are not always found, and the precise conditions mediating these differences are currently unclear. Furthermore, where predictive relationships have been observed, because of the low temporal resolution of fMRI, it is often equivocal to what extent the effects reflect stimulus-driven activity in sensory cortex, or consequences of activity in upstream regions that may both integrate inputs from sensory regions and shape their activity via top-down control mechanisms (Leopold & Logothetis, 1999; Meyer, 2011; Tong, 2003). Thus, as in monkey studies, it seems that higher-level interpretation of early sensory signals is often important in determining the percepts that inform human decisions.

In summary, whilst a number of specialised regions such as primary sensory cortex seem to encode the momentary fluctuations in evidence providing input to decision processes, neural evidence from humans and macaques suggests that (1) little to no evidence integration occurs in primary sensory cortices, and (2) persistent activity in sensory regions

cannot fully explain decision outcomes or subjective percepts. Thus, sensory regions are unlikely to play a major role in directly computing or maintaining representations of DVs. The following sections detail firing rate properties of neurons in anatomically downstream brain regions more likely to instantiate decision-making processes.

1.4. Integration of Evidence in the Monkey Brain

If sensory regions encode inputs to decision processes, then a natural hypothesis is that another set of anatomically-connected brain regions may monitor these signals and compute their integral, then pass the decision outcome on to regions involved in initiating a response. Over the last 20 years, mounting evidence has suggested that DVs are represented in sensorimotor integration regions of the parietal lobe of macaque monkeys. This section overviews the considerable body of work suggesting that specific regions within the macaque parietal cortex encode decision evidence for the spatially- and modality-specific responses monkeys use to indicate their decisions.

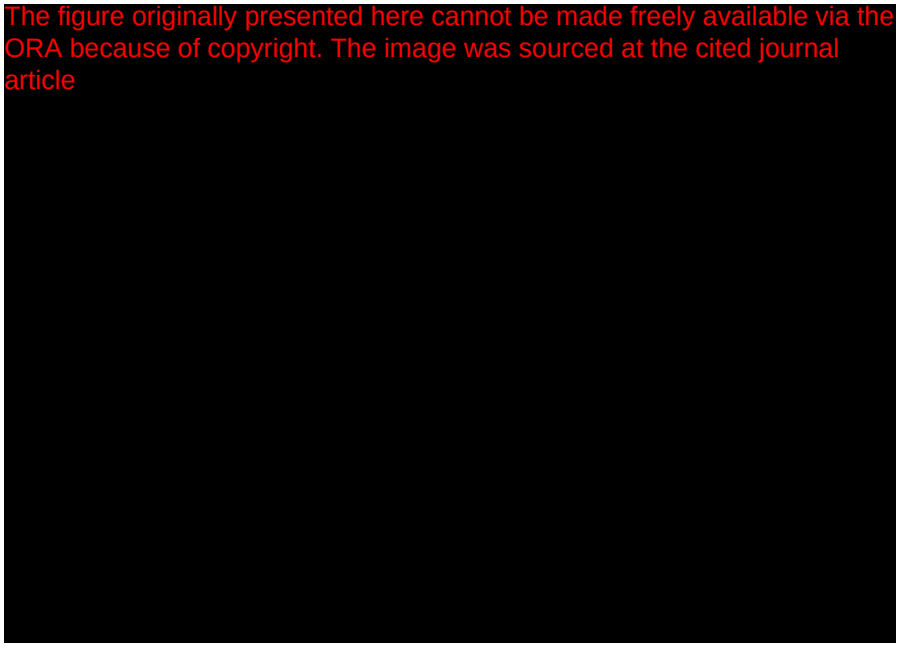


Figure 1-2. Anatomy of macaque parietal lobe. The inset view emphasizes the location of different parietal regions along the intraparietal sulcus (IPS). Medial intraparietal area (MIP) is on the medial bank of ths IPS, in the superior parietal lobule (SPL), whereas the anterior intraparietal area (AIP) and lateral intraparietal area (LIP) are on the ventral bank of the IPS, in the inferior parietal lobule (IPL). Taken from Buneo & Anderson (2006).

1.4.1. Macaque Parietal Lobe Anatomy and Subdivisions

The macaque parietal lobe is a highly heterogeneous structure with numerous anatomical and functional subdivisions (Averbeck et al., 2009; Grefkes et al., 2004; Lewis & Van Essen, 2000a, 2000b; Mars et al., 2011; Nelson et al., 2010; Orban et al., 2004). Anatomically, the intraparietal sulcus (IPS) is situated between the somatosensory and visual cortices, dividing the macaque parietal lobe into inferior and superior lobules (IPL and SPL, respectively) (Figure 1-2). The IPL corresponds to Brodmann's area 7 and includes caudal, rostral and intermediate regions 7a (PG), 7ab (PFG) and 7b (PF). The SPL includes Brodmann's area 5, also referred to as PE. The lateral intraparietal area (LIP) lies on the lateral wall of the IPS, caudal to the anterior intraparietal area (AIP) and rostral to the caudal intraparietal area (CIP). LIP receives ascending projections from visual regions including area MT. Its receptive fields are primarily in the ipsilateral hemisphere, frequently at

peripheral visual locations (Andersen et al., 1990; Baizer et al., 1991; Lewis & Van Essen, 2000a; Maunsell & van Essen, 1983). LIP is reciprocally connected with oculomotor regions including the supplemental and frontal eye fields (SEF and FEF), as well as the superior colliculus (SC) (Blatt et al., 1990; Cavada & Goldman-Rakic, 1989; Lynch et al., 1985; Schall et al., 1995). Area AIP is also located on the lateral IPS bank, but anterior to LIP. It is thought to have similar visual inputs to LIP (Nakamura et al., 2001), and has particularly strong connections with ventral premotor cortex (Tanné-Gariépy et al., 2002). The SPL includes Brodman's area 5, with anterior to caudal subdivisions sometimes referred to as PEa, PE and PEc, as well as the medial intraparietal area (MIP) on the medial wall of the IPS. MIP, V6a (sometimes called the parieto-occipital area, PO) and sometimes caudal parts of PE in the IPS are collectively referred to as the parietal reach region (PRR) (Buneo & Andersen, 2006; Cohen & Andersen, 2002; Grefkes & Fink, 2005). MIP receives strong visual inputs via V6a and other parietal subregions (Caminiti et al., 1996), and its middle-to-posterior aspects have strong reciprocal connections with dorsal premotor cortex (Pesaran et al., 2008; Tanné-Gariépy et al., 2002). More anterior regions of PRR receive stronger somatosensory inputs. For completeness, I note that whilst I adopt the use of PRR here, most electrophysiological studies using the nomenclature PRR have recorded almost exclusively from MIP.

1.4.2. Decision Integration by LIP Neurons

Consistent with its anatomical connectivity with sensory and motor regions, LIP has primarily been implicated in visual processing and control over eye movements (Andersen et al., 1992; Colby et al., 1996; Platt & Glimcher, 1997; Snyder et al., 1997). Early recordings demonstrated that a large proportion of LIP neurons not only respond when salient visual

stimuli are presented in their receptive fields, but also during delay periods during which a saccade is planned to that location, and as the saccade is performed (Barash et al., 1991; Gnadt & Andersen, 1988). Note that because LIP neurons' activity can reflect the presence of visual stimuli at circumscribed visuospatial locations and the intention to perform a saccade to that location, they can be referred to as having 'receptive fields' and/or 'response fields'. LIP response fields represent spatial locations in an eye-centred coordinate frame, and the locations to which they are sensitive updates anticipatorily shortly before a saccade, perhaps in anticipation of the retinal consequences of the saccade to allow a continuous representation of visual space (Duhamel et al., 1992).

Given their position in the middle of the sensorimotor hierarchy, parietal neurons such as those in LIP seem ideally placed to integrate perceptual information and convey this information to parts of the brain responsible for response execution. Accordingly, decision-making researchers were quick to investigate whether LIP neurons exhibiting spatially specific delay-period firing also had characteristics consistent with those predicted of accumulator neurons (Platt & Glimcher, 1999; Shadlen & Newsome, 1996). Response properties of LIP neurons have now been extensively studied in decision-making studies, most commonly using RDM discrimination tasks requiring monkeys to discriminate the direction of motion in a centrally presented RDM stimulus, and indicate their decisions with saccades to peripheral targets. Saccade target locations can then be presented inside a recorded-from neuron's response field (T_{in}) or outside it (T_{out}). Note that the RDM stimulus is not typically presented inside the response fields of recorded-from neurons. RDM stimulus onset leads to an initially non-specific response in LIP neurons, but after several hundred milliseconds firing rates begin to exhibit a number of characteristics consistent with

mathematical descriptions of accumulator model decision-making processes (Gold & Shadlen, 2007; Smith & Ratcliff, 2004) (Figure 1-3).

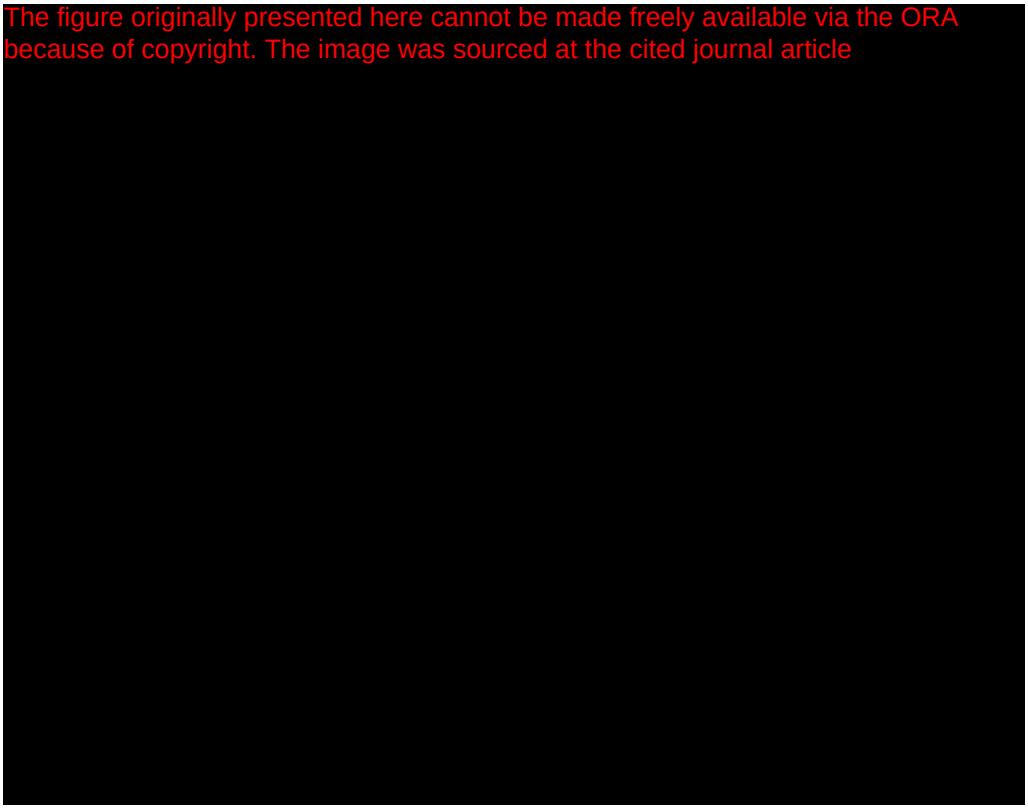


Figure 1-3. LIP neurons appear to integrate decision evidence. A schematic of the random-dot motion discrimination task is provided in the right-most panel. The left panel shows that after after an initial non-specific response lasting several hundred milliseconds, LIP firing rates increase or decrease at rates proportional to random dot motion evidence in favour of a saccade to the neuron's preferred response field. The more tonic motion-dependent responses in area MT are shown in the lower inset panel. The middle panel shows that decisions are terminated and a saccade made once firing rates hit a threshold level that is independent of the steepness with which firing rates increase. Taken from Gold and Shadlen (2008).

The first property of LIP activity suggestive of a decision-integration process is that the rate of change of LIP firing rates is proportional to the strength of motion coherence (Figure 1-3). Neurons increase their firing more quickly when motion coherence more strongly favours a saccade to their response field, and decrease more quickly when it favours a saccade in the opposite direction (Roitman & Shadlen, 2002; Shadlen & Newsome, 1996; Shadlen & Newsome, 2001). Thus, it appears LIP neurons robustly reflect the integral of task-relevant sensory evidence favouring specific decision outcomes.

Second, LIP neurons seem to reflect monkeys' decisions more than they do the objective visual properties of a stimulus (Park & Zhang, 2010). In addition to predicting responses on correct trials, their selective ramping activity predicts choices on error trials, and on trials where RDM stimuli contain no coherent motion (Roitman & Shadlen, 2002; Shadlen & Newsome, 1996; Shadlen & Newsome, 2001). The rate at which LIP firing rates increase also predicts reaction times independently of stimulus difficulty (Roitman & Shadlen, 2002). Furthermore, LIP activity is selectively modulated by task-relevant sensory dimensions, responding differently to identical visual stimuli depending on task demands (Shadlen & Newsome, 2001; Toth & Assad, 2002).

Third, LIP neuron firing rates also reflect decision biases in a manner consistent with both trial-to-trial and systematic changes in the starting point of an accumulation process. Trial-to-trial variations in LIP neuron pre-decision baseline firing rates predict monkeys' decisions, especially when the information provided by sensory stimuli is weak (Shadlen & Newsome, 2001). When reward is asymmetric, the apparent starting point of accumulation in LIP is similarly offset but in a consistent fashion (Rorie et al., 2010).

Fourth, in most cases LIP neurons' firing rates do not just reflect a categorical motor signal, but vary parametrically with evidence for responses. This has been suggested by

characterisation of the ramping rate of LIP neurons for different RDM stimulus coherences, demonstrations that firing rates are lower on error trials than correct trials resulting in a saccade to the same location, and analysis of the variance of LIP firing rates during the course of the decision period (Roitman & Shadlen, 2002; Shadlen & Newsome, 1996; Yang & Shadlen, 2007). Similarly, LIP firing rate modulation cannot be accounted for by changes in metrics of saccadic responses (Roitman & Shadlen, 2002; Shadlen & Newsome, 2001).

Fifth, aligning firing rate data to onset of a saccade reveals that the saccades are typically elicited when activity reaches a common level that is independent of the build-up rate (Roitman & Shadlen, 2002). This matches the prediction that decisions should be terminated, and responses initiated, as soon as the integrated evidence reaches a common threshold level. Accordingly, reaction times and the ramping rate of LIP neurons are inversely related. A predictive relationship between ramp rate and RT hold even at the single-trial level (Roitman & Shadlen, 2002), consistent with the idea that trial-by-trial variability in the accumulation process (i.e. the ramping rate) determines when the decision accumulation processes reaches the threshold (Ratcliff & Rouder, 1998).

Although the above studies relate LIP firing to the integral of evidence provided by sensory regions, LIP is also sensitive to other decision-relevant factors and more complex aspects of task structure. Evidence-dependent updating of LIP firing rates has also been shown in more discrete decision-making tasks, such as one that recently presented monkeys with symbolic shapes associated with specific evidence quantities, thereby allowing the experimenters to objectively manipulate fluctuations in the evidence for and against each saccadic response target over the course of each trial (Yang & Shadlen, 2007). LIP firing rates dynamically updated in response to the evidence provided by rapidly presented

sequences of these shapes, even when evidence quickly changed from strongly favouring one response to strongly favouring another.

Other studies have investigated how LIP activity is constrained by knowledge of the time available to make decisions. Ramping rates of LIP neurons increase as the expected available decision integration time for RDM discriminations is reduced, but without any apparent change in the threshold firing rate, possibly reflecting scaling of a DV by elapsed time in a manner that depends on the task-specific hazard rate (Shadlen & Newsome, 2001). Another study used an interval timing discrimination task requiring monkeys to saccade to different locations to indicate whether a test stimulus was presented for a shorter or longer duration compared with a reference stimulus. During the test stimulus display period, LIP firing rates were initially high for the response field for the 'short' response and low for the 'long' response, but this gradually reversed with viewing time, consistent with the notion that evolution of LIP activity reflected changes in the relative salience of each choice target over the viewing period (Leon & Shadlen, 2003). Similarly, LIP firing reflects monkeys' degree of anticipation about an upcoming target presentation, and closely matches learned hazard functions for its presentation schedule (Janssen & Shadlen, 2005). LIP neurons are also sensitive to numerosity within their response fields, independent of reward and stimulus-driven visual features (Roitman et al., 2007). Another important study demonstrated that LIP neuron activity varies with the prior probability of receiving a reward following a saccade to its response field, and with the magnitude of that reward (Platt & Glimcher, 1999). Subsequent studies have confirmed this idea, demonstrating that LIP activity reflects the subjective value of actions across a range of decision tasks (Dorris & Glimcher, 2004; Louie & Glimcher, 2010; Louie et al., 2011; Rorie et al., 2010; Seo et al., 2009; Sugrue et al., 2004). In summary, it appears that LIP activity can reflect integration of a wide range of

forms of behaviourally relevant evidence, suggesting it may encode decision variables or closely related quantities in a very general manner.

As the above studies only recorded activity in LIP, they were necessarily agnostic about whether decisions were actually formed in LIP. However, lesion and micro-stimulation work has confirmed that LIP is causally involved in saccadic planning and decision making towards saccades (Hanks et al., 2006; Li et al., 1999; Schiller et al., 2005). Hanks and Shadlen (2006) applied micro-stimulation to cortical columns in LIP from the time a RDM stimulus onset until a saccadic response was made, ensuring that stimulation was below the level that directly elicited saccades. Micro-stimulation consistently biased responses in favour of the response field of the stimulated area, especially when RDM stimulus coherence was low. This change could be characterised by a threshold decrease of ~2% for psychometric functions describing the RDM coherence necessary to elicit a T_{in} response (Hanks et al., 2006). Micro-stimulation also modulated RTs, decreasing them for T_{in} responses and increasing them for T_{out} responses. Importantly, this provides strong neural evidence against pure race models of the decision process, which posit the existence of independent accumulator processes for different responses. Instead, RT effects of T_{in} stimulation on T_{out} responses require negative coupling between neuronal pools representing competing responses, consistent with earlier mathematical model fits to behavioural data (see Section 1.1). Interestingly, the effects of LIP stimulation in the study by Hanks et al. (2006) were modest compared to those of earlier MT micro-stimulation studies. Although this difference may appear counter-intuitive, diffusion modelling of both sets of results was shown to be consistent with the idea that sustained LIP stimulation mimicked addition of a constant amount of evidence to the decision process, whereas MT micro-stimulation effects were integrated over time elsewhere in the brain, and thus had greater consequences on behaviour.

1.4.3. LIP is Not the Final Stage in Response Selection

Despite evidence for a role of LIP in decision making, dissociations between LIP activity and behavioural choice reveal that LIP activity is not the final stage in response selection. This can be seen, for example, when monkeys view highly coherent RDM stimuli but make an incorrect choice. In this situation, LIP firing seems to encode the correct choice, but perhaps due to a lapse in attention late in the trial the opposite response is made (Shadlen & Newsome, 2001). Intriguingly, on error trials monkeys' responses are predicted by pre-decision LIP firing rate biases (Shadlen & Newsome, 2001). However, this effect is only apparent before onset of the random motion stimulus and dissipates during motion viewing, suggesting the bias remains encoded in another region that exerts causal control over the decision process. Similarly, careful analysis of LIP data in several recent studies has further demonstrated that LIP activity is more closely predicted by factors associated with subjective value than behavioural choice on a trial-by-trial fashion (Louie & Glimcher, 2010; Louie et al., 2011).

1.4.4. Is LIP an Attentional or Intentional Structure?

In contrast to the view that LIP guides saccadic decisions, other investigators have argued that the primary role of LIP is related to visuo-spatial attention (Colby & Goldberg, 1999), and that apparently decision-related activity in LIP may be an artefact of the intimate link between attention and saccade planning (Deubel & Schneider, 1996; Kowler et al., 1995). Two findings of a prominent study by Gottlieb and colleagues (1998) support this notion by demonstrating de-coupling between LIP activity and saccades. First, LIP neurons fire in response to stimuli at salient or task-relevant visual locations regardless of whether or not they are saccadic targets. Second, LIP neurons do *not* fire in advance of a saccade to their response field when the saccade to that location is driven by memory and no salient target is

present there (Gottlieb et al., 1998). In another study utilising an anti-saccade task, LIP activity was shown to be more sensitive to the visual location of the informative visual cue than the saccade target on anti-saccade trials (Gottlieb & Goldberg, 1999). However, despite a wealth of other studies demonstrating further examples of de-coupling between attention and saccade planning in LIP activity, LIP micro-stimulation does causally influence decisions (Hanks et al., 2006), and even advocates of an attentional view acknowledge that some LIP neurons are sensorimotor in nature, jointly encoding action intention in addition to visual information (Oristaglio et al., 2006). In an attempt to unite the opposing attentional and intentional viewpoints, recent theorists have suggested that LIP neurons encode a spatially organised salience map indicating the behavioural relevance of visual locations (Bisley & Goldberg, 2010; Gottlieb, 2007; Gottlieb & Balan, 2010; Wardak et al., 2011). Under this view, the LIP salience map guides both covert attentional orienting and overt saccade planning, consistent with computational models of the visual system (Itti & Koch, 2001). Consistent with this idea, LIP micro-stimulation biases the probability a saccade is made to the stimulated response field during a reward-guided visual exploration task (Mirpour et al., 2010). Furthermore, a recent study highlighted that perceptual decision-making studies have typically recorded from cells showing sustained spatially specific firing during the delay period of memory-guided saccade tasks, whereas visual studies have utilised less strict cell selection criteria (Premereur et al., 2011). Analysing a wide range of cell types reveals that the response properties of spatially intermixed LIP cells are highly heterogeneous, and that the selection criteria of many decision studies biases results towards revealing oculomotor activity when in fact cells should be viewed as existing on a continuum from visual to 'motor intention'. Such a mixture of responses is consistent with the representation of a priority map reflecting the salience of objects that are potential targets of saccades (Premereur et al., 2011).

However, additional work is required to clarify how the notion of a unified LIP salience map relates to empirical data emphasising that the information represented by parietal neurons varies in a systematic and gradual manner both within and across the borders of parietal regions (Colby & Duhamel, 1991). For example, investigation of the behavioural consequences of reversible inactivation of dorsal and ventral LIP (LIPd and LIPv) subdivisions suggests a clear differentiation of functional roles even within LIP; LIPd inactivation primarily impairs oculomotor function whereas LIPv inactivation impairs both attentional and oculomotor behaviours (Liu et al., 2010). Another challenge to the salience map account for LIP activity is that it does not explain the relationship between LIP activity and nearby parietal reach region (PRR) activity, which seems to encode a spatial map in eye-centred coordinates for reach intentions (see next Section). It is possible that LIP encodes an attentional-saccadic salience map and MIP separately encodes a reach-related salience map, as these forms of attention seem dissociable (Jonikaitis & Deubel, 2011; Rushworth et al., 2001b). However, this may still be criticised as ignoring the graded changes in connectivity and neuronal functionality in these regions, as well as data suggesting that a more general role of the posterior parietal cortex (PPC) may be to perform coordinate transformations allowing visual, somatosensory, and motor inputs to be integrated within consistent spatial reference frames during both the planning and updating of actions plans (Andersen & Cui, 2009; Buneo et al., 2002).

Further countering the notion that LIP's sole role is to encode attentional or intentional information within a spatial reference frame, decision-related activity distinct from saccade planning can be observed in LIP neurons when the monkeys do not know the association between motion direction and saccade targets until the end of a trial (Bennur & Gold, 2011). LIP has also been reported to show activity that is shape selective but not

spatially specific, even during passive viewing (Sereno & Maunsell, 1998). Such data tacitly accord with recent suggestions that LIP and other frontoparietal structures in the dorsal stream may play a general role in both action-specific and action-independent decision making, where integration processes continuously tune planning circuits representing multiple potential action plans and/or representations of more abstract schemas, depending on current knowledge of environmental contingencies (Cisek & Kalaska, 2010; Freedman & Assad, 2011; Pezzulo & Castelfranchi, 2009). Still, the functional significance of non-spatial neural signals in LIP is unclear, as unilateral LIP inactivation seems to induce deficits on spatial, but not on non-spatial decisions (Balan & Gottlieb, 2009).

In summary, the activity of LIP neurons can play a causal role in determining monkeys' behavioural choices, and the temporal evolution of LIP firing rates during decision tasks is consistent with encoding of a quantity very similar to the decision variables postulated by psychologists modeling behavioural decision-making data. Although it is not currently possible to exhaustively define LIP functionality, within the context of decision tasks there is an overall consensus that LIP activity levels reflect the evidence for specific responses, or that LIP continuously tracks the salience of visual locations that may form the endpoints of saccades, and that this salience is near-indistinguishable from a DV. Under some circumstances LIP activity does not fully predict saccadic choice however, suggesting that LIP activity is not the final processing stage in an oculomotor decision circuit.

1.4.5. Function of Neurons in the Parietal Reach Region (PRR) and Area 5

PRR has been suggested to implement a similar sensorimotor interface to that in LIP, but specialised for reach rather than saccade planning (Andersen & Buneo, 2002; Buneo & Andersen, 2006; Cohen & Andersen, 2002; Cui & Andersen, 2007). Although PRR neuron

activity can also be modulated by attention, PRR specificity for the spatial location of planned reaching movements has been shown to be reasonably independent of attentional selection. This dissociation has been easier to achieve for PRR compared with studies of oculomotor intention in LIP because reaching movements are not as intimately coupled with visuospatial attention as saccades. PRR neurons are more active during the delay period of memory-guided reach tasks than memory-guided saccade tasks involving the same spatial locations (Snyder et al., 1997), consistent with the idea of a spatial map useful for the guidance of arm movements (Colby & Duhamel, 1991). Consistent with the opposite preference of LIP neurons for saccades than reaches (Snyder et al., 1997), reach movement vectors are better de-coded by population analysis of PRR neurons and saccade vectors better de-coded from LIP population activity (Quian Quiroga et al., 2006), and during an autonomous reach selection task, differential activity in PRR neurons is highly selective for the reach target location but is not selective for the target of saccades (Scherberger & Andersen, 2007). Similarly, during anti-reach tasks, almost half of the PRR cells showing spatial-selectivity are tuned only to the direction of the planned reach whereas relatively few cells show selectivity to the location of the instructive visual target before shifting to the movement target (Gail & Andersen, 2006). Furthermore, PRR activity predicts reaction times for reaches but not saccadic latencies (Snyder et al., 2006).

As in LIP, most PRR neurons' reference frames are mainly eye-centred (Batista et al., 1999; Buneo et al., 2002), but as the medial wall of the IPS is ascended towards area 5, more cells are encountered which are sensitive to a mixture of eye-centred and hand-centred positions, or to hand position alone (Buneo et al., 2002). This part of the posterior parietal cortex appears to transform eye-centred co-ordinates to body-centred co-ordinates within which motor intention vectors can be more naturally computed for communication with more

anterior parts of the brain that may encode actions in body-centred coordinates (Caminiti et al., 1996; Johnson et al., 1996). Inactivation of macaque area 5 leads to both neural and behavioural deficits in a task where the appropriate action depends on the numerosity of the executed movement within a sequence of movements (Sawamura et al., 2010).

Compared with LIP, PRR has not been rigorously studied within the context of decision tasks requiring accumulation of graded quantities of evidence. Specifically, to my knowledge, no previous studies have demonstrated a parametric relationship between firing rates of PRR neurons and confidence for a reaching action to the neuron's preferred spatial location. However, Cui and Andersen (2007) provided a compelling demonstration that PRR reflects, in the least, the outcome of the decision. LIP and PRR neuron activity was recorded as monkeys completed a free-choice task involving an instructive visual cue that specified that a response to a peripheral target should be made, but not what effector should be used to make it. During the pre-movement decision period of the task, PRR neuron firing rates showed sustained activity for reach compared with saccade choices, and LIP neuron firing rates showed sustained activity for saccade compared with reach choices. However, although this rate difference emerged gradually during the choice period, it is unclear whether this reflected gradual planning of the chosen response modality or gradual dis-preparation for the un-chosen response modality. The reason for this is that, in both regions, activity was high early in trials, and the effector-specific activity was due to a decay back to baseline firing rates for the un-chosen response (Cui & Andersen, 2007). Thus, this study does not clearly distinguish between neural activity reflecting the evolution and outcome of the decision.

In a remarkable study by Musallam and colleagues (2004), monkeys had multielectrode arrays implanted in their PRR, and activity recorded during memory-guided reach movements was used to train a computer classifier. This then allowed on-line decoding

of monkeys' intentions in the same task, but in the absence of movement (Musallam et al., 2004). Offline analysis demonstrated that the anticipated reward value, probability and magnitude could also be decoded from PRR data. Importantly, both the categorical choice and the overall expected value of the choice could be simultaneously read-out of neural data. Thus, whilst it must be acknowledged that this study did not demonstrate parametric integration of evidence over time in PRR as emphasised by the work of Shadlen and colleagues, it does suggest that many of the same high-level decision relevant quantities observed in LIP are also found in PRR.

It should be noted that consideration of choices between effector modalities raises another important and currently unresolved question. Current neurally plausible decision models such as the attractor models of the Wang and Deco laboratories involve competition (in the form of mutual inhibition) between cortical representations of evidence for each option (Albantakis & Deco, 2009; Lo & Wang, 2006; Soltani & Wang, 2010; Wang, 2002), and have been empirically tested within LIP. Given the anatomical separation between LIP and PRR, decisions about the spatial location towards which a saccade (or reach) is directed may primarily involve intra-areal neural interactions, whereas decisions about whether a saccade or reach is directed to a target predominantly involve inter-areal interactions. It is possible that such differences influence neural activity in ways that impose important constraints on decision-making models (though see Cisek, 2006, 2007; Cisek & Kalaska, 2010).

1.4.6. Decision Integration Neurons beyond the Parietal Lobe

Counter to the notion that decisions occur in discrete regions of the brain then pass their outputs to subsequent processing stages, similar decision-related signals to those

observed in the parietal lobe have been observed across a wide range of distal brain regions. As in the parietal lobe, many of these examples are from sensorimotor or motor regions involved in oculomotor or reach movement planning.

The macaque frontal eye fields (FEF) is located along the rostral bank of the arcuate sulcus close to the posterior end of the sulcus principalis (Walker's areas 8A and 45), and is strongly connected with dorsal stream visual regions including MT and LIP, as well as the superior colliculus (SC) and more anterior prefrontal regions (Amiez & Petrides, 2009; Cavada & Goldman-Rakic, 1989; Schall et al., 1995). Consistent with its connectivity with other regions implicated in oculomotor and attentional control, FEF activity precedes saccades (Bruce & Goldberg, 1985) and FEF micro-stimulation readily elicits saccades (Bruce et al., 1985; Robinson & Fuchs, 1969). FEF is also important in effecting top-down attentional modulation of parietal and visual regions, and micro-stimulation of FEF neurons modulates both visual sensitivity and V4 responses, enhancing them for stimulated response fields and attenuating them for other visual locations (Moore & Armstrong, 2003; Moore & Fallah, 2001). Though the relationship between attention and saccadic control in the FEF is topical (Juan et al., 2004), these functions seem at least somewhat dissociable at the neuronal level, with individual neurons being classifiable on a 'visuomotoric continuum' from mainly visual to mainly motoric (Bruce & Goldberg, 1985).

A seminal study by Hanes and Schall (1996) recorded from FEF neurons exhibiting spatially specific delay-period activity as monkey completed a go/no-go task. The results strongly supported a link between FEF neurons and accumulator decision processes. Saccadic reaction times were predicted by the rate of change in the spike rate during the decision period, consistent with the notion that faster accumulation led to quicker decisions. Importantly, FEF neuron activity reached a constant level 10-20 ms prior to saccade initiation

regardless of saccadic reaction time, consistent with the notion of a fixed decision threshold. Activity was also lower on no-go trials where saccades were successfully inhibited compared to no-go trials where a saccade was made (Hanes & Schall, 1996). Kim and Shadlen (1999) subsequently demonstrated that FEF neurons exhibit several of the same key decision-related properties as LIP cells in RDM tasks. In particular, (1) average firing rates and ramping rates of FEF neurons increased/decreased monotonically with the motion coherence favouring a saccade to the neurons' preferred/non-preferred response field, (2) FEF neurons' activity was lower preceding erroneous compared with correct saccades to their response field, and (3) saccadic choices could be predicted from neuronal activity not directly attributable to variance in the RDM stimuli (Kim & Shadlen, 1999). Several additional pieces of evidence suggest that local activity in the FEF may contribute to both target selection and decisions. Spiking activity of FEF neurons contains spatially specific information about the location of a salient visual target ~120 ms after onset of a target array, whereas this information is not present in local field potentials (LFPs) until ~20 ms later. Because LFPs are thought mainly to reflect dendritic inputs, whereas spike rates reflect output of the local neuronal population, this suggests the selection procedure is computed locally by FEF neurons (Monosov et al., 2008). Although the data of Monosov and colleagues pertained to covert attentional selection latencies rather than decision times, other evidence suggests the activity of visually-responsive FEF neurons contributes to categorical decisions requiring temporal integration of inputs. Specifically, when monkeys judge RDM stimuli as slow or fast, some FEF neurons exhibit stimulus speed preferences (Ferrera et al., 2009). Slow-preferring neurons fire more when RDM speed is slow than when it is fast, and fast-preferring neurons show the opposite preference. Furthermore, decision criteria changes result in predictable changes in the activity of these cells, with fast-preferring neurons firing more to the same stimulus when the category boundary between fast and slow is lower and vice versa for slow-preferring cells.

Modelling decisions based on these neural data accurately predicts monkeys' behavioural choices (Ferrera et al., 2009).

Preparatory motor activity occurs over a wide range of cortical areas in the monkey including primary and pre-motor cortex, supplementary motor cortices, the basal ganglia, and in spinal interneurons (Alexander & Crutcher, 1990; Bizzi et al., 2000; Godschalk et al., 1985; Godschalk et al., 1981; Kurata & Wise, 1988; Prut & Fetz, 1999). In general, intra-areal differences exist, with more rostral cortical motor areas having a higher proportion of neurons involved in preparatory but not movement-related activity (Alexander & Crutcher, 1990). Consistent with these data, it has been shown that decision-related signals propagate throughout the sensorimotor system, even reaching the superior colliculus (SC), only a few synapses away from the brainstem neurons that directly effect eye movements. About one third of SC cells show build-up activity that predicts when and whether a saccade will be made, and similar to LIP and FEF, firing rate growth rates scale with discriminability of visual targets and the probability of a reward, and predict behavioural choices (Basso & Wurtz, 1998; Horwitz et al., 2004; Horwitz & Newsome, 1999, 2001; Ikeda & Hikosaka, 2003; Munoz & Wurtz, 1995). Ratcliff and colleagues (2003) formally investigated the correspondence between SC activity and behaviour on a two-choice decision-making task using a drift-diffusion model. After establishing the model parameters that resulted in the best fit to monkey's behavioural data, they used the model to simulate the decision paths over a large number of decisions. They then compared the average temporal evolution of the simulated paths with the actual SC firing rates for slow, medium and fast choices, and found a near-perfect correspondence between them. Like LIP and FEF, inactivation studies have also demonstrated that the SC's role in the oculomotor decision process is causal. Chemical inactivation of specific SC movement fields impaired monkeys' abilities to saccade to that

location when it contained an oddball target (McPeek & Keller, 2004). This effect did not eliminate all saccades to the affected movement field, to which monkey's post-injection saccade rates depended on the difficulty of the discrimination task. Furthermore, a low contrast visual detection control task involving only a single target was not impaired. Thus, the inactivation-induced effects are best explained as a specific deficit in the ability to select between saccadic targets.

The evidence discussed so far indicates saccadic decision-related activity can be observed across virtually all brain regions involved in oculomotor control. What about non-sensorimotor/motor regions? It turns out that a number of frontal cortex regions have also been implicated as having a similar role in decision making. The nature of these effects have been systematically explored in the context of a somatosensory frequency discrimination task by Romo and colleagues. In this task, a monkey receives two pulses of vibrotactile mechanical stimulation to a fingertip, separated by a delay, and has to report whether the first pulse was higher or lower in frequency than the second one (see Figure 1-4B, top). Over a long series of experiments, Romo and colleagues have investigated how neural firing rates over a wide range of sensory, motor and prefrontal sites correlate with the encoding of stimulus frequencies, their delay period retention, and comparison of the two stimuli following presentation of the second vibrotactile pulse (Brody et al., 2003; de Lafuente & Romo, 2005; Haegens et al., 2011b; Hernández et al., 2010; Hernández et al., 2000, 2002; Lemus et al., 2007; Machens et al., 2005; Romo et al., 1999; Romo et al., 2004; Romo et al., 2000; Romo et al., 2002; Romo et al., 1998; Romo & Salinas, 2003; Salinas et al., 2000; Salinas & Romo, 1998). The most striking aspect of the results of this series of experiments is that decision-related neural activity has been observed in many of the regions recorded from, and that comparing activity between regions reveals more similarities than dissimilarities.

This was elegantly exemplified by a recent study by Hernández and colleagues (2010), who report analysis of over 2,500 neurons from seven brain regions as monkeys completed the frequency discrimination task (Figure 1-4). While primary somatosensory (S1) neurons only reflected the frequency of the two vibrotactile stimuli (f1 and f2, respectively) around the time they were presented, firing rates of neurons in secondary somatosensory (S2) cortex, prefrontal and premotor regions reflected both f1 and f2 over the entire trial duration. In addition, all regions other than S1 reflected a linear combination of the two stimulus frequencies to some extent, particularly around the time f2 was presented and the f1-f2 comparison decision was presumably made. Intriguingly, f1 persistence diminished somewhat during the f1-f2 delay, but resumed towards the end of the delay but before onset of f2, suggesting reactivation of a working-memory trace in these regions prior to the f1-f2 comparison. This was particularly the case in the prefrontal (PFC), ventral premotor (VPC) and medial premotor (MPC) cortices. Many of the neurons encoding f1 early in the trial subsequently reflected both f1 and f2 later in the trial. The strong comparison activity found in frontal, premotor and motor regions is once again consistent with the idea that the structures responsible for planning a response also encode persistent representations of the evidence on which the response is based. Notably, the investigators also examined how decision-relevant signals propagated through the brain over the task. The latency of f1 and f2 information representations was found in a predictable order, first in S1, then S2, then in the PFC and VPC, and finally in the MPC and premotor cortex (DPC), suggesting a degree of serialization in the processing hierarchy. However, the comparison signals did not appear in a staggered fashion, suggesting all regions recorded from are involved in the decision computation, or maintaining a working-memory representation of it (Curtis & Lee, 2010). In fact, other than the f1 and f2 latency differences, and the lack of f1-related delay period activity in the primary motor cortex (M1), the authors could make few distinctions between

responses across regions except for changes in the number of neurons representing each quantity. Intriguingly, these effects were closely related to behavior, and the extent with which f2 representations persisted more than f1 representations in all regions other than S1 and S2 during the delay period predicted behavioural decision biases to an equal degree.

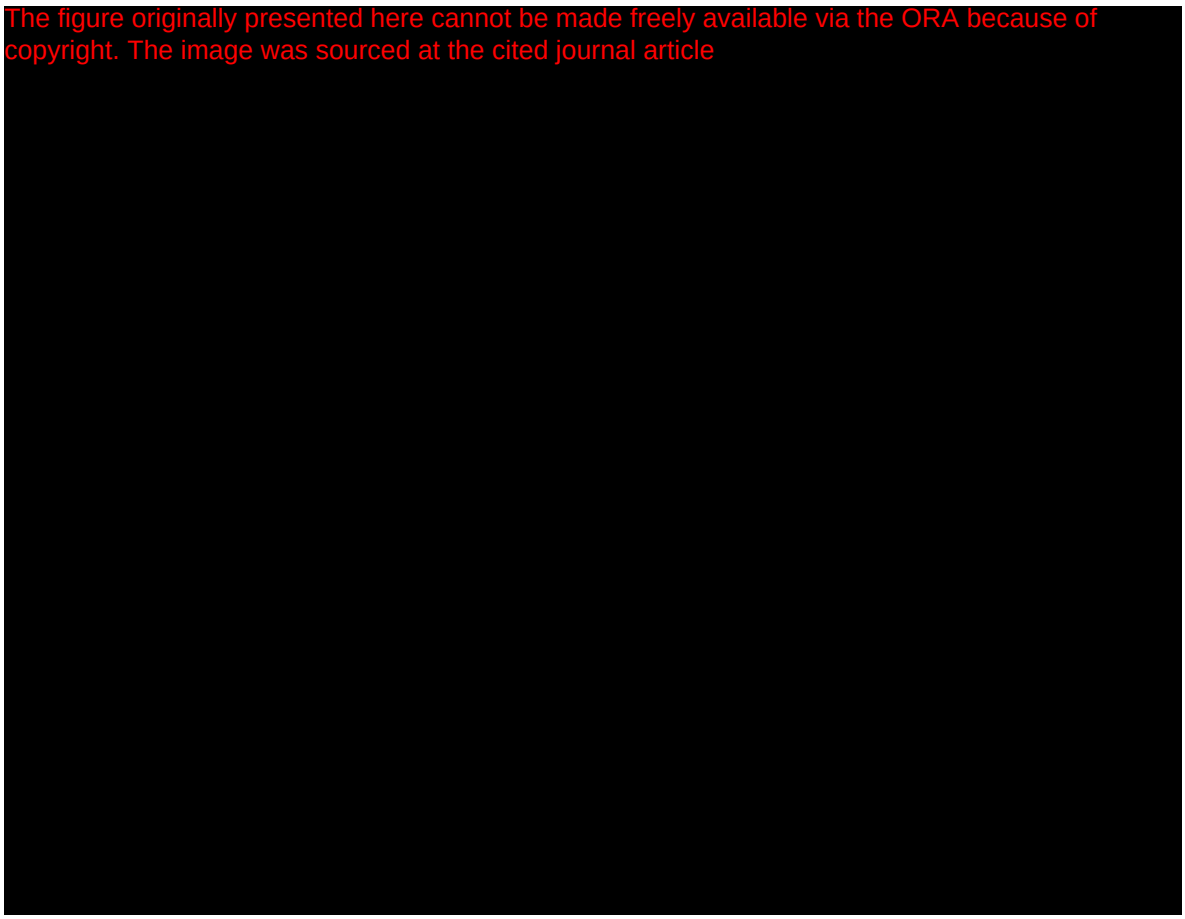


Figure 1-4. During a somatosensory frequency decision task, decision-related neural activity is observed across a wide range of cortical areas. (A) Recording sites include seven distinct sites, with four sites recorded from bilaterally. **(B)** (top) Schematic of the vibrotactile discrimination task, and (bottom) degree with which neural activity in each region correlates with different parts of the decision process, over the course of the trial. The final column shows data from the response period. The x-axis of each plot shows the impact of the frequency of the first stimulus (f1) on neural firing rates, and the y-axis shows the impact of f2. Green dots show neurons with significant f1 effects only, red dots neurons with significant f2 effects only. Blue dots show neurons more sensitive to both f1 and f2 but in opposite directions. Black dots show neurons responding to f1 and f2, but with significantly different sensitivity to f1 than f2, or vice versa. S1 and S2 = primary and secondary somatosensory cortex contralateral to the hand receiving vibrotactile stimulation, PFC = prefrontal cortex, VPC = ventral PFC, MPC = medial PFC, DPC = dorsal premotor cortex, M1 = primary motor cortex contralateral to the response hand. From Hernández et al (2010).

The apparent homogeneity of decision-related encoding across the somatosensory and prefrontal cortices in the work of Romo, Hernández and others belies that much is known about the roles of these regions in domains including arbitrary rules and conditional associations, working memory, cognitive control, error monitoring, and learning (Miller & Cohen, 2001; Wallis & Kennerley, 2010; Wise & Murray, 2000). However, the data of Hernández et al (2010) strikingly highlights the difficulty in isolating specific anatomical regions that may mediate decision integration in simple decision accumulation tasks, particularly given that most previous studies have reported data only from one or two brain regions (Kim & Shadlen, 1999). This difficulty is further apparent in studies attempting to identify the distinct contributions parietal and frontal regions may make to decision processes. In general, parietal cortex is most strongly associated with sensorimotor integration processes and transformations between multiple spatial reference frames, frontal regions are more associated with maintenance of task sets, and premotor/motor regions associated with planning and execution of motor responses (Buneo et al., 2002; Cisek & Kalaska, 2010; Wise & Murray, 2000). However, these differences are often not absolute, but are reflected in quantitative differences in the numbers of neurons sensitive to visual, attentional and intentional aspects of processing, or the duration over which visual versus motor signals persist (Coe et al., 2002; Crammond & Kalaska, 1996; Paré & Wurtz, 2001; Ratcliff et al., 2003a). Attempts to delineate functional differences on the basis of the temporal order of parietal and frontal activations have been a further topic of debate. Although a number of studies have reported that spatially-specific target activity in the eye fields and premotor cortex precedes parietal activity (Coe et al., 2002; Kalaska & Crammond, 1995; Pesaran et al., 2008; Westendorff et al., 2010), different results have been reported across studies (Buschman & Miller, 2007). One suggestion is that the temporal order of frontal and parietal activation associated with visual analysis and response planning depends

on task demands, with frontal activity being sensitive to target locations before parietal locations when visual analysis is complex or when target locations are determined by working memory (or other high level representations), and parietal activity potentially preceding frontal activity when target locations are of high visual salience (Bullier, 2001; Buschman & Miller, 2007; Cisek, 2007; Cisek & Kalaska, 2010) (see also Westendorff et al., 2010). It should be noted that many of the studies comparing parietal and frontal activations have required identification of visual targets followed by a saccade to the same location. Whilst some of the temporal differences reported are generally consistent with the notion that the eye fields are higher in a visual/attentional control hierarchy than the parietal cortex, they therefore do not dissociate between attentional selection and saccade planning sufficiently to justify the conclusion that *decision making* about an upcoming action occurred earlier in the FEF than parietal cortex. Greater clarity on this issue may be provided by a study comparing LIP, PRR and FEF activity when central visual cues instructed whether monkeys should saccade or reach to a single peripheral target (Lawrence & Snyder, 2006). Although visual transients to cues were observed earlier in the FEF than LIP and earlier in LIP than PRR, effector-specific signals were observed at similar latencies in LIP and PRR, and considerably earlier (~100 ms) than they were found in the FEF. Similarly, during reach/antireach tasks, neural activity in dorsal premotor cortex reflects the spatial location of a stimulus before the movement direction it instructs (Cisek & Kalaska, 2010). This suggests that parietal regions may play an earlier role in the neural processes guiding selection of responses than the FEF, and highlights the need for additional studies that distinguish between spatially specific attentional and intentional neural signals.

It is possible that a central decision-making circuit exists at or between several of the regions discussed so far, and that the output of this is continuously projected throughout other

regions, including the motor system, to allow constant biasing and preparation of motor states (Shadlen et al., 2008). On the other hand, decisions may be made over distributed networks, perhaps emerging as the result of co-ordinated inter-areal interactions (Pesaran et al., 2008) or as the result of computations that may be performed in any one of a number of brain regions (Cisek & Kalaska, 2010). Indeed, if one considers the generic nature of the neural processes which computational neuroscientists suggest may underlie accumulative decision making – namely, competitive processes between neuronal populations displaying persistent activity (Wang, 2002) – this functionality may be achieved across a wide range of frontoparietal and motor circuits (Cisek & Kalaska, 2010).

1.5. Integration of Evidence in the Human Parietal and Prefrontal Lobes

Although a great deal of similarities exist between the brains of macaques and humans (Astafiev et al., 2003; Mars et al., 2011), the frontal lobe and intraparietal sulcus are greatly expanded in humans compared to the macaque (Orban et al., 2004; Van Essen et al., 2001). These structural differences highlight the potential for functional differences between these two species. It has thus been important for investigations with human participants to investigate whether parietal, frontal and motor regions implicated by monkey electrophysiology also show dynamics consistent with accumulator decision processes in the human brain. This section overviews these studies and challenges in their interpretation, many of which arise due to the low temporal resolution of the haemodynamic responses measured by fMRI methods.

Similar to the macaque, human parietal cortex is also unequivocally implicated in perceptual processing, attentional control and motor planning. For example, human posterior parietal regions proximal to the IPS are sensitive to the spatial location of both visual targets

and hand positions in eye-centred co-ordinates (Beurze et al., 2007; Beurze et al., 2010; Medendorp et al., 2008; Medendorp et al., 2003) (see also Pertzov et al., 2011). Consistent with the distinction between macaque areas LIP and MIP, distinct regions along the banks of the human IPS show movement-related preparatory activity that is strongest contralateral to the movement target, and is more medial in location for reach preparation than saccade preparation, though there is also considerable overlap in the regions activated when saccades and reaches are planned (Astafiev et al., 2003; Beurze et al., 2009; de Lange et al., 2005; Filimon, 2010; Grefkes & Fink, 2005; Grefkes et al., 2004; Lindner et al., 2010; Mars et al., 2011; Medendorp et al., 2005; Medendorp et al., 2003; Sereno et al., 2001; Tosoni et al., 2008; Van Der Werf et al., 2009; Van Der Werf et al., 2008, 2010). Intraparietal regions and area 5 are also activated during motor planning, motor execution, and motor imagery (de Lange et al., 2005; Jeannerod & Frak, 1999; Wolbers et al., 2003), and parietal stimulation can trigger a strong intention to make movements, or even the belief that a movement had already been made (Desmurget et al., 2009). Together with the FEF, human posterior parietal cortex is also a key structure in exerting top-down control involved in the allocation of visuospatial attention (Capotosto et al., 2009; Corbetta & Shulman, 2002; Kastner et al., 1999; Kastner & Ungerleider, 2000; Nobre, 2001; Nobre et al., 1997; Yantis et al., 2002). Although neuroimaging studies have frequently reported bilateral parietal activations associated with attentional control and motor preparation, lesion and TMS studies have most strongly implicated a causal role of right-hemisphere regions in controlling attention (Capotosto et al., 2009; Chambers et al., 2007; Chambers et al., 2004a; Chambers et al., 2004b; Chao et al., 2011; Fuggetta et al., 2006; Heinen et al., 2011; Hodsoll et al., 2009; Hung et al., 2005; Mattingley et al., 1998; Mesulam, 1981; Müri et al., 2002; Rushworth et al., 2001a; Rushworth et al., 2003; Sack et al., 2007; Schenkluhn et al., 2008; Taylor et al., 2007; Vallar & Perani, 1986), whereas a dominant role of the left hemisphere has been

suggested in motor planning (Bunge et al., 2002; Cotti et al., 2011; Hesse et al., 2006; Króliczak & Frey, 2009; Mesulam, 1981; Mochizuki et al., 2005; Oliveira et al., 2010; Rushworth et al., 2001a; Rushworth et al., 2003; Rushworth et al., 2001b; Rushworth et al., 1997; Schluter et al., 2001; Schluter et al., 1998; Schluter et al., 1999).

An important study by Tosoni and colleagues (2008) more specifically addressed the neural regions that may carry out decision accumulation processes. Human participants made either pointing of saccadic responses based on discrimination judgements about noisy visual stimuli. Visual stimuli were carefully titrated to cover the full range of each subject's psychometric function, allowing investigation of haemodynamic responses as a function of decision difficulty and the response modality supported by the decision. Long trials of fixed duration were used to allow separation of decision making from the motor response stages of the task. To investigate how parietal and prefrontal areas involved in planning effector-specific responses were activated during decision making, analysis focussed on parietal and frontal regions of interest showing effector-specific preparatory activity, as identified in independent localiser scans. Consistent with saccade- and reach-specific planning activity reported in monkey parietal cortex and identified in the human brain in other neuroimaging studies (Bunge et al., 2002; Fernandez-Ruiz et al., 2007; Filimon, 2010; Grefkes & Fink, 2005; Mars et al., 2011; Rushworth et al., 2001a; Rushworth et al., 2001c; Van Der Werf et al., 2009; Van Der Werf et al., 2008, 2010), the localisers demonstrated that distinct frontal regions and parietal regions along the IPS showed effector-specific preparatory activity. In the decision task, the same regions showed parametric positive correlations between BOLD signal strength and sensory evidence in favour of the relevant effector. As in macaque LIP recordings, activity in each region was further reduced when evidence favoured the non-preferred response modality. Consistent with the idea that decisions were made soon after

stimulus presentation and subsequently gave way to categorical motor planning, parametric effects of stimulus strength were not found in BOLD responses around the time of motor execution. In contrast to the single-unit macaque recordings of Kim and Shadlen (1999), Tosoni and colleagues found no positive correlations between decision evidence and PFC BOLD responses. However, a number of regions showed negative effector-independent BOLD modulation by decision evidence, including the ventral and lateral PFC, bilateral insula, pre-SMA (pre-supplemental motor area), anterior cingulate cortex (ACC) and bilateral IPS. This relationship was argued to reflect greater activation due to increased attentional load rather than decision accumulation processes. In summary, these data place regions along the human IPS at an intermediate point between visual and motor codes in a manner that is highly concordant with monkey electrophysiological recordings (Tosoni et al., 2008).

Stimulation of human parietal structures along the intraparietal sulcus and in the superior parietal lobe can also affect motor parameters associated with expression of choice, such as accuracy and endpoint variability in saccades and reaches, and movement times (Davare et al., 2011; Striemer et al., 2011; Vesia et al., 2010; Vesia et al., 2008). Furthermore, when human participants complete a task involving speeded reaching movements to visual targets using a hand of their choice, TMS stimulation of a left hemisphere posterior intraparietal site just after target appearance can bias hand choice towards the ipsilateral hand, consistent with induction of a bias in hand preference or motor attention, or disrupted planning of a contralateral reach (Oliveira et al., 2010). Together, these TMS studies provide evidence for a causal role of the human parietal cortex in the generation and execution of motor plans, though it is equivocal how these results relate to the behavioural tasks more commonly used in the decision making literature. For example, in the experiment by Oliveira and colleagues (2010), participants were instructed to initiate

reaching movements as quickly as possible, but left- or right-hand choices could never be considered categorically 'wrong'. TMS may therefore have biased hand use preference without affecting decision making, or slowed contralateral hand responses, making ipsilateral reaches faster and thus more preferable. Thus, it remains unclear whether the human intraparietal cortex is causally involved in evidence integration processes.

An influential fMRI study by Heekeren and colleagues (2004) required human participants to discriminate whether noisy visual stimuli contained faces or houses, but did not provide participants with information about the mapping between decision outcomes and responses until after the decision stage of their task. Their fMRI analysis identified regions satisfying two key requirements. First, decision areas were identified as those regions showing activity increases when evidence was greatest and decisions easy. Second, it was required that activity in decision regions co-varied with BOLD differences in the fusiform face area and parahippocampal place area, which encode each stimulus category, on a trial-by-trial manner. The conjunction of these requirements was met only by a region in the left dorsolateral PFC (DLPFC) near the superior frontal sulcus (SFS), suggesting it supports the integration of perceptual evidence in decision making (Heekeren et al., 2004). Intraparietal and FEF activations were also found, but these exhibited greater activity on difficult trials. The authors interpreted these latter effects as evidence for increased attentional orienting when decisions are difficult rather than a signature of decision accumulation processes. Overall, these results thus suggest a role of the PFC in both human and monkey decision making, though they do not clarify whether the PFC's role is specific to situations in which decision-response mappings are unknown at the time of the decision (Rorie & Newsome, 2005). When decision-response mappings are known, however, parietal activations have been found, regardless of the response modality. For example, in a subsequent study by Heekeren

and colleagues, in alternating blocks human participants indicated their decisions using saccades or button presses (Heekeren et al., 2006). fMRI results showed a near-identical effect of stimulus visibility in the DLPFC as their earlier study, in addition to several other regions including the left intraparietal sulcus, posterior cingulate and fusiform/parahippocampal gyrus. Decision difficulty-related effects on left DLPFC activity have also been reported in the context of a somatosensory discrimination task (Pleger et al., 2006). Evidence for a causal role of the PFC in decision making is further provided by a recent TMS study that delivered inhibitory 1-Hz repetitive TMS (rTMS) to the left DLPFC (Philiastides et al., 2011). Both the accuracy and reaction times of decisions were impaired immediately after stimulation, but not before stimulation or after participants recovered from the effects of stimulation. Fitting the drift-diffusion model to their data, rTMS-induced behavioural changes were described by a specific reduction in the model parameter reflecting the rate at which decision evidence is accumulated. Zanto and colleagues (2011) have also reported that rTMS to the inferior frontal junction (IFJ) disrupted accuracy for colour discrimination when participants performed a match-to-sample task. Analysis of alpha-band phase coherence between frontal and posterior regions in post-rTMS electroencephalographic (EEG) recordings suggest this effect was driven by disruption of top-down control of visual processing, leading to reduced quality in working memory traces (Zanto et al., 2011). Together, these studies further highlight that motor systems may be downstream of higher-level cortical regions that implement decision-making processes. However, they may also be interpreted as evidence that the PFC plays an important role in the maintenance of working memory traces for decision-relevant quantities (Bechara et al., 1998; Curtis & Lee, 2010) and/or in exerting top-down control over sensory regions providing perceptual input to decisions (Rahnev et al., 2011). Current data thus provide causal evidence for a role of the

PFC in decision making but are agnostic about whether the PFC implements any kind of decision comparison processes.

While the above studies suggest similarities in the neural circuits underpinning monkey and human decision making, it is important to note two other features of these results. First, the regions implicated by Heekeren et al (2004, 2006) are parts of the default mode network, in which activity is typically suppressed during goal directed behaviour and during difficult or attentionally-demanding tasks (Raichle et al., 2001; Raichle & Snyder, 2007; Shulman et al., 1997). Indeed, several studies examining the time course of activity in these regions found that difficult decisions were associated with parametric decreases in BOLD responses compared to baseline activity, presumably a result of stronger or longer-lasting deactivations when decisions were difficult (Ho et al., 2009; Tosoni et al., 2008). Such deactivations do not readily accord with monkey single-unit findings of parametric evidence-related increases in neural activity compared to pre-stimulus baseline levels (Kim & Shadlen, 1999; Shadlen & Newsome, 1996; Yang & Shadlen, 2007).

A second point of contention in human decision-making fMRI research revolves around a more fundamental difficulty in translating single-unit decision-making findings into predictions about BOLD signals, which reflect the summed activity levels of many neurons over several cubic millimetres of cortex with a temporal resolution in the order of seconds. The inferences made in the human decision-making and neuroimaging studies of Tosoni and colleagues and Heekeren and colleagues relied on the assumption that BOLD responses due to decision processes should be largest when decision evidence is strongest. Although consistent with monkey data showing stronger single-unit activity when decisions are easy (Kim & Shadlen, 1999; Shadlen & Newsome, 1996; Yang & Shadlen, 2007), other investigators have suggested that careful consideration of the time-course of decision

processes results in an opposite predicted relationship between decision difficulty effects and BOLD responses in accumulator regions of the brain (Binder et al., 2004; Ho et al., 2009; Kayser et al., 2010a; Kayser et al., 2010b; Noppeney et al., 2010; Thielscher & Pessoa, 2007). These investigators have reasoned that BOLD correlates of decision processes should not merely reflect the strength of sensory information or the rate at which it is accumulated, but the integral of accumulator activity over the entire time over which a decision process occurs. Since accumulation processes take less time to hit an evidence threshold when evidence is strong, this leads to the prediction that easy decision accumulation processes should result in smaller BOLD responses compared with difficult ones. It should be noted that this prediction specifically relates to BOLD correlates of a decision accumulation period, and presumably of overall BOLD signal strengths when participants are instructed to respond as soon as they have made a decision. However, when tasks include a delay period between decisions and motor execution, this pattern may be expected to partially or completely reverse. When macaque decision tasks include such delays, firing rates in neurons carrying decision signals appear to accumulate until reaching a plateau level that is maintained during the delay period, and putatively reflects that the decision threshold has been crossed (e.g., Kim & Shadlen, 1999). Imposing a delay between decisions and responses could result in neurons spending longer in such a plateau state, with relatively high firing rates, following easy compared with difficult decisions. Thus, delay periods may result in a higher overall BOLD signal between the start of the decision and the response for easy compared with difficult decisions, but this effect would be driven by the maintenance of post-decision categorical motor planning rather than the metabolic needs associated with accumulation processes. As the task used by Tosoni and colleagues (2008) imposed a 10.5 second delay period between decisions and responses, the effects they report may have reflected motoric maintenance, and do not provide conclusive evidence for accumulator dynamics in the human

parietal cortex (Ho et al., 2009). It should be noted, however, that the decision process-BOLD predictions discussed above are somewhat speculative as prediction of BOLD responses requires knowledge of population level responses during decision making and delay periods. In contrast, most decision studies have not quantitatively compared firing rates between decision and delay periods of tasks, and have only reported single-unit firing rate data for a carefully selected subset of the neurons that could be isolated (e.g., Kim & Shadlen, 1999; Roitman & Shadlen, 2002; see also Kayser et al., 2010). Several studies, however, suggest there is considerable heterogeneity in delay-period activity between distinct sets of decision-making neurons across time. In particular, some neurons seem to fire around the time sensory signals providing evidence are observed, some show sustained delay-period firing, and others have firing rates that decline during delay periods but strongly reflect decision evidence towards the anticipated end of delay periods, when further decision-evaluation or motor responses are required (Barak et al., 2010; Bennur & Gold, 2011; Hernández et al., 2010; Hernández et al., 2002; Jun et al., 2010; Lemus et al., 2007; Martínez-García et al., 2011; Romo & Salinas, 2003).

A difficulty of predicting a negative correlation between decision accumulation processes and BOLD responses is that it makes it difficult to distinguish between effector-independent decision-related and attentional signals, as both would be expected to increase parametrically with decision difficulty. Ho and colleagues have attempted to overcome this issue using fMRI data from a carefully controlled four-alternative RDM decision task involving alternating saccadic and manual response modalities, and carefully controlled stimuli that ensured that decision evidence changes were never accompanied by sensory stimulation changes (Ho et al., 2009). Importantly, participants were able to respond as soon as their decision was made, allowing the assumption that BOLD activity was uncontaminated

by delay period response maintenance effects. Fitting of the linear ballistic accumulator model, which has many similarities to the Ratcliff diffusion model, suggested that task manipulations were effective in equating difficulty levels and decision thresholds across response modalities. To distinguish between parametrically varying attentional and decision-related neural activity, Ho and colleagues suggest that while attentional allocation should be maintained from the beginning of a decision period, decision-related ramping activity should be delayed for difficult compared with easy decisions, resulting in a small temporal delay in the latency of the early BOLD signal 'dip'. Results showed parametric modality-independent increases in the BOLD signal with decision difficulty across wide cortical networks including the right insula, intraparietal sulcus, medial and inferior frontal cortex and temporal parietal junction. Decision difficulty and onset delays were also found in the intraparietal sulcus for saccades, and in the contralateral central sulcus for manual responses, providing evidence for effector-dependent decision signals in these regions. However, only the right insula also showed a decision difficulty-related BOLD onset delay regardless of response modality, suggesting it may have a modality-independent role in decision integration.

Convergent support for insular involvement in decision making comes from several studies which demonstrated parametric increases in BOLD responses in the insula, as well as along the intraparietal sulcus and in premotor regions, when decision uncertainty was high (Grinband et al., 2006; Huettel, 2006; Huettel et al., 2005). Intriguingly, one study reported correlates of perceptual categorisation uncertainty in a fronto-striatal-thalamic network including the anterior insula, but did not observe any such effects in attentional networks including the frontal eye fields and intraparietal sulcus (Grinband et al., 2006). Insula activation appears to be specifically related to uncertainty about the appropriate behavioural response to make, and is not elicited by uncertainty about whether reward will be received

(Huettel, 2006). Insular activation has also been linked with difficulty of perceptual decision making in several other studies (Binder et al., 2004; Kayser et al., 2010a; Pessoa & Padmala, 2005, 2007; Pleger et al., 2006; Ploran et al., 2007; Thielscher & Pessoa, 2007), though these findings have not always been consistent. In contrast to the data of Ho and colleagues, one study reported greater insular activation when decisions were easy (Pleger et al., 2006), and another found phasic insular activations only at the end of a decision process (Ploran et al., 2007). Additionally, insular activation was not found in a task that allowed participants to avoid erroneous choices by declining to make a decision when they were uncertain, consistent with the idea these insula activations may have been related to anticipation of errors (Stern et al., 2010). As insula activation is also observed across a much wider range of contexts than decision studies, including even cigarette craving and maternal love, it has been suggested to reflect more generally the salience of items of which participants are currently aware of rather than decision integration processes per se (Craig, 2009). Whether or not the insula plays a causal role in guiding decision processes awaits empirical testing.

Human studies discussed so far provide convergent support for roles of a number of intraparietal and frontal regions in decision making that are highly comparable with monkey studies. However, such results have relied on carefully constructed but highly controversial models of the relationship between decision processes and BOLD responses. Further, the constraints on the temporal and spatial resolution of fMRI have prohibited direct observation of many of the key characteristics of monkey single-unit recordings suggesting the encoding an internal decision variable, such as sensory evidence strength-dependent changes in the rate at which accumulator neurons increase their firing rates. The high temporal resolution offered by non-invasive electrophysiological recording techniques, such as electroencephalography (EEG) and magnetoencephalography (MEG), make them ideal candidates for exploring

decision accumulation processes. However, few studies have attempted to investigate decision accumulation using these methods (Bankó et al., 2011; de Lange et al., 2010; Philiastides et al., 2006; Ratcliff et al., 2009). de Lange and colleagues (2010) presented a rapid stream of left or right arrows to participants, whom at the end of the trial were required to indicate whether the majority of arrows favoured a left or right response overall. Although this study did not reveal direct evidence for accumulator dynamics in the brain, a key finding of their MEG recordings was that when evidence was high, stimulus-evoked activity at parietal and central sensors was inversely related to the amount of accumulated evidence, suggesting attenuation of neural activity for new stimuli. This suggests top-down suppression of new sensory information when evidence was high, or similarly, that central and parietal activity evoked by sensory stimuli may be up-regulated under conditions of decision uncertainty.

Monkey data described in Section 1.4 suggest decisions affect the temporal evolution of neural activity even in effector-specific motor structures such as the superior colliculus. Similar to parietal cortex, human pre-motor and primary motor cortices are activated during motor planning and imagery, as evidenced by both neuroimaging (de Lange et al., 2005; Ehrsson et al., 2003; Guillot et al., 2009; Jeannerod & Frak, 1999; Mars et al., 2008a; Michelon et al., 2006; Porro et al., 1996; Roth et al., 1996) and lesion work (Tomasino et al., 2010). Compared with fMRI, EEG measures can reveal how preparatory motor processes evolve in the foreperiod before an instructed movement with superior temporal resolution. The 'contingent negative variation' (CNV) is a negative electrical potential that develops progressively during the foreperiod over parietal, central and frontal electrodes (Walter et al., 1964). It has been linked to both motoric and non-motor preparation, and is thought to be generated by bilateral parietal and frontal structures as well as the ACC, and supplemental

motor area (SMA) (Gomez et al., 2001; Gomez et al., 2003), though other subcortical structures including the insula and basal ganglia may also contribute to its generation (Nagai et al., 2004). The CNV is sensitive to the amount of information provided about an upcoming response, being greater in magnitude when additional movement parameters (such as the hand of response, direction and force) are specified (MacKay & Bonnet, 1990; Ulrich et al., 1998; Vidal et al., 1995). Prior to response onset, the CNV becomes asymmetric, with greater negativity contralateral to the responding hand. This asymmetry is known as the 'lateralized readiness potential' (LRP). The LRP is thought to be primarily generated in M1, and is considered to provide a measure of lateralized motor preparation (Gratton et al., 1988; Leuthold et al., 2004). An experiment by Scheibe and colleagues (2009) investigated what aspects of motor preparation are indexed by the CNV and LRP. On each trial, participants made magnitude discrimination judgments between two consecutively presented numbers. As the number stimuli were all single-digit, the identity of the first number provided parametrically varying information about which response was more probable. Behavioural reaction times and onset latencies of the LRP were modulated by this prior probability manipulation, but did not modulate the LRP amplitude, consistent with earlier data suggesting that the LRP only emerges once response hand selection is complete and response programming commences (Masaki et al., 2004). However, the amplitude of the CNV was parametrically modulated by the prior probability manipulation, suggesting that some premotor preparatory processes may have scaled with prior knowledge (Scheibe et al., 2009). A subsequent concurrent EEG-fMRI experiment identified a site in posterior medial frontal cortex as being sensitive to the same prior knowledge manipulation, however trial-to-trial variability in the CNV could be related to activity in a broader set of regions including the DLPFC, inferior parietal sites near the IPS, and the inferior frontal gyrus (Scheibe et al., 2010).

It has been suggested that slow negative potentials like the CNV and LRP may result from excitatory post-synaptic potentials at the apical dendrites of pyramidal neurons (Brunia, 1993). Consistent with this notion and the topographical foci of these potentials over central motor regions, response expectancy also impacts upon corticospinal excitability. In monkeys, pre-movement modulation of the excitability of spinal interneurons has been reported in the absence of afferent input changes. Excitatory changes specific to the prepared movement occur simultaneous with global inhibition that supresses muscular activity (Prut & Fetz, 1999). Spinal modulation of this nature may be generally important for planning and preparing movements (Bizzi et al., 2000). Task-related modulation of instantaneous corticospinal excitability can be probed in humans by applying TMS pulses to the relevant region of primary motor cortex – typically the hand region - and measuring the amplitudes of the resulting motor-evoked potential (MEP) in contralateral muscles – typically the contralateral hand. Corticospinal excitability selectively increases in the prime mover – the relevant muscle group – contralateral to a prepared movement, and decreases ipsilaterally and for other muscle groups. This effect appears to be specific to motor preparation, as it does not reflect sensory maintenance or attentional allocation (Mars et al., 2007; van den Hurk et al., 2007; van Elswijk et al., 2007). Corticospinal excitability in primary motor cortex is very specifically modulated by prior knowledge about the likelihood of upcoming responses. This was elegantly demonstrated by a study in which a sequentially presented series of cues provided probabilistic evidence about whether a subsequent imperative stimulus would instruct a right-handed button press using the thumb or the little finger (Bestmann et al., 2008a). As in previous studies, MEP amplitudes were affected by cues in a muscle-specific manner. However, Bestmann and colleagues could demonstrate that MEP amplitudes also varied parametrically with the strength of the expectation about the upcoming response, being higher when the prior evidence favoured that response. MEPs were also inversely related to

the degree of surprise at observing the cue stimulus. Thus, it appears that motor output is very flexibly shaped by contextual probabilities that are dynamically updated following observation of new information. Intriguingly, the specific and behaviourally adaptive corticospinal modulations reported by Bestmann and colleagues contrast with the insensitivity of LRP amplitudes to response probability information (Scheibe et al., 2009), suggesting the LRP reflects a relatively late stage of response preparation or execution. Speculatively, this dissociation may relate to the dual nature of corticospinal modulation observed in the monkey spinal cord (e.g., Prut & Fetz, 1999). TMS-related corticospinal excitability changes may reflect potentially fine-grained preparatory excitability modulation, whereas the LRP onset indicates when more global inhibitory suppression of a muscle group is removed.

1.6. Neural Oscillations

Synchronous and rhythmic electrical activity fluctuations in large populations of neurons can result in oscillations in local field potentials, EEG and MEG signals. Although ~10 and ~20 Hz oscillations were readily apparent even in the first electrical recordings of brain activity by Hans Berger (Berger, 1929), an emphasis by neuroscientists on rate coding information transmission schemes throughout most of the last century led to comparatively few investigations into the neurobiological basis and functional role of brain oscillations (Singer, 1993). Though the mechanisms underlying the generation of neural oscillations are still unclear, recent research has begun to reverse this trend by investigating the functional role of oscillations in normal cognitive functioning, and clinical correlates of abnormal oscillatory activity (Brown, 2006; Hari & Salmelin, 1997; Jensen et al., 2011; Singer, 1993; Uhlhaas & Singer, 2006, 2010). Rapid progress is also being made in understanding how

pacemaker cells, intrinsic cellular properties, and network architecture may contribute to a variety of neural oscillatory phenomenon that facilitate precise co-ordination of local and network-level neural communication with a relatively low energy cost (Buzsaki & Draguhn, 2004; Wang, 2010).

Neural oscillations are typically classified according to their frequency. Although the boundaries between frequency bands tend to vary between studies, in general researchers have focussed on five major frequency bands: delta (0.5 – 4 Hz), theta (4 – 7 Hz), alpha (8 - 14 Hz), beta (15 – 35 Hz) and gamma (>30 Hz, but most typically 40 – 80 Hz). At a functional level, lower frequency oscillations such as those in the delta bands have typically been associated with inter-areal communication, memory, and top-down control (Lakatos et al., 2008; Singer, 1993; Uhlhaas & Singer, 2010). They are thought to reflect synchronized modulation in excitability that occur over relatively large spatial scales in the brain, providing discrete windows during which network communication is facilitated. Through cross-frequency coupling, they may play an important role in organising higher-frequency oscillatory activity (Canolty & Knight, 2010). High frequency gamma-band activity is thought to be primarily generated through local network interactions, mainly due to phasic shunting inhibition from GABAergic basket cell interneuron populations, which rhythmically inhibits local excitatory activity (Fries, 2009). By concentrating local population spike activity within a small temporal window, local gamma-band synchronization can increase the chance that inputs will arrive at postsynaptic neurons within the short time window necessary for temporal summation to occur. Furthermore, if neural inputs are received in-phase with the high-excitability phase of local gamma band oscillations, which appears to be one consequence of selective visual attention under attentional control (Fries et al., 2001; Gregoriou et al., 2009), this can lead to powerful rhythmic input gain modulation (Fries,

2009; Salinas & Sejnowski, 2001). The amplitude of gamma-band activity recorded in MEG and EEG is therefore typically associated with elevated processing activity in the underlying cortical region (Niessing et al., 2005).

1.6.1. Alpha-Band Oscillations and Visual Attention

Although first described in scalp EEG recordings by Hans Berger (1929), ~10 Hertz alpha oscillations were not widely accepted as being of neural origin until Adrian and Matthews (1934) confirmed the presence of alpha oscillations in recordings in animals and systematically investigated their properties. In contrast to event-related potentials (ERPs), which typically require averaging over tens or hundreds of trials for reliable estimates to be made, alpha oscillations are readily visible in raw EEG traces, particularly over parieto-occipital regions. Alpha power is typically inversely related to visual arousal levels, being strongest when the eyes are closed or participants are drowsy or inattentive, and lowest when the eyes are open and participants are engaged in a visual task. Intriguingly, they are also absent in blind patients (Adrian & Matthews, 1934). Subsequent to Adrian and Matthews' work, alpha oscillations became widely regarded as an epiphenomenon of brain activity, merely reflecting that the brain is in an 'idling' state when the eyes are closed.

The last twenty years have seen a resurgence of interest in how alpha oscillations vary during cognition, particularly in the context of attention, movement and working-memory tasks. It is increasingly accepted that they actively shape cognitive processing (Foxe & Snyder, 2011; Hari & Salmelin, 1997; Palva & Palva, 2007; Pfurtscheller & Lopes da Silva, 1999). Occipito-parietal alpha power is suppressed when attention is allocated to the visual compared with auditory modality (Foxe et al., 1998). Supporting a much more specific role for alpha than might be expected under the 'idling' view, covert allocation of visual attention

results in lateralized modulation of alpha activity approximately 400 – 700 ms after the appearance of an attentional cue. Alpha activity is attenuated in the hemisphere contralateral to the cued side of space, and alpha synchronization increases ipsilateral to attention (Worden et al., 2000). Compellingly, these effects are highly topographically specific to the attended spatial location (Rihs et al., 2007). Furthermore, inter-individual differences and random fluctuations in alpha power predict the efficacy of TMS in eliciting visual phosphenes (Romei et al., 2008a; Romei et al., 2008b), and small changes in alpha lateralization just before onset of targets are predictive of behavioural accuracy and reaction times on detection and discrimination tasks (Kelly et al., 2009; Thut et al., 2006; Van Dijk et al., 2008). Alpha-band effects are not just observed when *visual* attention is allocated. Spatially- and temporally-specific alpha modulation can also be observed in somatosensory cortex in the context of somatosensory discrimination tasks (Haegens et al., 2011a; Jones et al., 2010; van Ede et al., 2011; van Ede et al., 2010). Overall, such findings suggest the presence of alpha reflects inhibitory processes that help ensure that only task-relevant sensory activity affects perception and behaviour.

Providing strong evidence for an active role of alpha activity, recent TMS data suggest a causal role for alpha oscillations in visual perception. Stimulation of occipital and parietal sites resulted in a short-lived reduction of detection performance for contralateral targets and an increase in performance for ipsilateral targets (Romei et al., 2010). These effects were frequency-specific, only being found for 10-Hz TMS, and not following 5- or 20-Hz stimulation, consistent with the notion that TMS modulated behaviour by entraining the cortex at the stimulated frequency (Thut et al., 2011). Thus, alpha-band activity levels appear to *actively* shape the perceptual information that guides behavioural decisions (see also Chapter 3).

The mechanisms by which alpha oscillations are generated are only partially understood. ~10-Hz sleep spindles recorded in sleeping and anaesthetised animals are principally generated via the thalamus, and have often been compared to alpha-band phenomena recorded in humans (Hughes & Crunelli, 2005), though a number of differences between sleep spindles and cortical alpha cast doubt on this relationship (see Foxe & Snyder, 2011, for discussion of this point). Consistent with a role of alpha in attentional control, and the idea that attention may operate via gating of sensory activity at the level of the thalamus (LaBerge, 1997; McAlonan et al., 2008; Wilke et al., 2009), negative relationships have been observed between resting-state alpha-band activity and positron emission tomography (PET) and fMRI measures of thalamic and cortical metabolism (Becker et al., 2011; Goldman et al., 2002; Laufs et al., 2003a; Lindgren et al., 1999). Furthermore, thalamic lesions can disrupt bilateral occipito-parietal alpha activity (Hari et al., 1997; Makela et al., 1998). However, monkey LFP analysis has suggested that cortical areas V2, V4 and IT are also important generators of cortical alpha oscillations (Bollimunta et al., 2008; Buffalo et al., 2011). Furthermore, in a recent TMS-EEG study, stimulation of the right IPS or right FEF during the orienting period of a covert attention task disrupted normal patterns of alpha lateralization, and the magnitude of these effects correlated with TMS-induced deficits in behavioural performance (Capotosto et al., 2009). Thus, frontoparietal cortical attentional networks appear to be crucial for establishing attentional modulation of alpha oscillations in posterior visual regions. One suggestion is that global arousal modulation linked to sustained attention operates via thalamo-cortical modulation, while attentional modulation operates primarily via cortico-cortico alpha mechanisms (Dockree et al., 2007; Foxe & Snyder, 2011; O'Connell et al., 2009).

Despite the ubiquity of alpha oscillations in the brain, the functional and information-theoretic mechanisms by which of alpha modulation affects cortical information processing are still unclear. On one hand, synchronization of thalamic inputs to the alpha cycle may facilitate information processing, and it is unclear how cortical alpha reductions correspond to thalamic alpha activity (Lorincz et al., 2008; Lorincz et al., 2009). Another possibility is that attentionally mediated synchronization of noise correlations across populations of neurons may reduce the overall information-coding capacity, thereby reducing the efficacy of information transmitted to downstream decision regions. Comparison of spike correlations in simultaneous recordings from multiple V4 columns supports this latter notion, suggesting that attention-driven noise correlation reductions may impact behavioural performance to a much greater extent than firing-rate modulation (Cohen & Maunsell, 2009; Mitchell et al., 2009) (though see Britten et al., 1992; Gu et al., 2011; Poort & Roelfsema, 2009). Laminar analysis of noise correlations in areas V2 and V4 suggests that attention-driven noise correlation reductions in the alpha band may be specific to layer 2/3 neurons projecting to upstream processing regions (Buffalo et al., 2011).

1.6.2. Alpha-Band Oscillations – From Visual Attention to Motor Preparation

Alpha-band fluctuations can be observed across a variety of contexts other than attention, including motor preparation. Similar to attention, execution of unimanual movements results in desynchronization of alpha-band activity in central somatomotor regions that is strongest over the motor cortex contralateral to the upcoming movement, and varies topographically depending on the body part moved in a manner consistent with the somatotopic organization of the motor cortex (Crone et al., 1998b; Pfurtscheller & Berghold, 1989; Pfurtscheller et al., 2006; Pfurtscheller et al., 1997; Pineda, 2005). Movement-related

alpha desynchronization (sometimes called 'mu' activity) is observed up to several seconds before the movement (Nagamine et al., 1996), as well as when movements are imagined (McFarland et al., 2000; Neuper et al., 2006; Pfurtscheller et al., 2006; Schnitzler et al., 1997; Wolpaw et al., 2002). Compared with visually reactive alpha-band activity, movement-related ~10 Hz modulation often occurs at a slightly higher frequency, tends to be comparatively smaller in amplitude, and is less bilaterally coherent (Chatrian et al., 1959; Pineda, 2005; Schoppenhorst et al., 1980). Momentary alpha-band power over motor cortex is also inversely related to the likelihood that application of a TMS pulse to M1 will evoke a motor-evoked potential (Sauseng et al., 2009).

1.6.3. Beta-Band Oscillations and Motor Preparation

Beta-band activity (15 – 35 Hz) over somatomotor cortex undergoes a very similar desynchronization to the alpha band before movements and during motor imagery, and has low bilateral coherence (Andrew & Pfurtscheller, 1997, 1999; Crone et al., 1998b; de Lange et al., 2008; Leuthardt et al., 2004; McFarland et al., 2000). However, movement-related beta modulation is clearly distinct from movement-related alpha-band activity in several qualitative respects. Movement-related beta-band desynchronization typically begins slightly later than in the alpha band, and although they tend to co-occur, desynchronization in both frequency bands does not always co-occur (Jones et al., 2009; McFarland et al., 2000; Pineda, 2005; Salmelin & Hari, 1994b). This separability has resulted in somatomotor alpha and beta activity being useful as independent control signals in two-dimensional brain-computer interface systems (Wolpaw et al., 2002; Wolpaw & McFarland, 2004). Furthermore, beta-band activity undergoes a strong post-movement rebound contralateral to the movement that is not found in the alpha band. Although beta-band desynchronization is greatest contralateral

to an upcoming movement, peak beta desynchronization is typically found at EEG/MEG electrodes over the vertex (e.g., McFarland et al., 2000; Schoffelen et al., 2011). Source reconstructions and electrocorticographic (ECoG) data indicate that peri-movement modulation of both frequency bands occurs diffusely over somatomotor cortex, but with peak beta sources commonly localized to the posterior frontal lobe, superior and anterior to the peak alpha sources found in area 3b of the post-central gyrus (Jones et al., 2009; Miller et al., 2010; Salmelin & Hari, 1994a, 1994b). Because the alpha source is located in somatosensory cortex, some investigators have considered somatomotor alpha-band activity to be a signature of somatosensory processing and beta of somatomotor processing (Salmelin et al., 1995; Salmelin & Hari, 1994a). However, there is also evidence for involvement of ~10 Hz activity in organizing motor activity, potentially via rhythmic descending control of motoneuron pools via corticospinal neurons (Farmer, 1998; Hari & Salmelin, 1997; Vallbo & Wessberg, 1993). It is currently unclear why peri-movement somatomotor alpha- and beta-band activity is so broadly distributed in the cortex, in contrast to the focal and somatotopically organized gamma-band power increases seen in primary motor cortex in the same recordings (Miller et al., 2010). However, subtracting oscillatory beta-band responses to left and right responses typically produces much more focal effects over somatomotor cortex (e.g., de Lange et al., 2008), consistent with a specific role in preparatory motor processes. Furthermore, source reconstructions from the foreperiod of a simple reaction-time task suggest pre-movement beta-band modulations follow a similar time-course of evolution and topography to the CNV (Fischer et al., 2010). Transcranial alternating current stimulation (tACS) has been used to demonstrate the causal nature of beta-band activity, with imperceptible 20-Hz stimulation subtly reducing movement velocity changes during reaching movements (Pogosyan et al., 2009).

Investigations of corticomuscular coherence provide further strong evidence that beta modulation is linked to preparatory motor processes. In humans, the spatially specific beta desynchronization observed following response cuing is often accompanied by beta-band coherence between the cued hand and the contralateral motor cortex (Baker et al., 1997; Conway et al., 1995; Salenius et al., 1997; Schoffelen et al., 2008; van Wijk et al., 2009). In animals, similar beta coherence has also been demonstrated between the motor cortex, spinal cord, basal ganglia, and thalamus (see Schoffelen et al., 2008). Similarly, movement-related beta-band desynchronization may also be accompanied by gamma-band coherence between the cued hand and the contralateral motor cortex (Schoffelen et al., 2005; Schoffelen et al., 2011). Importantly, movement-related beta synchrony is not simply an artefact of actual movement. Although beta-band corticomuscular coherence does increase with response force (Chakarov et al., 2009), the latency of pre-movement beta desynchronization is not tightly coupled with muscle activity changes, suggesting beta reflects a more general aspect of motor preparation (Sanes & Donoghue, 1993). Furthermore, beta and alpha imagery effects can occur in the absence of any concurrent muscle activation (Vaughan et al., 1998; Wolpaw & McFarland, 2004), and task context can modulate beta-band corticomuscular phase coherence in the absence of any change in muscle force output (Kilner et al., 2000; Schoffelen et al., 2011). The time course and topography of peri-movement beta desynchronization is also similar to changes in corticospinal excitability (Leocani et al., 2001), and the amplitude of MEPs is a smooth cosine function of the beta phase in the stimulated muscle at the time of stimulation (van Elswijk et al., 2010). Together, these findings provide strong support for the idea that somatomotor beta-band activity modulation plays important roles in the generation of motor-unit synchronization underlying binding and movement preparation within the motor system (Conway et al., 1995; Farmer, 1998; Salenius et al., 1997).

1.6.4. Oscillatory Correlates of Decision Processes

Changes in oscillatory activity can be observed over a time course of tens or hundreds of milliseconds, providing substantially higher temporal resolution than neuroimaging methods such as fMRI. Several recent studies have exploited this advantage to assess oscillatory correlates of decision processes, and how neural activity evolves during decision periods (Donner & Siegel, 2011; Siegel et al., 2011). It should be noted that many of these findings were reported after the work presented in this thesis commenced.

Gamma-band activity in sensory cortex appears to index local sensory encoding during perceptual decision making. This has been demonstrated in an MEG study in which participants were presented with RDM stimuli of parametrically varying coherence levels. Gamma-band activity in area MT+ varied parametrically with the motion coherence (Siegel et al., 2007). The integral of MT+ activity is also closely tied with perceptual decision choices, consistent with the notion this gamma-band activity is accumulated by a downstream decision region (Donner et al., 2009).

Donner and colleagues (2009) further characterized whether the lateralization of oscillatory activity evolving in motor cortex displayed dynamics consistent with accumulator decision models in a clever MEG experiment. Participants completed a near-threshold yes/no motion detection task in with each response was associated with a different hand. An enforced delay period ensured responses were made after the period during which participants viewed the RDM stimulus and made their decisions, allowing analysis of oscillatory lateralization during decision making uncontaminated by response execution effects. The lateralization of beta- and gamma-band activity in motor and pre-motor cortex were increasingly strong predictors of participants' choices as time into the stimulus viewing

period increased, with beta-band activity showing contralateral desynchronization and/or ipsilateral synchronization relative to the upcoming response hand, and the opposite pattern for gamma-band activity. These findings held regardless of whether trials were hits or false alarms in the case of 'yes' responses, or correct rejections or misses in the case of 'no' responses. Two possible explanations for these results are that (1) oscillatory activity scaled *parametrically* with accumulated evidence on each trial, and (2) that oscillatory activity reflected *categorical* response preparation during the decision period, and was able to more accurately predict responses later in time simply because of the distribution of latencies over which decisions were made and categorical states entered into. To distinguish between these possibilities, estimates of accumulated decision evidence throughout the decision period were made by taking the integral of gamma-band activity in area MT+, and correlating these with momentary gamma- and beta-band lateralization from motor regions. Strong correlations were found in both cases. Critically, in the case of gamma-band activity, this correlation held regardless of the response made at the end of each trial, and so these results provide direct evidence that the build-up of gamma-band activity in motor regions continuously and parametrically reflects the output of a decision integration process. Unfortunately, this important final analysis was not reported for the beta band. In another recent study, as participants completed a mental imagery task, the amplitude of occipitoparietal gamma-band activity was negatively coupled on a trial-by-trial basis with beta-band activity amplitudes over motor cortex, again perhaps reflecting greater desynchronization as gamma-band activity in other cortical regions is integrated (de Lange et al., 2008).

In contrast to the aforementioned findings that beta-band activity decreases in contralateral motor cortex when a movement is planned, other data suggest that *increased* beta-band synchrony may be observed throughout decision-making networks during accurate

decision making. In a separate analysis of the RDM dataset discussed above, Donner and colleagues (2007) compared the whole-brain spectral profiles associated with correct and erroneous responses. On correct trials, beta-band activity was higher bilaterally along the IPS, bilaterally in the DLPFC, and in right-hemispheric motor cortex (Donner et al., 2007). These data were interpreted as providing evidence that inter-areal beta-band synchrony is a signature of long-range network interactions underlying integration of activity in sensory regions towards motor plans in this task. In contrast, gamma-band activity might be a signature of local processing (Donner & Siegel, 2011). Of course, it is difficult to distinguish the extent to which these effects reflect direct integration of evidence, as opposed to reflecting co-ordination of activity within frontoparietal networks involved in attentional control. Still, this idea perhaps explains the fact that peri-movement beta modulation is widely distributed across somatomotor cortex (Siegel et al., 2011). It is also consistent with computational modelling that suggests the beta frequency is better suited to synchronize activity over long distances in the brain than the gamma band (Kopell et al., 2000). Beta synchrony has also been associated with long-range network organization and sensorimotor integration across a variety of other human and monkey studies (Brovelli et al., 2004; Buneo et al., 2003; Buschman & Miller, 2007, 2009; Gross et al., 2004; Haegens et al., 2011b; Pesaran et al., 2008; Pesaran et al., 2002; Sehatpour et al., 2008; Spitzer et al., 2010; von Stein et al., 1999). For example, Pesaran and colleagues (2008) calculated spike-field coherence – which quantifies the ability of action potentials to predict LFPs in another region – from recordings taken from dorsal premotor cortex (PMd) and the parietal reach region whilst monkeys completed a free-choice saccade task. PMd-to-PRR spike-field coherence preceded PRR-to-PMd spike-field coherence by 30ms, which corresponds to half a 15-Hz beta-band cycle, consistent with the idea information was reverberating between these two regions at that frequency. Brovelli and colleagues (2004) also identified synchronous beta-

band networks across somatomotor and intraparietal regions as monkeys completed a visual discrimination task. An additional finding supporting a role for beta synchrony in dynamically organising network communication comes from an experiment where human participants viewed an ambiguous stimulus, where two moving lines could be perceived as either passing each other or colliding and bouncing off each other (Hipp et al., 2011). When participants perceive the stimulus as 'bouncing', beta synchrony was found to be higher across a network including bilateral frontal, parietal and sensory regions, but with right-hemispheric parietal cortex acting as a hub. At the single-trial level this allowed above-chance prediction of participants' subjective percepts. Rhythmic TMS at beta-band frequencies also has differential effects on global and local perceptual tasks. Potentially consistent with the idea that it promoted inter-areal interactions, rhythmic 20-Hz TMS of right-hemisphere parietal cortex reduced performance on a local, but not a global visual task (Romei et al., 2011). The opposite effect was found for theta-frequency (5-Hz) TMS delivery. However, it is unclear from these data whether the frequency-specific disruptive effects of stimulation reflect the frequencies that are task-relevant or task-irrelevant for the global versus local tasks, as the results do not clarify whether TMS affected behaviour by disrupting endogenous oscillations or inducing artificial ones.

1.7. Thesis Experiments

Previous experiments with human participants have implicated similar parietal and frontal regions in decision-integration processes to those identified by monkey electrophysiology. However, given the comparatively low temporal and spatial resolution of fMRI, it remains a challenge to distinguish decision-related neural activity from activity related to other factors, like attention. As these difficulties are unlikely to be resolved on the

basis of indirect arguments about the relationship between single-unit phenomena and BOLD changes, several avenues of research seem particularly likely to be fruitful in resolving these issues. First, one could directly resolve the debate via further single-unit studies and concurrent fMRI and single-unit studies as monkeys complete decision-making tasks. An alternative approach is to investigate human decision making using neuroimaging techniques with higher temporal resolution than fMRI. The present thesis adopts the latter approach. Two EEG (Chapters 3 and 4) and one concurrent EEG-TMS (Chapter 5) experimental datasets are presented, all of which investigate the oscillatory correlates of perceptual processes and motor preparation during human decision making, and the regions that causally contribute to decision making in the human brain.

The first experiment (Chapter 3) follows on from previous visual studies that have demonstrated that fine-grained differences in alpha-band power over parieto-occipital cortex are associated with graded differences in behavioural choice and reaction times. On the basis of previous studies it was unclear, however, whether such effects reflected random fluctuations in neural activity or are under top-down control. Chapter 3 therefore reports the results of an experiment that validated the use of oscillations as a parametric index of participants' preparatory states. Specifically, we investigated whether parametric variations in the lateralization of alpha (~8-14 Hz) oscillations recorded over occipito-parietal cortex would be flexibly modulated by graded differences in top-down attentional goals. When this work commenced, no previous studies had reported parametric beta-band modulations linked with motor parameters or decision certainty (Donner et al., 2009; Tzagarakis et al., 2010b). In preparation for the experiments presented in Chapters 4 and 5, a secondary goal of this experiment was therefore to investigate whether graded changes in alpha- and beta-band

activity recorded over the motor cortex can provide a parametric index of participants' preparatory motor states.

The aim of the second thesis experiment (Chapter 4) was to directly investigate whether the temporal dynamics of preparatory activity changes in human motor planning structures reflect encoding of a decision variable. A novel sequential decision integration task was adapted for use with humans, allowing investigation of whether the temporal evolution of alpha- and beta-band EEG activity may reflect the perception and integration of information for decision making. To investigate the brain regions causally contributing to decision-integration processes underlying behaviour in the experiment described in Chapter 4, we then adapted the decision-integration task for use with concurrent TMS-EEG (Chapter 5). Behavioural and neural effects of transiently disrupting a medial intraparietal region were investigated. We hoped that these efforts would provide important insights about how decision-accumulation processes evolve over time in the human brain, and elucidate the relevance of findings from monkey electrophysiological recordings and micro-stimulation studies in understanding the neural basis of human decision making.

Chapter 2 - Methods

This chapter reviews the principles underlying the methods used in this thesis to study brain activity: transcranial magnetic stimulation (TMS), electroencephalography (EEG) and combined online TMS-EEG. The chapter concludes with a brief discussion of why these techniques were chosen given the aims of this thesis.

2.1. Transcranial Magnetic Stimulation (TMS)

TMS operates according to Faraday's principle of electromagnetic induction. Passing an electric current through a primary coil produces a magnetic field with strength proportional to the stimulating current. This can result in induction of an electric field, and in turn an electric current, in a nearby secondary coil, the strength of which depends on the rate of change of the primary magnetic field. In the context of TMS, the primary coil is a TMS stimulation coil held over a participant's head, and the secondary coil is the brain (Figure 2-1). Thus, 'magnetic stimulation' is misleading in the sense that TMS does not involve direct neural stimulation, but involves induction of an electrical field that may, in turn, affect neural activity.

Although electromagnetic stimulation of the brain has a long history (reviewed in Walsh & Pascual-Leone, 2003), contemporary use of TMS did not begin until Anthony Barker and colleagues demonstrated that discharge of a magnetic pulse over the human visual cortex could result in induction of visual phosphenes (Barker et al., 1985a), and stimulation over the vertex could elicit visible hand movements accompanied by measurable changes in accompanying EMG activity (Barker et al., 1985b). Barker and colleagues also developed the

precursor to modern TMS systems, which generate magnetic pulses by discharging a large current (typically ~8 kA) from a capacitor into a stimulator coil. The induced secondary current strength depends on the rate of change of the current in the primary coil, which must have a very short rise time (100-200 μs) in order to induce a secondary current of sufficient intensity to stimulate cortical neurons (Walsh & Cowey, 2000) (Figure 2-1).

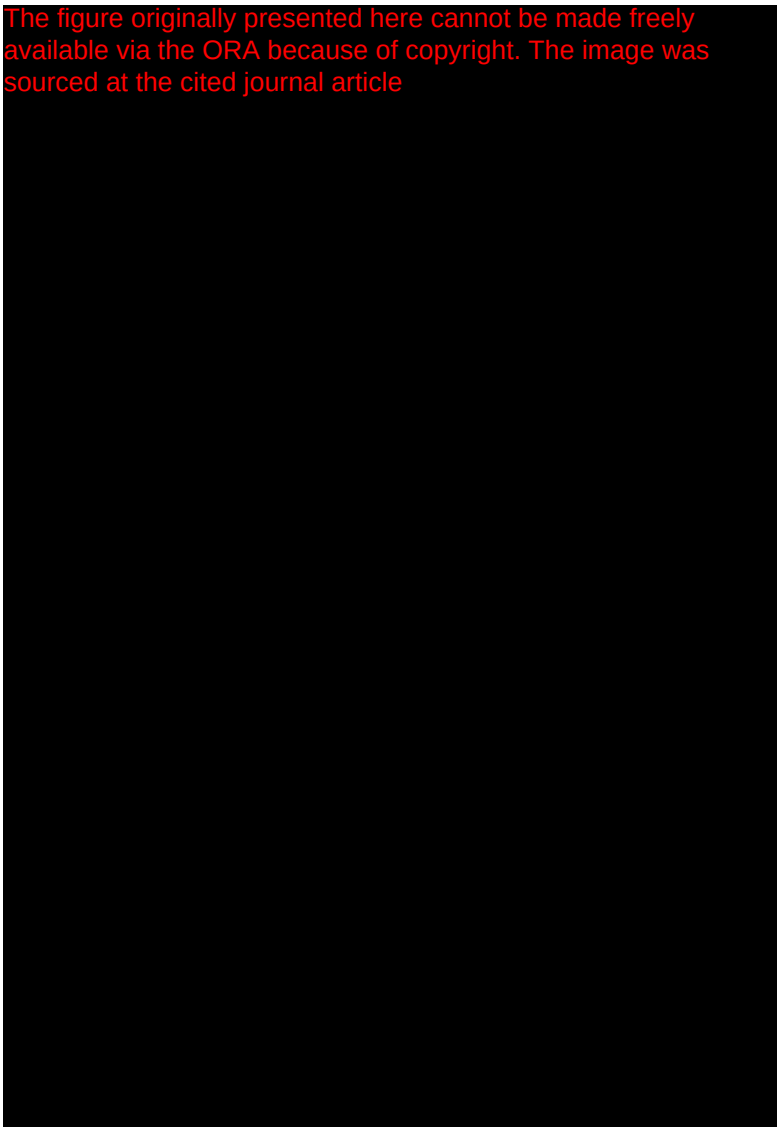


Figure 2-1. Transcranial magnetic stimulation. Shown here is the sequence of events occurring when a monophasic TMS pulse is delivered at the scalp. **(a)** Discharge of an electrical current into a stimulating coil produces **(b)** a magnetic field peaking at ~2 Tesla with a rise time of ~200 μs. **(c)** The time-varying magnetic field **(d)** induces an electric field, resulting in **(e)** induction of current in the brain that may lead to changes in behavioural performance. Taken from Walsh & Cowey (2000).

TMS machines typically discharge either monophasic pulses (as in Figure 2-1A) or biphasic pulses, in which the stimulating coil current undergoes a full oscillation before being damped. Biphasic stimulation has two main benefits. First, the second half of the biphasic oscillation returns up to 60% of the original pulse energy to the capacitor, reducing the time required for capacitors to recharge and allowing repetitive TMS (rTMS) pulses to be delivered. The initial rise time for biphasic pulses is also shorter, reducing the field intensities needed to induce currents in neural tissue (Walsh & Pascual-Leone, 2003).

Early TMS coils were circular (Barker et al., 1985b). This design results in close to zero stimulation under the coil centre, and maximal stimulation intensity in a circular region directly under the coil windings (Hovey & Jalinous, 2008). Non-clinical cognitive neuroscience research more typically utilises figure-of-eight stimulation coils comprising two sets of copper windings placed side by side in the same plane, as depicted in Figure 2-1. The advantage of this design is that when stimulation currents are passed in opposite directions through the two sets of windings, the induced secondary currents are maximal at the midpoint between the two coils, allowing more focal stimulation of the cortex (Figure 2-2) (Ueno et al., 1988).

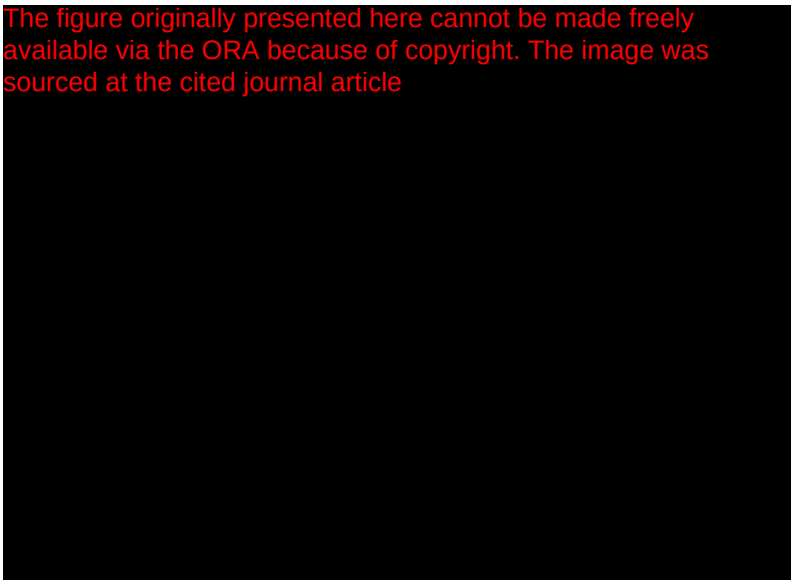


Figure 2-2. Distribution of electric fields induced by stimulation of common TMS coils. Shown are plots of the fields at a depth of 20mm below the coil surface for **(a)** a 90mm circular coil and **(b)** a 90mm figure-of-eight coil. From Pascual-Leone et al. (1999).

Neuronal stimulation is not a direct result of magnetic fields in the brain, but can arise when a TMS-induced electric field results in transmembrane current flow. The mechanism by which TMS affects neural activity thus depends on the spatial relationship between the stimulation-induced electric field and underlying neuronal geometries (Amassian et al., 1992; Ruohonen & Ilmoniemi, 1999). Specifically, the neuronal activation function is proportional to the spatial rate of change of the electric field along the neuron's membrane (Walsh & Pascual-Leone, 2003).

The strength of induced current decreases with distance from the TMS coil following an inverse square law. Although spread of the TMS-induced magnetic field increases with the distance from the coil and cannot be eliminated, effective stimulation is generally thought to occur over a region of cortex several cubic centimetres underneath the stimulation coil (Pascual-Leone, 1999; Walsh & Pascual-Leone, 2003). Proof of this specificity is difficult given the complexity of the head models required to predict accurately the effects of TMS

(Wagner et al., 2004), however surface validity for the focality of TMS is provided by the observation that differences in motor-evoked potentials and phosphenes can be distinguished when the stimulation coil is moved from the optimal position by as little as one centimetre (Brasil-Neto et al., 1992; Cowey & Walsh, 2000). Furthermore, neuroimaging studies have demonstrated the spatial specificity of TMS in selectively modulating activity levels within a circumscribed region directly under the coil, as well as in distal regions anatomically connected with the stimulation site (Bestmann et al., 2008b; Ilmoniemi et al., 1997; Paus et al., 1997; Ruff et al., 2009; Wassermann et al., 1996).

TMS has been popularised as a method for producing 'virtual lesions', thus permitting 'virtual neuropsychology' studies in healthy patients (Pascual-Leone, 1999; Walsh & Cowey, 2000). When delivered 'online' – as participants complete a behavioural task – it has also been commonly described as adding 'noise' to neural processing, appealing to the intuition that TMS induces activity in excitatory and inhibitory neuronal populations that is random with respect to normal cortical activity, and may thus potentially disrupt behaviour (Walsh & Cowey, 2000; Walsh & Pascual-Leone, 2003). These descriptions highlight several of the key advantages of TMS. First, TMS allows investigation of the *causal* role of stimulated brain regions in behaviour, whereas neuroimaging methods can only interrogate correlational relationships. Second, the focality and rapid induction of TMS effects are major advantages compared with lesion studies, in which much larger cortical areas are typically damaged than those of interest to the investigator, and post-lesion brain reorganisation may have compensated for any initial deficits. As the duration of TMS pulses is around 1 millisecond, TMS has the potential to interrogate the time course of neural processing with high temporal resolution. This has allowed the times at which cortical areas causally contribute to task-related processing to be identified with a precision of tens of milliseconds (e.g., Chambers et

al., 2004a; Koch et al., 2006; O'Shea et al., 2007b; Silvanto et al., 2005), and allowed characterisation of the precise timing of inter-regional functional connectivity with millisecond precision (e.g., Davare et al., 2010; Mars et al., 2009).

Although intuitively appealing, descriptions of TMS as producing 'virtual lesions' or 'noise' are not informative about the neural mechanisms affected by TMS, and bely the diversity of neural and behavioural consequences that can result from TMS, depending on factors including the stimulation intensity, the stimulation context, the frequency and number of pulses delivered in each train of TMS, and the interval between TMS pulse trains. Rather than increasing the effects of stimulus noise, careful psychophysical investigations suggest that the effect of single-pulse TMS delivered to the occipital pole or V5/MT is to suppress the strength of relevant visual signals when stimulation intensity is high (i.e., above phosphene threshold) (Harris et al., 2008; Ruzzoli et al., 2011), but to enhance participants' ability to detect low-contrast visual stimuli when stimulation intensity is low (i.e., below phosphene threshold) (Abrahamyan et al., 2011). The cause of these differences is still unclear, but one suggestion is that TMS activates cortical neurons non-specifically, and this impacts behaviour in a context-specific manner (Abrahamyan et al., 2011; Silvanto et al., 2008; Tadin et al., 2011). A detailed characterisation of the effects of short trains of high frequency (>1 Hz) rTMS is also lacking, however it has been suggested to have potentially different disruptive effects due to temporal summation in the effects of multiple pulses, increased spread of activity compared with single-pulse stimulation, or rhythmic entrainment of neural oscillations (Ruzzoli et al., 2011; Ruzzoli et al., 2010; Thut & Miniussi, 2009; Thut et al., 2011). In contrast, 1-Hz rTMS delivered for 15 minutes or longer decreases cortical excitability in the stimulated region of cortex for at least 15 minutes afterwards (Chen et al., 1997), and patterned TMS protocols employing repeated bursts of very high frequency TMS

(e.g., 3 pulses at 50Hz, repeated every 200ms) at low intensities can have long-lasting excitatory or inhibitory effects, or no effect at all, on motor cortex excitability depending on the precise stimulation protocol (Huang et al., 2005). Counter to the 'virtual lesion' and 'noise' accounts, TMS is therefore best thought of as a tool that provides a variety of means by which an experimenter may transiently perturb normal neural functioning.

Finally, but most importantly, the primary concern in any TMS experiment is participant safety. There are several potential adverse effects of TMS, with the most common ones being short-lasting headaches and syncope. Transient hearing loss has also been reported in several cases, highlighting the need for earplugs to mask the loud (up to 140 dB) auditory click associated with TMS pulse discharge (Rossi et al., 2009). The most serious consequence of TMS is induction of epileptiform seizure activity. Only a handful of seizures due to TMS have been reported, and the majority of these were prior to the definition of TMS safety guidelines in 1998 (Wassermann, 1998). Of the nine seizures reported in non-epileptic populations between 1998 and the 2009 updating of the TMS safety guidelines (Rossi et al., 2009), half of the cases involved stimulation parameters outside the 1998 guidelines, and one involved a relatively new stimulation paradigm, 'theta-burst' patterned TMS, at a higher stimulation intensity than normally used. The remaining four cases all involved rTMS, but three cases involved patients taking pro-epileptiform medication, and two may have been non-epileptic events. The risks associated with TMS are therefore very low. However, it is of great importance that all TMS investigators strictly adhere to the most recently published safety guidelines (Rossi et al., 2009).

2.2. Electroencephalography

Electroencephalographic (EEG) recordings are measurements of voltage potential differences between locations on the outer surface of the scalp, typically from between 20 and 256 electrodes. Although electrical recordings from the cortex were made in the 19th century (Beck, 1890; Brazier, 1963; Caton, 1875), EEG recordings from humans were not pioneered until several decades later (Berger, 1929), and brought to the awareness of the broader scientific community by Adrian and Matthews (1934). Since then, mainstream use of EEG research has been hindered by uncertainty about the sources of EEG signals, their relationship with brain activity, and questions regarding the functional interpretation of EEG results. Indeed, until relatively recently, EEG research was seen by many psychologists as being:

"*.... irrelevant to the study of brain or mind, as merely a kind of artifact like amplifying the signal from a bowl of jelly or listening to a computer signal with a stethoscope*" – (M. Posner, in Rugg & Coles, 1996)

As a result of empirical advances and methodological and technological developments, EEG has come to be seen as an essential non-invasive tool for investigating the dynamics of neural activity with high temporal precision. Magnetoencephalography (MEG), which measures magnetic flux changes outside the skull, provides higher spatial resolution compared with EEG, and has further contributed to the utility of non-invasive neurophysiological investigations with human participants.

2.2.1. Measurement and Biophysical Origins of EEG signals

The high temporal resolution of EEG and MEG recordings enables measurement of elecetromagnetic signals at the timescale of neuronal activity, on the order of tens of milliseconds (Baillet et al., 2001; Hamalainen et al., 1993). Although the signals resulting from activation of any single neuron are small, signals strong enough to be measurable outside the head may result from the superposition of signals from thousands or millions of synchronously active neurons (Hämäläinen & Hari, 2002). Biophysical considerations affecting the capacity for such signal summation therefore provide important constraints on the sensitivities of EEG and MEG.

Neural activity gives rise to afferent volleys of action potentials that may lead to excitatory or inhibitory post-synaptic potentials (PSPs) in the dendrites of other neurons. Whilst action potentials and PSPs both have electromagnetic signatures, EEG/MEG recordings are thought to have a higher sensitivity to PSPs partly because their duration (usually tens of milliseconds) allows for greater temporal summation compared with action potentials (~1-2 ms), which are both fast and whose propagation across neighbouring axons is not perfectly synchronized (Hamalainen et al., 1993). During transient excitatory PSPs, inward current flow across the apical dendritic membranes causes them to become electronegative with respect to distal parts of the neuron, including the soma. This potential difference is counterbalanced by outward capacitative currents across the cell membrane of the soma and more basal dendrites (Gloor, 1985). The associated electric field can be approximated by an electrical dipole consisting of spatially separated positive and negative charges. The strength of a dipole's electric field decreases exponentially with distance (Scott, 1997, in Hamalainen et al., 1993), biasing EEG recordings in favour of superficial (i.e., cortical) sources in the brain.

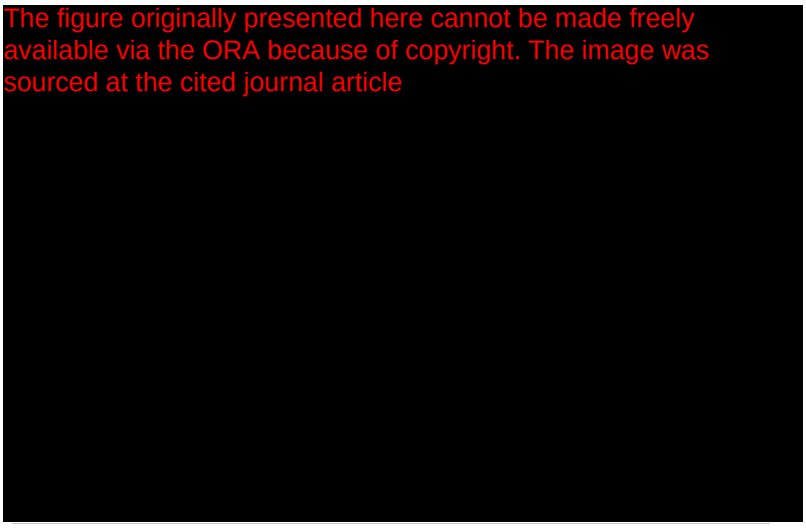


Figure 2-3. Theoretical current flow and potential fields produced by synchronous activation of neurons in different spatial configurations. (taken from Lorente de Nó, 1947; in Allison et al., 1986)

The relative spatial configuration within a neural population is an important determinant of the EEG signal resulting from their synchronous activation. The consequences of different neural geometries were described by Lorente de Nó (1947). Modeling of the interaction between nearby dipoles suggests that when neurons within a population are radially oriented, their electric fields will sum to zero at large distances (see Figure 2-3). This is known as a 'closed-field' configuration, and the activity of neurons arranged in such a fashion is likely to be undetectable from the scalp. In contrast, if populations of homogenously oriented neurons form an 'open-field' configuration, the superposition of their electric fields should be non-zero, potentially leading to detectable EEG signals at the level of the scalp (Allison et al., 1986; Lorente de No, 1947). EEG and MEG signals are thought to reflect primarily synchronous activity across macrocolumns of homogenously oriented pyramidal cells in the cortex, as these may be described by open-field geometries, or at least

by ‘open-closed field’ geometries in which there is only partial cancellation between the electromagnetic fields resulting from source current flowing in opposite directions, resulting in weaker signals at the scalp (see Figure 2-3). Despite these limitations, it should be noted that some researchers have reported EEG and MEG signals reflecting activation of deeper cortical structures predicted to have near-closed geometries, including the hippocampus, cerebellum, amygdala and thalamus (e.g., Cornwell et al., 2008; Litvak et al., 2010; Llinas et al., 1999; Quraan et al., 2011; Tesche & Karhu, 1999).

The location and orientation of a cortical region relative to the scalp also influence whether neural activity results in electromagnetic signals measurable outside the head. While EEG can detect activity from both gyral and sulcal sources, MEG is most sensitive to sulcal sources. The reason for this is that radially oriented dipoles (i.e., gyral pyramidal neurons) do not produce any external magnetic field outside a spherically symmetric volume conductor, regardless of the sensor orientation (Hamalainen et al., 1993). Inter-areal interactions may also affect the signal recordable at the scalp. For example, the electric fields from two open-field configurations on opposing sides of a sulcus may be expected to cancel out (Clark & Hillyard, 1996).

2.2.2. Recording, Preprocessing and Analysis of EEG signals

The electrical potential at each EEG electrode must be made in comparison with a reference electrode. Choice of an appropriate reference is an important determinant of observed waveforms. For example, choice of a lateralized electrode can bias recordings towards showing effects in the contralateral hemisphere. Different researchers have advocated a variety of references. A common approach is to make use of a reference that is

not contaminated by neural activity, typically the earlobe or a linked mastoid. In practice, however, such efforts do not completely attenuate neural activity. For example, temporal lobe epileptiform activity is readily reflected in these reference (Reilly, 2005), as is normal alpha-wave activity. Another popular approach is to reference EEG data to the average of many or all scalp electrodes recorded from. This is an effective method of averaging out small deviate voltages showing up in only a few electrodes, but has the disadvantage that wide-spread artefacts and artefacts with large voltages may be introduced over the scalp but with different polarities (Reilly, 2005). Another advantage of the average reference is its widespread use, facilitating comparison of results between laboratories (Nunez, 1981) (see also Murray et al., 2008).

EEG recordings are sensitive to a number of factors other than brain activity. It is therefore important to minimise contributions of noise sources to the recording. The impedance between electrodes and the scalp should be kept low (<5 kΩ) to minimise the likelihood of noise or drift in recorded signals. Signals may also be filtered to attenuate high and low frequency activity that is not of interest to the experimenter (e.g., a bandpass filter from 0.01 to 100 Hz). A 50-Hz notch filter is also commonly used to attenuate effects related to the mains power supply. Appropriate artefact rejection is also crucial to minimise noise due to muscular activity such as jaw clenching and blink-related artefacts, which can produce widespread electromyographic (EMG) artefacts across the scalp. During experiments, most researchers take electrooculogram (EOG) recordings from electrodes placed around the eyeball to facilitate identification of blinks and saccade-related artefacts, which can introduce noise or systematic confounds to recordings if not identified. Although many researchers use analysis methods such as independent component analysis to remove the artefacts associated with blinks or eye movements, such approaches cannot control for the neural consequences of

participants closing or moving their eyes, and so a more conservative approach is to discard data contaminated by blinks or saccades.

Preprocessed EEG signals from many trials may be averaged to produce grand-averaged waveforms with a higher signal-to-noise ratio than single trial data. Event-related potentials (ERPs) are average waveforms time-locked to a relevant sensory, motor or cognitive process of interest. The latency, amplitude and topographic distribution of reliable deflections in ERP components (e.g., the P100, a positive waveform appearing at posterior sensors approximately 100 ms after onset of a visual stimulus) may then be compared to investigate how experimental manipulations affect neural processing (Allison et al., 1986; Luck, 2005; Luck et al., 2000; Murray et al., 2008; Picton et al., 2000; Rugg & Coles, 1996). The latency of significant differences between two ERPs provides an upper bound on the time that neural activity differed between conditions.

Identifying the spatial location of neural generators on the basis of EEG waveform differences is challenging. This in part reflects the consequences of the head acting as a volume conductor, resulting in spatial smearing of neural signals at the scalp. At a more fundamental level, however, while the 'forward problem' – computing the voltages observed at the scalp given a head model and a set of electric dipoles at known locations and orientations – is well defined, the 'inverse problem' – estimating the dipole sources of observed EEG data is ill-posed, as there are an infinite number of dipole configurations that can produce any scalp topography (Baillet et al., 2001; Helmholtz, 1853).

Even in the earliest intracranial and scalp recordings, researchers realised that a variety of events could trigger modulation in the power of ongoing neural oscillations (Beck, 1890, in Brazier, 1963; Berger, 1929). These changes can be characterised by a variety of spectral (or 'time-frequency') analysis methods such as Fourier and wavelet analysis, which

decompose a time-varying signal (e.g., a raw EEG trace) into amplitude measures within specific frequency bands (Pfurtscheller & Lopes da Silva, 1999; Torrence & Compo, 1998). Changes in spectral activity over time can be assessed by applying spectral analysis methods to EEG data using a sliding time window. Time-frequency analysis is sensitive to induced oscillatory amplitude changes, regardless of the phase of the oscillation or jitter in the timing of oscillatory changes relative to an experimental event of interest. In contrast, ERP analysis is only sensitive to evoked waveforms that are time-locked and phase-locked to a particular point in time.

2.2.3. Relationship Between Oscillatory EEG Activity and Neural Activity

Recent investigations have begun to elucidate how oscillatory EEG/MEG activity co-varies with fluctuations in simultaneously recorded BOLD responses, neuronal firing rates, and LFPs recorded from depth electrodes or electrocorticographic (ECoG) recordings from the surface of the brain. Increases in broadband oscillatory power and gamma-band power have generally been reported to show positive correlations with spike rates and BOLD activity (Koch et al., 2009; Lachaux et al., 2007; Mukamel et al., 2005; Mulert et al., 2010; Niessing et al., 2005; Rasch et al., 2008; Scheeringa et al., 2011; Yuan et al., 2010; Zaehle et al., 2009), and low-frequency signals between approximately 4 and 30 Hz (i.e., including the alpha- and beta-bands) to show negative correlations (Becker et al., 2011; Laufs et al., 2006; Laufs et al., 2003a; Mukamel et al., 2005; Niessing et al., 2005; Scheeringa et al., 2011; Scheeringa et al., 2009; Stevenson et al., 2011; Whittingstall & Logothetis, 2009). Combined EEG-fMRI data further suggest that BOLD signal variance explained by alpha- and beta-band activity is independent of that explained by gamma-band fluctuations (Scheeringa et al., 2011). In contrast, the variance explained by alpha- and beta-band activity overlap to a large

degree – alpha-band activity only explains a marginal amount of BOLD variance independently, and beta-band activity explains a small but significant amount of BOLD variance on its own (Scheeringa et al., 2011). Previously, linear relationships have often been assumed between spectral power modulation and firing rate data (Miller et al., 2009a; Mukamel et al., 2005; Rasch et al., 2008; Whittingstall & Logothetis, 2009). Although this has not been explicitly validated in most studies, where model comparisons were performed the majority of variance in spike-rate data has been explainable by simple linear models (e.g., >90% in Rasch et al., 2008), justifying the use of linear models when dealing with spectral power in general (Miller et al., 2010; Stevenson et al., 2011). It should also be noted that most previous studies have compared single-unit firing rates to LFP or ECoG activity, firing rate data or LFPs to BOLD signals, or oscillatory EEG/MEG phenomenon to BOLD signals. The qualitative similarities between spectral power modulations in intracranial and EEG/MEG recordings make it reasonable to assume that similar relationships hold between local spiking activity and spectral power in non-invasive EEG/MEG recordings. However, until further empirical data are available, caution is required in making assumptions about the broader consequences of EEG/MEG oscillatory power changes on local firing rates.

Despite showing reliable relationships, different measures of neural activity do not reflect identical neurophysiological processes, and can undergo different modulatory patterns (Logothetis et al., 2007; Logothetis & Wandell, 2004; Maier et al., 2008; Niessing et al., 2005; Sirotin & Das, 2009). Inconsistent findings have been particularly common in attempts to characterize the broader neural consequences of oscillatory power changes in the lower frequency bands. For example, alpha-, beta-, and theta-band activity have under some circumstances been reported to show positive correlations, or no relationship at all, with BOLD activity (Donner & Siegel, 2011; Giraud et al., 2007; Goldman et al., 2002; Laufs et

al., 2003b; Manning et al., 2009; Mantini et al., 2007; Whittingstall & Logothetis, 2009). It has been suggested that increases in local oscillatory power under ~30 Hz are often accompanied by local activity decreases, but that local cortical activity may increase in the same regions when oscillatory power changes reflect increased oscillatory synchrony between regions (Donner & Siegel, 2011). However, it is currently unclear whether such differences reflect differences in behavioural tasks when recordings are made, inter-regional differences in the relationship between oscillatory phenomena and neural activity, differences in the sensitivities and/or biases of surface ECoGs, depth LFPs and single/multi-unit recordings, or interactive effects of frequency-specific and broad-band power changes (Manning et al., 2009; Miller et al., 2009a; Miller et al., 2009b).

2.2.4. Concurrent EEG and TMS

The simultaneous use of TMS and neuroimaging methods such as EEG can combine the strengths of both methods, allowing the neural and behavioural consequences of brain disruption to be concurrently observed (Driver et al., 2009; Miniussi & Thut, 2010; Siebner et al., 2009; Taylor et al., 2008; Thut & Miniussi, 2009; Thut & Pascual-Leone, 2010a, 2010b). The main obstacles to concurrent TMS-EEG are the technical challenges associated with the large electrical artefacts induced at the scalp by TMS pulses, which can saturate EEG amplifiers for several seconds. Several solutions to this problem have been developed over recent years. The sample-and-hold approach clamps the EEG signal for several milliseconds around the time of the TMS pulse (Ilmoniemi et al., 1997). It is also possible to use slew-rate limited amplifiers to prevent amplifier saturation by the TMS pulse (Thut et al., 2003). The experimental work presented in this thesis employs a simpler approach to this problem. Use of EEG amplifiers offering a wide dynamic range can allow continuous recording of EEG

data without saturation during TMS delivery (Bonato et al., 2006). As a result, usable data may be obtained after the TMS artefact has subsided, as little as 50ms after TMS onset. To minimise the duration of the TMS artefact it is important to ensure that EEG recordings are made without any filters, as this can result in long-lasting 'ringing' artefacts following the sudden onset of the TMS pulse artefact (Taylor et al., 2008). It is also important to prevent physical contact between the TMS coil and EEG electrodes as this can induce additional noise in the EEG recording (Taylor et al., 2008) and increase the likelihood of TMS-induced electrode heating (Rossi et al., 2009). Placement of EEG electrodes away from the TMS coil and apparatus can also minimise artefacts associated with stimulation and recharging of the TMS boosters (Veniero et al., 2009).

2.3. Methodological Rationale

As stated in Section 1.7, the aims of the present thesis were to investigate the oscillatory correlates of perceptual processes and motor preparation during human decision making, and the regions that causally contribute to decision making in the human brain. In Chapter 3, EEG was used to investigate whether parametric variations in the lateralization of alpha oscillations recorded over occipito-parietal cortex would be flexibly modulated by graded differences in top-down attentional goals. In Chapter 4, EEG was used to investigate whether the temporal dynamics of preparatory activity changes in human motor planning structures are consistent with the encoding of a decision variable. We note that while use of MEG would have provided a higher spatial resolution, both of these experiments utilised EEG as this method provides a sufficient spatial resolution to discriminate between signals originating in left- and right-hemisphere visual (Chapter 3) and motor (Chapter 4) regions. The use of EEG in Chapter 4 also provided a foundation for Chapter 5, in which concurrent

TMS-EEG was used to investigate the behavioural and neural consequences of transiently disrupting a medial intraparietal region during the decision integration task developed in Chapter 4.

Chapter 3 - Indexing the Graded Allocation of Visuospatial Attention Using Anticipatory Alpha Oscillations

Lateralization in the desynchronization of anticipatory occipito-parietal alpha (8-12 Hz) oscillations has been implicated in the allocation of selective visuospatial attention. Previous studies have demonstrated that small changes in the lateralization of alpha-band activity are predictive of behavioral performance, but have not directly investigated how flexibly alpha lateralization is linked to top-down attentional goals. To address this question, we presented participants with cues providing varying degrees of spatial certainty about the location at which a visual target would appear. Time-frequency analysis of EEG data demonstrated that manipulating spatial certainty led to graded changes in the extent to which alpha oscillations were lateralized over occipito-parietal cortex during the cue-target interval. We found that individual differences in alpha desynchronization contralateral to attention predicted reaction times, event-related potential measures of perceptual processing of targets, and beta-band (15-25 Hz) activity typically associated with response preparation. These results support the hypothesis that anticipatory alpha modulation is a plausible neural mechanism underlying the allocation of visuospatial attention, and is under flexible top-down control.

3.1. Introduction

The ability to select and process relevant sensory stimuli flexibly underlies our ability to make decisions and act upon appropriate sensory inputs, and is critically important for our ability to maintain goal-directed behaviour within a noisy environment. A major goal of modern neuroscience research has therefore been to understand the neural mechanisms underlying the allocation of selective attention. Selective visuospatial attention has been extensively characterized as modulating baseline and target-evoked neural activity in cortical areas involved in processing attended versus unattended stimuli (Chawla et al., 1999;

Chelazzi et al., 1993; Hillyard et al., 1998; Kastner et al., 1999; Luck et al., 1997; McAdams & Maunsell, 1999; McMains et al., 2007; Moran & Desimone, 1985; Ress et al., 2000; Reynolds et al., 2000; Stokes et al., 2009). Some of these effects may reflect modulation of thalamic input to cortex (Crick, 1984; McAlonan et al., 2008). Recently, anticipatory modulation of occipito-parietal alpha-band (8-12 Hz) oscillations during cue-target delays has also been identified as a possible neural mechanism underlying the allocation of selective visuospatial attention (Foxe et al., 1998; Worden et al., 2000). Similar to attention, alpha oscillations have been related to thalamocortical interactions (Hughes & Crunelli, 2005; Lopes da Silva, 1991). Occipito-parietal alpha oscillations are attenuated when visual information is attended compared with auditory information (Foxe et al., 1998; Fu et al., 2001). When visuospatial attention is covertly allocated, topographically organized modulation of alpha activity is also observed (Rihs et al., 2007; Worden et al., 2000). Increased anticipatory alpha synchronization is typically observed ipsilateral to the locus of attention, perhaps reflecting suppression of processing of unattended locations (Kelly et al., 2006; Rihs et al., 2007; Rihs et al., 2009; Worden et al., 2000), whilst decreased synchronization has been observed contralateral to attention, perhaps reflecting enhancement of processing for attended locations (Kelly et al., 2009; Rihs et al., 2009; Sauseng et al., 2005; Thut et al., 2006; Yamagishi et al., 2008). This pattern of effects is disrupted by TMS stimulation of parietal and frontal regions implicated in top-down control of attention (Capotosto et al., 2009).

Selective attention is advantageous to the extent it can be flexibly allocated. For example, attention can allow perceptual processing to be optimized given knowledge of probabilities of events occurring at different spatial locations within the visual environment (Eckstein et al., 2004; Eckstein et al., 2002; Egner et al., 2008; Kingstone, 1992; Yantis &

Jonides, 1990). Ideally, it should be possible to understand the flexibility with which attention can be allocated across space in terms of its neural underpinnings. In this regard, it is interesting to note that trial-to-trial variability in alpha power can predict accuracy and reaction times on visual judgement tasks (Dockree et al., 2007; Ergenoglu et al., 2004; Kelly et al., 2009; Mathewson et al., 2009; O'Connell et al., 2009; Thut et al., 2006; Van Dijk et al., 2008), and that alpha power is inversely related to the probability that applying TMS pulses to occipital cortex will result in perception of phosphenes (Romei et al., 2008a). Importantly, however, the evidence that trial-to-trial variability in alpha power is correlated with behavioral changes does not constitute evidence for flexible, voluntary control over alpha modulation. The co-variance between small changes in alpha power and behavior may merely reflect that this measure provides an index of intrinsic variability in cortical excitability.

To investigate directly how flexibly anticipatory alpha lateralization is linked to voluntary attentional goals, we presented participants with spatially predictive cues of varying validity and examined whether the magnitude of anticipatory alpha rhythm lateralization co-varied with the degree to which attention was allocated to a particular location. We hypothesized that, to the extent that the lateralization of alpha oscillations is a neural mechanism underlying the top-down allocation of attention, the lateralization of alpha rhythms should vary in a graded fashion with graded changes in the direction of voluntary attention. We also examined the functional relevance of observed alpha modulation by investigating, at a within-subject level, how attentional modulation of alpha-band activity was related to modulation of behavioural accuracy and reaction time measures of performance, early sensory event-related potentials reflecting perceptual analysis of target stimuli, and to beta-band (15-25 Hz) activity over motor cortex electrodes providing a neural index of motor

preparation (Donner et al., 2009; Doyle et al., 2005; Tzagarakis et al., 2010a; van Wijk et al., 2009).

3.2. Materials and Methods

3.2.1. Participants

Fourteen paid volunteers (mean age 28; 6 female) participated after giving informed written consent. All participants were right-handed (Oldfield, 1971), and reported having normal or corrected-to-normal visual acuity and no history of neurological disorders. The methods and procedures used in the study were non-invasive and had ethical approval from the University of Oxford Central University Research Ethics Committee.

3.2.2. Task and Stimuli

Participants were asked to discriminate the orientation of a peripheral target stimulus, which was preceded by a spatial cue. A schematic of the display sequence is shown in Figure 3-1A. Participants were instructed to maintain central fixation throughout experimental trials, and completed the task seated comfortably in a dimly lit room with their head position stabilized by a chin rest. Stimuli were presented at 60 Hz on a 22-inch Sony Trinitron CRT monitor at a viewing distance of 100 cm. Stimulus presentation and response acquisition were controlled using Presentation 13.0 (Neurobehavioral Systems).

All stimuli were presented against a uniform mid-gray background. Trials commenced with a 1,500-ms presentation of a fixation cross consisting of two 0.3^{o} x 0.06^{o} black lines. A central cue stimulus was then presented for 500 ms. The cue on each trial was drawn randomly from a set of six cue shapes (Figure 3-1B), each of which had a diameter of

approximately 2.3^{o} and a line width of 0.02^{o}. Cues indicated that target stimuli would appear on the left or right side of the screen with a 'spatial certainty' (i.e., probability) of 60%, 80% or 100%. Participants were explicitly informed about the cued direction and validity associated with each cue shape. The cued direction and validity associated with specific cue shapes was randomised across participants.

Target stimuli were presented following a cue-target inter-stimulus interval (ISI) of 750 ms (50% of trials), 1,850 ms (25% of trials), or 2,950 ms (25% of trials). This truncated geometric distribution of ISIs was used to avoid the possibility that strong effects of temporal expectation might influence our results. Target arrays were presented for 67 ms, followed by a 67-ms bilateral backwards-mask array. Target arrays consisted of a horizontally or vertically oriented target Gabor patch (Gaussian-vignetted sinusoidal grating), and a ±45^{o} tilted distracter Gabor patch. Presentation of a bilateral array including similar target and distracter stimuli avoided any automatic attentional capture by the target stimulus. The short array duration and bilateral mask further prevented re-orienting to the target after it was presented. This ensured that performance levels were determined by participants' attentional state when the target array was presented, and encouraged them to orient their attention in a graded fashion based on spatial certainties provided by cues. Target, distracter and backward mask stimuli were presented 4.8^{o} below the horizontal meridian and ±3.2^{o} from the vertical meridian. Gabor patch stimuli were presented in greyscale at 90% contrast, and with a spatial frequency of 2.5 cycles per degree. The Gaussian envelope had a space constant of 0.457^{o}. The location of the target and distracter were determined probabilistically by the cue. The orientations of the target and distracter were randomly selected on each trial. Backward-mask stimuli were constructed by applying a Gaussian-vignette to the convolution of 90% contrast square-wave gratings at the four target and distracter orientations. Target, distracter and mask

stimuli were presented atop 10% contrast luminance pedestals, which were present throughout the experiment to aid target localisation and the allocation of visual attention (see Figure 3-1A).

Participants discriminated the target orientation (horizontal or vertical) by making a right-handed index or middle finger button-press during a response period of up to 1,500 ms. Response mappings were counterbalanced between participants. Feedback was provided for 250 ms after the response period by coloring the fixation cross green for correct responses or red for incorrect responses or misses. The subsequent inter-trial interval (ITI) was 1,500 ms.

All participants completed two testing sessions within one week. In the first session participants completed 540 training trials, practising first with single cues, then pairs of cues at each cue validity level. The number of cues within each block was then increased to 4, and then to 6 for the last 290 trials. In the experimental session, participants completed 30 practice trials with all 6 cues, then 450 trials during which EEG was recorded. Rest breaks were provided every 30 trials. Statistical analysis was performed using Matlab and SPSS. Where appropriate, the Greenhouse-Geisser correction for non-sphericity was applied. All post-hoc pairwise comparisons were Bonferroni-corrected.

3.2.3. Electroencephalography (EEG) Recording and Pre-Processing

EEG was recorded continuously (1,000-Hz sampling rate; left mastoid reference; NuAmps digital amplifiers; Neuroscan, El Paso, TX) from 36 scalp sites using Ag/AgCl electrodes mounted on an elastic cap (Easy Caps, Germany) according to the 10-20 international system. The montage included 7 midline sites (OZ, POZ, PZ, CPZ, CZ, FCZ and FZ), 12 sites over each hemisphere (O1/O2, PO3/PO4, PO7/PO8, P3/P4, P7/P8,

CP3/CP4, C3/C4, FC3/FC4, FT7/FT8, F3/F4, F7/F8 and FP1/FP2), left and right mastoids, HEOG and VEOG electrodes to monitor the EOG bipolarly, and an additional electrode (AFZ) used as ground. Vertical EOG was calculated as the bipolar derivation between FP2 and the lower VEOG electrode. Recordings were re-referenced offline to the average of the mastoids. Continuous epochs from 100 ms before fixation onset to the end of the response period were included in analyses except when showing recording artefacts, if saccades or blinks occurred in the EOG, or if participants made early (<300 ms) or late (>1500 ms) responses (80% ± 14% S.E. trials accepted). Epochs were defined using digital codes sent to the EEG recording computer to mark the presentation of the cue and target in each trial type. A low-pass filter (40 Hz, 24 dB/octave) was applied to data used in event-related potential analyses prior to epoching.

3.2.4. Determination of Individual Alpha Frequency Bands

Time-frequency analysis of alpha-band EEG data was performed with respect to each participant's individual alpha frequency (IAF) to allow for individual variations in alpha bands (Doppelmayr et al., 1998; Klimesch et al., 1998). IAF frequencies were defined from the fast Fourier transform over occipital and parieto-occipital electrodes (O1/2, PO3/4, PO7/8, P3/4) across all short-trial epochs (4,000 ms), giving a frequency resolution of 0.25 Hz. Each participant's IAF was defined as the frequency with the largest power in the 8-12-Hz range. The frequency band subsequently analysed was defined as the participant's IAF ± 2 Hz, as modulation of this frequency band has been demonstrated in previous attentional orienting studies (e.g., Thut et al., 2006). The mean IAF was 9.9 Hz (± 0.25 S.E.).

3.2.5. Time-Frequency Analysis

Time-frequency analysis was performed on all epochs using a multi-taper approach (2-30 Hz, 0.5-Hz steps, 500-ms temporal smoothing window, 2-Hz frequency resolution) using Fieldtrip (Donders Institute for Brain, http://www.ru.nl/neuroimaging/fieldtrip) under Matlab (The Mathworks). Raw power data at each time-frequency sample were log-transformed, yielding approximately normally distributed data suitable for standard parametric statistical tests (Kiebel et al., 2005). Log-transformed data were linearly baselined relative to the 200-ms preceding cue onset.

Time-frequency analysis of alpha power data was conducted in 3 bilateral regions of interest (ROI) within which electrodes showed similar effects. The 'parieto-occipital' ROI included O1/O2 and PO7/PO8, electrodes commonly reported as showing lateralized alpha modulation in attentional tasks (Kelly et al., 2006; Thut et al., 2006). The 'parietal' ROI included PO3/PO4 and P3/P4, and the 'parieto-central' ROI included CP3/CP4 and C3/C4, electrodes commonly reported as showing mu (8-12 Hz) and beta de-synchronization in motor planning and imagery studies (McFarland et al., 2000; van Wijk et al., 2009).

Repeated-measures ANOVAs were performed on alpha (IAF ± 2 Hz) frequency data 1,050-1,250 ms after onset of the cue stimulus. This time window corresponds to the 200 ms before the first possible time at which a target could be presented, when attention should have been strongly engaged (Rihs et al., 2009; Sauseng et al., 2005). To investigate motor preparation, beta-band (15-25 Hz) data from the parieto-central ROI was also analysed over the same time window (Donner et al., 2009; Doyle et al., 2005; McFarland et al., 2000; van Wijk et al., 2009). As participants did not know when the target would appear at this stage in the trial, data were pooled across all cue-target ISIs to maximise statistical power in our analyses.

3.2.6. Event-Related Potential (ERP) Analysis

To test for the consequences of spatial attention on visual processing of the target, we also analysed target-evoked visual ERPs at electrodes O1/2 and PO7/8 (epochs: -50 to 600 ms; baseline: -50 to 0 ms). As enhancement of both the P1 and N1 potentials is a common consequence of spatial attention and is likely to reflect the operation of gain control mechanisms (Hillyard & Anllo-Vento, 1998; Hillyard et al., 1998), we used the peak-to-peak P1-N1 complex amplitude to characterise the overall effects of gain control by attention on visual ERPs. The amplitude of the P1-N1 complex evoked by validly cued targets was calculated by subtracting the mean voltage around the peak N1 latency (192-222 ms) from that around the peak P1 latency (104-124 ms). These P1 and N1 time windows correspond to ± 10 ms from the peak P1 and N1 latencies, the values of which were determined from group averages using Scan 4.4 (Neuroscan). Data from invalidly cued targets (i.e., trials with a spatial predictability of 20% or 40%) were not analysed due to there being relatively few trials in these conditions (~24 trials when spatial predictability was 20%, after artefact rejection).

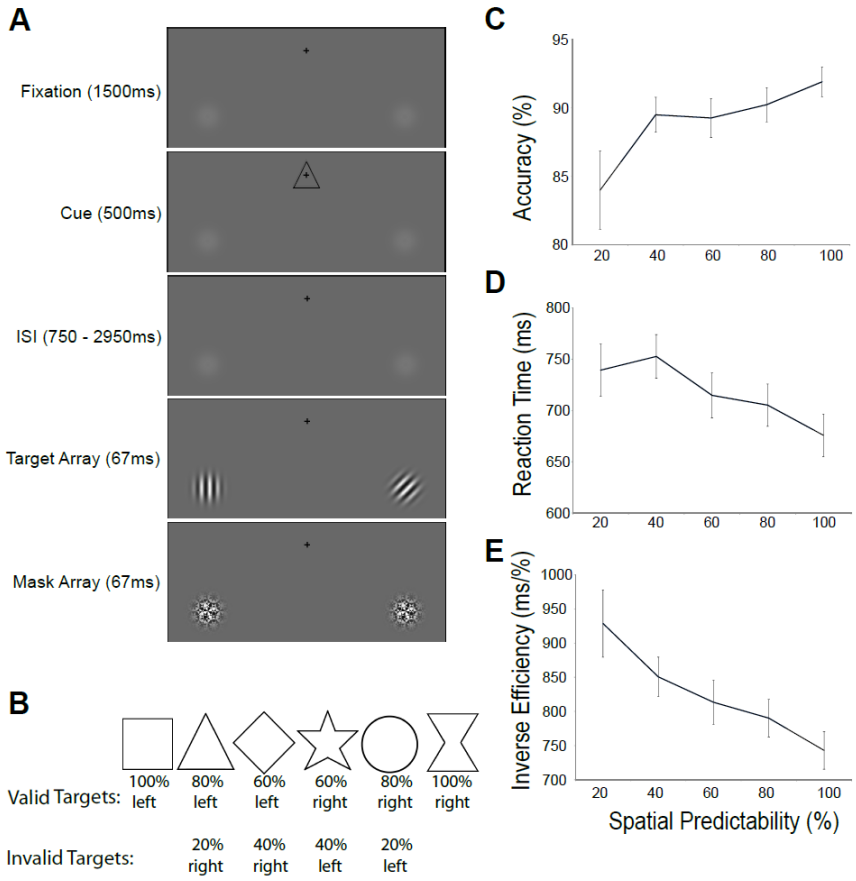


Figure 3-1. Task Design and Behavioral Results. (A) Schematic of the attentional orienting task. On each trial, a symbolic cue instructed that a target would appear in the left or right visual field with a 'spatial certainty' of 60%, 80% or 100%. Participants then discriminated the orientation (horizontal or vertical) of a target Gabor patch. **(B)** The six cue stimuli used in the task, and the cued direction and target probabilities associated with each cue shape for one participant. **(C)** Average accuracy increased whereas **(D)** reaction times on correct trials and **(E)** inverse efficiency decreased with increases in 'spatial predictability' of the actual target location. Note that spatial predictabilities of 20% and 40% describe targets following invalid cues that provided spatial certainty of 80% and 60%, respectively.

3.3. Results

3.3.1. Behavioral Results

Repeated-measures ANOVAs were carried out on accuracy, reaction times from correct trials, and inverse efficiency (calculated as reaction time divided by accuracy) data with factors of 'spatial predictability' (the cued probability of the target Gabor patch

appearing in the visual field it was presented; 20%, 40%, 60%, 80%, 100%) and ISI (short, medium, long).

Behavioral data are presented in Figure 3-1C-E. Significant main effects of spatial predictability were observed on both accuracy ($F_{(4,52)} = 3.84$, $p = 0.04$) and reaction time ($F_{(4,52)} = 4.27$, $p = 0.045$). The effects of spatial predictability were related to an increase in accuracy with spatial predictability (linear contrast: $F_{(1,13)} = 9.59$, $p = 0.008$) and a decrease in reaction time with spatial predictability (linear contrast: $F_{(1,13)} = 7.54$, $p = 0.017$). To investigate whether speed-accuracy tradeoffs affected the reaction-time and accuracy data, we performed an ANOVA on inverse efficiency measures. This revealed a main effect of spatial predictability ($F_{(4,52)} = 8.39$, $p = 0.005$) due to inverse efficiency decreasing with spatial predictability (linear contrast: $F_{(1,13)} = 14.6$, $p = 0.002$), confirming that task performance improved with spatial predictability. No other significant main effects or interactions were observed, including all effects involving the ISI factor.

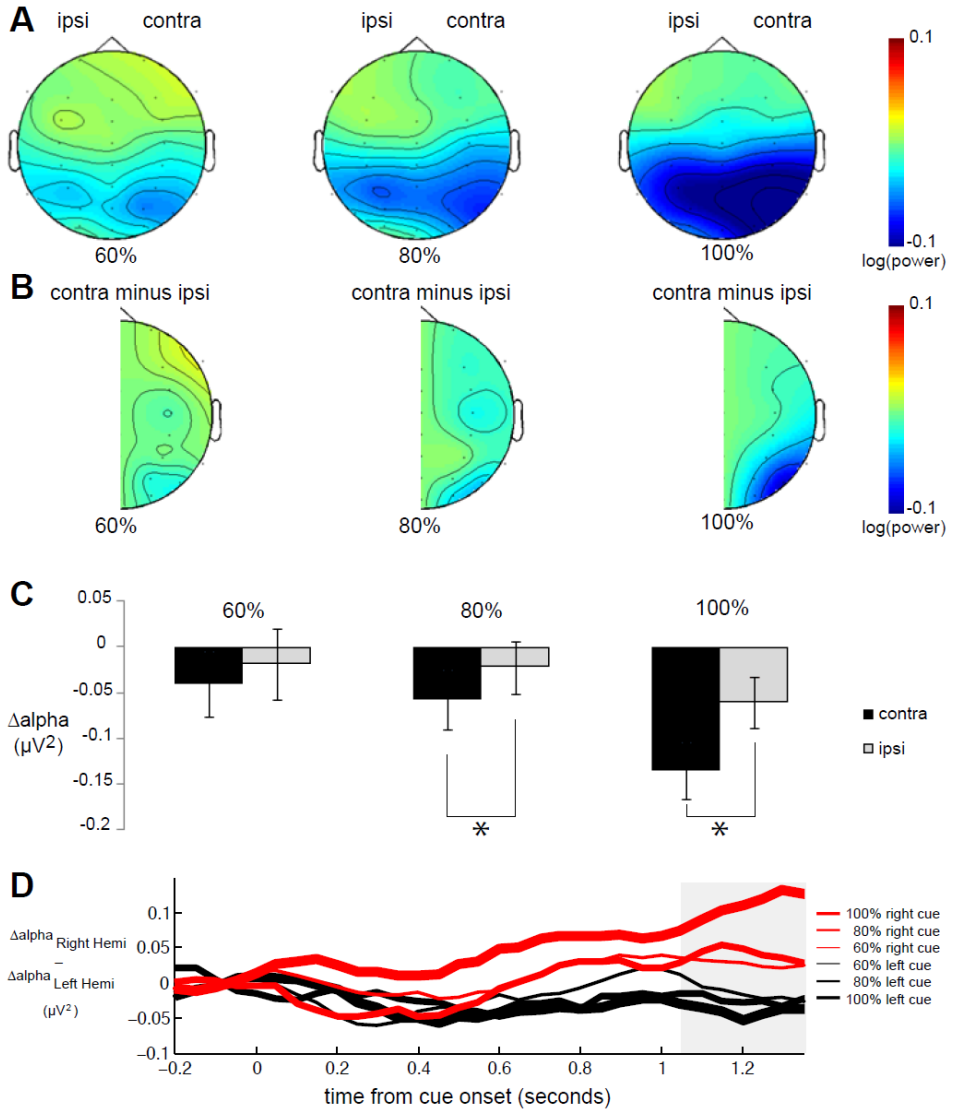


Figure 3-2. Lateralization of parieto-occipital alpha synchronization increased with spatial certainty. **(A)** Topography of alpha desynchronization following cues providing spatial certainty of 60%, 80% and 100% 1050-1250ms after cue onset. Ipsilateral hemisphere data are presented on the left, and contralateral data on the right. **(B)** Contralateral minus ipsilateral subtractions reveal that lateralization in alpha desynchronization at posterior electrodes increases with spatial certainty. **(C)** Mean contralateral and ipsilateral alpha modulation at each spatial certainty level at posterior electrodes O1/2 and PO7/8 (error bars are S.E.). **(D)** The graded lateralization of alpha oscillations emerged gradually at posterior electrodes, for both left and right cue directions. Values greater than zero indicate a rightwards bias in alpha asymmetry, and negative values a leftwards bias. The region highlighted in gray indicates the 200 ms before the earliest time at which targets could appear, where cuing effects on alpha-band data were strongest.

3.3.2. Alpha Power

The topography of changes in alpha-band power relative to the pre-cue baseline is presented in Figure 3-2. A 4-way ANOVA of alpha-band power was performed with factors of ROI (parieto-occipital, parietal, centro-parietal), hemisphere (ipsilateral or contralateral relative to the cued direction), cue direction (left, right), and the cued spatial certainty (60%, 80%, 100%). This analysis revealed a significant main effect of hemisphere ($F_{(1,13)} = 12.83$), $p = 0.003$) and spatial certainty ($F_{(2,26)} = 6.0$, $p = 0.007$), a cue direction X hemisphere interaction ($F_{(1,13)} = 7.6$, $p = 0.017$). Most importantly, the analysis revealed a ROI X cue direction X hemisphere interaction ($F_{(2, 26)} = 4.35$, $p = 0.043$), and a ROI X hemisphere X spatial certainty interaction ($F_{(4,52)} = 3.27$, $p = 0.044$). To clarify the nature of these interactions, subsidiary 3-way ANOVAs and pairwise comparisons were carried out within each ROI.

Results from the occipito-parietal ROI are presented in Figure 3-2C-D**.** A significant main effect of hemisphere ($F_{(1,13)} = 21.58$, $p < 0.001$) was observed, reflecting greater alpha-band desynchronization at contralateral electrodes relative to ipsilateral electrodes (pairwise comparisons: $p < 0.001$). A main effect of spatial certainty ($F_{(2,26)} = 4.30$, $p = 0.024$) was also observed, reflecting greater desynchronization when spatial certainty was higher (linear contrast: $F_{(1,13)} = 6.61$, $p = 0.023$). Critically, a hemisphere X spatial certainty interaction ($F_{(2,26)} = 4.12$, $p = 0.028$) was also observed, indicating that the degree with which alpha-band desynchronization was lateralized increased linearly with spatial certainty (linear contrast: $F_{(1,13)} = 6.42$, $p = 0.025$). This effect was primarily driven by a significant effect of spatial certainty at contralateral electrodes (linear contrast: $F_{(1,13)} = 10.96$, $p = 0.006$), where alpha power decreased progressively as spatial certainty increased. At ipsilateral electrodes a

similar trend was observed (see Figure 3-2C), however this effect was not significant (linear contrast: $F_{(1,13)} = 2.13$, $p > 0.16$)

For the parieto-central ROI, there was a main effect of spatial certainty ($F_{(2,26)} = 5.35$, $p = 0.011$), due to a bilateral desynchronization that increased linearly with spatial certainty (linear contrast: $F_{(1,13)} = 6.80$, $p = 0.022$). A significant cue direction X hemisphere interaction was also observed ($F_{(1,13)} = 19.96$, $p = 0.001$). Consistent with the right-handed responses made in the task, this reflected greater desynchronization in the left versus right hemisphere; following left cues contralateral alpha was greater than ipsilateral alpha (pairwise comparisons: $p = 0.046$), and following right cues ipsilateral alpha was greater than contralateral alpha (pairwise comparisons: $p < 0.001$).

Results for the parietal ROI showed a combination of the effects observed at the parieto-occipital and parieto-central ROIs. Main effects of hemisphere ($F_{(1,13)}= 8.31$, $p = 0.013$) and spatial certainty ($F_{(2,26)}= 6.53$, $p = 0.005$) were observed, reflecting greater contralateral than ipsilateral desynchronization (pairwise comparisons: $p = 0.013$), and desynchronization that increased linearly with spatial certainty (linear contrast: $F_{(1,13)} = 8.27$, $p = 0.013$). A cue-direction X hemisphere interaction was also observed ($F_{(1,13)} = 5.59$, $p = 0.034$). Pairwise comparisons revealed that for rightward cues, ipsilateral hemisphere alpha was greater than contralateral alpha (pairwise comparisons: $p = 0.003$), however there was no significant hemisphere difference for leftwards cues ($p > 0.4$). Unlike the occipito-parietal ROI the hemisphere X spatial certainty interaction was only of marginal significance ($F_{(2,26)} = 2.65$, $p = 0.089$), due to a trend towards increasingly lateralized alpha-band activity as spatial certainty increased (linear contrast: $F_{(1,13)} = 4.46$, $p = 0.055$).

3.3.3. Beta Power

Beta-band effects were predominant at electrodes over left hemisphere motor areas (Figure 3-3A). To investigate how beta-band activity linked to motor preparation was modulated in the task, we performed a repeated-measures ANOVA on beta-band power at the parieto-central ROI with factors of cue direction (left, right), hemisphere (ipsilateral, contralateral) and spatial certainty (60%, 80%, 100%). This revealed a significant main effect of spatial certainty ($F_{(2,26)} = 4.1$, $p = 0.029$), with greater beta desynchronization when spatial certainty was high (Figure 3-3B; linear contrast: $F_{(1,13)} = 8.7$, $p = 0.011$). A significant cue direction X hemisphere interaction ($F_{(1,13)} = 9.6$, $p = 0.008$) was also observed. As for this ROI in the alpha-band frequency range, this reflected greater desynchronization over left versus right hemisphere following both leftwards (pairwise comparisons: $p = 0.024$) and rightwards (pairwise comparisons: $p = 0.006$) cues.

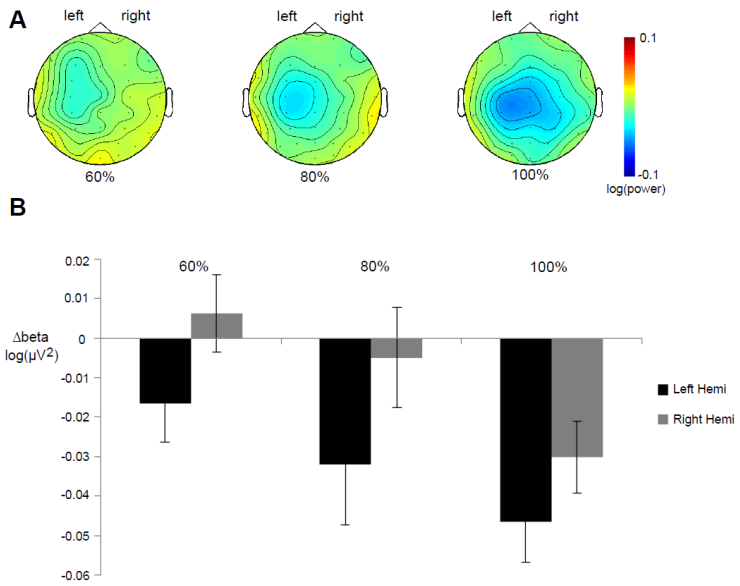


Figure 3-3. Beta-band desynchronization was predominant over left hemisphere motor areas 1050-1250ms after cue onset, and increased in magnitude with spatial certainty. Note that the left hemisphere is contralateral to motor responses, which were always made with the right hand. **(A)** Topography of beta desynchronization at 60%, 80% and 100% spatial certainty levels. **(B)** Mean beta power at parieto-central electrodes CP3/4 and C3/4 at each spatial certainty level (error bars are S.E.).

3.3.4. Visual Potentials

To investigate how spatial certainty affected the amplitude of early sensory event-related potentials elicited by the target array at electrodes showing graded alpha-band lateralization (Figure 3-4), a repeated-measures ANOVA was performed on P1-N1 amplitude data from the parieto-occipital ROI, with factors of hemisphere (contralateral or ipsilateral relative to the cued direction), and spatial predictability (60%, 80%, 100%). The ANOVA revealed a spatial predictability X hemisphere interaction ($F_{(2,26)} = 7.6$, $p = 0.002$). Posthoc analyses revealed that as spatial predictability increased, the P1-N1 potential amplitude was larger in the contralateral hemisphere relative to the ipsilateral hemisphere (linear contrast: $F_{(1,13)} = 11.1$, $p = 0.005$). Consistent with this effect, pairwise comparisons revealed an increase in the contralateral relative to ipsilateral P1-N1 amplitude that was significant when spatial predictability was 100% ($p = 0.006$) and 80% ($p = 0.01$), but not 60% ($p = 0.10$).

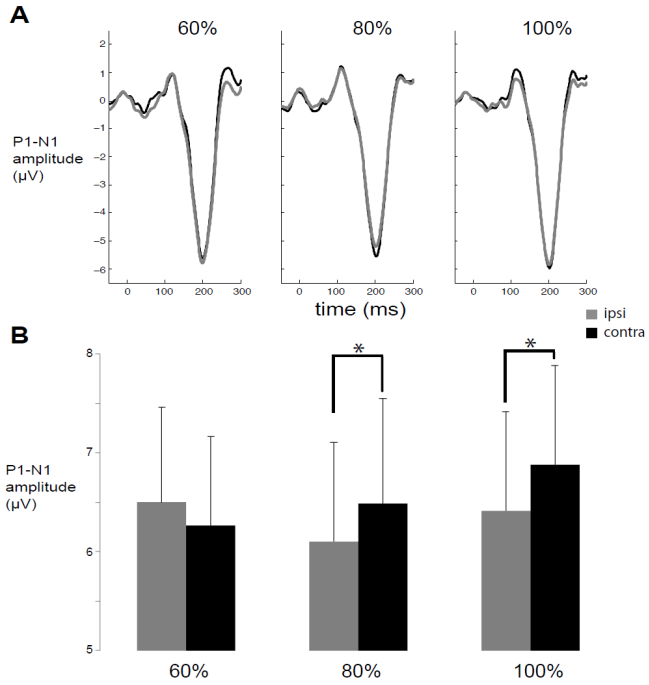


Figure 3-4. Target-evoked event-related potentials. **(A)** Target-evoked potentials for validly cued target arrays as a function of spatial predictability. **(B)** Contralateral and ipsilateral modulation of the P1-N1 complex amplitude as a function of spatial predictability.

3.3.5. Correlation Between Behavioral and Neural Results

To investigate the relationship between individual subjects' behavior and neural effects, for each individual we regressed the behavioral and neural measures described above against the spatial certainty indicated by the cues (for alpha and beta power) or against the spatial predictability of the target location (for behavioral measures and target-evoked ERPs). The resulting regression slope coefficients were then compared across subjects using two-tailed Pearson correlations.

For the P1-N1 complex, the slopes were calculated as the average contralateral-ipsilateral difference at electrodes O1/2 and PO7/8. Supporting a tight link between ERP measures of target processing and behavior, P1-N1 complex slopes were positively correlated with the slopes of individuals' accuracy measures (r = 0.63, p = 0.016) and negatively correlated with their reaction-time slope (r = -0.82, p < 0.001) (Figure 3-5A-B).

Previous studies have specifically linked facilitation of attended stimulus processing to contralateral alpha desynchronization (Kelly et al., 2009; Sauseng et al., 2005; Thut et al., 2006; Yamagishi et al., 2008) and/or suppression of distracter stimuli processing to increased ipsilateral alpha synchronization (Kelly et al., 2006; Rihs et al., 2009; Worden et al., 2000). We therefore calculated the slopes of alpha modulation separately for the contralateral and ipsilateral hemispheres in the occipito-parietal ROI. Contralateral alpha was positively correlated with reaction time (r = 0.70, p = 0.005) (Figure 3-5C), whereas ipsilateral alpha was only marginally associated with reaction times (r = 0.53, p = 0.053). Given that there was high multicollinearity between ipsilateral and contralateral alpha slope measures (r = 0.73, p = 0.003), we calculated one-tailed partial correlations to investigate whether significant reaction-time variance was uniquely accounted for by ipsilateral and/or contralateral alpha. Alpha desynchronization over the contralateral hemisphere explained a

significant amount of reaction time variance after controlling for ipsilateral hemisphere alpha (partial r = 0.54, p = 0.027), however a non-significant relationship was observed between ipsilateral alpha and reaction times after controlling for contralateral alpha (partial r = 0.034, p > 0.45). Further supporting a tight link between contralateral alpha and target processing, there was also a significant correlation between P1-N1 slopes and contralateral (r = -0.565, p = 0.035) (Figure 3-5D) but not ipsilateral (p > 0.2) alpha slopes.

Finally, we correlated beta-power slopes from parieto-central electrodes with behavioral performance slopes, and with alpha-modulation slopes. Significant positive correlations were found between left-hemisphere beta slopes and reaction-time slopes (r = 0.56, p = 0.039), and between left-hemisphere beta slopes and contralateral alpha slopes (r = 0.62, p = 0.018). The correlation between beta slopes and ipsilateral alpha slopes was of marginal significance (r = 0.48, p = 0.084).

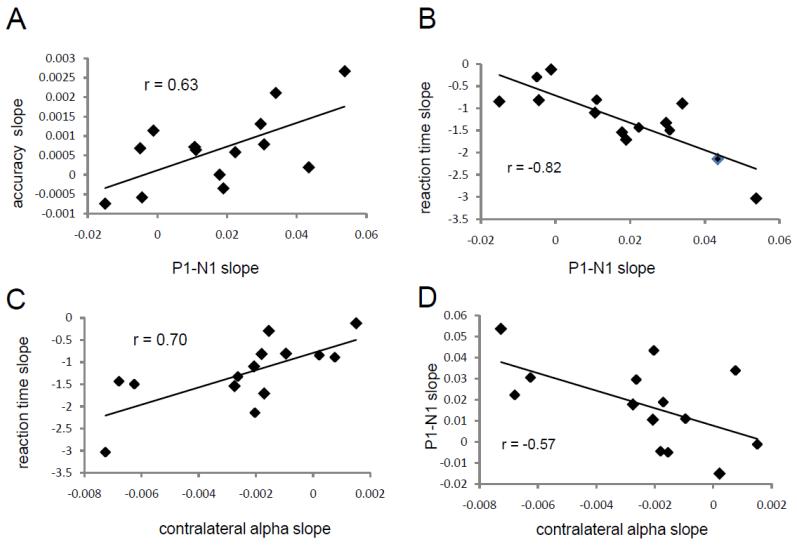


Figure 3-5. Correlations in the effects of attentional cues on individuals' behavioral and neural data. The magnitude of each slope co-efficient reflects the degree with which each participant's behavioral or neural effects varied with spatial certainty (see text for details). P1-N1 slopes were associated with **(A)** accuracy and **(B)** reaction time. Contralateral alpha slopes were associated with **(C)** reaction time and **(D)** P1-N1 complex slopes.

3.4. Discussion

The primary aim of this study was to investigate whether graded changes in alpha lateralization are associated with graded changes in the direction of voluntary attention. Presenting participants with central symbolic cues of varying validity levels resulted in a graded lateralization of alpha-band activity over occipito-parietal electrodes. To our knowledge, these results provide the first demonstration that parametric changes in top-down attentional goals can modulate the anticipatory lateralization of alpha rhythms in a graded manner. The consistency of the relationship supports the hypothesis that lateralization of alpha rhythms contributes to the neural mechanisms underlying the allocation of selective attention (Foxe et al., 1998; Worden et al., 2000). We also characterised the relationship between spatial certainty provided by cues and individual subjects' anticipatory modulation of alpha-band activity, and the relationship between spatial predictability and subjects' behavioral and neural measures of target processing. We found that alpha modulation contralateral to attention during a preparatory period significantly predicted three subsequent measures: lateralization of the early sensory P1-N1 complex, reaction times, and a beta-band measure of motor preparation. Together, these results suggest that greater modulation of alpha-band activity may reflect larger attentional shifts, resulting in greater attentional effects on behavioral performance. This finding complements previous studies which did not distinguish whether variations in lateralization of alpha-band activity reflected variations in the top-down control of attention or simply spontaneous variations in cortical excitability (Kelly et al., 2009; Thut et al., 2006), as well as studies emphasizing a link between visual detection performance and tonic differences in individuals' alpha-band activity (Dockree et al., 2007; Romei et al., 2008b).

For this task, behavior was more closely linked with the slope of contralateral than ipsilateral hemisphere alpha modulation. Although our results highlight the relationship between contralateral alpha activity and behavioral performance, such effects may depend on precise aspects of task configuration. For example, in a steady-state visual evoked potential study by Kelly and colleagues (2006), a continuous stream of bilateral stimuli was presented while participants attended to one side of the display. Increased alpha synchronization was observed ipsilateral to the attended side, however attention did not affect contralateral alpha activity. Although the authors did not directly link the increases in ipsilateral alpha power to behavior, and acknowledge that the lack of contralateral alpha modulation may have resulted from the continuous bilateral visual stimulation in their task, their data provide compelling evidence that allocation of attention can also result in ipsilateral alpha enhancement. Given the high contrast stimuli used in our task, a recent fMRI study is also of note. Sylvester and colleagues (2008) demonstrated that when participants expected either low or high contrast targets, spatial attention led to anticipatory increases in prestimulus BOLD activity contralateral to the attended side (Sylvester et al., 2008). However, a greater BOLD signal reduction was observed ipsilateral to the attended side, and this predicted behavior when low-contrast versus high-contrast targets were expected. More generally, a range of studies have suggested that attentional selection affects behavioral performance via the operation of different mechanisms as a function of task difficulty (Boudreau et al., 2006; Prinzmetal et al., 2009; Rees et al., 1997), stimulus contrast (Martinez-Trujillo & Treue, 2002; Reynolds et al., 2000; Sylvester et al., 2008), individual differences in behavioral strategies (Abbey & Eckstein, 2006; Boudreau et al., 2006), the presence and location of distracters (Shiu & Pashler, 1994), spatial certainty (Gould et al., 2007; Palmer et al., 1993; Pelli, 1985), external noise levels (Lu et al., 2002), the nature of the visual judgement being made about targets (Abbey & Eckstein, 2006; Smith, 2000), and the nature of attentional cues (Prinzmetal et al.,

2005). Additional research is necessary to clarify whether such differences influence whether behavioral performance is associated with modulation of alpha activity contralateral and/or ipsilateral to attention.

At parietal and parieto-central electrodes we observed bilateral modulation of alpha power with changes in spatial certainty, regardless of the cued direction. Given that alpha sources are widely distributed across occipito-parietal cortex (Basar et al., 1997; Hari & Salmelin, 1997; Pineda, 2005), and that modulation of alpha-band activity results from a wide range of task manipulations (Hari & Salmelin, 1997; Palva & Palva, 2007; Rihs et al., 2009; Salenius et al., 1995; Salmelin et al., 1994; Snyder & Foxe, 2010; Tuladhar et al., 2007; Vanni et al., 1997), this bilateral effect may reflect additional cortical activity that scales with spatial uncertainty. Speculatively, the bilateral effect we report here may be related to the extent with which attention was shifted or maintained (Banerjee et al., 2011; Kelley et al., 2008; Vandenberghe et al., 2001; Yantis et al., 2002).

Given that participants made right-handed button responses in our task, our observation of greater beta desynchronization over left hemispheric motor regions is consistent with the well-established role of beta desynchronization in motor preparation (Donner et al., 2009; Doyle et al., 2005; McFarland et al., 2000; Tzagarakis et al., 2010a; van Wijk et al., 2009). In addition, we found that beta desynchronization scaled with the spatial certainty provided by cues, and the slope of this effect correlated with participants' alpha modulation at occipito-parietal electrodes contralateral to attention, and with their reaction times. As the spatial cues in this study did not provide information about the target orientation, they did not allow participants to prepare a specific motor response. However, when spatial certainty was higher participants may have been able to anticipate being able to respond more quickly to the target array when it appeared, resulting in greater generalized

motor preparation at the end of the cue-target interval. This finding is consistent with the suggestion that the role of beta-band desynchronization in response preparation may be similar to the role of alpha-band desynchronization in visual attention (van Wijk et al., 2009).

Chapter 4 - Oscillatory Correlates of Motor-Related Decision Making in the Human Brain

To decide effectively information must not only be integrated from multiple sources but it must be distributed across the brain if it is to influence structures such as motor cortex that execute choices. We tested whether oscillatory brain activity over motor cortex reflected not just motor preparation but also the perception, integration, and distribution of information for decision making. This chapter presents results from an experiment in which human participants integrated information from multiple, but only partially informative, cues in a probabilistic reasoning task in an optimal manner. Lateralization of alpha- and beta-band activity in the electroencephalogram reflected the logarithm of the likelihood ratio associated with each new piece of information witnessed – a key quantity for decision making – as well as the sum of the log likelihoods associated with previous cues.

4.1. Introduction

Everyday decision making may be underpinned by neural processes that integrate relevant perceptual inputs over time to guide action selection. Key support for this idea has come from electrophysiological studies with non-human primates which demonstrated that the temporal dynamics of neuronal firing rates in frontal cortex, motor planning regions and sensorimotor integration regions such as the lateral intraparietal area (LIP) are consistent with encoding of a decision variable (Cui & Andersen, 2007; Gold & Shadlen, 2007; Ratcliff et al., 2003b; Shadlen & Newsome, 1996; Shadlen & Newsome, 2001; Smith & Ratcliff, 2004). A wide range of human and monkey decision-making behaviours are well described by the same sets of mathematical accumulator models, which account for accuracy and reaction-time distributions (Bogacz et al., 2006; Brown & Heathcote, 2005; Ratcliff & Smith, 2004;

Smith & Ratcliff, 2004; Soltani & Wang, 2010; Wang, 2002). Despite an apparent consensus that activity in motor and premotor structures reflects how much evidence has been integrated in favour of specific responses (Donner & Siegel, 2011; Donner et al., 2009; Forstmann et al., 2010a; Forstmann et al., 2010b; Gold & Shadlen, 2007; Hanks et al., 2006; Heekeren et al., 2008; Kable & Glimcher, 2009; Tosoni et al., 2008) and evidence that prefrontal regions play a causal role in decision making (Kim & Shadlen, 1999; Philiastides et al., 2011), it remains unclear how the temporal dynamics of neural activity in human motor planning structures reflect encoding of a decision variable. It is also unclear whether human motor planning structures causally underpin categorical decision choices.

A recent experiment required monkeys to associate arbitrary shapes with likelihoods of receiving a reward when a saccade was made to one of two peripheral targets, and to track the sum of the evidence provided by a sequence of these shapes in order to decide whether to make a leftward or rightward saccade (Yang & Shadlen, 2007). Throughout a delay period following the presentation of each shape, firing rates of LIP neurons appeared to track this sum of evidence, with firing rates proportional to the log likelihood of evidence for a particular response. For the present experiment, we developed a human analogue of this task that was suitable for use with non-invasive electrophysiological recordings taken from the scalp. We recorded EEG while presenting humans with between one and four pieces of evidence before they were required to make a left- or right-handed response on the basis of the sum of the observed evidence. Our primary hypothesis was that updating of evidence would be linked to dynamic updating of response preparation, and that this would result in modulation of lateralized beta-band synchrony over primary motor and/or premotor regions of the cortex in proportion the precise amount of evidence available to participants (Donner & Siegel, 2011; Donner et al., 2009; Engel & Fries, 2010; van Wijk et al., 2009).

4.2. Materials and Methods

4.2.1. Participants

Twenty-four paid volunteers (mean age 26, standard deviation 3.9, range 19-34; 13 female) participated after giving informed written consent. All participants were right-handed (Oldfield, 1971), and reported having normal or corrected-to-normal visual acuity and no history of neurological disorders. The methods and procedures used in the study were non-invasive and had ethical approval from the University of Oxford Central University Research Ethics Committee.

4.2.2. Probabilistic Categorization Task

The task used is an adaptation of the sequential version of the Weather Prediction Task employed by Yang and Shadlen (2007) (Knowlton et al., 1996; Knowlton et al., 1994). In summary, on each trial participants attempted to determine whether the world was in a 'left' or 'right' state by integrating the evidence provided by up to four sequentially presented cue shapes (see Figure 4-1). After pressing a response button with either the left or right index finger, they received positive or negative feedback depending on whether their guess was correct.

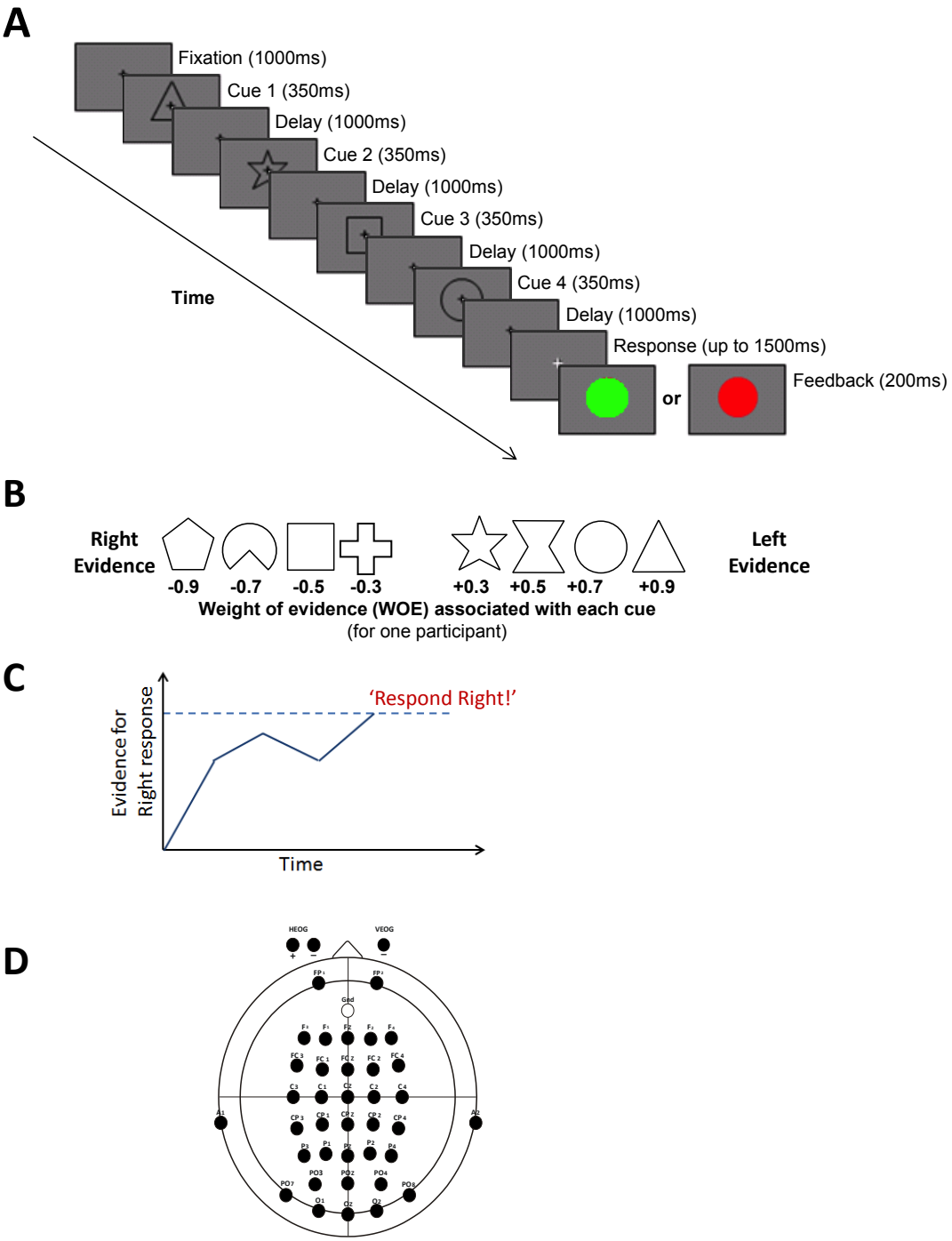


Figure 4-1. Experimental Task. (A) Schematic of a typical trial, in which four cue stimuli are shown providing information about whether a left or right response will be rewarded**. (B)** The set of eight cue shapes and their mappings onto WOEs for one participant. **(C)** A schematic of fluctuations in the evidence for a right response for the example trial in (A) assuming the shape-WOE mappings shown in (B). At the end of the trial the evidence is in favour of a right response and the participant should respond with a right-hand button-press. **(D)** Electrode montage used in the EEG experiment.

Prior to each trial, the stimulus presentation computer randomly set the world to be in either a 'left' or 'right' state. Between one and four cue shapes $\{s_1, s_2, s_3, s_4\}$ were then selected from a set of 8 shapes $\{S_1, S_2, \ldots, S_8\}$. On average, all eight shapes were equiprobable ($P(s_i = S_x) = 1/8$ for all x). However, on each trial the probabilities of observing specific cue shapes were biased depending on the world state. Observation of the selected shapes thus provided probabilistic evidence about the world state. Specifically, each shape was associated with a fixed weight from the set of weights $w = \{-0.9, -0.7, -0.5, -0.3, +0.3, +0.5, +0.7, +0.9\}$. The relationships between shape weights and world state probabilities were defined such that shape weights were equal to the change in log-odds that observing a shape provided in favour of a left- or right-handed response (see Figure 4-2). Arbitrarily, positive weights were associated with leftwards world states. Shapes associated with positive weights were therefore more likely to be observed when the world was in a 'left state' and shapes associated with negative weights were more likely to be selected when the world was in a 'right state':

$$w_i = \log_N \frac{P(L|s_i)}{P(R|s_i)} \qquad \textit{Eq. 4-1.}$$

$$\mathrm{P}(s_i|L) = \frac{1}{\mathrm{P}(L)} \times \frac{1}{N} \times \frac{N^{w_i}}{(1 + N^{w_i})} \qquad \textit{Eq. 4-2.}$$

$$\mathrm{P}(s_i|R) = \frac{1}{\mathrm{P}(R)} \times \frac{1}{N} \times \frac{N^{-w_i}}{(1 + N^{-w_i})} \qquad \textit{Eq. 4-3.}$$

$$= \frac{1}{\mathrm{P}(L)} \times \frac{1}{N} - \mathrm{P}(s_i|L)$$

where $P(s_i|L)$ and $P(s_i|R)$ are the probabilities of observing cue shape s_i given a left (L) or right (R) world state. N is the total number of cue shapes and is thus a constant with $N = 8$ during the main experiment. $P(L)$ and $P(R)$ are the probabilities of the computer selecting a

left or right world state and are constant, with P(L) = P(R) = 0.5. Cue shapes were sampled independently and with replacement, and the mapping between shapes and weights was randomised across participants.

Following observation of a sequence of n shapes the overall evidence accumulated in favour of a left versus right state is the posterior log-odds – the logarithm of the ratio of the probabilities of the world being in a left versus right world state given the observed shapes. Given Equations 4.1 to 4.3 and Bayes' rule, the posterior log-odds is equal to the sum of the weights associated with the observed shapes. Because left and right world states were equi-probable, the posterior log-odds is also equal to the log-likelihood ratio (the logarithm of the ratio of the probabilities of observing the presented cue shapes under the assumption of a left versus right world state). That is:

$$WOE = \log_N \frac{P(s_1, \ldots, s_n|L)}{P(s_1, \ldots, s_n|R)} = \log_N \frac{P(L|s_1, \ldots, s_n)}{P(R|s_1, \ldots, s_n)} = \sum_{i=1}^{n} w_i \qquad \textit{Eq. 4-4.}$$

For convenience, we hereafter refer to all three of the above quantities (the sum of one of more cue weights, the log-likelihood ratio and the posterior log-odds) using the term 'weight of evidence' (WOE) (Eq. 4-4). However, in our analyses we make several subtle distinctions regarding the WOE, which we define here. The 'overall WOE' or 'accumulated WOE' describes the WOE at the end of an epoch or trial, whereas the 'prior WOE' is the accumulated WOE at the start of an epoch, and is zero when the first shape appears. The term 'cue WOE' describes the weight associated with a cue shape presented in a particular epoch of a trial, and is equal to the update value that should be added to the prior WOE upon observation of the shape. Thus, at the end of any epoch, the overall WOE is equal to the sum of the prior WOE and the cue WOE.

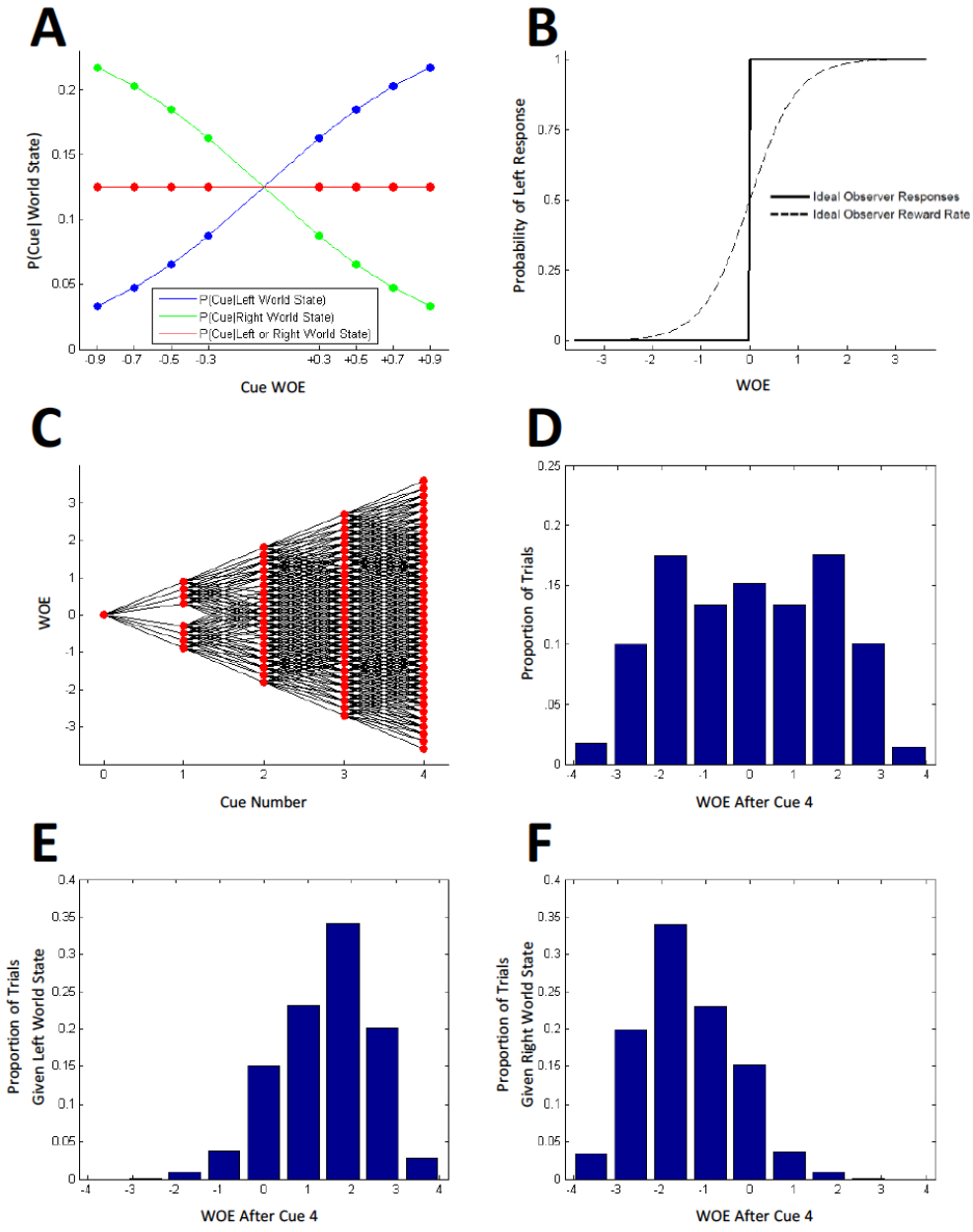


Figure 4-2. Key design features of the experimental task. (A) The relationship between cue WOEs and the probabilities of observing each cue given a left or right world state (blue and green lines) and on average (red line). **(B)** Response pattern of an ideal observer (solid line) and the associated expected reward rate (dashed line). Note that the curve depicting the reward rate also describes a probability-matching response pattern. **(C)** All possible evidence states at each stage in the task (red dots) and all possible trajectories that can lead to each state (black lines). **(D)** Histogram of WOEs after the fourth cue for 10,000 simulated trials shows the broad distribution of WOEs achieved with this design. This distribution reflects summation of two skewed distributions of WOEs when the world was in **(E)** a 'left state' or **(F)** a 'right state'.

Given any WOE, the optimal estimates of the underlying world state are therefore:

$$P(L|s_1, \ldots, s_n) = \frac{N^{WOE}}{1 + N^{WOE}} \qquad \textit{Eq. 4-5.}$$

$$P(R|s_1, \ldots, s_n) = 1 - P(L|s_1, \ldots, s_n) \qquad \textit{Eq. 4-6.}$$

We highlight a subtle but significant difference between the formulation of our task and the task of Yang and Shadlen (2007). Their design involved selection of shapes from a uniform random distribution, and the world state was probabilistically determined at the end of the trial based on the sum of the weights associated with the observed shapes. This led to what is known as a 'failure of conditional independence' in their task (see Yang & Shadlen, 2007, Appendix A), with the consequence that Eq. 4-4 only held in their task after presentation of the fourth shape. The overall change in the log-likelihood provided by a shape in their task could differ by a factor of up to ~3x, depending on when in the trial the shape was presented (see Yang & Shadlen, 2007, Table 1). In contrast, we ensured that log-likelihoods were conditionally independent by selecting shapes from biased distributions according to Equations 4.1 to 4.3. We believe this conditionally independent design has greater ecological validity, since it formally reflects a context in which independent samples of evidence about an underlying world state are observed (Stern et al., 2010). This was particularly important in the context of this experiment, in which human participants were required to learn the task in a relatively short time, and since we wished to model the effects of partial evidence during each trial (see also de Lange et al., 2010).

4.2.3. Procedure – EEG Session

Participants completed the task seated comfortably in a dimly lit room with their head position stabilized by a chin rest. They were instructed to maintain central fixation and asked not to blink during experimental trials.

A schematic of a typical trial is shown in Figure 4-1. Each trial commenced with presentation of a central fixation cross for 1,000 ms. One or more cue shapes were then presented sequentially. Each cue shape was presented for 350 ms, followed by a 1,000 ms delay period in which only the central fixation cross was visible. On most trials (70% of trials), participants observed four symbolic cue shapes. To ensure that participants were integrating the evidence provided by the cue shapes in an on-going fashion, we also included shorter trials in which only one (10% of trials), two (10% of trials) or three (10% of trials) cue shapes were presented. The fixation cross then turned white as a 'go signal', indicating that the sequence of shapes was complete and that participants should respond. Participants responded with a left- or right-hand index finger button press using a DirectIN response box (Empirisoft, USA). They were instructed to emphasize accuracy in the task, but also to respond in a timely fashion. The maximum allowed response time was 1,500 ms. After the response period participants received feedback indicating whether they correctly guessed the world state. If participants exceeded the maximum response time or responded during the trial but before onset of the go stimulus, feedback indicated the trial was a 'miss'.

Participants completed a 1.5-hour training session less than one week before the EEG session (see below). In the EEG session participants completed 40 practice trials with all eight cues, then 400 trials during which EEG was recorded. Rest breaks were provided every 40 trials.

4.2.4. Procedure - Training Session

In an initial training session, participants were instructed that the task involved observation of a sequence of shapes providing probabilistic evidence about whether the computer had assigned the world state to be 'left' or 'right', and that their task was to infer this hidden world state and respond accordingly with a unimanual button press. To assist learning, at the start of the training session participants were told that the order of cue presentation did not affect the impact the evidence provided and were shown a ranking of the shapes reflecting how predictive they were and whether they provided evidence for a left or right response. They were explicitly informed that they would never be told the exact weighting of each shape or how to combine the shapes, and that their main aims in the training session were to learn how much weight to give each shape through trial-and-error and to work out how to combine information from multiple shapes.

The training session was broken down into two parts. For the first part participants were told the main aim was to familiarise themselves with the task and get a rough idea of the weighting appropriate for each pair of shapes, and that they should refine this throughout the session. To begin with, participants first completed practice trials with the most predictive pair of shapes ($w = \pm 0.9$), then with the next most predictive pairs of shapes ($w = \pm 0.7$). They then completed a practice block with both of these pairs of shapes together (w = -0.9, -0.7, +0.7, +0.9). This procedure was then repeated with the less predictive four shapes (w = -0.5, -0.3, +0.3, +0.5). Practice continued until participants reported feeling comfortable using the shapes in that block, typically 10-20 trials with single pairs of shapes and 20-40 trials with sets of four shapes. Participants then completed a 40-trial practice block with six shapes (excluding only the most predictive pair of shapes) and a practice block with all eight cue shapes (40 trials). To ensure the evidence provided by shapes was constant throughout the

training, the cue set size *N* was varied appropriately in Equations 4.1 to 4.6 to determine the probabilities of observing each cue shape.

After a short break, participants completed the second part of the training session. This was a shortened version of the main experimental task - participants completed 240 trials with all eight cue shapes, with rest breaks every 40 trials. In this part of the training session, participants were instructed to try and refine their estimates of the weighting to apply to each shape. They were also asked to try and maintain central fixation and not to blink during experimental trials.

Except for the changes in the cue set size described above, all task parameters in the training session were identical to those in the EEG session.

4.2.5. Visual Stimuli

Stimuli were presented at 60 Hz on a 22-inch Sony Trinitron CRT monitor at a viewing distance of 100 cm, with stimulus presentation and response acquisition controlled using Presentation 13.0 (Neurobehavioral Systems). All stimuli were presented centrally and against a uniform mid-gray background. The fixation cross consisted of two 0.3^{o} x 0.06^{o} black lines. The eight cue stimuli had a diameter of approximately 2.3^{o} and a line width of 0.02^{o}. The go signal was identical to the fixation cross except that it was coloured white. Feedback consisted of a 2.5^{o} disc, coloured green if the participant correctly guessed the world state, red if their guess was incorrect, and yellow if they responded too slowly or before the onset of the go stimulus.

4.2.6. Data Analysis Software

Analysis of behavioural and EEG data was performed using SPSS (IBM) and custom Matlab scripts in conjunction with code from the FieldTrip (Oostenveld et al., 2011) and EEGLab (Delorme & Makeig, 2004) toolboxes for Matlab (The Mathworks).

4.2.7. Behavioural Data Analysis

We used logistic regression to estimate the impact of each cue shape on participants' choices from trials in which four cues were presented, as in previous studies (Philiastides et al., 2010; Yang & Shadlen, 2007). To individual subjects' data we fit:

$$P(L) = \frac{8^K}{1 + 8^K}, \text{where } K = \beta_0 + \sum_{i=1}^{8} w^*_i N_i \qquad \textit{Eq. 4-7.}$$

where P(L) is a binary vector indicating whether a left or right response was made on each trial, N_i is the number of times shape s_i was observed on trial i, and w^*_i is the fitted subjective weight of evidence (SWOE) for shape s_i. To characterise the relative relationship between true shape WOEs and participants' SWOEs, we calculated the Pearson correlation co-efficient between each participant's SWOEs and the true shape WOEs. The estimated SWOEs for several observers were very large due to their high performance (note that the SWOEs for an ideal observer, who always makes right-hand responses when the overall WOE is negative and left-hand responses when it is positive, are proportional to the true shape WOEs but infinite). We therefore normalized the set of w^*_i values within each subject for display purposes.

To analyse reaction times, four-cue trials were binned according to the WOE in favour of the response made on each trial. As there were relatively few trials on which participants' responses were not consistent with the sign of the WOE, we put all such trials into a single bin. The remaining trials were separated into another six equally spaced bins with edges between WOEs of 0 and ±3.6. Reaction times were then subjected to repeated-measures ANOVA with factors of bin number (1 to 7) and response hand (left or right).

To assess overall performance on shorter trials we subjected accuracy, reward, and miss rates to repeated-measures ANOVAs. Note that accuracy refers to whether the participant made the optimal response, but given the probabilistic nature or the task this does not always correspond with whether or not a reward was received.

Where appropriate, all statistical comparisons were Greenhouse-Geisser-corrected for lack of sphericity.

4.2.8. EEG Recording and Pre-Processing

EEG was recorded continuously (1,000-Hz sampling rate; left mastoid reference; NuAmps digital amplifiers; Neuroscan, El Paso, TX) from 40 scalp sites using Ag/AgCl electrodes mounted on an elastic cap (Easy Caps, Germany) according to the 10-20 international system. The montage included 7 midline sites (OZ, POZ, PZ, CPZ, CZ, FCZ and FZ), 14 sites over each hemisphere (O1/O2, PO3/PO4, PO7/PO8, P1/P2, P3/P4, CP1/CP2, CP3/CP4, C1/C2, C3/C4, FC1/FC2, FC3/FC4, F1/F2, F3/F4 and FP1/FP2), left and right mastoids, HEOG and VEOG electrodes to monitor the EOG bipolarly, and an additional electrode (AFZ) used as ground (see Figure 4-1D). Vertical EOG was calculated as the bipolar derivation between FP2 and the lower VEOG electrode. Recordings were re-

referenced offline to the average EEG. Due to the low numbers of trials in which one, two or three cue shapes were presented, EEG data were only analysed for trials in which four cue shapes were presented. For these trials, continuous epochs from 1,000 ms before onset of the first cue shape to the end of the response period were included in analyses except when showing recording artefacts, when saccades or blinks occurred in the EOG, or when participants made early or late responses. This resulted in inclusion of 222 trials per subject on average (79% of all four-cue trials, standard deviation 9.9%). Epochs were defined using digital codes sent to the EEG recording computer to mark the presentation of the cue and target in each trial type.

4.2.9. Spectral Analysis

Power spectra were computed for single-trial data using the multi-taper method (Mitra & Pesaran, 1999; Thomson, 1982) with a single Hanning taper (1-35 Hz, 0.5 Hz frequency steps, 600-ms temporal smoothing window, 50-ms window step size) using Fieldtrip (Oostenveld et al., 2011). The relatively long temporal smoothing window was chosen to allow us to discriminate between oscillatory activity in the alpha- and beta-band frequencies. Using shorter temporal smoothing windows resulted in qualitatively similar results, but reduced the frequency resolution such that clear distinction between the alpha and beta bands was not possible.

Raw power data at each time-frequency sample were converted to decibel (dB) units by $\log_{10}$-transforming the raw data then multiplying it by 10, yielding approximately normally distributed data suitable for standard parametric statistical tests (Kiebel et al., 2005). Spectral representations of phase-locked responses on the task were obtained by averaging

over all trials for each participant, and then performing spectral analysis on the average waveform using the procedures above. To characterise the overall and phase-locked spectral profile on the task, averaged overall and phase-locked data for each participant were baseline corrected using the 500-ms prior to onset of the first cue shape. A student's t-test was subsequently performed on all sensor-time-frequency bins.

4.2.10. Region of Interest Selection and Beta Rebound

Our key hypotheses relate to the spectral power difference between left- and right-hemisphere motor regions. Based on previous motor planning and imagery studies (McFarland et al., 2000; Pfurtscheller et al., 1996; van Wijk et al., 2009; Wolpaw & McFarland, 2004), we pre-defined a left-hemisphere region of interest (ROI) as the average spectral power at electrodes C3 and CP3, and a right-hemisphere ROI as the average at electrodes C4 and CP4. We also validated this ROI using an independent data set. For this, we aligned raw EEG data to participants' responses and re-computed time-frequency data as described above. We then identified the peak electrodes at which differential beta modulation was present following left- versus right- hand responses (the 'beta rebound').

4.2.11. Statistical Analysis of Spectral Data

We applied several simple or multiple linear regression models to single-trial spectral data. Single-trial data were either raw data from individual sensors, an average over several sensors, or a 'lateralization index' (LI), calculated as the left-hemisphere minus right-hemisphere difference for left/right symmetric electrode pairs or ROIs.

In general we used a data-driven approach to identify the times and frequency-bands of significant effects (Donner & Siegel, 2011). Under this approach, each regression model was fit independently for each subject and at every sensor, frequency and time bin of interest. We then identified contiguous clusters of time-frequency bins at each sensor showing significant power modulation using one-sample *t* tests against zero with a threshold at $p < 0.01$ (two-tailed). Statistical significance of clusters was assessed at the group-level whilst controlling the type I false alarm rate using a cluster-based non-parametric randomization method (Maris & Oostenveld, 2007). We defined a second-level test statistic $\sum_T$ as the sum of the T scores of all time-frequency bins in each cluster, and evaluated the significance of each cluster by comparing the original $\sum_T$ statistics to an estimated null distribution from 2,000 randomizations of the data. On each randomization, we permuted the correspondence between each participant's vector of predictor regressors and the observed spectral data, then fit the model and calculated $\sum_T$ statistics as above. The maximum positive and negative cluster statistics from each randomization defined the estimated null distribution. We then estimated two-tailed Monte Carlo *p* values for each original $\sum_T$ statistic against the estimated null distribution. All *p* values were Bonferroni-corrected for multiple comparisons when analysing multiple sensors.

In cases where we wished to investigate more clearly the temporal evolution of effects within already-defined frequency bands of interest, we averaged over the power data in the frequency bands of interest before fitting the regression model and assessing significance of results. In these instances clustering was performed as described above, but on adjacent time-bins rather than time-frequency bins.

To test whether oscillatory signals reflected the accumulated WOE, we first fit a simple linear model:

$$y = \beta_0 + \beta_1 WOE_i\,, \quad i = 1,2,3, \text{or } 4 \qquad \textit{Eq. 4-8.}$$

where y is a vector of single-trial spectral power data for a sensor-frequency-time bin for a single participant, and WOE_i is a vector containing the WOEs after the i-th cue on each trial. The fitted co-efficient β_1 describes the effect of the WOE on the spectral power, and the fitted co-efficient β_0 is a fitted constant term.

To dissociate the contributions of the prior WOE and cue WOE to spectral data, we fit the following multiple regression model to spectral data across all four epochs:

$$y_i = \beta_0 + \beta_1 WOE_{i-1} + \beta_2 Q_i + \beta_3 i\,, \quad i = 1,2,3,4 \qquad \textit{Eq. 4-9.}$$

where all β_j are fitted co-efficients, y_i is the spectral power from a sensor-frequency bin at a time-point relative to onset of the i-th cue, Q_i is the WOE provided by the i-th cue, and WOE_{i-1} is the total WOE provided by previous cues at the time the i-th cue is presented, with WOE_{i-1}=0 for i=1. The co-efficient β_3 was included in the model to ensure any non-specific effects of time in the task were modelled.

We conducted two control analyses to investigate whether the relationships we observed between the WOE and oscillatory activity reflected a parametric relationship or could be explained by planning of a categorical (left or right hand) motor response.

The first control model investigated whether 8-14 Hz and 15-25 Hz activity reflected the WOE or the categorical response made at the end of the trial. To maximise sensitivity for this analysis, for each frequency band and for each trial, we averaged 1,000 ms of power data, starting 500 ms after each cue was presented. Within this time window oscillatory activity reflected the most recently presented cue, but not the subsequently presented cue (see Figure 4-8). We then fit linear regression models separately to the data for each frequency band and each of the four epochs:

$$y = \beta_0 + \beta_1 WOE_i + \beta_2 R\,, \quad i = 1,2,3 \text{ or } 4 \qquad \textit{Eq. 4-10.}$$

where y is the average power across the time window following presentation of the i-th shape, WOE_i is the total WOE after presentation of the i-th shape, and R is the response made at the end of the trial. β_0, β_1, and β_2 are fitted co-efficients. We then performed a two-way repeated-measures ANOVA to investigate whether the fitted co-efficients for β_1 and β_2 varied with the epoch number i. A dummy variable was included in the ANOVA model to allow us to test whether the β-parameters were significantly different from zero.

A second control model investigated whether oscillatory power reflected planning of a categorical response which flipped in direction over the course of trials due to fluctuations in the evidence presented to participants. This model was identical to the previous control model except for two changes. First, we only considered data from trials on which participants made the optimal response, suggesting that they correctly tracked the WOE over the course of the trial. Second, R was replaced by the term S_i, which reflected the sign of the WOE after presentation of the i-th shape:

$$y = \beta_0 + \beta_1 WOE_i + \beta_2 S_i\,, \quad i = 1,2,3,4 \qquad \textit{Eq. 4-11.}$$

We performed an additional control analysis to ensure the results were not affected by non-specific factors associated with task difficulty or cue-related surprise. For this, we extended the model in Eq. 4-9 to include terms describing the absolute values of the prior WOE and the cue-related surprise. The model therefore took on the form:

$$y_i = \beta_0 + \beta_1 WOE_{i-1} + \beta_2 Q_i + \beta_3 i + \beta_4 |WOE_{i-1}| + \beta_5 Z_i\,, \quad i = 1,2,3,4 \qquad \textit{Eq. 4-12.}$$

$$Z_i = \log\left(P(s_j|L)P(L)_i + P(s_j|R)P(R)_i\right) \qquad \textit{Eq. 4-13.}$$

where $|WOE_{i-1}|$ denotes the absolute value of the prior WOE and s_j is the cue shape presented in the i-th epoch. $P(s_j|L)$ and $P(s_j|R)$ are the probabilities of observing shape s_j in the i-th epoch under the assumption of a Left or Right world state, respectively. These conditional probabilities are constant for each shape (see the blue and green lines in Figure 4-2A). $P(L)_i$ and $P(R)_i$ are the prior probabilities of a Left or Right world state given the WOE provided by all previously presented shapes on the trial, calculated using Eqs 4.5-4.6. Z_i is therefore the overall log-probability of observing the cue stimulus under the prior WOE and is more negative when the presented cue is surprising given $P(L)_i$ and $P(R)_i$. Note also that this term corresponds to log of the denominator in Bayes' rule when calculating the posterior probability of either world state given the value of the i-th cue:

$$P^*(L|s_i) = \frac{\mathrm{P}(s_j|L)P(L)_i}{\mathrm{P}(s_j|L)P(L)_i + \mathrm{P}(s_j|R)P(R)_i} \qquad \textit{Eq. 4-14.}$$

Finally, we investigated the statistical significance of observed differences in the onset times of effects for the model described in Eq. 4-12. We took the latency at which each regressor was strongest for each individual subject between 0 and 1,000 ms after cue onset and performed two-tailed paired t-tests on these latencies.

4.3. Results

4.3.1. Behavioural Data

Despite the large number of possible shape combinations (8^4 permutations; 330 unique permutations), after the training session participants were able to integrate the information provided by multiple shapes using highly accurate weightings, making right-hand responses when the WOE was negative and left-hand responses when the WOE was

positive (Figure 4-3A). At intermediate WOEs participants made a sharper transition between left and right responses than expected by a probability-matching explanation of behaviour. Confirming that participants learned the proportional weighting to apply to each shape, individual participants' subjective WOEs correlated with the objective cue WOEs (Figure 4-3B; mean $R = 0.97$, $p < 0.001$ for all single-subject correlations).

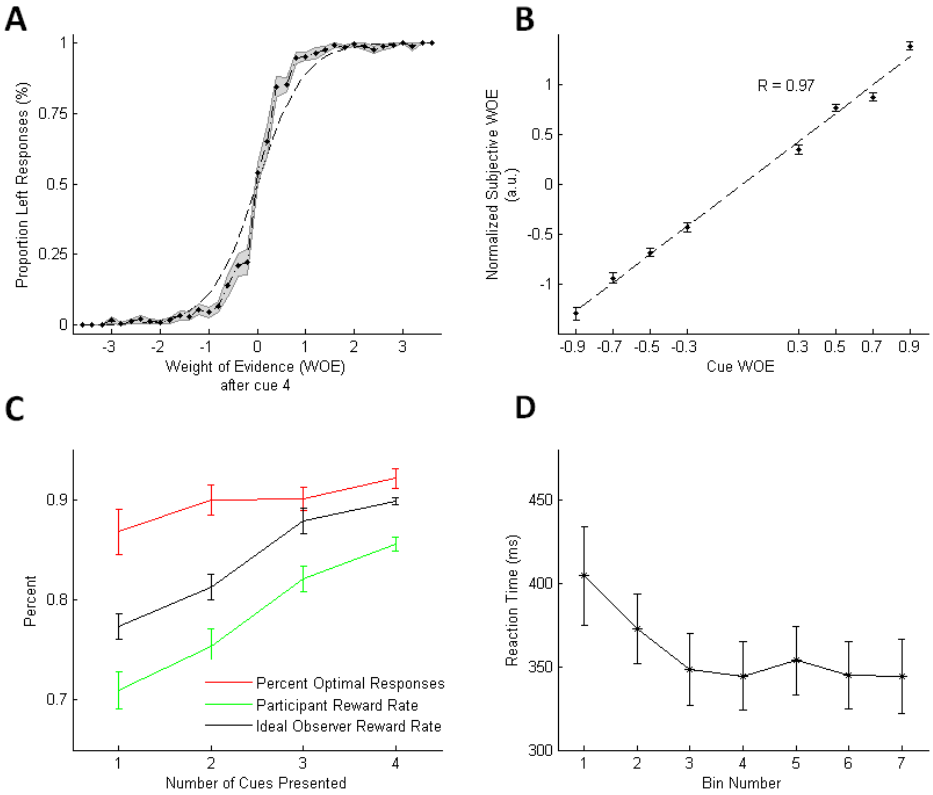


Figure 4-3. Behavioural Data. (A) Participants' responses accurately reflected the total evidence after the fourth cue shape was presented, making a sharp transition from right to left hand responses when the sum of the evidence changed polarity. The dashed line describes a probability-matching response pattern. **(B)** Logistic regression reveals the relative weight of each cue shape on participants' responses closely matched their objective log-likelihood ratio. **(C)** Accuracy was high overall, including on shorter trials on which less than four cues were presented before the go cue (red line), resulting in a reward rate for participants (green line) which increased with the number of shapes as did the reward rate for an optimal observer (black line). **(D)** Response times binned by the WOE after the fourth cue. The WOE in favour of the response increases with the bin number, and the first bin contains all trials where the WOE did not favour the response made.

Accuracy was high on the task, with participants making the optimal choice on 92% of trials with four cues. Accuracy was also high on shorter trials on which less than four cues were presented (87% accuracy for trials with one cue), and increased with the number of shapes presented ($F(3,69) = 5.73$, $p < 0.01$; linear contrast: $F(1,23) = 10.0$, $p < 0.01$). Since |WOE| (the absolute value of the WOE) tended to increase with the number of cues presented, the effect of time on accuracy may reflect lower performance on shorter trials or that small errors in SWOEs have greater impacts when the overall |WOE| is lower. To clarify this, we compared reward rates of real participants and an ideal observer using a repeated-measures ANOVA with factors of number of cues (1 to 4) and observer type (real or ideal). Main effects revealed that reward rates increased with time ($F(3,69) = 37.2$, $p < 0.001$), and that participants' performance was lower than that of the ideal observer ($F(1,23) = 37.1$ $p < 0.001$). However, this performance difference did not change with time ($F(3,69) = 0.65$, $p = 0.58$), suggesting that the quality of evidence integration was not reduced on shorter trials. A repeated-measures ANOVA revealed that the proportion of miss trials did not depend on the number of cue shapes presented before the go cue ($F(3,69) = 2.7$, $p > .05$).

A repeated-measures ANOVA of RT data from four-cue trials binned according to the WOE at the end of the trial (Figure 4-3D) revealed a main effect of the bin number ($F(6,132) = 8.5$, $p < 0.01$). Pairwise comparisons suggest this effect was driven by trials with low WOEs. RTs in the lowest WOE bin were slower than in all other WOE bins (all $ps < 0.01$), and slower in the second WOE bin than all but the first and fifth bins (all $ps < 0.05$).

In summary, behavioural data demonstrate that participants were highly sensitive to the WOE provided by cue shapes on experimental trials. In the following section, we therefore analyse neural data in relationship to our WOE manipulations.

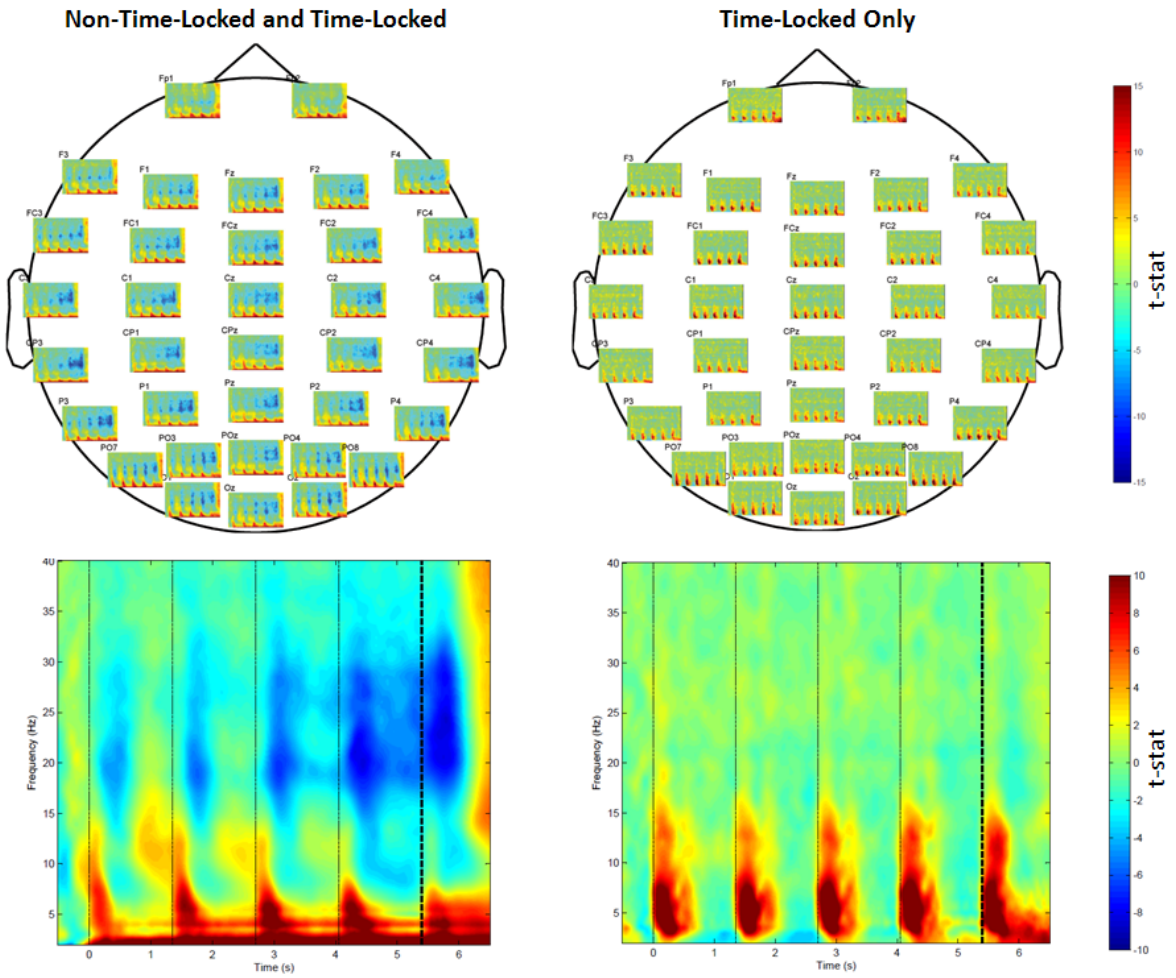


Figure 4-4. Characterisation of overall and time-locked time-frequency responses throughout trials on which four cue stimuli were presented. In the overall response but not the time-locked response, alpha and beta modulation followed presentation of each cue stimulus, and progressively desynchronized as the trial progressed. The upper panels show the average effects at individual sensors. The lower panels show the average effect across sensors in greater detail. The light vertical lines indicate onset times of each of the four cue stimuli and the heavy dashed line indicates the onset of the go cue.

4.3.2. EEG Results

We first characterised the average time-course and spectral profile of EEG responses in our task (Figure 4-4). Presentation of cues was followed by beta-band desynchronization, becoming increasingly prominent towards the end of the trial. Alpha-band activity also tended to be more desynchronized towards the end of trials. These effects were not present in

a phase-locked analysis, suggesting they reflect induced oscillatory neural activity. Induced activity modulation in these frequency bands has been reported in several previous attentional and decision-making tasks (e.g., Donner et al., 2007, 2009; Siegel et al., 2008).

Our primary hypothesis was that if preparatory motor activity continuously updates to reflect available evidence, the left-hemisphere minus right-hemisphere lateralization index (LI) at electrodes overlying motor cortices should correlate with fluctuations in the overall WOE in favour of a left- versus right-hand response. Consistent with this hypothesis, there was evidence of a strong relationship between the overall WOE and alpha- and beta-band lateralization. Figure 4-5A shows the results of the regression analysis between the overall WOE after the fourth cue and the LI for 2-35 Hz activity throughout experimental trials (Eq. 4-8). Significant effects of the overall WOE were observed in the alpha- and beta-bands, particularly towards the end of the trial. Performing the same analysis separately for each cue period relative to the accumulated WOE after each cue presentation, correlates of the WOE were observed in the alpha- and beta-bands in all epochs, strengthening towards the end of the trial and dissipating after a response was made (Figure 4-5B). Data in Figure 4-5 are computed from left- and right-hemisphere ROIs including electrodes commonly implicated in motor planning and imagery (McFarland et al., 2000; Wolpaw & McFarland, 2004). Fitting the model to individual electrode data verified the strongest correlations between the WOE and the LI were observed at these sensors (Figure 4-6). The topography of effects also matched that of the post-response beta-band rebound (Figure 4-7), consistent with the effects being driven by differential activity in the primary motor and/or premotor cortices.

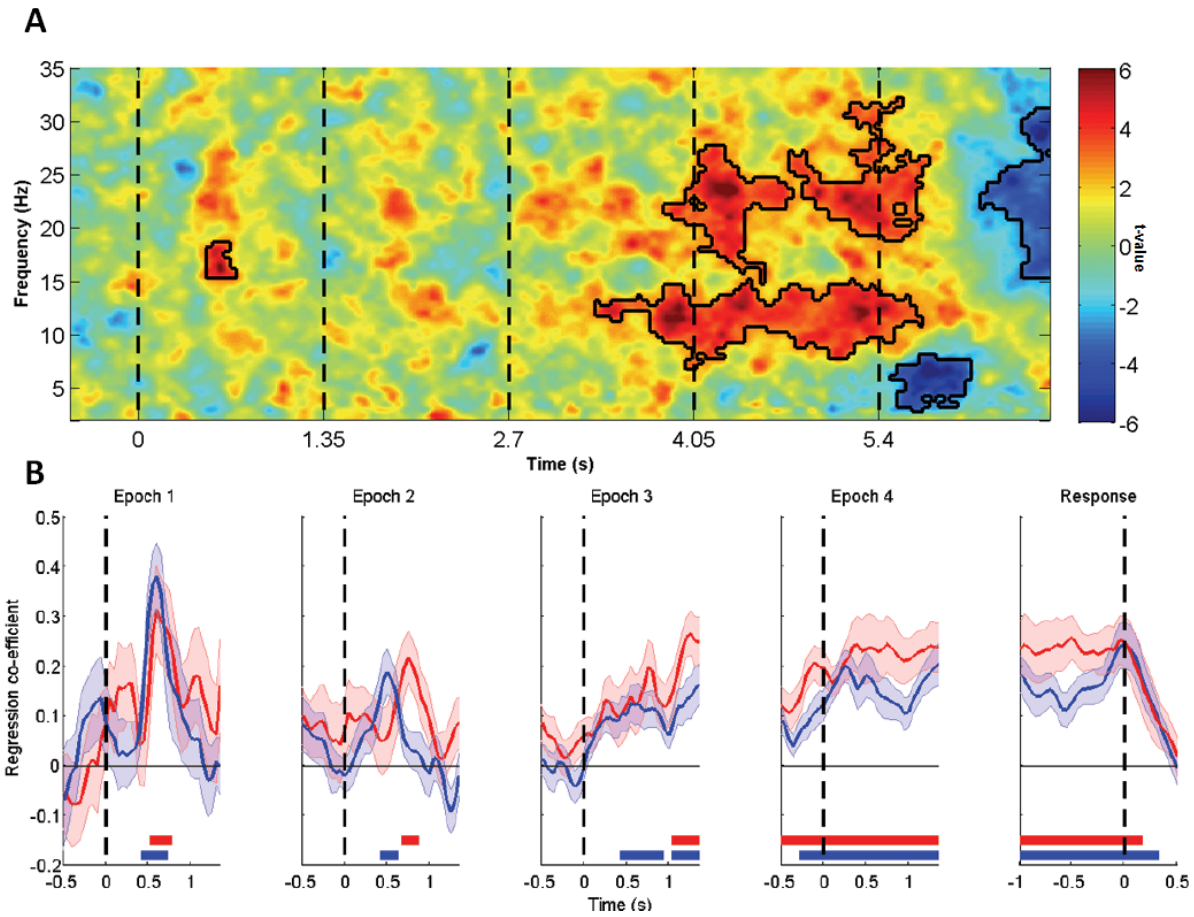


Figure 4-5. Correlates of the Overall and Partial WOE in Oscillatory Lateralization. (A) The evolution of lateralization of 8-14 Hz and 15-25 Hz activity over motor electrodes correlates with the total evidence at the end of the trial for a left- versus right-hand response. Dashed lines indicate onset times of the four cue stimuli and the start of the response period. Solid black lines encircle significant effects. Onset of the first cue stimulus was at time zero. **(B)** Regression coefficient between the WOE after each shape presentation and lateralization of 8-14 Hz (thin red line) and 15-25 Hz (thin blue line) lateralization. Error bars are s.e.m. Dashed lines indicate onset times for each shape and the time of the response. Evidence preceding the response was correlated with the evidence after the fourth cue shape. Thick red and blue horizontal lines indicate significant effects.

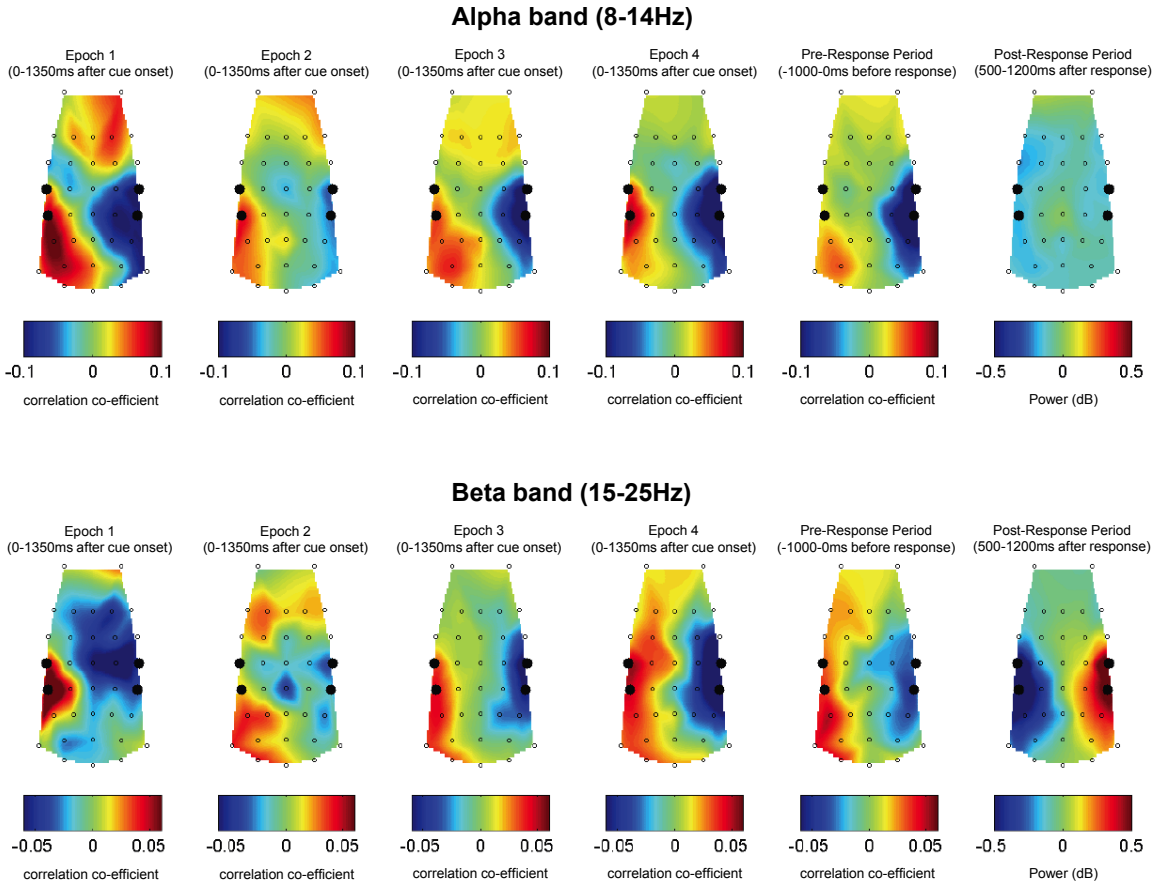


Figure 4-6. Topography of alpha- and beta-band correlations with the WOE at each stage of the trial. The WOE correlated with alpha (8-14 Hz) and beta (15-25 Hz) bands at consistent central and parietal scalp locations (left 5 plots in each row). As positive WOEs favoured left responses, the WOE correlated positively with changes in left hemisphere oscillatory activity and negatively with changes in right hemisphere oscillatory activity. The topography of the difference between left and right responses reveals a classic post-response beta-band rebound at the same electrode locations (right-most plot in each row), and no effect in the alpha band. Note the opposite direction of the power modulation in the beta-band rebound compared with the correlation coefficients depicted in the other plots. All topographies depict a birds-eye view of the scalp, with anterior locations at the top. Small black dots are electrode locations. Large black dots highlight electrodes where peak beta-band rebound effects were observed. The average of these electrodes in each hemisphere provided regions of interest for analyses of WOE-related oscillatory activity.

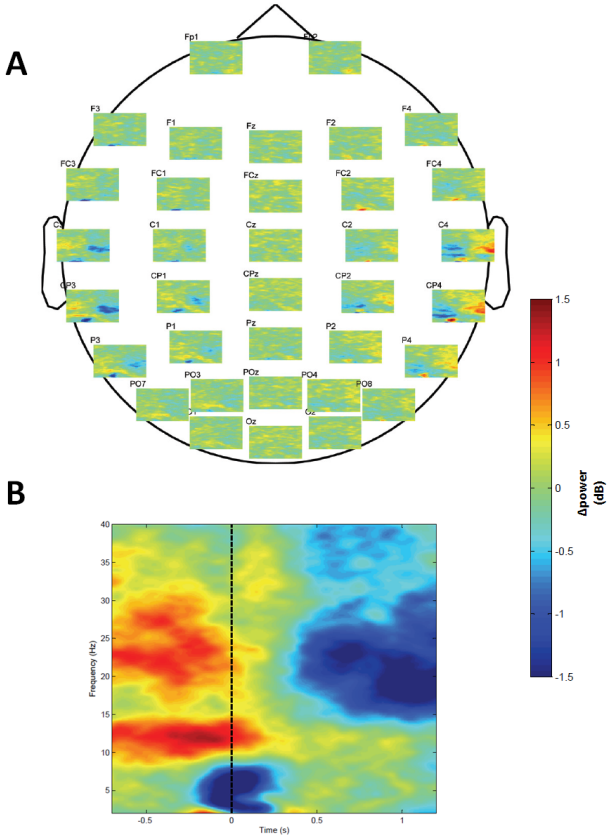


Figure 4-7. (A) Topography of the beta rebound lateralization is evident in the average time-frequency map for the subtraction of left- and right-handed responses. All plots depict the same time and frequency range as in (B). **(B)** As in (A) but showing the further subtraction between a left-hemisphere ROI (C3, CP3) and a right-hemisphere ROI (C4, CP4). The black vertical line marks the time at which a response was made.

The results plotted in Figure 4-5 reveal the effect of the overall WOE on oscillatory signals, but not how oscillatory activity changes as each new piece of evidence is witnessed and integrated with the prior evidence. We therefore fit a regression model to identify the unique contributions to oscillatory activity provided by the prior WOE and the WOE update provided by the most recently observed cue (Eq. 4-9). Both aspects of the decision evidence make dissociable contributions to the LI (Figure 4-8). The prior evidence was reflected in both frequency bands throughout the epoch. Correlates of the most recently presented cue were only apparent 400-500ms after the cue was presented, presumably reflecting the

processing times associated with the task. Both effects appeared more sustained for 8-14 Hz than for 15-25 Hz activity, and had similar topographies to the overall WOE.

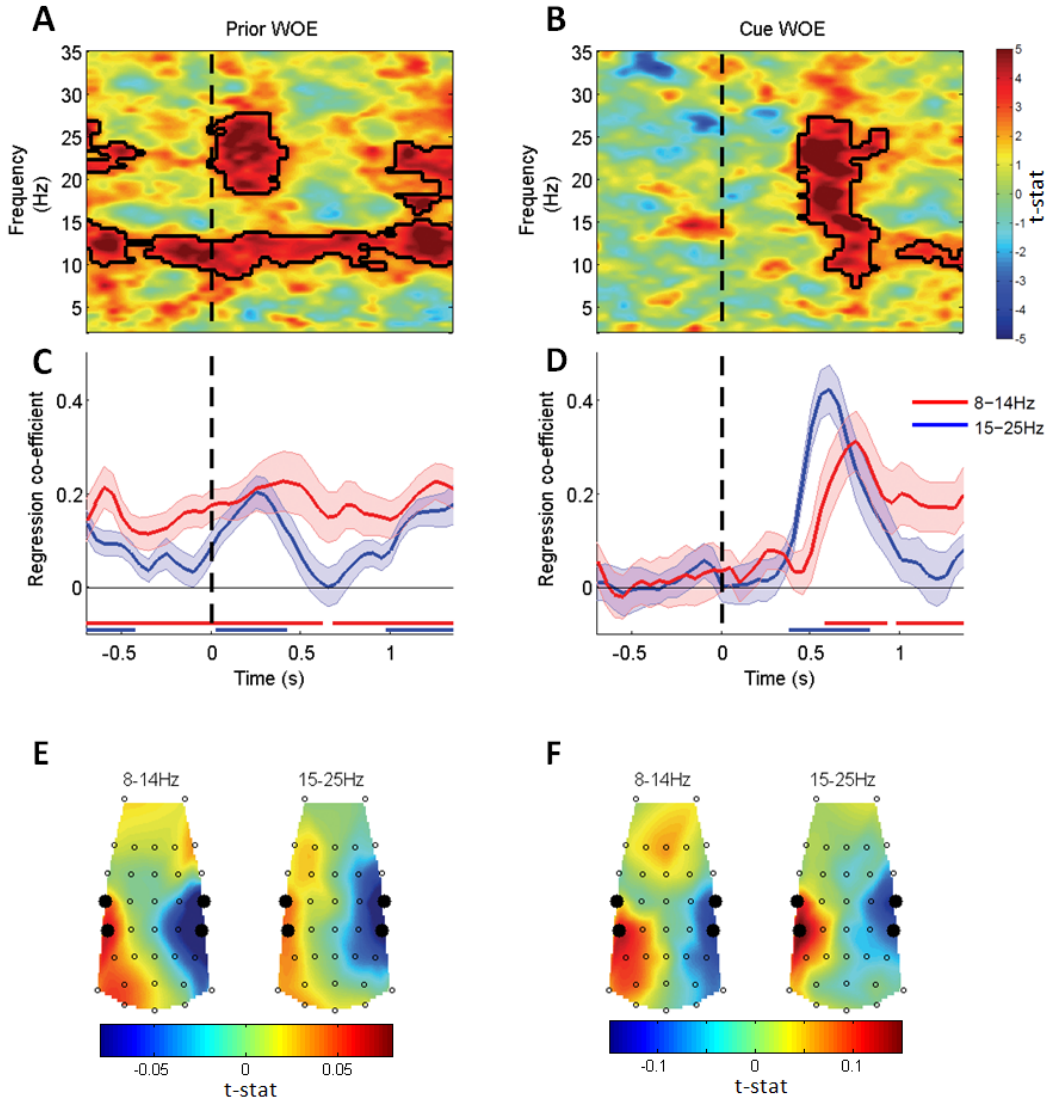


Figure 4-8. Temporal dynamics of oscillatory activity lateralization within epochs. (A) The prior evidence was reflected in lateralization of oscillatory activity over motor electrodes throughout the epoch, whereas **(B)** correlates of the evidence provided by the most recently seen cue were only observed after the cue has been processed. Solid black lines encircle significant effects. **(C, D)** The average time-course of 8-14 Hz and 15-25 Hz activity reflecting the prior and cue log-odds relative to onset of the cue stimulus. Horizontal red and blue lines indicate significant effects. **(E, F)** Topographic plots of the regression co-efficients averaged across the entire epoch for the Prior WOE regressor, and from 400 ms until the end of the epoch for the Cue WOE regressor. All topographies depict a birds-eye view of the scalp, with anterior locations at the top. Small black dots are electrode locations. Large black dots highlight electrodes where peak effects were observed in the beta-band rebound.

We further investigated whether the observed relationships between oscillatory signals and decision evidence were parametric by considering several alternative hypotheses. We first considered whether they merely reflected planning of the categorical response made at the end of the trial (Eq. 4-10). This possibility could be rejected for both frequency bands, as a significant effect of the WOE was present even when the effect of the response was modelled at each stage of the trial (Figure 4-9) (8 to 14 Hz: $F(1,23) = 22.79$, $p < 10^{-3}$; 15-25 Hz: $F(1,23) = 4.82$, $p = 0.038$). For both frequency bands, we also observed a main effect of epoch number on regression co-efficients modelling the effect of the response (8 to 14 Hz: $F(3, 69) = 9.94$, $p < 10^{-3}$; 15 to 25 Hz: $F(3, 69) = 20.47$, $p < 10^{-3}$). For both frequency bands, post-hoc tests revealed no significant response-related effects at Epochs 1 and 2 (pairwise comparisons, all ps > 0.05), even though significant effects were observed at Epoch 3 (pairwise comparisons, ps < 0.05) and Epoch 4 (pairwise comparisons, ps < 0.001). Thus, both frequency bands also reflected the response, and displayed ramping effects reflecting the response towards the end of the trial.

Alternatively, we reasoned our effects might not have reflected the planning of the precise responses actually made at the end of trials but instead a closely related variable – the planning of a response where the intended direction flipped as each of the four cues was presented and evidence in favour of one response or the other fluctuated. We tested this possibility by considering an additional model incorporating a term that reflected the sign of the WOE in each epoch (Eq. 4.11). Importantly, for this analysis we only considered trials on which participants made the optimal response, suggesting that they correctly tracked the WOE over the course of the trial. Results were similar to the previous analysis, and a significant effect of the WOE was again found for both frequency bands (Figure 4-10) (8 to 14 Hz: $F(1,23) = 22.9$, $p < 10^{-3}$; 15-25 Hz: $F(1,23) = 6.12$, $p = 0.021$). Similar to the effect of

the response in the previous model, a significant main effect of epoch number was observed on the co-efficients modelling the effect of the sign of the WOE (8 to 14 Hz: $F(3,69) = 7.79$, $p < 10^{-3}$; 15 to 25 Hz: $F(3,69) = 10.87$, $p < 10^{-3}$). Post-hoc tests revealed significant effects of the WOE sign on 8-14Hz power at Epochs 2, 3 and 4 (all ps < 0.05). For 15-25 Hz power, post-hoc tests revealed a marginal effect of the WOE sign at Epoch 3 ($p = 0.07$) and a significant effect at Epoch 4 ($p < 10^{-3}$).

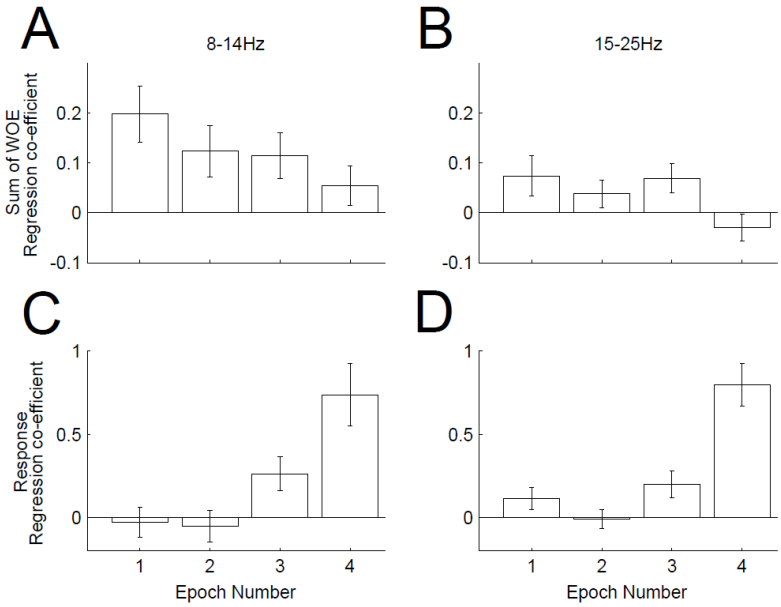


Figure 4-9. Effects of the WOE on oscillatory activity did not just reflect participants' responses. (A, B) After controlling for the categorical response at the end of the trial significant effects of the WOE were found for 8-14 Hz and 15-25 Hz activity. **(C, D)** The response at the end of the trial became increasingly correlated with both frequency bands as the trial progressed.

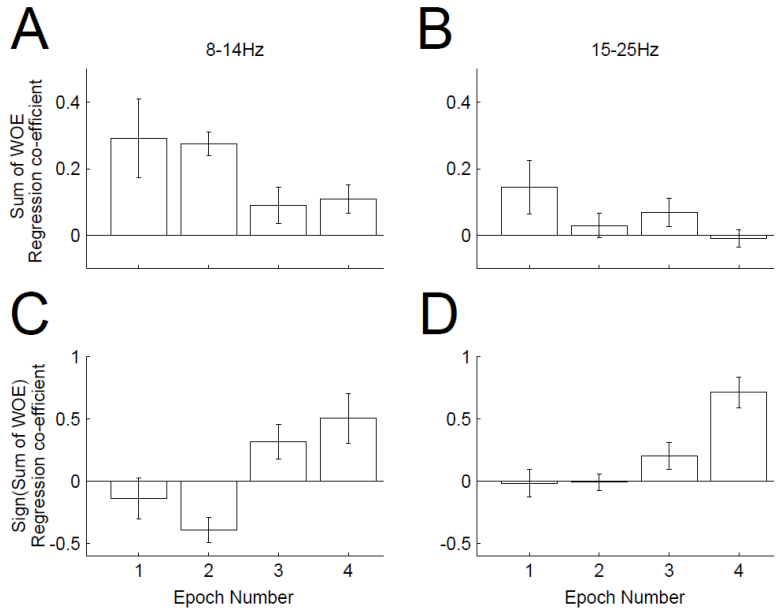


Figure 4-10. Effects of the WOE on oscillatory activity did not just reflect the categorical response favoured by the WOE at each stage of the trial. Plots are as in Figure 4-9, but controlling for the response the participant would have made based on the WOE at each point in the trial.

To ensure effects associated with general arousal, task difficulty or surprise were not responsible for our observed link between evidence and the LI, we further extended our regression model to include a parameter reflecting the absolute value of the prior evidence, and a parameter reflecting the log-probability of observing the cue given the prior WOE (Eq. 4-12). This latter term is identical (though opposite in sign) to the surprise at observing the cue (Bestmann et al., 2008a). Inclusion of these terms did not mediate the impact of the prior and cue WOEs on the LI (Figure 4-11A), though significant effects were found in the average over electrodes contributing to the LI (Figure 4-11B). Positive effects of the absolute value and surprise parameters were also found at a range of individual electrode sites (Figure 4-12 and Figure 4-13).

The average time-course of the regressors for the prior WOE, cue WOE and surprise-related effects are shown in Figure 4-14. Analysis of within-subject differences in peak latencies of these regressors supports the notion that beta-band effects preceded alpha-band effects, and that the prior WOE, cue WOE and surprise-related effects emerged sequentially. The prior WOE effect in the beta band occurred earlier than all other effects (380ms vs 519 to 696ms; all ps < 0.05) except for the cue WOE in the alpha band, which occurred marginally later (380ms vs 554ms; $p = 0.056$). The cue WOE effect occurred earlier in the alpha- and beta-bands (554 and 585 ms, respectively) than the surprise effect in the alpha-band (696 ms; both ps < 0.05), and the surprise-related effect occurred earlier in the beta-band than the alpha-band (519 ms vs 696 ms; $p = 0.009$).

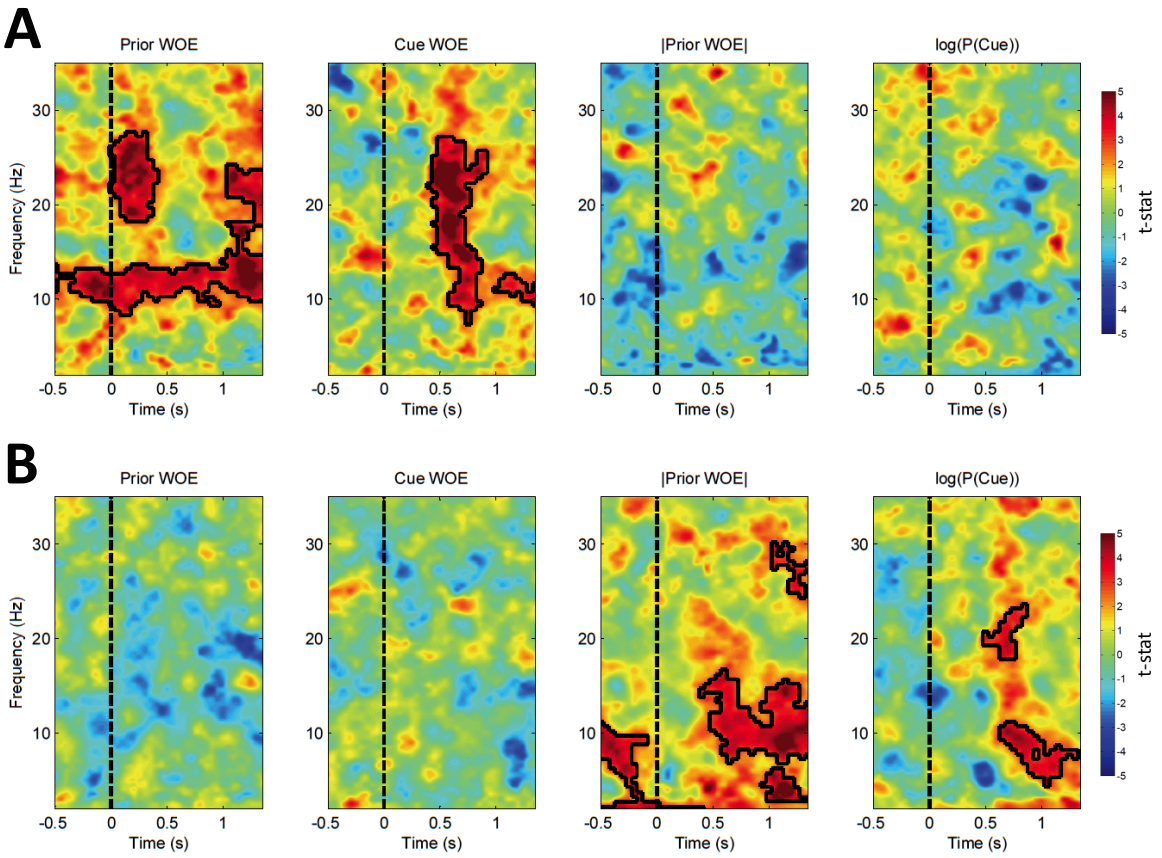


Figure 4-11. Effects of Decision Evidence, Certainty and Cue-Related Surprise on Lateralized and Non-Lateralized Oscillatory Activity. (A) The absolute value of the prior WOE and surprise associated with the most recently observed cue did not significantly modulate the LI. Inclusion of these terms did not mediate the effects of the prior WOE or cue WOE on the LI. **(B)** In the average across electrodes used to calculate the LI the prior WOE and cue WOE had no significant effects, but significant effects of the |Prior WOE| and surprise-related terms were found.

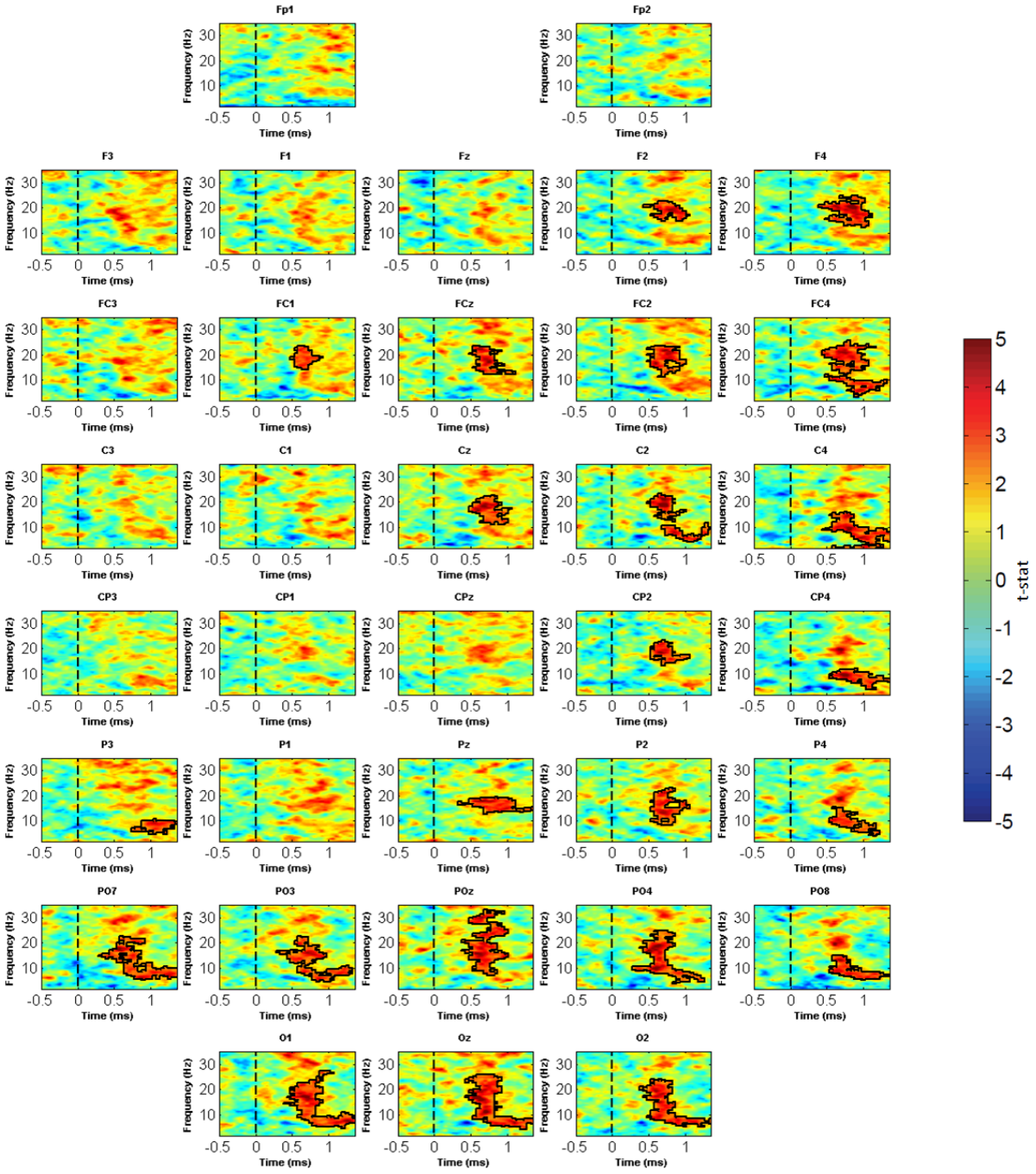


Figure 4-12. Significant effects of the surprise/Bayesian normalization term parameter were observed across a range of electrodes, and were strongest at frontal and parieto-occipital electrodes.

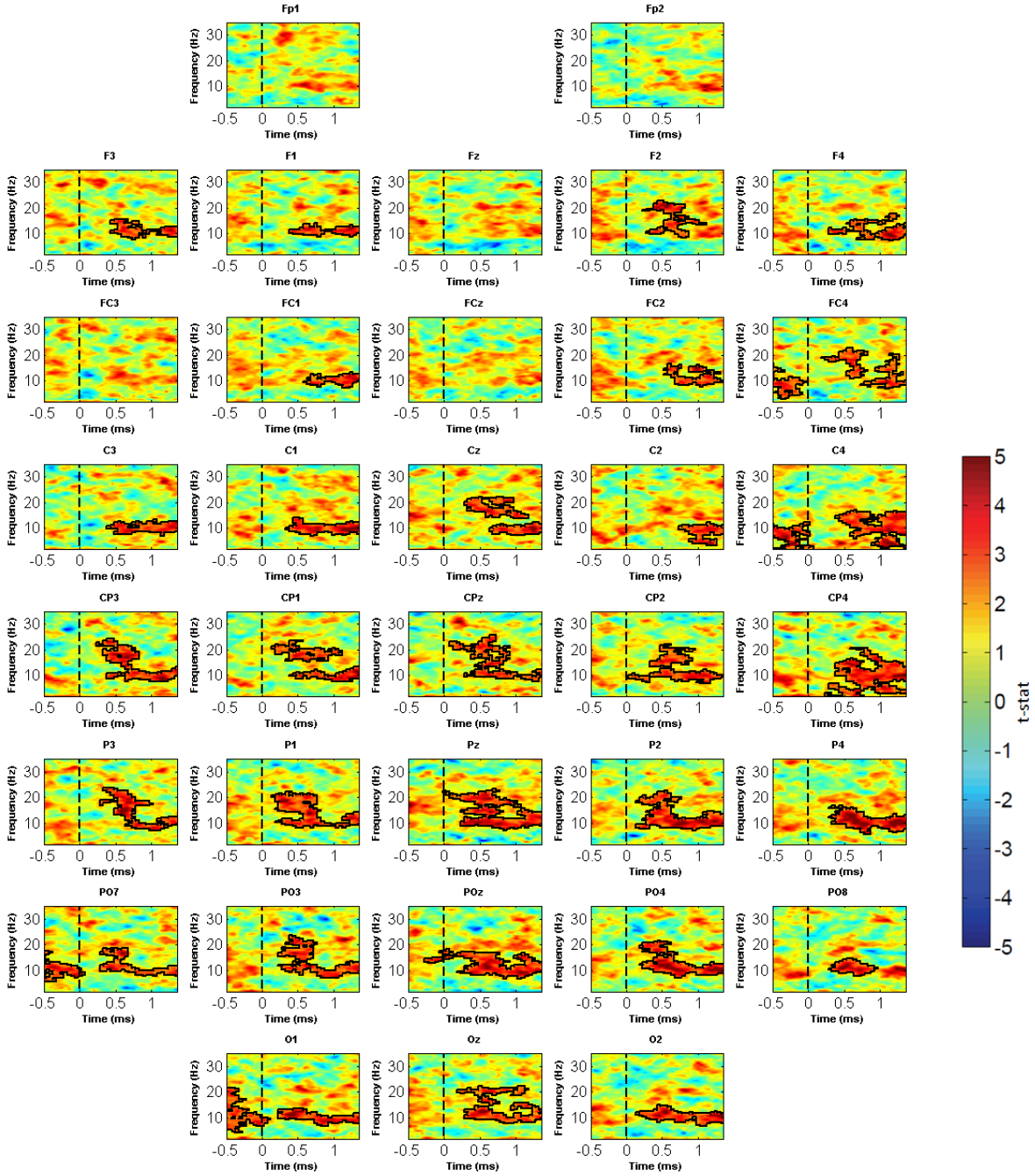


Figure 4-13. The absolute value of the Prior WOE modulated oscillatory activity in the alpha and beta bands across a wide range of electrodes.

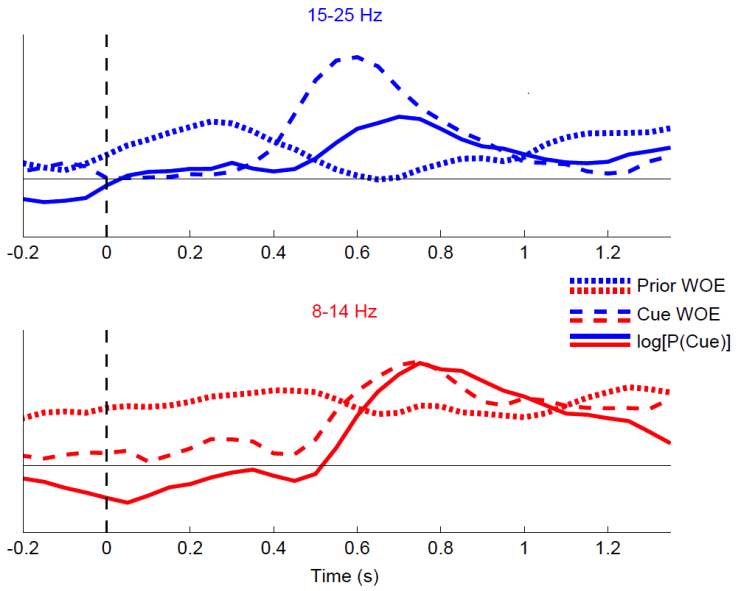


Figure 4-14. Time-course comparison for the WOE and surprise-related regressors in each frequency band.

4.4. Discussion

This study utilised a novel behavioural task requiring human participants to integrate sequentially presented pieces of evidence towards a decision about which of two potential actions should be performed. Behavioural results demonstrated participants were highly effective at integrating the information provided by the symbolic cue shapes. Optimal responses were made on over 90% of trials with four cues, and reaction times were elevated when decision uncertainty was high.

The first key finding of the present study is that lateralization of alpha- and beta-band activity recorded at motor electrodes was parametrically related to the signed evidence for left- or right-handed responses over the course of experimental trials. Although categorical choice-related activity was increasingly apparent towards the end of trials, control analyses confirmed the parametric relationship between evidence and oscillatory activity in each

epoch of the trial after controlling for response-specific effects. Further control analyses established that evidence tracking in the alpha- and beta-bands could not be attributed to non-specific effects related to the overall amount of accumulated evidence or to cue-related surprise. These results thus suggest that the state of participants' motor systems updated in an on-line manner to reflect the available evidence about the upcoming response. These results complement the large number of previous studies demonstrating that alpha-band and beta-band activity becomes lateralized up to several seconds before a voluntary or instructed unimanual response (Crone et al., 1998b; Pfurtscheller & Berghold, 1989). A close link between effector-specific preparatory activity and the participant's internal decision variable was also recently demonstrated by Donner and colleagues (2009), who reported that beta- and gamma-band lateralization in M1 can predict participants' behavioural choices towards the end of a decision period. In their study, both beta- and gamma-band lateralization correlated with estimates of the sensory evidence participants extracted from a random dot motion stereogram – the integral of single-trial gamma-band activity in the task-relevant sensory area, MT. However, whilst these authors reported a significant residual correlation between sensory evidence and gamma-band lateralization in M1 after controlling for participants' specific choices, they did not report a similar effect for the beta-band. Our results therefore extend those of Donner et al. (2009) by demonstrating that beta-band lateralization in motor circuits is parametrically linked to decision evidence independent of choice behaviour. To our knowledge, our results are also the first to demonstrate a similar parametric relationship between alpha-band lateralization and decision evidence.

Our results also complement previous TMS studies demonstrating that effector-specific motor excitability varies dynamically with the probability of an expected response (Bestmann et al., 2008a; Mars et al., 2007; van den Hurk et al., 2007; van Elswijk et al.,

2007). Other studies have established that in the absence of changes in muscular output, motor preparation may result in increased corticomuscular gamma-band synchrony at M1 contralateral to the response hand and decreased contralateral beta-band power, perhaps in conjunction with increased ipsilateral corticomuscular beta-band synchrony (Murthy & Fetz, 1996; Prut & Fetz, 1999; Schoffelen et al., 2005, 2008; Schoffelen et al., 2011; Soteropoulos et al., 2011; van Wijk et al., 2009). As we did not perform electromyographic recordings, our data can only establish a link between oscillatory power and motivation to prepare a motor response, however we presume that preparatory corticomuscular synchrony would be modulated in a similar parametric manner.

Our parametric alpha- and beta-band effects appear at odds with a recent spectral analysis of LFP data from a single monkey involved in a somatosensory discrimination task (Haegens et al., 2011b). In this study, categorical differences in beta activity were associated with specific behavioural choices. Importantly, however, the monkey in this task always received tactile stimulation to one hand and responded with the other hand. LFP analysis in this experiment therefore focussed on activity at specific frontal sites rather than the lateralization differences we report, and we suggest this may underlie discrepancies between our findings. Consistent with this interpretation, several ECoG data suggest that beta activity undergoes modulation over a broad network within each hemisphere during motor execution and imagery, and is not effector-specific like gamma activity (Crone et al., 1998a; Crone et al., 1998b; Miller et al., 2010) (see also Ohara et al., 2000). Investigations into the utility of MEG for brain-machine interface control have also concluded that beta power does not allow classification of different movements performed by the same effector (Waldert et al., 2008). Alternatively, since the task used by Haegens and colleagues only involved one integration period, their categorical effects may reflect that the monkey was able to plan a categorical

response earlier than in our task. Consistent with this interpretation, we also observed categorical choice-related beta activity towards the end of trials. Further work is required to clarify the basis of these differences.

The second key finding from the present study relates to how specific decision-relevant quantities were reflected in the time-course of rhythmic activity over motor regions. The prior WOE and cue WOE made dissociable contributions to lateralized rhythmic activity in each epoch. Prior decision evidence was reflected in alpha-band lateralization in a sustained fashion throughout each epoch of the task, and was significantly modulated by the WOE associated with cue stimuli in a sustained manner starting approximately 500 ms after their presentation. This temporal profile is similar to the dynamic updating of monkey LIP neuron firing rates in a saccadic version of this task, and suggests encoding of a decision variable which is updated as new evidence is observed (Yang & Shadlen, 2007). Beta lateralization also exhibited decision-variable like dynamics, but with more complex temporal dynamics. Beta-lateralization significantly reflected the cue WOE from approximately 450 ms after its presentation, slightly earlier than in the alpha band, but this effect was transiently significant, only lasting approximately 250 ms. In further contrast to the sustained alpha-band effects, beta-band lateralization most clearly reflected the prior decision evidence early in each epoch, before the cue stimulus had been processed, but was not significant during the period at which the cue WOE was significant. Beta-band lateralization again reflected the prior WOE towards the end of the trial, just before onset of the next stimulus.

The phasic nature of beta-band lateralization we report is remarkably similar to modulation of neuronal firing rates in prefrontal cortex reported in a somatosensory discrimination tasks by Romo and colleagues. In this task, monkeys were required to

maintain a working-memory representation of the frequency of an initial vibrotactile pulse during a delay before a second comparison stimulus. Firing rates in prefrontal and premotor regions were found to transiently encode the frequency of the first stimulus after it was delivered, but persistence of this signal was reduced during the delay period. Towards the end of the delay period, however, significant coding of the initial stimulus frequency resumed before presentation of the second stimulus (Hernández et al., 2010). These authors therefore suggested that frontal regions are more engaged in the read-out of sensory information when it is necessary to compare these working-memory representations with new sensory inputs. Our data suggest beta activity may reflect similar dynamics. This interpretation is consistent with recent suggestions that beta-band synchrony arises when cortical networks are involved in long-range integrative functions, particularly decision-making computations requiring co-ordination of neural activity across regions involved in transforming stimulus evidence into action plans (Donner & Siegel, 2011; Donner et al., 2007; Haegens et al., 2011b; Pesaran et al., 2008). Under this view, transient beta activity may occur as regions prepare for and engage in decision-updating processes, but may not encode the decision variable per se. This account naturally explains why beta-band correlates of the cue stimulus may occur slightly earlier than the other cue-related effects in both frequency bands. Of course, caution is required in interpreting the apparently phasic nature of the beta-band response, as this may in part be a false negative, especially given the multi-collinearity between the cue WOE and prior WOE regressors (R=0.33). However, the similar signal-to-noise ratio for the WOE-related effects observed in the alpha and beta bands suggests the dissociation in their time-courses warrants further investigation.

Previous decision-making studies have reported that activation levels at a range of parietal and frontal regions scale with overall decision uncertainty (de Lange et al., 2010;

Donner et al., 2007; Grinband et al., 2006; Huettel et al., 2005; Stern et al., 2010; Volz et al., 2004), perceptual difficulty or attentional load (Bankó et al., 2011; Heekeren et al., 2004; Heekeren et al., 2006; Ho et al., 2009; Tosoni et al., 2008), and surprise (Bestmann et al., 2008a; Mars et al., 2008b). To ensure such general affects were not responsible for our observed link between evidence and the LI, we further extended our regression model to include two additional parameters. The first reflected the absolute value of the prior evidence. The second parameter reflected the log-probability of observing the cue given the prior WOE and was identical (though opposite in sign) to the surprise at observing the cue (Bestmann et al., 2008a). Significant effects of both parameters were found in the average over motor electrodes used to calculate the LI. Positive effects of the absolute value term were also found at a range of individual electrode sites. These results complement evidence that decision correctness is positively correlated with bilateral ~15-Hz activity in parietal and prefrontal cortices (Donner et al., 2007), perhaps reflecting elevated spectral power when more evidence has been accumulated. As noted by de Lange and colleagues, these effects may also reflect top-down suppression of future sensory inputs when evidence is high (de Lange et al., 2010). Spectral power was also higher approximately 500 ms after observation of less-surprising cues at a wide range of electrodes. These effects complement studies demonstrating changes in cortico-spinal excitability following surprising stimuli (Bestmann et al., 2008a) as well as the enhancement of the P300 component elicited by surprising events (Mars et al., 2008b).

Optimal updating of a decision variable in light of new evidence can be simply described in Bayesian terms as a function of (1) the weight of the prior evidence, (2) the weight of the new piece of evidence, and (3) a divisive normalization term (Eq. 4.14). Our effects on the LI suggest that oscillatory signals in the human brain encode the first two of

these terms. Speculatively, it is interesting to note that the surprise-related parameter we report here is equal to the logarithm of the third term used for Bayesian updating. It is also a component in models describing how Bayesian decision updating occurs via cortico-basal ganglia loops. These models predict that log-probabilities of prior decision variable states are combined with new decision information in cortical integrators, then subsequently normalized by such a term via diffuse projections from the subthalamic nucleus and globus pallidus leading back to the cortex (Bogacz & Gurney, 2007; Frank, 2006). The same cortico-basal ganglia circuits can also generate strong beta-band activity (Mallet et al., 2008; Nevado Holgado et al., 2010). Our data suggest that all three of these quantities are represented in the human brain in a sequential order that is consistent with the model proposed by Bogacz and Gurney (2007), raising the possibility that the oscillatory signals we report here provide a direct window into the neural computations involved in decision making. This notion is, of course, highly speculative given the present data set. We consider this an important issue for future studies to investigate, and suggest that one effective strategy to investigate this further is via MEG recordings in tasks such as that used here, where prior decision variables are updated given new evidence. A critical empirical question is whether source reconstructions of the broad topography of the surprise/normalization term effects reported here implicate regions that also parametrically track changes in decision evidence. Such effects may also be observed in motor structures and/or parietal and prefrontal regions mediating decision making (Gold & Shadlen, 2007; Heekeren et al., 2008; Ho et al., 2009; Philiastides et al., 2011; Tosoni et al., 2008).

The possibility of interrogating the time-course over which quantities involved in decision updating are represented in the brain raises another important question – what exactly are those quantities? The normalization term discussed above is a core aspect of basal

ganglia decision-making models, which predict decision-making neurons encode the log-probability in favour of their decision outcome (Bogacz, 2009; Bogacz & Gurney, 2007). In contrast, another popular computational model predicts that firing rates should scale with the log-posterior odds (Soltani & Wang, 2010; Wang, 2002), while electrophysiologists have argued that LIP firing rates encode log-likelihood ratios (LLRs) (Yang & Shadlen, 2007). Empirical investigations have not yet established which of these quantities are represented in decision-making neurons. To test between the latter of these two options, neural data are needed from decision-making tasks involving unequal priors at onset of the decision process (Soltani & Wang, 2010). Testing the basal ganglia hypothesis, however, is in principle possible using data from the current sequential decision-making task. Indeed, in the data of Yang and Shadlen (2007), from a similar task to ours, LIP firing rates seem to decrease with negative evidence more than they increase with positive evidence (Figures 2-3, Yang & Shadlen, 2007), consistent with encoding of log-probabilities rather than LLRs (R. Bogacz, personal communication). We attempted to discriminate between these accounts in the present dataset (data not shown), however the signal-to-noise ratio was not sufficient to discriminate the slight non-linearity predicted between log-probability and LLR/log-posterior odds accounts (see also Roitman et al., 2007). Future MEG and electrophysiological studies using tasks such as ours should further investigate this issue. In addition to yielding a higher signal-to-noise than EEG, MEG would allow examination of gamma-band activity in motor structures, and potentially in integration regions of the prefrontal and posterior parietal cortices. Interpretation of local gamma-band modulations may also be more straightforward, as the relationship between oscillatory activity and neural activity is particularly equivocal in the low-frequency ranges, where synchrony changes may regulate long-range neural interactions rather than changes in local activity (Donner & Siegel, 2011; Engel & Fries, 2010; Pesaran et al., 2008).

Functionally, we have interpreted our results as providing evidence for parametric modulation of preparatory motor processes. Such interpretation of beta-band effects is consistent with numerous studies demonstrating peri-movement beta-band modulation (Crone et al., 1998b; McFarland et al., 2000; Ohara et al., 2000; Pfurtscheller, 1981; Pfurtscheller & Lopes da Silva, 1999; Tzagarakis et al., 2010b), as well as MEG source reconstructions and ECoG evidence that consistently localise beta generators to primary motor and premotor regions (Crone et al., 1998b; Donner et al., 2009; Jones et al., 2010; Jones et al., 2009; Jones et al., 2007; Marsden et al., 2000; Miller et al., 2010; Pineda, 2005; Salenius et al., 1997; Salmelin & Hari, 1994a, 1994b). Alpha-band (or 'mu') activity, however, is more commonly localized to area 3b of the post-central gyrus, in somatosensory cortex. It has therefore classically been interpreted as a somatomotor rhythm (Hari & Salmelin, 1997; Salmelin et al., 1995; Salmelin & Hari, 1994b). Alpha-band activity does have an unequivocal role in somatosensory processing. For example, similar to the posterior attentional alpha rhythm modulated by visual attention (Foxe et al., 1998; Gould et al., 2011; Worden et al., 2000), somatosensory alpha-band lateralization varies parametrically with somatosensory attention (Haegens et al., 2011a), and pre-stimulus somato-motor alpha-band power differences predict detection rates for subsequent somatosensory targets (Jones et al., 2010). On the other hand, there is also evidence that ~10 Hz activity has a role in organizing motor activity, potentially via rhythmic descending control of motoneuron pools via corticospinal neurons (Farmer, 1998; Vallbo & Wessberg, 1993). For example, one recent study has demonstrated that ~10 Hz activity over motor cortex predicts how likely a motor-evoked potential will be elicited by application of a TMS pulse to primary motor cortex (Sauseng et al., 2009). The low spatial resolution of EEG does not allow us distinguish between neural generators in motor and somatosensory cortex, and this is left to future studies. This distinction is important in determining whether the alpha-modulation we observe reflects preparatory motor or

somatosensory processes. A somatosensory source would suggest the parametric alpha-band effects we report here could reflect an attentional mnemonic used by participants rather than motor preparation.

Although four cues were presented on the majority of trials in our task, we included shorter trials so that participants would be encouraged to integrate cues as the trial proceeded so that they could respond at any stage during the integration period. Under these conditions we observed clear preparatory activity throughout experimental trials. An important question is whether our decision-related effects early in trials depend on this manipulation. Although the data presented here cannot address this question, electrophysiological recordings suggesting the presence or absence of such preparatory activity reflects whether or not the subject is involved in an active decision-process (Haegens et al., 2011b; Hernández et al., 2002; Pesaran et al., 2008), suggesting alpha and beta modulation is likely to occur regardless of the presence of shorter trials. This caveat is more directly addressed in Chapter 5. Conversely, if the evidence is high enough after the second or third cue – say, for example, the first two cues provided the strongest possible evidence for a left response – then a 'point of no return' may be crossed where participants can cease decision making without sacrificing optimality in decision behavior (de Lange et al., 2010). Our control analyses are consistent with this notion, suggesting that categorical motor planning increases in the last two epochs of the trial. Although non-significant, it is tempting to interpret the trend for our parametric evidence regressor amplitudes to decrease over time (Figure 4-9). We are hesitant to do so as this effect may either be due to participants switching from maintaining graded preparatory sets to categorical ones, or may merely reflect multicollinarity between our evidence and response regressors, which interacted with time. One way of addressing this in future work would be to allow participants to self-terminate the decision process at any point

in the trial, as soon as they have accumulated sufficient evidence. Pilot data we have collected suggest that participants can easily learn to effect such decisions using the same cue stimulus set to the present experiment (data not shown).

Although mathematical models commonly describe decision making as a process whereby multiple independent samples of evidence are taken from the world and integrated towards an internal decision variable, most studies investigating the neural basis of decision making in humans have manipulated the strength of the perceptual information provided by presentation of a single stimulus or stimulus array (e.g., Bankó et al., 2011; Forstmann et al., 2010; Heekeren et al., 2004; Heekeren et al., 2006; Ho et al., 2009; Tosoni et al., 2008; though see Stern et al., 2010). Especially when combined with modelling of accuracy and reaction time distributions (e.g., Ho et al., 2009; Forstmann et al., 2010), such manipulations may allow inferences to be drawn about the average rate at which sensory-driven information accumulates in the brain but do not allow an experimenter to make *a priori* assumptions about the exact state of a participant's internal decision variable at any time within a single-trial, since multiple decision-related processes may vary between (e.g., drift rate, starting-point bias, time at which the decision threshold is crossed) and within (e.g., noise in sensory cortex) trials. One solution to this problem is to infer single-trial inputs to decision variables via analysis of neural recordings from sensory processing regions (Donner et al., 2009; Philiastides et al., 2011; Rahnev et al., 2011; Ratcliff et al., 2009; Siegel et al., 2007). However, the simultaneity of perception and decision-updating in such tasks makes it somewhat equivocal whether any observed changes in sensory activity reflect bottom-up stimulus drive and/or allocation of attention to salient visual features during the time-course of decision making. Attention and stimulus intensity can have interactive effects on behavioural and neural responses (Bankó et al., 2011; Carrasco et al., 2004; Martinez-Trujillo

& Treue, 2002; Reynolds & Chelazzi, 2004; Treue & Trujillo, 1999), and can both modulate stimulus-driven gamma-band activity (Fries, 2009; Fries et al., 2001; Tiitinen et al., 1993; Wyart & Tallon-Baudry, 2008). Indeed, Donner and colleagues reported decision-related effects between 64 and 100 Hz, encompassing frequencies recently reported to reflect attention-related (76-90 Hz) but not awareness-related (54-64 Hz) effects on stimulus-driven gamma band activity (Wyart & Tallon-Baudry, 2008). A further problem is that it can be difficult to distinguish between sensory-cortex activity modulation due to information versus perceptual noise in stimuli (Bankó et al., 2011). In contrast, the present task required participants to integrate well-learned, supra-threshold, symbolic information, eliminating confounds between sensory input strength and decision evidence. Given their accurate behavioural performance, this allowed us to make precisely quantified *a priori* assumptions about participants' internal decision variables and how they changed over the course of each experimental trial. Given the high temporal resolution of the signals analysed versus the relatively long duration of epochs in the task, we were also able to identify distinct components related to decision updating. We therefore suggest this approach provides a simple but powerful paradigm for investigating the temporal dynamics of decision-related activity across the brain.

In conclusion, our data link preparatory processes in motor circuits with encoding of a decision variable, complimenting previous neurophysiological recordings with monkeys, and suggesting that human motor planning signals are continuously updated on the basis of participants' expectancies. Our results do not, however, distinguish whether any specific brain regions or signals had a causal role in the decision process, or were downstream of decision-making nodes and constantly updated. To investigate this question, Chapter 5

describes a concurrent TMS-EEG study attempting to establish the causality of a medial intraparietal region in the decision process.

Chapter 5 - Investigation of the Causal Role of Intraparietal Cortex in Motor-Related Decision-Making

5.1. Introduction

Recent electrophysiological recordings, human neuroimaging and mathematical modelling results have converged to suggest that every-day decision making occurs via integration of sensory signals over time towards a decision variable (Gold & Shadlen, 2007; Platt et al., 2008; Smith & Ratcliff, 2004). The experimental results presented in Chapter 4 complement these findings by providing evidence that lateralization of oscillatory alpha- and beta-band activity in human motor regions reflects neural encoding of a decision variable.

Importantly, however, like all data collected using non-interventional neural recording techniques, the results of Chapter 4 are correlational in nature and cannot establish whether the decision-related signals observed in motor regions are *causally* involved in the decision-making processes underpinning behaviour on our sequential integration task. Indirect inference about the causal role of this decision-related activity is also difficult because previous studies have differed in the functional roles ascribed to somatomotor oscillatory activity. On one hand, a causal role for beta-band activity in decision making is supported by data suggesting that beta-band synchrony occurs between brain regions involved in decision-related integration via long-range neural interactions (Donner & Siegel, 2011; Engel et al., 1991). However, other research has emphasized that contralateral desynchronization and ipsilateral synchronization of beta-band activity are associated with motor planning, execution and imagery (Crone et al., 1998b; Donner et al., 2009; McFarland et al., 2000;

Miller et al., 2010; Tzagarakis et al., 2010b). These two views are not mutually exclusive – for example, beta-band synchrony in motor regions may reflect maintenance of motor inhibition via long-range interactions with the basal ganglia. Thus, in the context of the somatomotor decision-related oscillatory effects reported in Chapter 4, it is unclear whether beta-band activity reflects decision processes *per se*, or that downstream motor structures are continuously updated as new evidence is integrated (Ho et al., 2009; Kim & Shadlen, 1999; Shadlen et al., 2008; Spivey et al., 2005). Similar difficulties apply to functional interpretations of somatomotor alpha-band activity we have reported in Chapter 4. Whilst this activity may reflect a decision variable, it is unclear whether somatomotor structures play a causal role in computing decision variables locally or receive a downstream copy of the decision variable, and whether the alpha-band activity reflects motor preparation and/or motor attention.

In addition to evidence that neural activity in parietal and motor regions of both humans and monkeys represents decision information (Donner et al., 2009; Donner et al., 2007; Gold & Shadlen, 2007; Hanks et al., 2006; Horwitz et al., 2004; Shadlen & Newsome, 2001; Tosoni et al., 2008), human neuroimaging studies have emphasized the involvement of prefrontal structures during decision making, particularly the left dorsolateral prefrontal cortex (DLPFC) and insula (Heekeren et al., 2004; Heekeren et al., 2006; Ho et al., 2009; Philiastides et al., 2011; Philiastides et al., 2010). Evidence for a causal role of the PFC in decision-making has also been provided by TMS data demonstrating that delivering inhibitory 1-Hz rTMS to the left DLPFC impairs accuracy and reaction times of decisions in a manner that is well described by a reduction in the drift-diffusion decision model parameter reflecting the rate at which decision evidence is accumulated (Philiastides et al., 2011). Zanto and colleagues (2011) have also reported that rTMS to the inferior frontal junction (IFJ)

disrupted accuracy for colour discrimination when participants performed a match-to-sample task. Analysis of alpha-band phase coherence between frontal and posterior regions in post-rTMS EEG recordings suggest this effect was driven by disruption of top-down control of visual processing, leading to reduced quality in working-memory traces (Zanto et al., 2011). Together, these studies further highlight that motor systems may be downstream of higher-level cortical regions that implement decision-making processes. However, they may also be interpreted as evidence that the PFC plays an important role in the maintenance of working-memory traces for decision relevant quantities (Bechara et al., 1998; Curtis & Lee, 2010) and/or in exerting top-down control over sensory regions providing perceptual input to decisions (Rahnev et al., 2011). Current data thus provide evidence for a causal role of the PFC in decision making, but are agnostic about whether the PFC implements any kind of decision-comparison processes.

Whereas on-going updating of the human motor system, such as that reported in Chapter 4 and by other investigators (Bestmann et al., 2008a; Donner et al., 2009; Donner et al., 2007; Tosoni et al., 2008), is consistent with these structures being downstream of regions mediating decision making, other data support a causal role of human intraparietal structures in guiding choice behaviour. When monkeys are engaged in a random-dot motion discrimination task towards a saccadic response, sub-threshold excitatory stimulation of LIP neurons biases monkeys' decisions towards the stimulated neuron's response field (Hanks et al., 2006). Stimulation of structures along the human intraparietal sulcus (IPS) and superior parietal lobe (SPL) can also affect motor parameters associated with expression of choice, such as accuracy and endpoint variability in saccades and reaches, and movement times (Davare et al., 2011; Vesia et al., 2010; Vesia et al., 2008). More compellingly, when human participants complete a task involving speeded reaching movements to visual targets using a

hand of their choice, TMS of a left hemisphere posterior IPS site just after target appearance can bias hand choice towards the ipsilateral hand (Oliveira et al., 2010), consistent with induction of a bias in hand preference or motor attention, disrupted planning of a contralateral reach, or a disruption of the spatial updating or co-ordinate transformations that may have been involved in integrating visual and somatosensory information about current hand position with the spatial location of the visual target such that response selection could proceed appropriately (Buneo & Andersen, 2006; Morris et al., 2007). Together, these TMS studies provide evidence for a causal role of the human parietal cortex in the generation and execution of motor plans in response to sensory stimuli, but it is equivocal how these results relate to the behavioural tasks more commonly used in the decision-making literature. For example, in the experiment by Oliveira and colleagues (2010), participants were instructed to initiate reaching movements as quickly as possible but hand choice could never be considered categorically 'wrong'. TMS may therefore have biased hand use preference without directly affecting decision making, or it may have slowed contralateral hand responses, making ipsilateral reaches faster and thus more preferable[1]. Thus, it remains unclear whether the human parietal cortex also plays a causal role in decision-making processes involving integration of evidence over time, such as random-dot motion discrimination judgements or the shape-integration task used in Chapter 4 (Hanks et al., 2006; Yang & Shadlen, 2007).

This chapter presents data from a concurrent TMS-EEG experiment aiming to determine whether human intraparietal cortex plays a causal role in decision making. We adapted the task developed in Chapter 4 for use with concurrent TMS-EEG, and investigated whether applying online rTMS trains at 10 Hz during decision making affected decision-

[1] Note that in arguing against TMS having induced an attentional bias, Oliveira et al. (2010) report control analysis results showing that TMS did not modulate reaction times for left versus right hemifield targets. However, they did not report whether TMS affected the speed of reaches as a function of response hand. If TMS simply slowed contralateral hand responses, this may have in turn biased hand preferences.

making behaviour. TMS was delivered to a putative human homologue of macaque area MIP in the left hemisphere (Mars et al., 2011). To control for non-specific consequences of TMS, effects of intraparietal TMS were compared with those at a left hemisphere control site, V5 (Kolster et al., 2010). TMS trains were delivered during the decision-making period of each trial and finished almost two seconds before participants responded, ensuring transient disruption of action planning and execution unrelated to a decision variable did not influence participants' choice behaviour.

We investigated how TMS affected behaviour by characterising the effects of TMS on logistic psychometric functions describing how participants' responses varied with the evidence at the end of the trial. As the online rTMS protocol we used is thought to have disruptive effects on neural processing (Walsh et al., 2005), we reasoned that stimulating regions causally involved in decision making may have two consequences. If TMS disrupted a neural representation of the overall decision variable or the updating associated with a cue stimulus, the slope of psychometric functions should be reduced, reflecting decreased sensitivity of behavioural choices to decision evidence. Alternatively, since we stimulated a left hemisphere cortical site, we reasoned that TMS might disrupt the neural representation of evidence in favour of a contralateral (right-hand) response. If this is the case, TMS should induce a consistent bias on choice behaviour described by a leftwards shift in psychometric function thresholds. This latter effect is predicted by a monkey microstimulation study suggesting that choice behaviour can be biased towards the response field of stimulated LIP neurons (Hanks et al., 2006).

Despite a consensus that beta-band activity in human motor/premotor regions can reflect the consequences of sensorimotor integration, and emerging evidence indicating that some beta-band activity reflects long-range integrative decision processes, there has not yet

been a direct test that beta-band activity is causally dependent on an evolving decision process occurring through interactions between brain areas. We predicted that if this is the case, TMS should also modulate beta-band power, and that the magnitude of TMS-induced changes in behaviour and neural effects would be correlated.

5.2. Materials and Methods

5.2.1. Participants

Twelve paid volunteers (mean age 27, range 20-35; 7 female) participated after giving informed written consent. A safety-screening questionnaire was completed prior to all TMS sessions. All participants were right-handed (Oldfield, 1971), and reported having normal or corrected-to-normal visual acuity and no history of neurological disorders. TMS parameters were within established safety guidelines (Rossi et al., 2009; Wassermann, 1998), and the study was approved by the Central Oxfordshire Research Ethics Committee and in accordance with the Declaration of Helsinki. All participants completed an initial induction session (1 hour), a motor and comfort threshold measurement session (2 hours), a behavioural training session (1.5 hours), then two TMS-EEG sessions (2.5 hours each). T1-weighted structural MRI scans were also obtained for all participants prior to the motor threshold session.

5.2.2. TMS-EEG Procedure

A schematic of the experimental task is shown in Figure 5-1. The task was identical to the sequential decision-making task developed in Chapter 4 except for several modifications to make the task more suitable for use with TMS. First, in order to maximise the chance of

observing an effect of TMS on behavioural choice, we reduced the total amount of evidence observed on each trial to three shapes. Second, we removed all shorter trials on which fewer than three cue shapes were presented, simplifying the design and maximising the number of trials from which usable data were obtained. Third, TMS was delivered on 50% of trials. On TMS trials, 5 pulses of 10-Hz TMS (i.e. lasting 400 ms) were delivered starting 50 ms after onset of the second cue stimulus. This time period was chosen based on the results of Chapter 4, which suggest that cue stimulus processing and decision variable updating occur in this time window. TMS was delivered using a MagStim Rapid biphasic stimulator with a 70-mm figure-of-eight coil positioned tangentially to the scalp and with the handle oriented towards the vertex.

Prior to the TMS-EEG sessions, participants completed a behavioural training session identical to that described in Chapter 4 except for the changes in trial length noted above. To familiarise participants with the auditory artefacts associated with the TMS stimulation protocol, TMS was delivered with the coil held in the air approximately 1 meter behind participants' heads during the training session. In each TMS-EEG session, TMS was delivered to a different site over the left hemisphere (see Section 5.2.3). The order of site stimulation was counterbalanced across participants. In each session, participants completed one practice block of 40 trials during which TMS was delivered, then 360 trials during which TMS was delivered and EEG recorded. Rest breaks were provided every 40 trials.

TMS output intensity was matched across sites according to each participant's resting motor threshold (Stokes et al., 2007; Stokes et al., 2005). Between individual participants, TMS output intensity was varied between 90% and 100% distance-adjusted motor threshold (mean 95%) to ensure stimulation was comfortable and did not induce blinks. Resting motor threshold was assessed in a separate session prior to the training and TMS-EEG sessions.

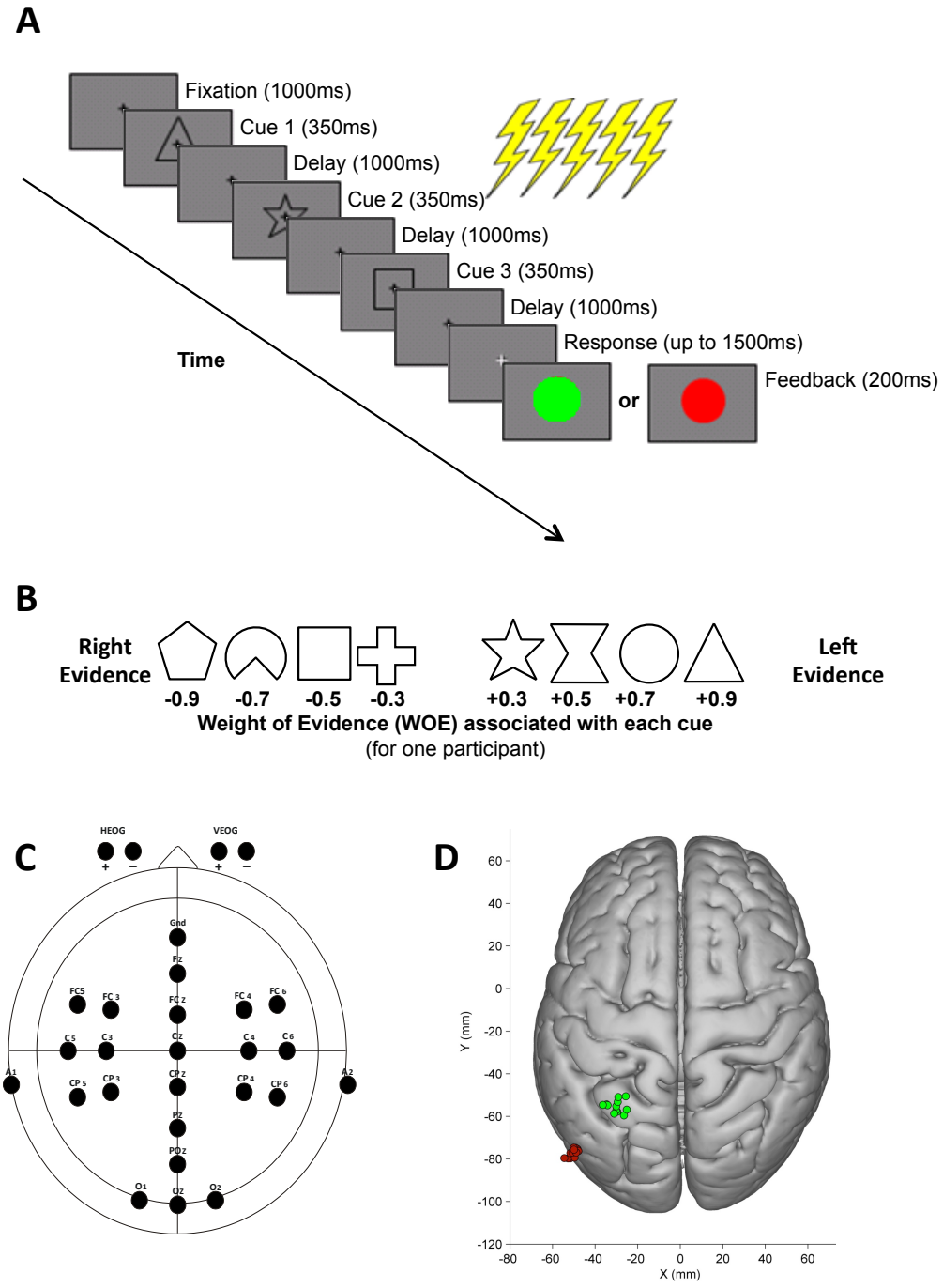


Figure 5-1. Experimental Task. (A) Schematic of a typical trial. Three cue stimuli were presented on all trials, providing probabilistic information about whether a left- or right-hand response would be rewarded. On 50% of trials, 5 pulses of TMS were delivered at 10 Hz, starting 50 ms after onset of the second cue shape. **(B)** The set of eight cue shapes and their mappings onto WOEs for one participant. **(C)** Electrode montage recorded from in all TMS-EEG sessions. **(D)** MNI coordinates of stimulated sites in each participant projected onto the MNI template brain (green = MIP; red = V5).

5.2.3. TMS Site Localisation

In separate sessions, TMS was delivered to a putative human homologue of the macaque area MIP (referred to hereafter as MIP) and V5 as control site. Both TMS sites were over the left hemisphere, controlling for any lateralized somatosensory and acoustic effects that may have directed attention to one side of space. We restricted stimulation to the left hemisphere for several reasons. First, although neuroimaging decision-making studies have reported bilateral activations along the intraparietal sulcus and superior parietal lobule, previous studies suggest a dominant role of the left hemisphere in motor planning (Cotti et al., 2011; Hesse et al., 2006; Króliczak & Frey, 2009; Mesulam, 1981; Mochizuki et al., 2005; Oliveira et al., 2010; Rushworth et al., 2001a; Rushworth et al., 2003; Rushworth et al., 2001b; Rushworth et al., 1997; Schluter et al., 2001; Schluter et al., 1998; Schluter et al., 1999). Stimulation of left-hemisphere sites thus maximised the chance that TMS would disrupt motor planning during our task. Second, a causal role of right-hemispheric regions has been strongly implicated in the control over spatial attention by lesion and TMS studies (Chambers et al., 2007; Chambers et al., 2004a; Chambers et al., 2004b; Chao et al., 2011; Fuggetta et al., 2006; Heinen et al., 2011; Hodsoll et al., 2009; Hung et al., 2005; Mattingley et al., 1998; Mesulam, 1981; Müri et al., 2002; Rushworth et al., 2001a; Rushworth et al., 2003; Sack et al., 2007; Schenkluhn et al., 2008; Taylor et al., 2007; Vallar & Perani, 1986). By stimulating the left hemisphere we minimized the chance of attentional disruption confounding our results (though see Gillebert et al., 2011).

Stimulation sites were identified in T1-weighted structural MRI scans for each participant using MNI co-ordinates from previous studies and local neuroanatomical landmarks. MNI co-ordinates of the brain stimulation sites for each participant are illustrated in Figure 5-1D. The MIP stimulation site was located on the medial bank of the middle part

of the intraparietal sulcus based on a recent diffusion-weighted imaging tractography-based parcellation of the parietal cortex (Mars et al., 2011) (average MNI brain co-ordinate: -30, -55, 63; average MNI scalp co-ordinate: -38, -63, 79). This region displays resting-state connectivity with PMd, and has been reported to show activity when hand and arm movements are made or hand and arm intentions updated (Grefkes et al., 2004; Hinkley et al., 2009; Mars et al., 2011; Rushworth et al., 2001c). The V5 stimulation site was defined based on recent fMRI data placing the human middle temporal (MT)/V5 complex in a region bounded by the lateral, anterior and inferior occipital sulci (Kolster et al., 2010) (average MNI brain co-ordinate: -50, -77, 8; average MNI scalp co-ordinate: -63, -87, 9). Coil placement was guided using Brainsight frameless stereotaxy (Rogue Research, Montreal, Canada).

5.2.4. EEG Recording, Pre-Processing and Spectral Analysis

EEG was recorded continuously (1,000-Hz sampling rate; Cz reference; NuAmps digital amplifiers; Neuroscan, El Paso, TX) from 32 scalp sites using Ag/AgCl electrodes mounted on an elastic cap (Easy Caps, Germany) according to the 10-10 international system (Chatrian et al., 1985). The montage included seven midline sites (OZ, POZ, PZ, CPZ, CZ, FCZ and FZ), nine sites over each hemisphere (O1/O2, PO3/PO4, PO7/PO8, CP3/CP4, CP5/C6, C3/C4, C5/C6, FC3/FC4, and FC5/6), left and right mastoids, HEOG and VEOG electrodes to monitor the EOG bipolarly, and an additional electrode (AFZ) used as ground (see Figure 5-1C). Electrode wires were arranged on the scalp to be loop free and oriented away from the centre of the TMS coil in order to minimise TMS-induced artefacts (Veniero et al., 2009). Recordings were re-referenced offline to the average EEG. Epochs were defined using digital codes sent to the EEG recording computer to mark the presentation of the cue

and target in each trial type. Continuous epochs from 1,000 ms before onset of the first cue shape to the end of the response period were included in analyses except when showing recording artefacts, if saccades or blinks occurred in the EOG, or if participants made early or late responses. On average, this resulted in inclusion of 162 TMS trials (S.D. = 15) and 163 no-TMS trials (S.D. = 19) per subject. A repeated-measures ANOVA compared the number of trials included for each subject with factors of TMS Condition (TMS, no-TMS) and TMS Site (MIP, V5). The number of rejected trials did not differ between sites or TMS conditions (all $Fs < 1.3$, all $ps > 0.3$).

Power spectra were computed for single-trial data using the multi-taper method (Mitra & Pesaran, 1999; Thomson, 1982) with a single Hanning taper (2-35 Hz, 0.5 Hz frequency steps, 600-ms temporal smoothing window, 50-ms window step size) using Fieldtrip (Oostenveld et al., 2011). Raw power data at each time-frequency sample were converted to decibel (dB) units by $\log_{10}$-transforming the raw data then multiplying it by 10, yielding approximately normally distributed data suitable for standard parametric statistical tests (Kiebel et al., 2005).

5.2.5. Region of Interest Selection and Beta Rebound

As in Chapter 4, our key hypotheses relate to the spectral power difference between left- and right-hemisphere motor planning regions. Based on previous motor planning and imagery studies (McFarland et al., 2000; Pfurtscheller et al., 1996; van Wijk et al., 2009; Wolpaw & McFarland, 2004), we pre-defined a left-hemisphere ROI as the average spectral power at electrodes C3 and CP3, and a right-hemisphere ROI as the average at electrodes C4 and CP4. We also validated this ROI using an independent data set. For this, we aligned raw

EEG data to participants' responses and performed the time-frequency analysis as described above. We then identified the peak electrodes at which differential beta modulation was present following left- versus right-hand responses (the 'beta rebound').

5.2.6. Visual Stimuli

Visual stimuli were presented at 60 Hz on a 17-inch Mitsubishi Diamond Pro CRT monitor at a viewing distance of 75 cm, with stimulus presentation and response acquisition controlled using Presentation 13.0 (Neurobehavioral Systems). All stimuli were presented centrally and against a uniform mid-grey background. The fixation cross consisted of two 0.2^{o} x 0.05^{o} black lines. The eight cue stimuli had a diameter of approximately 1.7^{o} and a line width of 0.02^{o}. The go signal was identical to the fixation cross except that it was coloured white. Feedback consisted of a 1.9^{o} disc, coloured green if the participant correctly guessed the world state, red if their guess was incorrect, and yellow if they responded too slowly or before the onset of the go stimulus

5.2.7. Behavioural Effects of TMS

To characterise how delivering TMS to MIP affected choice accuracy and miss rates (the proportion of trials on which participants failed to respond during the response period), we performed a 2-way repeated-measures ANOVA comparing performance in the MIP session with that of the V5 control session. ANOVA factors were TMS condition (TMS, no-TMS) and site (active, control).

For each TMS-EEG session and TMS condition, we further characterised how each participant's responses varied with the WOE at the end of each trial using a logistic psychometric function:

$$P(L) = \frac{1}{1 + 8^{-\beta(WOE-\alpha)}} \qquad \textit{Eq. 5-1.}$$

where *P(L)* is a vector describing the proportion of left responses the participant made at each WOE, and β and α describe the slope and threshold of the psychometric function, respectively. Fits were performed using the Palamedes toolbox for Matlab (Prins & Kingdom, 2009). A 2-way repeated-measures ANOVA was then performed to compare obtained slope and threshold parameters for the MIP session with those obtained for the control site, with factors of TMS condition (TMS, no-TMS) and site (active, control).

We also investigated whether TMS changed the impact of the first, second or third cue on participants' behaviour. To do this we performed a logistic regression separately for TMS and no-TMS trials in each TMS-EEG session:

$$P(L) = \frac{8^K}{1 + 8^K}, \text{where } K = \beta_0 + \beta_1 WOE_1 + \beta_2 WOE_2 + \beta_3 WOE_3 \qquad \textit{Eq. 5-2.}$$

where P(*L*) is a binary vector indicating whether a left or right response was made on each trial, WOE_i is the WOE provided by the *i*-th cue, and β_1, β_2 and β_3 are fitted coefficients describing the impact of each cue on behaviour. β_0 is a fitted constant term. We then performed 3-way repeated-measures ANOVAs to investigate whether the fitted coefficients β_1, β_2 and β_3 varied with the factors cue number (1, 2 or 3), TMS condition (TMS, no-TMS) and site (active, control).

To investigate the effects of TMS on reaction times, trials were binned according to the WOE in favour of the response made on each trial. As there were relatively few trials on

which participants' responses were not consistent with the sign of the WOE, we put all such trials into a single bin. The remaining trials WOEs were separated into another 3 equally spaced bins with edges between WOEs of 0 and ± 2.7. A repeated-measures ANOVA was then used to investigate whether MIP TMS modulated reaction times compared to the control site, with factors of bin number (1 to 4), response hand (left or right), TMS condition (yes or no), and TMS site (active, control).

5.2.8. Validation of EEG data - Analysis of Spectral Data from no-TMS Trials

We first investigated whether our EEG data replicated the pattern of results observed in Chapter 4, demonstrating that oscillatory activity in motor regions continuously updated to reflect available evidence. To maximise statistical power for this analysis, we pooled single-trial spectral data from no-TMS trials across all TMS sessions for each participant, then applied simple or multiple linear regression models to these data as in Chapter 4. Single-trial data were either raw data from individual sensors, an average over several sensors, or a 'lateralization index' (LI), calculated as the left-hemisphere minus right-hemisphere difference for left/right symmetric electrode pairs or ROIs.

In general we used a data-driven approach to identify the times and frequency-bands of significant effects (Donner & Siegel, 2011). Under this approach, each regression model was fit independently for each subject and at every sensor, frequency and time bin of interest. We then identified contiguous clusters of time-frequency bins at each sensor showing significant power modulation using one-sample *t* tests against zero with a threshold at $p < 0.01$ (two-tailed). Statistical significance of clusters was assessed at the group-level whilst controlling the type I false alarm rate using a cluster-based non-parametric randomization method (Maris & Oostenveld, 2007). We defined a second-level test statistic $\sum_T$ as the sum of

the T scores of all time-frequency bins in each cluster, and evaluated the significance of each cluster by comparing the original $\sum_T$ statistics to an estimated null distribution from 2,000 randomizations of the data. On each randomization, we permuted the correspondence between each participant's vector of predictor regressors and the observed spectral data, then fit the model and calculated $\sum_T$ statistics as above. The maximum positive and negative cluster statistics from each randomization defined the estimated null distribution. We then estimated two-tailed Monte Carlo *p* values for each original $\sum_T$ statistic against the estimated null distribution. All *p* values were Bonferroni-corrected for multiple comparisons when analysing multiple sensors.

To test whether spectral data reflected the accumulated WOE, we fit a simple linear model:

$$y = \beta_0 + \beta_1 WOE_i\,, \quad i = 1,2, \text{or } 3 \qquad \textit{Eq. 5-3.}$$

where *y* is a vector of single-trial spectral power data for a sensor-frequency-time bin from for a single participant, and WOE_i is a vector containing the overall WOE after the *i*-th cue on each trial. The fitted co-efficient β_1 describes the effect of the overall WOE on the spectral power, and the fitted co-efficient β_0 is a fitted constant term.

To dissociate the contributions of the prior WOE and cue WOE to spectral data, while controlling for non-specific factors associated with task difficulty and cue-related surprise, we extended the model described in Eq. 5.3 to include terms describing the absolute values of the prior WOE and the cue-related surprise. The model therefore took on the form:

$$y_i = \beta_0 + \beta_1 WOE_{i-1} + \beta_2 Q_i + \beta_3 i + \beta_4 |WOE_{i-1}| + \beta_5 Z_i\,, \quad i = 1,2,3 \qquad \textit{Eq. 5-4.}$$

$$Z_i = \log\left(P\left(s_j \middle| L\right) P(L)_i + P\left(s_j \middle| R\right) P(R)_i\right) \qquad \textit{Eq. 5-5.}$$

where $|WOE_{i-1}|$ denotes the absolute value, and $P(s_i|L)$ and $P(s_i|R)$ are the probabilities of observing shape s_j in the i-th epoch under the assumption of a Left or Right world state, respectively. $P(L)_i$ and $P(R)_i$ are the prior probabilities of a Left or Right world state given the overall WOE provided by all previously presented shapes on the trial. Z_i is therefore the overall log-probability of observing the cue stimulus under the prior WOE and is more negative when the presented cue is surprising given $P(L)_i$ and $P(R)_i$. Note also that this term corresponds to log of the denominator in Bayes' rule when calculating the posterior probability of either world state given the value of the i-th cue.

As in Chapter 4, we conducted two control analyses to investigate whether the relationships we observed between the WOE and oscillatory activity reflected a parametric relationship, or could be explained by planning of a categorical motor response.

The first control model investigated whether 8-14 Hz and 15-25 Hz activity reflected the WOE or the categorical response made at the end of the trial. To maximise sensitivity for this analysis, for each frequency band and for each trial, we averaged 500 ms of power data, starting 500 ms after each cue was presented. This time window captures the times at which oscillatory activity most strongly reflected the most recently presented cue, but not the ramping activity suggestive of categorical response planning (see Figure 5-5). We then fit linear regression models separately to the data for each frequency band and each of the four epochs:

$$y = \beta_0 + \beta_1 WOE_i + \beta_2 R\,, \quad i = 1,2 \text{ or } 3 \qquad \textit{Eq. 5-6.}$$

where y is the average power across the time window following presentation of the i-th shape, WOE_i is the overall WOE after presentation of the i-th shape, and R is the response made at the end of the trial. β_0, β_1, and β_2 are fitted coefficients. We then performed a two-way repeated-measures ANOVA to investigate whether the fitted coefficients for β_1 and β_2 varied

with the epoch number *i*. A dummy variable was included in the ANOVA model to allow us to test whether the β-parameters were significantly different from zero.

A second control model investigated whether oscillatory power reflected planning of a categorical response that flipped in direction over the course of trials due to fluctuations in the evidence presented to participants. This model was identical to the previous control model except for two changes. First, we only considered data from trials on which participants made the optimal response, suggesting that they correctly tracked the WOE over the course of the trial. Second, *R* was replaced by the term S_i, which reflected the sign of the WOE after presentation of the *i*-th shape:

$$y = \beta_0 + \beta_1 WOE_i + \beta_2 S_i , \quad i = 1,2,3 \qquad \textit{Eq. 5-7.}$$

5.2.9. Analysis of TMS Effects on EEG and their Relation to Behavioural TMS Effects

To investigate the mean effect of TMS on EEG-recorded oscillations over and above any variance explainable by task demands common to TMS and no-TMS trials, we extended the GLM model in Eq. 5-4 to include a term reflecting the effects of TMS:

$$y_i = \beta_0 + \beta_1 WOE_{i-1} + \beta_2 Q_i + \beta_3 i + \beta_4 |WOE_{i-1}| + \beta_5 Z_i + \beta_6 T_i, \quad i = 3 \qquad \textit{Eq. 5-8.}$$

where *T* is a binary term (0 or 1) describing whether TMS was delivered on each trial, and all other terms are as described for Eq. 5-4. This analysis was performed separately for each channel-frequency-time bin of each participant's data from each TMS-EEG session. The TMS-induced EEG artefact in TMS trials prevented us from analysing spectral data immediately before or after TMS pulses. We therefore fit the model described in Eq. 5-8 for data from the third epoch of each trial only. The model was fit to data from the earliest time

at which artefact-free EEG time-frequency data were available, 550 ms before onset of the third cue. This time point corresponds to 800 ms after onset of the second cue shape, reflecting that the first ~780 ms of the second epoch was not analysable since the last TMS pulse was delivered 450 ms after onset of the second cue, the TMS artefact extended ~30 ms, and the half-width of our temporal smoothing window was 300 ms. The latest time-point included in the analysis was the beginning of the response period. To maximise the sensitivity of the cluster statistics, the model was fit on *a priori* grounds to time-frequency data between 3 and 27 Hz (Maris & Oostenveld, 2007), within which range task-related effects were observed in Chapter 4. The 3-Hz lower limit also ensured data were not contaminated by low-frequency TMS artefacts associated with re-charging of TMS boosters, which we observed at electrodes proximal to the stimulation site.

After characterizing the overall time-frequency effects of TMS in each TMS-EEG session using cluster-based statistics, we statistically compared the effects between active and control TMS-EEG sessions. This was done by averaging the regression coefficients describing the mean effects of TMS (Eq. 5-8) over time and frequency windows of interest for each participant in the MIP TMS-EEG session, and then subtracting the same measure calculated for the V5 control session. This computation was performed separately for left- and right-hemisphere ROIs. Data were then subjected to a 2-way repeated-measures ANOVA to investigate whether beta-band power differed in left and/or right hemisphere ROIs following MIP stimulation. Factors were hemisphere (left, right) and TMS site (MIP, V5).

Finally, we investigated whether individual participants' TMS-induced changes in EEG time-frequency data correlated with TMS-induced changes in behaviour using two-tailed Pearson correlations. Behavioural changes considered were modulation of the threshold and slope parameters of logistic functions estimated as described in Section 5.2.7. To assess

both lateralized and non-lateralized neural consequences of TMS, correlations were performed separately for the average effects over left- and right-hemisphere ROIs, and the difference between them (i.e., the LI).

5.3. Results

5.3.1. *Behavioural Consequences of TMS*

Overall performance on the task was high across all sessions and TMS conditions (range: 91.1% to 92.5%). A repeated-measures ANOVA comparing accuracy for MIP and control-site V5 sessions did not reveal any significant main effects or interactions (all $Fs < 1.6$, all $ps > 0.2$). Miss rates were low (<0.5% in all sessions), and performing the same repeated-measures ANOVAs on miss rates did not reveal any significant effects.

We more sensitively characterised how individual participants' choices varied with the overall WOE by fitting logistic psychometric functions to their choice data in each session and TMS condition. The slope and threshold parameters were fit independently in each case. Psychometric functions and the TMS-induced change in threshold and slope parameters are shown for each site in Figure 5-2. No significant effects on slope parameters were found (ps for all F-tests > 0.1). For the threshold parameter, however, a significant interaction was found between TMS condition and TMS site ($F(1,11) = 5.41$, $p = 0.04$), reflecting that psychometric function threshold parameters were shifted leftwards on TMS trials compared with no-TMS trials when MIP was stimulated (see Figure 5-2). This suggests a behavioural bias towards right-hand responses, which are favoured by negative WOEs. Qualitatively identical effects were obtained when holding the slope parameter constant and allowing only the threshold parameter to vary between logistic function fits (data not shown).

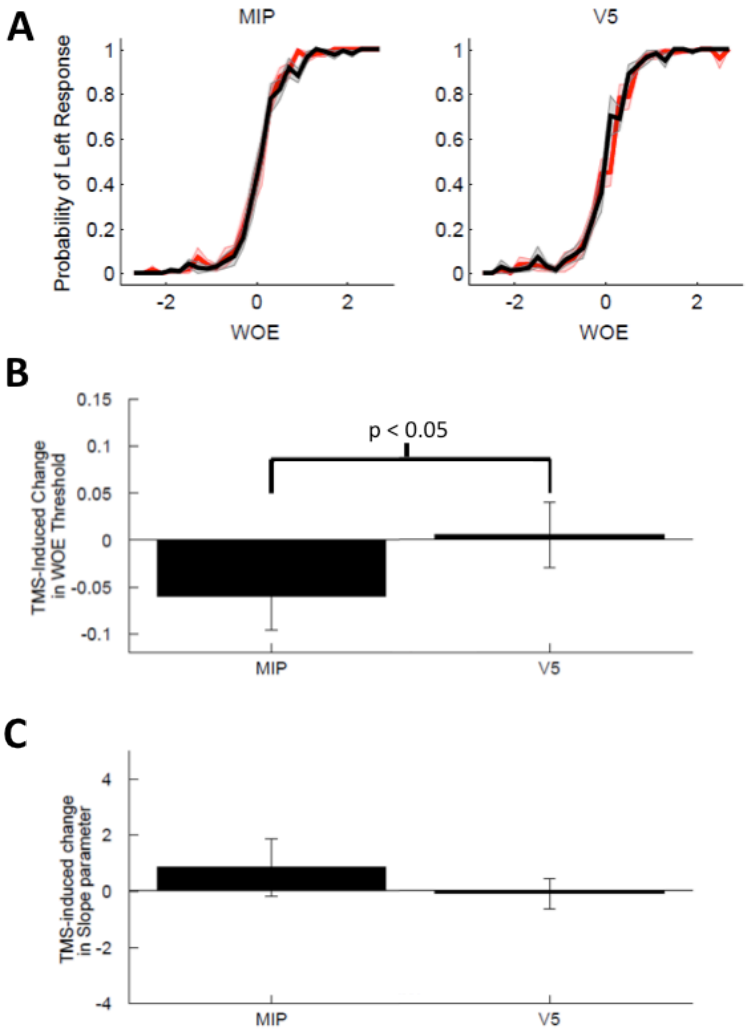


Figure 5-2. **Effects of TMS on choice behaviour. (A)** Psychometric functions for TMS and no-TMS trials in each experimental session. Red and black lines describe responses on TMS and no-TMS trials, respectively. **(B)** TMS induced a significant leftwards shift in threshold parameters of participants' psychometric functions, reflecting a bias towards left-handed responses**. (C)** No effects of TMS were found on the psychometric function slope parameter.

We wondered whether the shift in psychometric functions with MIP-TMS reflected an overall bias in participants' decisions, or resulted from a specific change in the weighting participants gave to different cues. Specifically, we wondered whether the effects of TMS altered the weights of the first or second cue stimulus on participants' decisions. A 3-way

repeated-measures ANOVA analysed the estimated weights of cues with factors of cue number (1, 2 or 3), TMS condition (TMS, no-TMS) and TMS site (active, control). No interactions with TMS site were observed, suggesting that the biasing of TMS towards right-handed responses cannot be attributed to changes in processing of any particular cue shape. The only significant effect was a main effect of cue number ($F(2,22) = 12.22$, $p = 0.002$). Overall, this reflected that the subjective weights given to cue stimuli were ~15% lower for the first cue than the third cue ($p < 0.002$) and ~12% lower for the second cue than the third cue ($p < 0.003$) regardless of the stimulation site and TMS condition.

Separate repeated-measures ANOVAs were performed to investigate whether TMS modulated reaction times (RTs) differently between the MIP and control-site sessions. Most importantly, no significant effects were found involving the factor TMS site. Several non-specific effects were observed however. A significant main effect of response hand was found ($F(1,11) = 12.37$, $p < 0.005$), reflecting overall faster RTs for left- (345 ms) than right-hand responses (361 ms) (pairwise comparison, $p < 0.01$). A main effect of TMS was also found ($F(1,11) = 9.12$, $p = 0.012$), reflecting overall faster RTs on TMS than no-TMS trials (345 vs 361 ms; pairwise comparison, $p < 0.05$). Finally, we observed a main effect of RT bin ($F(3,33) = 17.5$, $p < 0.01$). Post-hoc tests revealed that RTs were slower when participants made incorrect responses (bins 1-4: 406 ms, 343 ms, 336 ms and 328 ms, respectively; pairwise comparisons, ps < 0.05 comparing bin 1 with all other bins), but did not differ between any other bins (pairwise comparisons, all ps > 0.29).

5.3.2. EEG Results from no-TMS Trials

We first conducted analyses to investigate whether lateralization of preparatory motor activity was continuously updated to reflect available evidence as observed in Chapter 4. This

was achieved by investigating whether the lateralization index (LI) for electrodes overlying motor cortex correlated with fluctuations in the overall WOE in favour of left- versus right-hand responses. To maximise statistical power and for brevity, we report here analysis of data pooled across no-TMS trials from all TMS-EEG sessions. As in Chapter 4, key analyses were performed on the LI computed using *a priori* regions of interest in each hemisphere based on previous motor execution and imagery studies (McFarland et al., 2000; Wolpaw & McFarland, 2004) and which we confirmed showed the strongest post-response beta-band rebound (Figure 5-3).

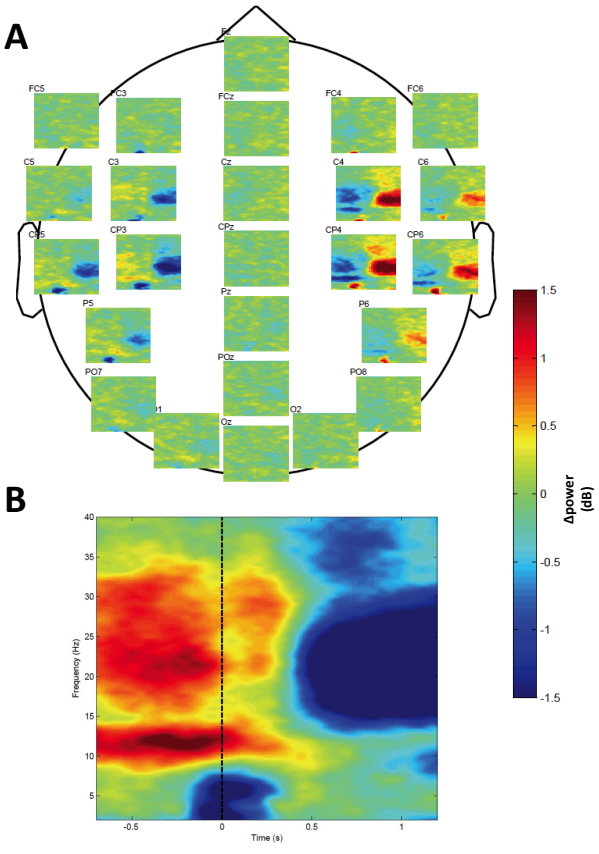


Figure 5-3. (A) Topography of the beta rebound lateralization is evident in the average time-frequency map for the subtraction of left- and right-handed responses. All plots depict the same time and frequency ranges as in (B). **(B)** As in (A) but showing the further subtraction between a left-hemisphere ROI (C3, CP3) and a right-hemisphere ROI (C4, CP4). The black vertical line marks the time at which a response was made.

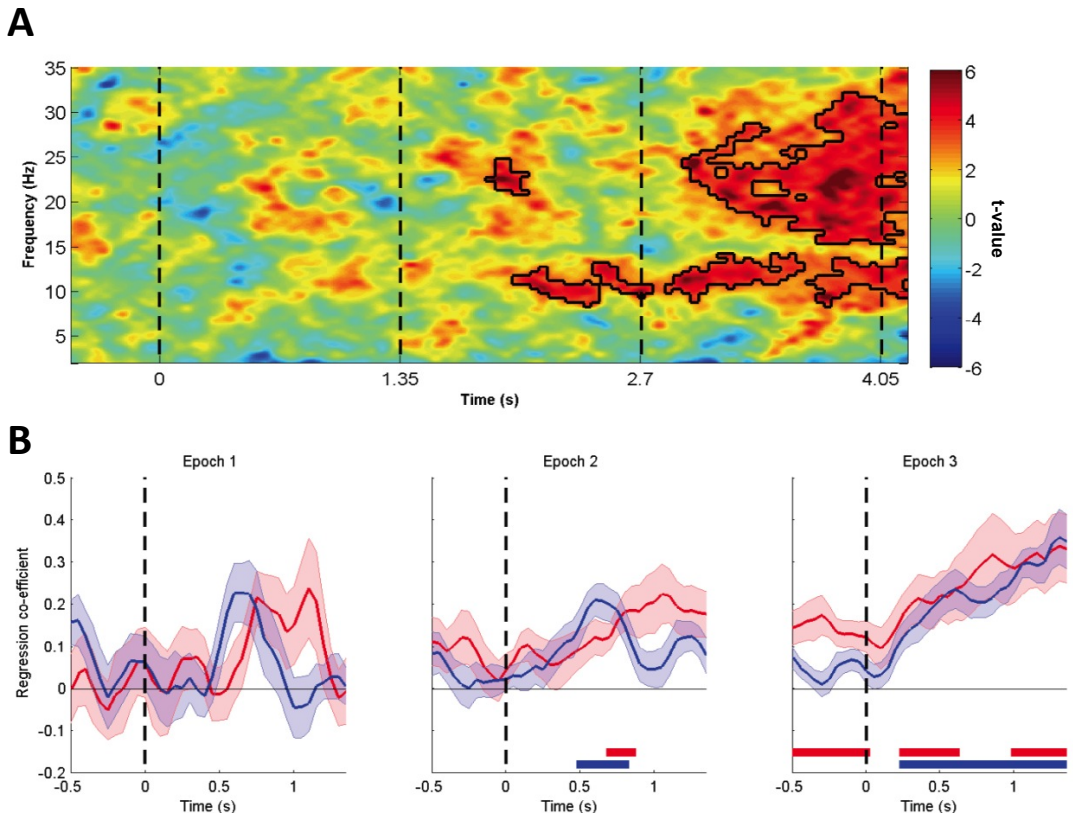


Figure 5-4. (A) The evolution of lateralization of 8-14 Hz and 15-25 Hz activity over motor electrodes correlates with the total evidence at the end of the trial for a left- versus right-hand response. Dashed lines indicate onset times of the three cue stimuli and the start of the response period. Solid black lines encircle significant effects. Onset of the first cue stimulus was at time zero. **(B)** Regression coefficient between the WOE after each shape presentation and lateralization of 8-14 Hz (thin red line) and 15-25 Hz (thin blue line) lateralization. Error bars are s.e.m. Dashed lines indicate onset times for each shape. Thick red and blue horizontal lines indicate significant effects.

As in Chapter 4, there was evidence of a relationship between the WOE at the end of the trial and alpha- and beta-band lateralization (Figure 5-4). Regression analyses of alpha- and beta-band activity in each cue period revealed significant correlations between the LI and activity in both frequency bands during the second and third epoch of the trial. A similar trend was observed in the first epoch, but did not reach significance in either band.

We then fit a regression model identifying the unique contributions to oscillatory activity provided by the prior WOE and the WOE provided by the most recently observed cue, whilst controlling for effects associated with general arousal, task difficulty and surprise (Eq. 5-4). Both the prior WOE and cue WOE made dissociable contributions to the LI (Figure 5-5A). The prior WOE was reflected in both frequency bands from early in the epoch or before onset of the cue stimulus, whereas correlates of the cue WOE were only significant starting approximately 500 ms after onset of the cue, presumably reflecting the processing times associated with the task. Positive effects of the absolute value parameter were also found in the average over electrodes contributing to the LI (Figure 5-5B), and both the absolute value and surprise parameters had significant effects at a range of individual electrode sites (Figure 5-6 and Figure 5-7).

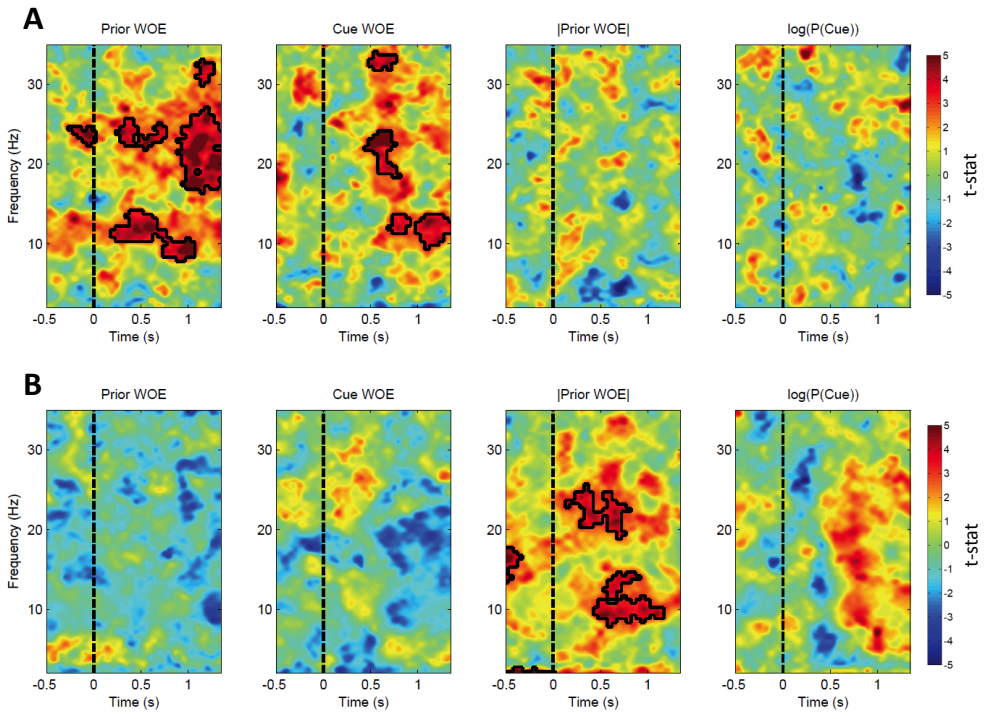


Figure 5-5. (A) The prior and cue WOEs were reflected in the LI over motor electrodes throughout the epoch, but not the |Prior WOE| or surprise associated with the most recently observed cue. **(B)** In the average across electrodes used to calculate the LI the prior WOE and cue WOE had no significant effects, but significant effects of the |Prior WOE| term were found.

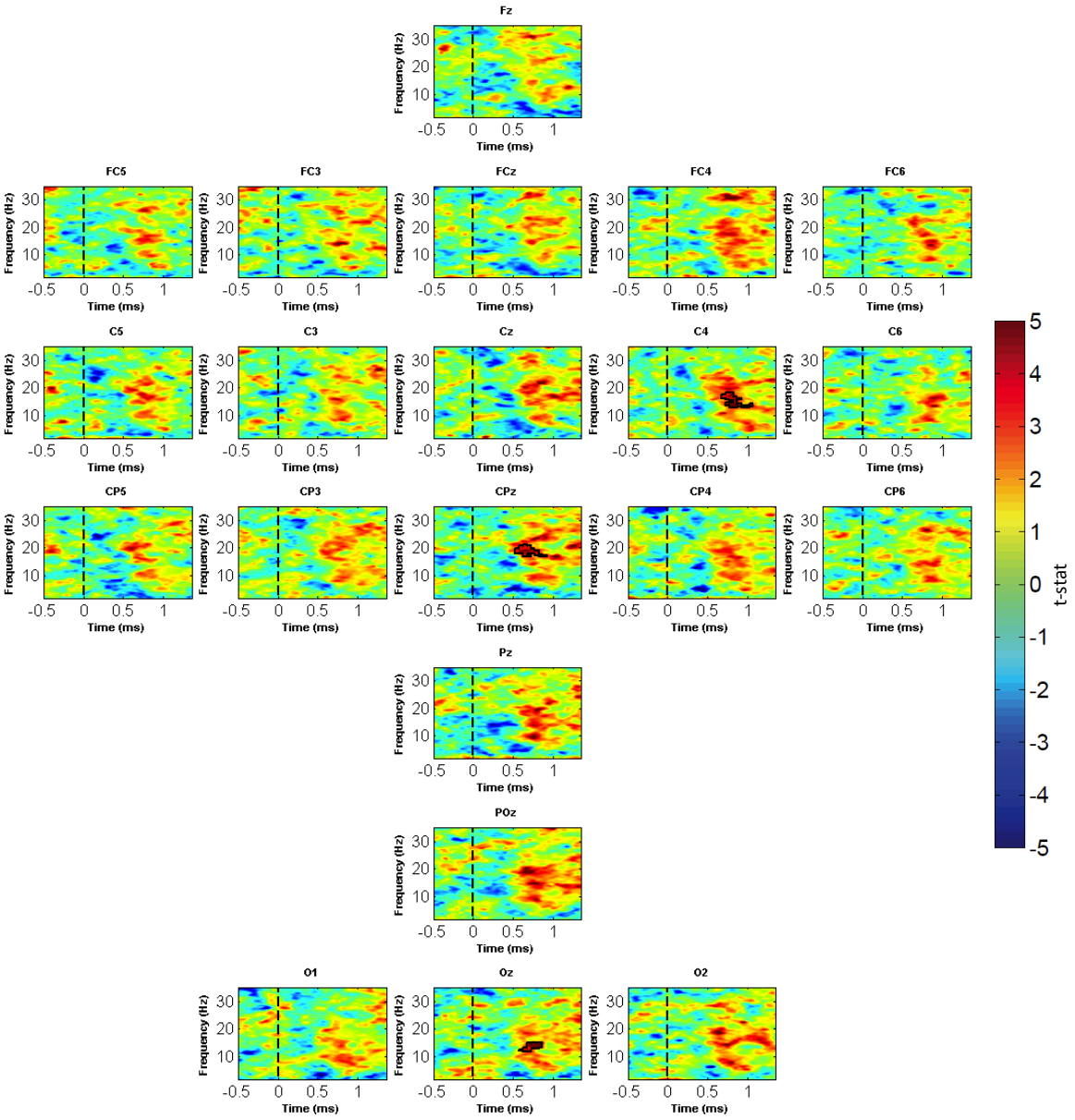


Figure 5-6. Effects of the Bayesian normalization term parameter were observed across a range of electrodes, and were strongest at central and occipital electrodes.

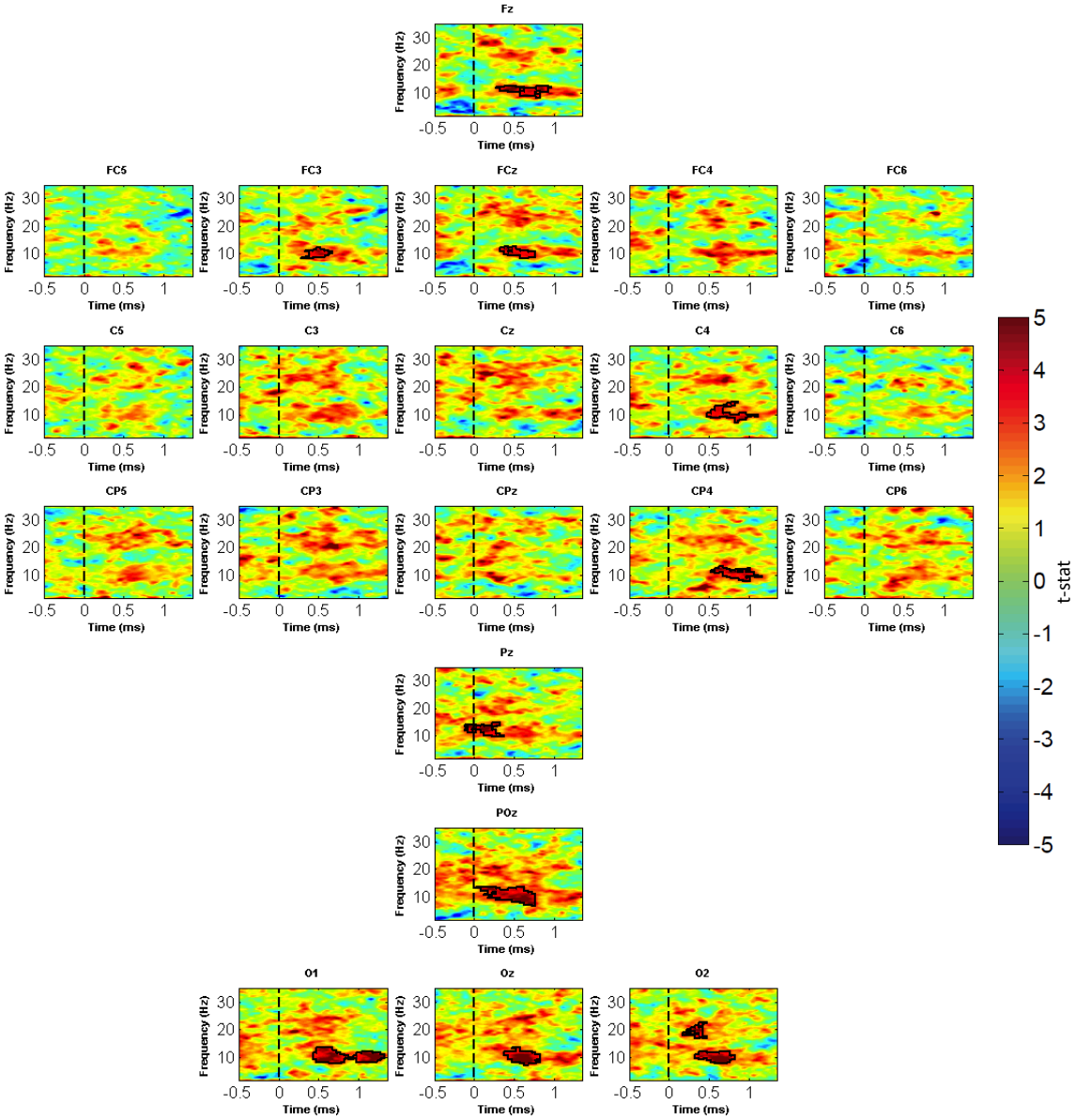


Figure 5-7. The absolute value of the Prior WOE modulated oscillatory activity in the alpha and beta bands across a wide range of electrodes.

As in Chapter 4, we further investigated whether the observed relationships between alpha- and beta-band signals and decision-evidence were parametric by considering two alternative hypotheses. We first considered whether the observed effects merely reflected planning of the categorical response made at the end of each trial (Eq. 5-6). This possibility could be rejected for both frequency bands, as a significant effect of the WOE was present

even when the effect of the response was modelled in each epoch of the trial (Figure 5-8) (8 to 14 Hz: $F(1,11) = 5.91$, $p = 0.03$; 15 to 25 Hz: $F(1,11) = 7.14$, $p = 0.02$). There was also a significant main effect of the response on 8 to 14 Hz ($F(1,11) = 18.9$, $p = 0.001$) and 15 to 25 Hz activity ($F(1,11) = 27.4$, $p < 0.001$). For 15 to 25 Hz activity there was also a significant effect of epoch number on regression coefficients modelling the effect of the response ($F(2,22) = 13.5$, $p < 0.001$). Pairwise comparisons revealed the response had significant effects on beta-band activity only during Epochs 2 and 3 ($ps = 0.012$ and 0.002, respectively). Thus, both frequency bands also reflected the categorical response, and beta-band activity displayed ramping effects, reflecting the response more strongly towards the end of the trial.

We then tested the alternate hypothesis that our effects did not reflect the planning of the response made at the end of trials, but a closely related variable – the planning of a response where the intended direction flipped as each of the three cues was presented and evidence in favour of one response or the other fluctuated. We tested this possibility by considering an additional model incorporating a term that reflected the sign of the WOE in each epoch (Eq. 5-7). Importantly, for this analysis we only considered trials on which participants made the optimal response, suggesting that they correctly tracked the WOE over the course of the trial. Results were similar to the previous control analysis, with a significant effect of the WOE found for both frequency bands (Figure 5-9) (8 to 14 Hz: $F(1,11) = 5.01$, $p = 0.047$; 15 to 25 Hz: $F(1,11) = 6.58$, $p = 0.026$). Similar to the effect of the response in the previous control model, a marginal main effect of epoch number was observed on coefficients modelling the effect of the sign of the WOE for 8 to 14 Hz activity ($F(2,22) = 3.65$, $p = 0.05$), as well as a significant effect of epoch number for 15 to 25 Hz activity ($F(2,22) = 4.11$, $p = 0.038$). Post-hoc tests revealed significant effects of the WOE sign at Epoch 3 for both 8 to 14 Hz ($p = 0.02$) and 15 to 25 Hz activity ($p < 0.001$).

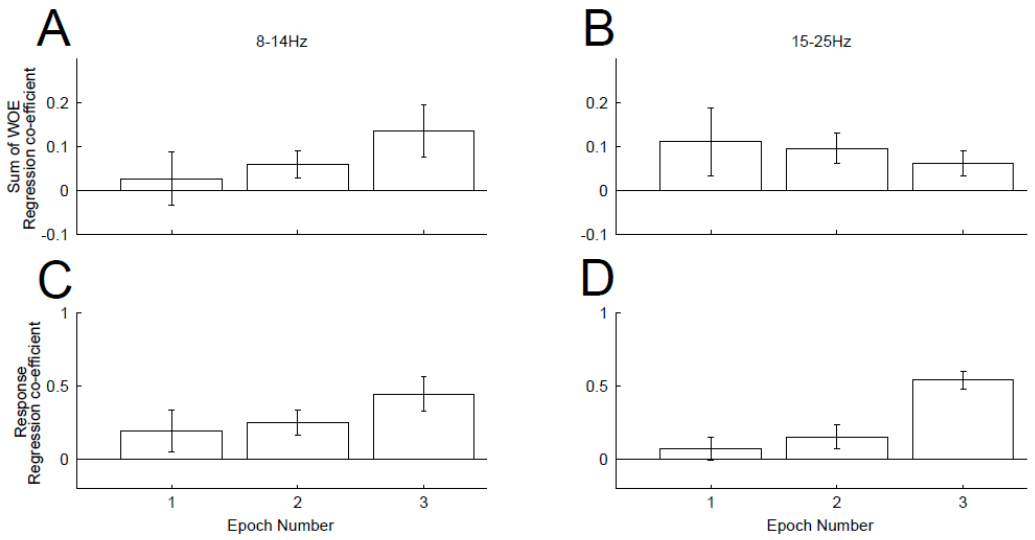


Figure 5-8. Effects of the WOE on oscillatory activity did not just reflect participants' responses. **(A, B)** After controlling for the categorical response at the end of the trial significant effects of the WOE were found for 8-14 Hz and 15-25 Hz activity. **(C, D)** The response at the end of the trial became increasingly correlated with beta-band lateralization as the trial progressed.

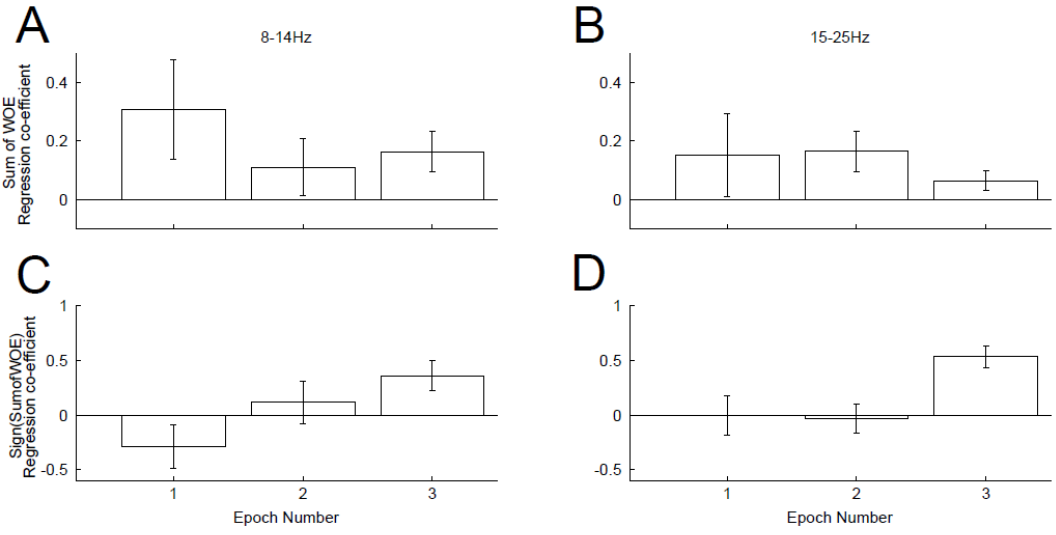


Figure 5-9. Effects of the WOE on oscillatory activity did not just reflect the categorical response favoured by the WOE at each stage of the trial. Plots are as in Figure 5-8 but controlling for the response the participant would have made based on the WOE at each point in the trial.

5.3.3. *EEG Effects of TMS*

Behavioural analyses described above suggest that, compared with control site stimulation, MIP stimulation biased participants' choices towards left-handed responses. In characterizing the neural effects of TMS, we first investigated whether TMS had a comparable effect on the average spectral power in each TMS-EEG session over and above the spectral responses associated with performance of the decision-making task. To do so, we extended the regression model fit to spectral data to include a term describing the average effects of TMS, and then fit this model separately to spectral data from each TMS-EEG session (Eq. 5-8). The model was fit to data from 550 ms before onset of the third cue shape (the earliest time at which time-frequency data undistorted by TMS pulses were available) until the beginning of the response period. No significant effects were found for the regressor describing the effects of TMS on the LI, however significant modulation of beta-band activity was observed in the average across the electrodes contributing to the LI (Figure 5-10A). In both TMS-EEG sessions these effects were present after delivery of the rTMS train and before the beginning of the third epoch of the trial. Exploration of the topography of beta-band modulation in the 550 ms before onset of the third cue reveals the specificity of this effect to electrodes contributing to the LI (Figure 5-10B).

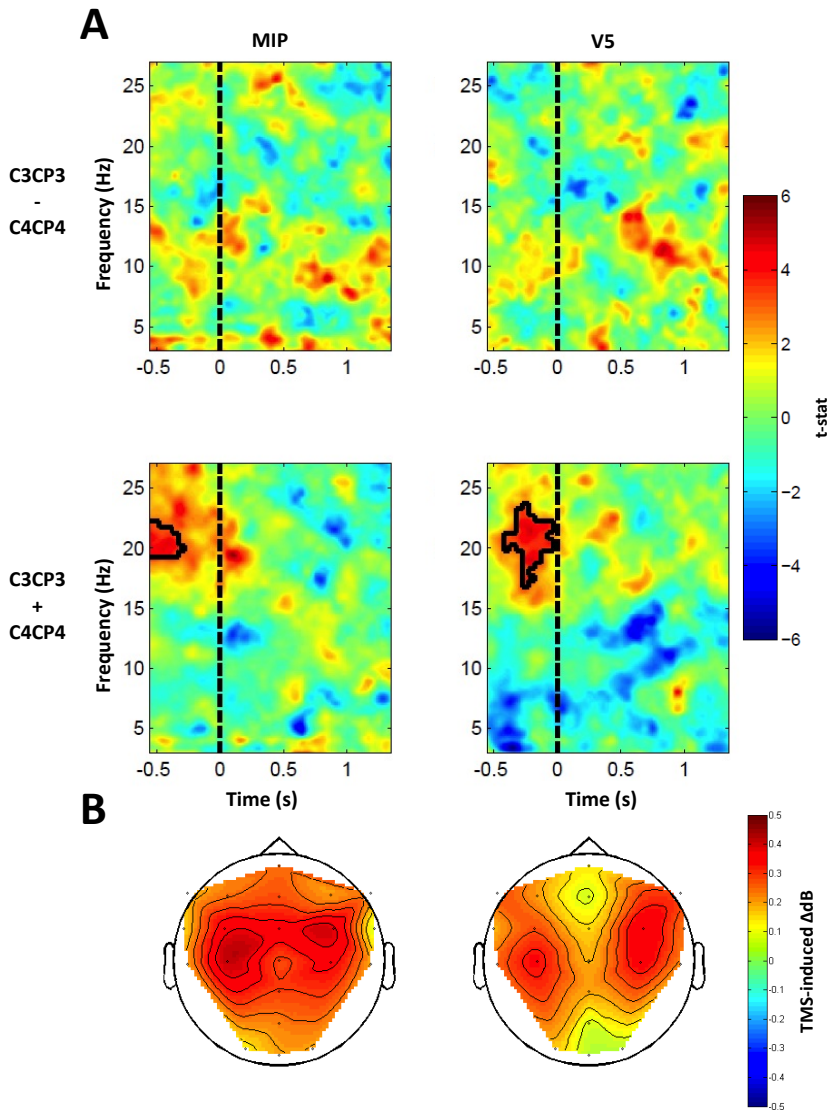


Figure 5-10. Mean effect of TMS on EEG time-frequency responses in the third epoch in each TMS-EEG session. (A) No significant lateralized effects of TMS were observed in the LI for any TMS-EEG session **(upper panel)**, however on average there was significant modulation over motor electrodes **(lower panel)**. Dashed vertical lines indicate the onset of the third cue shape. Solid black lines encircle significant effects **(B)** Topography of 15-25 Hz modulation due to TMS in the 550 ms before onset of the third cue reveals the specificity of TMS-induced beta-band modulation to central motor electrodes.

Given that TMS-induced modulation of beta-band activity resulted from stimulation of both sites, such a response is likely to reflect non-specific effects of TMS. To investigate the relationship between TMS-induced changes in behavioural and neural data, we conducted two sets of analyses. The first of these investigated whether the effects of TMS on beta-band

activity differed between control and active TMS-EEG sessions. To do this, for each TMS-EEG session we calculated the average TMS-induced 15 to 25 Hz effect for each participant over two time windows. The first time window included the 550 ms before onset of the third cue shape, corresponding to the time window during which significant beta-band modulation was observed in both TMS-EEG sessions. The second time window covered the entire period from 550 ms before onset of the third cue shape until the end of the third epoch, and was intended to investigate whether sustained effects of TMS persisted throughout the remainder of the trial. Repeated-measures ANOVAs investigated whether these effects differed significantly for the MIP TMS-EEG session compared with the V5 control session. No significant effects were found in beta-band activity in either time window following MIP stimulation (all $Fs < 0.9$, all $ps > 0.35$).

A second analysis aimed to investigate more sensitively whether, regardless of mean power changes, the effects of TMS on spectral power in individual subjects predicted the effects of TMS on their behavioural decision-making performance. Behavioural data analysed were the MIP versus V5 changes in the psychometric function threshold parameter reported in Section 5.3.1 and Figure 5-2. Neural data analysed were the subtractions between estimated regression coefficients describing the effects of TMS on beta-band activity for MIP versus V5. Correlations were performed separately for the two time windows of interest, and for three ROIs: the left-hemisphere ROI, the right-hemisphere ROI and the difference between them (i.e., the LI). We were primarily interested in investigating whether we could observe a correlate of the psychometric function threshold shift resulting from MIP stimulation. Supporting this idea, in the 550 ms preceding onset of the third cue, significant negative correlations were found between MIP minus V5 behavioural and neural measures for the ROIs in both hemispheres (left-hemisphere ROI: $R = -0.62$, $p = 0.03$; right-

hemisphere ROI: R = -0.60, p = 0.04) (Figure 5-11). Note that as TMS shifted thresholds leftwards (i.e., in a negative direction), this negative correlation suggests that bilateral beta power was *higher* in participants who were most strongly affected by TMS. However, no significant correlation was found for the LI (R = 0.01, p = 0.97). Over the longer time window, no correlations remained significant, though the right-hemisphere effect was marginal (R = -0.51, p = 0.09). To test the specificity of the correlations observed between TMS-induced behavioural and beta-band changes, we also repeated the correlation analysis described above for the 8 to 14 Hz frequency band. This did not reveal any significant effects.

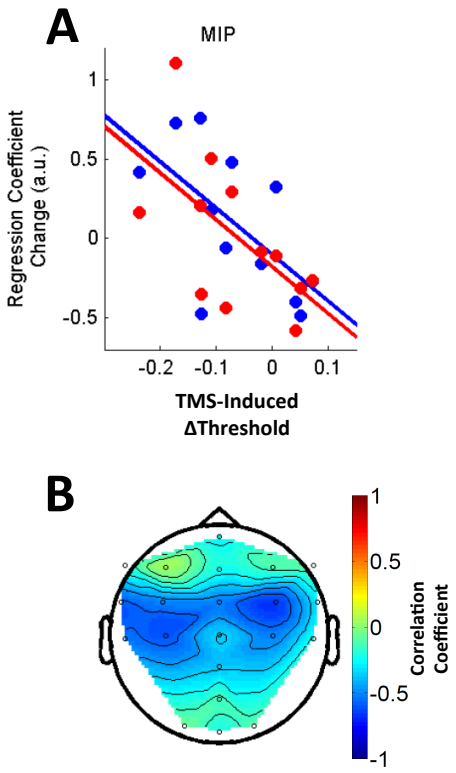


Figure 5-11. Correlations between TMS-induced beta-band changes and TMS-induced changes in the threshold parameter of psychometric functions describing participants' decision-making behaviour. (A) Following MIP TMS, negative correlations were found between threshold parameter changes and effects of TMS on beta-band activity for left- (blue line and dots) and right-hemisphere (red line and dots) motor electrodes. **(B)** This effect was topographically specific to central electrodes overlying motor cortex in both hemispheres.

5.4. Discussion

This study utilised concurrent TMS-EEG to investigate whether the process of integrating sequentially presented pieces of evidence towards a motor decision is causally dependent on a medial intraparietal region that resembles macaque area MIP in its estimated connections and functions (Mars et al., 2011). When TMS was delivered to MIP, participants were significantly biased to make ipsilateral (left hand) responses. Such a bias is expected if, as has been recently shown, areas in human parietal cortex are primarily concerned with preparation of contralateral hand responses when the two hands are competing to be chosen to respond (Oliveira et al., 2010). TMS causes destructive interference, as opposed to the constructive interference induced by microstimulation targeted to neurons with particular response fields. Nevertheless, TMS and microstimulation effects can often be related; intraparietal microstimulation (Hanks et al., 2006), just like TMS in the present experiment, induced reliable response biases, as opposed to changes in evidence accumulation that would have been indexed by changes in the slope of a fitted psychometric function. To our knowledge, our data provide the first direct demonstration that human intraparietal cortex plays a causal role in the process of integrating sensory evidence towards a response. Given the known anatomical and functional differences between the intraparietal and frontal cortices of monkey and man (Mars et al., 2011; Orban et al., 2004), this finding provides an important bridge between human and macaque decision-making studies.

Before investigating the consequences of TMS on oscillatory EEG activity, we first investigated whether data from no-TMS trials replicated the results of Chapter 4. Our analyses confirmed all of the major findings in Chapter 4. Lateralization of somatomotor alpha and beta-band activity correlated with the accumulated evidence in favour of left- versus right-hand responses throughout experimental trials, and these effects remained

significant even after controlling for categorical response-related variables. Once again, our GLM analysis approach also allowed us to isolate how the prior WOE and cue WOE made unique contributions to this oscillatory lateralization, and to demonstrate that similar non-lateralized correlates of decision certainty and cue-related surprise were observed compared with Chapter 4. These results are important in three respects. First, they provide an independent replication of the key results presented in Chapter 4. Second, because oscillatory activity was closely related to decision making in this experiment, any behaviourally relevant effects of TMS on somatomotor oscillatory activity are likely to reflect modulation of the process by which decision-related evidence is computed in the motor cortex, or communicated to it from distant brain regions. Finally, in the experiment reported in Chapter 4, participants were typically presented with four cues, but on catch trials had to respond after between one and three cues, making it equivocal whether our observation of lateralized oscillatory activity depended on the need to actively prepare responses. In contrast, in the present experiment participants observed three shapes on every trial, so had no need to prepare a motor response prior to the final cue period. Still, decision evidence in earlier epochs correlated significantly with the LI for both the alpha and beta frequency bands, suggesting that such activity may occur during decision making regardless of response expectations.

Not only participants' decisions, but also beta-band modulation associated with decision parameters, was causally dependent on the intraparietal sulcus; individual variability in decision threshold biases were correlated with individual differences in the beta-band effects seen shortly after MIP, as opposed to control, TMS. Although it was clear that MIP TMS-induced changes in beta-band activity were most prominent over the same motor areas showing activity correlated with decision evidence, their precise nature merits further

investigation. Amongst other possibilities, the beta-band changes may have reflected reduced responsiveness to further evidence (de Lange et al., 2010) or reduced response preparation. While the intraparietal TMS manipulation probably directly affected a limited region of cortex (Walsh & Cowey, 2000; Walsh et al., 2005), it is likely to have had an impact on activity in distant but interconnected areas that change as a function of the areas' coupling during task performance (Bestmann et al., 2008b; Bestmann et al., 2008c; Davare et al., 2010; Heinen et al., 2011; O'Shea et al., 2007a; Ruff et al., 2009). It may, therefore, make sense that TMS effects are correlated with aspects of beta-band changes if the beta-band changes themselves reflect long-range interactions (Donner & Siegel, 2011; Engel & Fries, 2010; Wang, 2010). Beta-band modulations have been reported between MIP and dorsal premotor cortex (Pesaran et al., 2008) and between adjacent parts of the superior parietal lobule and primary motor cortex (Witham et al., 2007), and at least in the former case they have been noted during visually-guided response selection.

The correlations we report between TMS-induced threshold parameter changes and beta-band activity stand in contrast to the fact that, at the group level, TMS did not significantly affect alpha- or beta-band activity following MIP compared with control site TMS. However, the correlated changes in decision behaviour and beta-band activity following MIP stimulation underscores the intimacy of the relationship between beta-band activity in the EEG and decision making. Several features of the results suggest they cannot be dismissed as simply the consequence of non-specific factors such as volume conduction: (1) the differential nature of the effects as opposed to control TMS, (2) that no similar effects were seen in other frequency bands, and (3) the distribution of the effects over motor areas.

Although MIP TMS did not significantly modulate alpha- or beta-band activity compared with our V5 control site, comparing TMS with no-TMS trials within each session

revealed that our 10-Hz stimulation regime induced transient changes in beta-band power regardless of the stimulated site. Significant modulation was not found in the alpha frequency band. The frequency-specific but site-independent consequences of TMS observed here complement several studies that applied TMS to motor regions and observed transient increases in beta-band synchrony (Fuggetta et al., 2005; Paus et al., 2001; Van Der Werf & Paus, 2006; Van Der Werf et al., 2006; Veniero et al., 2011), as well as one study showing that TMS of M1 or the SMA modulates beta-band activity in the sub-thalamic nucleus (Gaynor et al., 2008). Although alpha-band synchrony induction is more commonly reported in the TMS-EEG literature, we may not have observed such effects here because the ability of TMS to entrain the alpha cycle appears to require careful matching of the stimulation frequency to the peak frequency of participants' endogenous alpha rhythm (Thut et al., 2011).

A number of other studies have observed behavioural changes following intraparietal stimulation attributable to disruption of visuospatial attention rather than motor disruption. Spatial attentional disruption is unlikely as an explanation of the MIP TMS effects reported here for three main reasons. First, the behavioural modulation we report was a result of left-hemisphere intraparietal stimulation, whereas visual attention and visual search disruption is more typically reported to arise from right-hemisphere disruption (Rushworth et al., 2003). Second, we stimulated a site on the medial bank of the IPS, in the superior parietal lobule, whereas attentional disruptions from TMS have typically been reported following stimulation of the inferior parietal lobe (Chambers & Heinen, 2010). Third, all stimuli in our task were centrally presented, requiring maintenance of attention to foveal regions given that participants maintained fixation during the task. In contrast, spatial attention deficits are more typically found in the context of covert orienting or visual search tasks involving peripherally presented stimuli (Chambers & Heinen, 2010). Thus, it is more likely our effects reflect

disruption of decision integration activity rather than induction of a bias in visuospatial attention.

We note that the present experiment was designed using a conventional rTMS disruption paradigm involving online delivery of 10-Hz rTMS trains as participants carried out a behavioural task. Although our data suggest a close link between beta-band activity and decision making, because we did not systematically vary the frequency of stimulation it is unclear whether the effects we have observed were a direct result of disrupting endogenous beta-band activity, as may be expected if beta synchrony mediates inter-areal interactions underlying decision-related integration (Donner & Siegel, 2011; Engel et al., 1991). A recent study demonstrated that delivery of 20-Hz transcranial alternating current stimulation (tACS) over the motor cortex slows human movements, providing evidence for a causal relationship between neurophysiological oscillations and concurrent motor behaviour (Pogosyan et al., 2009). Future studies should further investigate whether TMS and tACS of parietal and motor structures in the human brain have frequency-specific effects on decision-making behaviour.

In summary, together with Chapter 4, the present study suggests that beta-band activity reflects not simply motor preparation but multiple sources of evidence bearing on the probabilistic reasoning that should guide optimal response selection and on the updating of this evidence as new information is revealed. Medial intraparietal TMS systematically biased decisions towards the ipsilateral hand, consistent with disruption of a decision variable in favour of a contralateral response, and the magnitude of these changes correlated with transient beta-band activity changes over somatomotor cortex.

Chapter 6 - General Discussion

Evidence from a large body of electrophysiological recordings and microstimulation studies suggests that signals reflecting the current state of monkeys' decisions are encoded throughout intraparietal, frontal, and motor circuits. In contrast, relatively few previous studies have explored whether the temporal dynamics of decision-related activity in the human brain undergo similar modulation. The main aim of this thesis was to investigate whether the amplitude of neural oscillations in the human brain reflect the selective modulation of sensory signals providing inputs to decision-making processes, and the current state of participants' internal decision variable as they integrate evidence towards manual motor responses. The second aim of this thesis was to elucidate whether human decision making is causally dependent on the intraparietal sulcus using concurrent TMS and EEG.

6.1. Alpha- and Beta-Band Neural Oscillations Provide an Ongoing Index of Attentional and Intentional States

Prior to this thesis work commencing, several studies had established that parametric modulation of oscillatory activity occurs as a result of several factors including task difficulty or memory load, however such effects may have reflected modulation of cortical excitability or thalamocortical information transmission at reasonably central levels (Jensen et al., 2002; Tuladhar et al., 2007). The three experiments presented in this thesis investigated whether alpha- and beta-band oscillations can provide an ongoing index of continuous change in participants' attentional and intentional states.

In the study described in Chapter 3, participants viewed symbolic cues associated with varying levels of spatial certainty about imperative stimuli which they were required to discriminate. EEG recordings revealed graded changes in the extent to which anticipatory alpha oscillations were lateralized over occipito-parietal cortex during the cue-target interval. Individual differences in this modulation predicted reaction times, ERP measures of perceptual processing of targets, and anticipatory beta-band desynchronization that was topographically focussed over the motor cortex contralateral to the hand used to make responses. Desynchronization of beta-band activity was also parametrically related to spatial certainty, being strongest for participants showing the greatest effects of spatial certainty on reaction times, and presumably reflecting increased response preparation when certainty was higher.

In the study described in Chapter 4, participants integrated information provided by a sequence of partially informative cues, which guided an upcoming left- or right-handed button-press response. Analysis of alpha- and beta-band lateralization over the motor cortex revealed that, as in the monkey, human motor planning signals are continuously and parametrically updated to reflect the precise amount of available evidence. The GLM analysis approach further allowed identification of distinct components reflecting prior evidence and cue-related evidence update signals in the alpha- and beta-bands. Information coded in each band showed qualitative differences – the alpha band reflected available decision evidence in a relatively tonic manner, whereas effects in the beta-band appeared much more phasic in nature, appearing at a reliable latency with respect to the onset of the cue stimulus. Beta-band effects also tended to precede those in the alpha band. These results thus raise the possibility that somatomotor alpha-band activity reflected ongoing maintenance of a decision variable,

whereas beta-band activity reflected more transient processes underlying updating of decision-related activity in somatomotor cortex.

In the study described in Chapter 5, the experimental task utilised in Chapter 4 was adapted for use with concurrent TMS-EEG. Control analyses from no-TMS trials replicated the EEG results of Chapter 4, and further demonstrated that alpha and beta lateralization proportional to the available evidence could be seen even during periods when participants knew a response would not be immediately required. Left hemisphere intraparietal TMS reliably biased the threshold parameters of psychometric functions in favour of an ipsilateral response, in a manner that was consistent with disruption of the representation of a decision variable. Across the participant group, the magnitude of this behavioural disruption was correlated with bilateral beta-band modulation over the motor cortex, but not with other frequency bands. In accordance with the hypothesis that this beta-band activity reflected TMS-induced increases in the functional coupling between the motor cortex and distant but interconnected regions such as the intraparietal cortex, bilateral beta-band activity was greatest for participants showing larger (more negative) threshold shifts.

Since this thesis was commenced, several key findings concordant with the parametric oscillatory modulations presented here have been reported. Similar to Chapter 3, one MEG study demonstrated that graded lateralization of alpha oscillations can be observed in the somatosensory cortex depending on the spatial certainty with which participants expect to receive target tactile stimulation at the cued hand (Haegens et al., 2011a). This highlights the difficulty in establishing whether the alpha-band decision variable correlates we have observed (Chapters 4 and 5) reflect modulation of motor preparation and/or somatomotor attention. Donner and colleagues (2009) also used MEG to show that beta-band lateralization in motor and premotor cortex was proportional to the integral of gamma-band activity

estimates in area MT+, and became increasingly strong predictors of participants' responses as time into the random-dot motion task decision period increased. An additional MEG study demonstrated that motor cortex beta-band activity varied parametrically with motor uncertainty, with desynchronization in a delay period being greatest when only one potential movement target appeared, smallest when three potential targets appeared, and intermediate in level when two targets were shown (Tzagarakis et al., 2010b). Furthermore, several theories have recently been put forward in which beta-band activity in the motor cortex is suggested to reflect, amongst other things, a running index of the extent to which internal and external cues combine to predict the need to initiate action (Donner & Siegel, 2011; Jenkinson & Brown, 2011; Siegel et al., 2011).

Overall, the results of Chapters 3 to 5 thus accord with a rapidly growing body of findings underscoring the flexibility with which moment-by-moment fluctuations in the amplitude of oscillatory neural activity may reflect active modulation of functional networks involved in perception, decision-making and action preparation (Foxe & Snyder, 2011; Jensen & Mazaheri, 2010; Siegel et al., 2011). However, several outstanding challenges remain. First, before the functional significance of these sorts of findings can be understood, considerable efforts will need to be made in investigating the causal consequences of oscillatory phenomena such as those reported here (see Section 6.2 below). The utility of being able to characterise these signals is also still being explored, though brain-computer interface (BCI) systems are increasingly focussing on oscillatory signals such as those focussed on here in the alpha- and beta-bands (Jensen et al., 2011; Miller et al., 2010; Waldert et al., 2008; Wolpaw et al., 2002; Wolpaw & McFarland, 2004). It will be of continuing interest for future research to attempt to quantify exactly how much information about movement intentions and actual movement dynamics can be predicted by oscillatory

activity in EEG, MEG and ECoG signals, and to characterise how these oscillatory signals explain common or independent variance compared with other neural signals such as firing rates and BOLD responses (Scheeringa et al., 2011; Whittingstall & Logothetis, 2009). Further clarification of the neural changes accompanying the oscillatory modulations reported in Chapters 4 and 5 is also necessary. While gamma-band oscillations are reliably positively correlated with local BOLD activity, it has been suggested that increases in the power of beta-band oscillations are often accompanied by local activity decreases, but that local cortical activity may be increased when beta power modulation reflects increased functional coupling between regions (Donner & Siegel, 2011). Corticospinal excitability varies parametrically with expectations about an upcoming response (Bestmann et al., 2008a), providing indirect evidence that at least some of the beta-band modulations reported in Chapters 4 and 5 are likely to have been accompanied by changes in corticospinal excitability. However, future work is required to investigate directly the extent with which these effects reflect modulation of functional coupling in the beta band between motor cortex and other regions involved in decision computations such as intraparietal regions (Pesaran et al., 2008). Given the higher signal-to-noise ratio, spatial resolution and reduced problems of volume conduction for MEG as compared with the EEG methods utilised here, MEG recordings along with the present task are likely to provide a fruitful approach for investigating such questions. MEG coherence analysis might aid attempts to dissociate the neural pathways along which synchronization is modulated during decision making (Schoffelen et al., 2005; Schoffelen et al., 2011). In particular, it would be valuable to attempt to distinguish the extent with which the decision-related oscillatory changes reported here reflect modulation of cortico-cortical, cortico-spinal and cortico-basal ganglia phase coupling (Jenkinson & Brown, 2011). While cortico-spinal coherence may be readily assessed using MEG-EMG data, identifying contributions to MEG signals from subcortical structures such

as the basal ganglia may be extremely challenging. Although technically demanding, analysis of MEG and concurrently recorded LFPs from deep brain stimulation electrodes in the subthalamic nucleus of Parkinson's disease patients may in the future allow clearer conclusions about such relationships to be made (Litvak et al., 2010).

6.2. Do Neural Oscillations Causally Shape Attention and Decision Making?

Future work is required to establish further the causal importance of the oscillatory phenomenon reported in this thesis, though it must be noted that several initial attempts to explore the causal nature of alpha- and beta-band activity have been highly successful. This is particularly the case in the context of the occipitoparietal alpha rhythm, where TMS delivered to the parietal cortex at a frequency matched to participants' peak individual alpha frequency appears to be able to entrain local alpha oscillations (Thut et al., 2011), and TMS delivered at the alpha frequency, but not other frequencies, impairs visual performance in the contralateral visual hemifield and improves it ipsilaterally (Romei et al., 2010). TMS of parietal and frontal attentional control regions also disrupts behaviour and attentional alpha lateralization in a correlated manner (Capotosto et al., 2009). Given the results of Chapter 3, together with reports that variation in the local amplitude or lateralization of occipitoparietal alpha power predicts the efficacy of TMS in eliciting phosphenes, or behavioural performance on detection and discrimination tasks (Kelly et al., 2009; Thut et al., 2006; Van Dijk et al., 2008), it seems reasonable to conclude that graded changes in the lateralization of alpha power are under top-down control, and causally impact upon visual perception, though the mechanism by which alpha modulation results in functional inhibition is still unclear (Buffalo et al., 2011; Foxe & Snyder, 2011; Jensen & Mazaheri, 2010).

Recent neurodisruption studies have also begun to explore the causal role of beta-band activity. Imperceptible 20-Hz transcranial alternating current stimulation (tACS) slows the velocity of parameters of reaching movements (Pogosyan et al., 2009). Furthermore, corticospinal excitability increases with beta-frequency tACS to the motor cortex (Feurra et al., 2011a) and varies sinusoidally with corticomuscular beta-band phase (van Elswijk et al., 2010). Intriguingly, beta-band TMS of the parietal lobe also seems to differentially affect global versus local visual processing tasks (Romei et al., 2011). While such data suggest that beta-band modulation has causal consequences, interpretation of such studies is made difficult by the relative complexity and multitude of beta-band phenomena reported in cortical, subcortical and spinal contexts. The results reported in Chapter 4 are correlational by nature, and cannot directly address the putative causal role of somatomotor alpha and beta oscillations in decision making. In Chapter 5, TMS-induced behavioural changes were closely related to modulation of somatomotor beta-band activity. It is possible that the intraparietal TMS manipulation disrupted long-range interactions mediated by beta band synchrony, leading to behavioural changes. However, because TMS affected both behaviour *and* beta-band activity, it is also possible that TMS-related beta effects were a consequence of the behavioural changes (Bestmann et al., 2008b). Future work is needed to clarify this issue. Support for a long-range interaction account could come from phase coherence analysis of EEG data from combined TMS-EEG experiments, though this would be challenging given that changes in beta power may affect the reliability of beta-band phase estimates, potentially biasing inter-regional coherence measures in a systematic manner. A more useful approach may be to investigate the consequence of manipulating activity in particular frequency bands with non-invasive stimulation techniques. For example, one could investigate the behavioural consequences of parametrically varying the frequency of tACS delivered to parietal, motor/premotor, or frontal regions in a decision integration task. Care would have to be taken

when designing such experiments, as tACS may induce visual phosphenes due to direct retinal stimulation at particular frequencies (Kanai et al., 2008), and when delivered to the somatosensory cortex can elicit tactile sensations (Feurra et al., 2011b). tACS could therefore impair performance on visual RDM discrimination and somatosensory vibrotactile discrimination tasks due to non-specific factors, making it preferable for decision making studies involving tACS to utilise tasks with supra-threshold stimuli, as in Chapters 4 and 5. TMS could also readily be applied to test the causal role of beta-band activity in decision integration. For example, if beta-band activity mediates long-range neural interactions, this may occur via coupling of other oscillatory phenomena, such as gamma-band power, to the phase of the beta oscillation. To test this, one could investigate whether the behavioural consequences of TMS depend on the phase of endogenous beta-band oscillations at the time of stimulation (van Elswijk et al., 2010). As TMS may result in a phase-reset of cortical beta oscillations (Paus et al., 2001), this would most readily be accomplished using single-pulse TMS in the context of an integrative task such as a random-dot motion task or the shape-integration task used in Chapters 4 and 5. Note that one disadvantage of the shape-integration task utilised in this thesis is the relative insensitivity of reaction times to decision certainty (see Figure 4-3D). In the context of neurodisruption studies, use of a task on which reaction times vary more strongly with evidence levels would be preferable, as drift diffusion model fits could then be applied to the data, allowing the consequences of TMS on decision variables to be investigated more systematically (Philiastides et al., 2011). Of course, such effects would need to be compared with an appropriate control condition to ensure that disruption effects on reaction-time performance were specific to decision-integration contexts, and not due to effects on motor execution (Hanks et al., 2006).

6.3. What Can We Conclude About How Decisions Evolve in the Human Brain?

"It seems that the comparison between stored and ongoing sensory information takes place in a distributed fashion – no single area can be identified as the unique site of decision-making" - (Romo & Salinas, 2003, p216).

The decision-making task utilized in Chapters 4 and 5 investigated updating of oscillatory activity over the motor cortex when the responses associated with decision outcomes were known throughout the decision period. This approach capitalized on the lateralization and somatotopic organization of the motor cortex to allow spatial dissociation of rhythmic neural activity associated with specific decision outcomes in motor/premotor regions. Results demonstrate that changes in decision evidence resulted in ongoing and parametric modulation of lateralization of oscillatory activity (Chapters 4 and 5), consistent with monkey studies suggesting that decision information propagates throughout motor planning networks (Gold & Shadlen, 2007). It would be expected that, as in the monkey, such effects propagate until relatively late stages in the motor system and also parametrically modulate cortiomuscular coherence (Schoffelen et al., 2005; Schoffelen et al., 2011), though further MEG-EMG work is needed to test this. Correlations between the behavioural and neural consequences of medial intraparietal TMS (Chapter 5) further suggest that intraparietal cortex is causally involved in decision-integration processes, providing evidence that the same neural structures involved in planning actions can also be involved in making decisions about what actions should be made. Together with data suggesting a causal role of the DLPFC in perceptual decision making (Philiastides et al., 2011), our results suggest that, as

in the monkey, human decision making is causally dependent on a distributed network of regions. It remains to be seen whether discrete areas in this network are functionally specialised for different aspects of the decision process (e.g., integration of sensory information versus maintenance of a decision variable), or whether it makes more sense to consider these networks as functionally coupled sets of accumulators, with decisions emerging as the result of competitive processes at any point in the network (Cisek & Kalaska, 2010). In attempting to dissociate functional differences throughout decision networks, it may be helpful to investigate whether dissociable behavioural effects result from TMS timed to disrupt specific parts of decision-updating processes suggested by Chapters 4 and 5 (e.g., the 'updating phase' at ~500ms after cue onset, versus the 'maintenance phase' towards the end of each epoch), and whether these effects vary depending on whether parietal, motor or frontal regions are stimulated.

The precise nature of the role of the human motor and premotor cortices (PMd) in decision-integration processes is also currently unclear. MEG source reconstruction (Donner et al., 2009; Hari & Salmelin, 1997) and ECoG data (Crone et al., 1998b; Miller et al., 2010) strongly suggest the decision variable correlates presented in Chapter 4 may have originated in primary motor and premotor structures, highlighting the importance of investigating whether these regions are actively involved in computing these quantities, or are simply in constant receipt of this information from other regions such as intraparietal cortex. The latter view – continuous updating of motor preparation as new information is acquired – might make sense from an ecological perspective as it would facilitate continuous interactions with the world (Cisek & Kalaska, 2010; Shadlen et al., 2008), however there is also considerable evidence suggesting an important role for PMd in response-selection processes. Previous monkey and human studies have demonstrated that PMd in both species has a causal role in

the selection of actions that are to be immediately executed when these responses are based on deterministic stimulus-response mapping rules (O'Shea et al., 2007a; O'Shea et al., 2007b; Wise & Murray, 2000). Monkey electrophysiological findings further suggest that a wider repertoire of decisions about responses may rely on competitive activity within a sensorimotor map of potential actions represented in PMd (Pastor-Bernier & Cisek, 2011), possibly via reciprocal PMd-MIP interactions (Pesaran et al., 2008). However, the causal role of human PMd in decision-integration tasks has not yet been established. It will therefore be important for future human neurodisruption studies to investigate whether PMd plays a causal role in the decision-integration processes that lead towards reaching movements.

An important limitation of the fixed response mappings in Chapters 4 and 5 is that it is unclear how these findings relate to other sorts of decisions. Intuitively, we often feel perfectly able to make decision about abstract ideas, and about ideas not associated with immediately executable actions. Experimentally, monkeys are able to make decisions about random-dot motion stimuli when saccadic target locations are unknown during decision making, and it is unclear how parts of the brain concerned with spatially-specific intentional planning (e.g., LIP) contribute to such decisions (Bennur & Gold, 2011; Gold & Shadlen, 2003). It should be noted that such decisions may be mediated by different neural paths, as accuracy tends to be higher when responses contingencies are established before onset of the RDM stimulus (Bennur & Gold, 2011; Gold & Shadlen, 2003). Recent computational models suggest that the same sorts of competitive neural processes thought to underlie decision making may be a ubiquitous neocortical mechanism (Cisek & Kalaska, 2010; Cisek et al., 2009; Wang, 2002). It may thus be conjectured that regardless of whether decision-response associations are known at the time the decision is made, similar accumulative processes may guide decision processes, but involving different brain regions. As noted by Gold and

Shadlen (2003), the PFC, particularly Walker's area 46, contains neurons that appear to encode more abstract behavioural rules such as 'if the motion is leftwards, choose the green saccade target' (Wallis et al., 2001). It remains an open question whether accumulative processes towards more abstract decisions may also be found in such regions. As in the past, single-unit recordings may help resolve these questions, though given the inhomogeneity of neural properties in area 46 compared with LIP, the FEF and SC, such studies are likely to be technically challenging. Given the discrete time periods over which parametric decision-related quantities were observed over motor/premotor regions in the experiments reported in Chapters 4 and 5, another possibility is that human MEG recordings may prove useful to investigate whether, in the context of decisions made without knowledge of response contingencies, regions like the DLPFC show a similar set of responses. Although our results – i.e., TMS-induced reductions in bilateral beta-band activity over motor regions that correlated with TMS-induced behavioural changes – are consistent with involvement of beta-band activity in inter-areal communication, beta-band activity has more classically been associated with preparatory states in motor and premotor regions. These views are not mutually exclusive. Beta-activity in the motor cortex may reflect interactions with the basal ganglia (Jenkinson & Brown, 2011), which also carries decision signals (Ding & Gold, 2010). However, such ideas still need to be rigorously empirically tested. By shifting the emphasis away from the motor system, adapting the task used in Chapters 4 and 5 for use with task in which decisions are made without knowledge of response contingencies may make it possible to gain important insights into the generality of beta-band activity. Such approaches may help discriminate between the array of regions implicated by fMRI studies of human perceptual decision making.

It should be noted that the work presented in this thesis has been exclusively concerned with identifying parametric relationships between decision evidence and lateralized oscillatory activity. Looking beyond this, another key property of 'decision-making neurons' in the monkey brain is that when activity levels reach a common decision threshold, the accumulation process terminates and a response is initiated (Gold & Shadlen, 2007). The shape-integration task from which we have presented data was designed to allow precise, objective manipulation of our participants' internal decision variables. However, an optimal observer might realize when they crossed a 'point of no return' during a sequence of shapes and terminate their decision (de Lange et al., 2010). In the shape-integration task used in Chapters 4 and 5, for example, if the first two shapes a participant sees both provide the strongest evidence for a left response, subsequently presented shapes can never outweigh this evidence. In such situations, participants might as well terminate their decision process and plan to make a left response. Although we did not formally model such a process, our control analyses in Chapters 4 and 5 suggest that categorical response planning occurred in the later epochs of trials, consistent with the idea that some decisions were terminated before the response stage of the task. It would be particularly interesting to collect MEG data as participants complete a version of the shape-integration task used in Chapters 4 and 5 incorporating several modifications. First, participants would be able to self-terminate the decision process at any point in the trial, and would be compelled to do so as a result of there being a cost associated with observing each additional piece of information. This would be likely to minimize any confounding effects of categorical response planning in neural responses, and might demonstrate that decisions are executed as soon as a threshold level of neural activity is reached. Second, the reward for a correct decision and punishment for an incorrect decision would be varied between blocks of the task, allowing investigation of whether oscillatory decision-related activity scales linearly with available evidence (i.e., the

effects of quantities of evidence would remain constant, but the decision threshold would change), or represents the relative distance to a common decision bound (i.e., the effects of evidence would change, but the threshold remain constant).

In conclusion, I hope that the work presented here will contribute to bridging the gap between non-human primate electrophysiological studies and non-invasive human investigations into the neural basis of decision making. It is also hoped that the experimental tasks developed here may be adapted for use in future studies, and thereby make further contributions to advances in our understanding of how the brain implements the variety of decision-making processes we take for granted in every day of our lives.

Bibliography

Abbey, C. K., & Eckstein, M. P. (2006). Classification images for detection, contrast discrimination, and identification tasks with a common ideal observer. *Journal of Vision, 6*(4).

Abrahamyan, A., Clifford, C. W. G., Arabzadeh, E., & Harris, J. A. (2011). Improving Visual Sensitivity with Subthreshold Transcranial Magnetic Stimulation. *The Journal of Neuroscience, 31*(9), 3290-3294.

Adrian, E. D., & Matthews, B. H. C. (1934). The Berger Rhythm: potential changes from the occipital lobes in man. *Brain, 57*, 355-384.

Afraz, S.-R., Kiani, R., & Esteky, H. (2006). Microstimulation of inferotemporal cortex influences face categorization. *Nature, 442*(7103), 692-695.

Albantakis, L., & Deco, G. (2009). The encoding of alternatives in multiple-choice decision making. *Proceedings of the National Academy of Sciences, 106*(25), 10308-10313.

Alexander, G. E., & Crutcher, M. D. (1990). Preparation for movement: neural representations of intended direction in three motor areas of the monkey. *Journal of Neurophysiology, 64*(1), 133-150.

Allison, T., Wood, C., & McCarthy, G. (1986). The Central Nervous System. In M. G. H. Coles (Ed.), *Psychophysiology* (pp. 5-25). New York: The guilford Press.

Amassian, V. E., Eberle, L., Maccabee, P. J., & Cracco, R. Q. (1992). Modelling magnetic coil excitation of human cerebral cortex with a peripheral nerve immersed in a brain-shaped volume conductor: the significance of fiber bending in excitation. *Electroencephalography and Clinical Neurophysiology/Evoked Potentials Section, 85*(5), 291-301.

Amiez, C., & Petrides, M. (2009). Anatomical organization of the eye fields in the human and non-human primate frontal cortex. *Progress in Neurobiology, 89*(2), 220-230.

Andersen, R. A., Asanuma, C., Essick, G., & Siegel, R. M. (1990). Corticocortical connections of anatomically and physiologically defined subdivisions within the inferior parietal lobule. *The Journal of Comparative Neurology, 296*(1), 65-113.

Andersen, R. A., Brotchie, P. R., & Mazzoni, P. (1992). Evidence for the lateral intraparietal area as the parietal eye field. *Current Opinion in Neurobiology, 2*(6), 840-846.

Andersen, R. A., & Buneo, C. A. (2002). Intentional Maps in Posterior Parietal Cortex. *Annual Review of Neuroscience, 25*(1), 189-220.

Andersen, R. A., & Cui, H. (2009). Intention, Action Planning, and Decision Making in Parietal-Frontal Circuits. *Neuron, 63*(5), 568-583.

Andrew, C., & Pfurtscheller, G. (1997). On the existence of different alpha band rhythms in the hand area of man. *Neuroscience Letters, 222*(2), 103-106.

Andrew, C., & Pfurtscheller, G. (1999). Lack of bilateral coherence of post-movement central beta oscillations in the human electroencephalogram. *Neuroscience Letters, 273*(2), 89-92.

Ashby, F. G., & Townsend, J. T. (1980). Decomposing the reaction time distribution: Pure insertion and selective influence revisited. *Journal of Mathematical Psychology, 21*(2), 93-123.

Astafiev, S. V., Shulman, G. L., Stanley, C. M., Snyder, A. Z., Van Essen, D. C., & Corbetta, M. (2003). Functional organization of human intraparietal and frontal cortex for attending, looking, and pointing. *Journal of Neuroscience, 23*(11), 4689-4699.

Averbeck, B. B., Battaglia-Mayer, A., Guglielmo, C., & Caminiti, R. (2009). Statistical Analysis of Parieto-Frontal Cognitive-Motor Networks. *Journal of Neurophysiology, 102*(3), 1911-1920.

Baillet, S., Mosher, J. C., & Leahy, R. M. (2001). Electromagnetic brain mapping. *Signal Processing Magazine, IEEE, 18*(6), 14-30.

Baizer, J., Ungerleider, L., & Desimone, R. (1991). Organization of visual inputs to the inferior temporal and posterior parietal cortex in macaques. *The Journal of Neuroscience, 11*(1), 168-190.

Baker, S. N., Olivier, E., & Lemon, R. N. (1997). Coherent oscillations in monkey motor cortex and hand muscle EMG show task-dependent modulation. *The Journal of Physiology, 501*(1), 225-241.

Balan, P. F., & Gottlieb, J. (2009). Functional Significance of Nonspatial Information in Monkey Lateral Intraparietal Area. *The Journal of Neuroscience, 29*(25), 8166-8176.

Banerjee, S., Snyder, A. C., Molholm, S., & Foxe, J. J. (2011). Oscillatory Alpha-Band Mechanisms and the Deployment of Spatial Attention to Anticipated Auditory and Visual Target Locations: Supramodal or Sensory-Specific Control Mechanisms? *The Journal of Neuroscience, 31*(27), 9923-9932.

Bankó, É. M., Gál, V., Körtvélyes, J., Kovács, G., & Vidnyánszky, Z. (2011). Dissociating the Effect of Noise on Sensory Processing and Overall Decision Difficulty. *The Journal of Neuroscience, 31*(7), 2663-2674.

Barak, O., Tsodyks, M., & Romo, R. (2010). Neuronal Population Coding of Parametric Working Memory. *The Journal of Neuroscience, 30*(28), 9424-9430.

Barash, S., Bracewell, R. M., Fogassi, L., Gnadt, J. W., & Andersen, R. A. (1991). Saccade-related activity in the lateral intraparietal area. I. Temporal properties; comparison with area 7a. *Journal of Neurophysiology, 66*(3), 1095-1108.

Barker, A. T., Freeston, I. L., Jalinous, R., Merton, P. A., & Morton, H. B. (1985a). Magnetic stimulation of the human brain. *The Journal of Physiology, 369*(Suppl), 3P.

Barker, A. T., Jalinous, R., & Freeston, I. L. (1985b). Non-invasive magnetic stimulation of human motor cortex. *The Lancet, 325*(8437), 1106-1107.

Basar, E., Schürmann, M., Basar-Eroglu, C., & Karakas, S. (1997). Alpha oscillations in brain functioning: an integrative theory. *International Journal of Psychophysiology, 26*(1-3), 5-29.

Basso, M. A., & Wurtz, R. H. (1998). Modulation of Neuronal Activity in Superior Colliculus by Changes in Target Probability. *The Journal of Neuroscience, 18*(18), 7519-7534.

Basten, U., Biele, G., Heekeren, H. R., & Fiebach, C. J. (2010). How the brain integrates costs and benefits during decision making. *Proceedings of the National Academy of Sciences*.

Batista, A. P., Buneo, C. A., Snyder, L. H., & Andersen, R. A. (1999). Reach Plans in Eye-Centered Coordinates. *Science, 285*(5425), 257-260.

Bechara, A., Damasio, H., Tranel, D., & Anderson, S. W. (1998). Dissociation Of Working Memory from Decision Making within the Human Prefrontal Cortex. *The Journal of Neuroscience, 18*(1), 428-437.

Beck, A. (1890). Die strome der nervencentren. *Centerblatt fur Physiologie, 4*, 572-573.

Beck, J. M., Ma, W. J., Kiani, R., Hanks, T., Churchland, A. K., Roitman, J., Shadlen, M. N., Latham, P. E., & Pouget, A. (2008). Probabilistic Population Codes for Bayesian Decision Making. *60*(6), 1142-1152.

Becker, R., Reinacher, M., Freyer, F., Villringer, A., & Ritter, P. (2011). How Ongoing Neuronal Oscillations Account for Evoked fMRI Variability. *The Journal of Neuroscience, 31*(30), 11016-11027.

Bennur, S., & Gold, J. I. (2011). Distinct Representations of a Perceptual Decision and the Associated Oculomotor Plan in the Monkey Lateral Intraparietal Area. *The Journal of Neuroscience, 31*(3), 913-921.

Berger, H. (1929). Über das Elektrenkephalogramm des Menschen. *Archiv für Psychiatrie und Nervenkrankheiten, 87*(1), 527-570.

Bestmann, S., Harrison, L. M., Blankenburg, F., Mars, R. B., Haggard, P., Friston, K. J., & Rothwell, J. C. (2008a). Influence of Uncertainty and Surprise on Human Corticospinal Excitability during Preparation for Action. *Current Biology, 18*(10), 775-780.

Bestmann, S., Ruff, C., Blankenburg, F., Weiskopf, N., Driver, J., & Rothwell, J. (2008b). Mapping causal interregional influences with concurrent TMS–fMRI. *Experimental Brain Research, 191*(4), 383-402.

Bestmann, S., Swayne, O., Blankenburg, F., Ruff, C. C., Haggard, P., Weiskopf, N., Josephs, O., Driver, J., Rothwell, J. C., et al. (2008c). Dorsal premotor cortex exerts state-dependent causal influences on activity in contralateral primary motor and dorsal premotor cortex. *Cerebral Cortex, 18*(6), 1281-1291.

Beurze, S. M., de Lange, F. P., Toni, I., & Medendorp, W. P. (2007). Integration of Target and Effector Information in the Human Brain During Reach Planning. *Journal of Neurophysiology, 97*(1), 188-199.

Beurze, S. M., de Lange, F. P., Toni, I., & Medendorp, W. P. (2009). Spatial and Effector Processing in the Human Parietofrontal Network for Reaches and Saccades. *J Neurophysiol, 101*(6), 3053-3062.

Beurze, S. M., Toni, I., Pisella, L., & Medendorp, W. P. (2010). Reference frames for reach planning in human parietofrontal cortex. *Journal of Neurophysiology, 104*(3), 1736-1745.

Binder, J. R., Liebenthal, E., Possing, E. T., Medler, D. A., & Ward, B. D. (2004). Neural correlates of sensory and decision processes in auditory object identification. *Nat Neurosci, 7*(3), 295-301.

Bisley, J. W., & Goldberg, M. E. (2010). Attention, Intention, and Priority in the Parietal Lobe. *Annual Review of Neuroscience, 33*(1), 1-21.

Bizzi, E., Tresch, M. C., Saltiel, P., & d'Avella, A. (2000). New perspectives on spinal motor systems. *Nat Rev Neurosci, 1*(2), 101-108.

Blatt, G. J., Andersen, R. A., & Stoner, G. R. (1990). Visual receptive field organization and cortico-cortical connections of the lateral intraparietal area (area LIP) in the macaque. *J Comp Neurol, 299*(4), 421-445.

Bogacz, R. (2007). Optimal decision-making theories: linking neurobiology with behaviour. *Trends in Cognitive Sciences, 11*(3), 118-125.

Bogacz, R. (2009). Optimal decision-making theories. In J. C. Dreher & L. Tremblay (Eds.), *Handbook of Reward and Decision Making* (pp. 375-397): Academic Press.

Bogacz, R., Brown, E., Moehlis, J., Holmes, P., & Cohen, J. D. (2006). The physics of optimal decision making: A formal analysis of models of performance in two-alternative forced-choice tasks. *Psychological Review, 113*(4), 700-765.

Bogacz, R., & Gurney, K. (2007). The Basal Ganglia and Cortex Implement Optimal Decision Making Between Alternative Actions. *Neural Computation, 19*(2), 442-477.

Bollimunta, A., Chen, Y., Schroeder, C. E., & Ding, M. (2008). Neuronal mechanisms of cortical alpha oscillations in awake-behaving macaques. *Journal of Neuroscience, 28*(40), 9976-9988.

Bonato, C., Miniussi, C., & Rossini, P. M. (2006). Transcranial magnetic stimulation and cortical evoked potentials: A TMS/EEG co-registration study. *Clinical Neurophysiology, 117*(8), 1699-1707.

Boorman, E. D., Behrens, T. E. J., Woolrich, M. W., & Rushworth, M. F. S. (2009). How Green Is the Grass on the Other Side? Frontopolar Cortex and the Evidence in Favor of Alternative Courses of Action. *62*(5), 733-743.

Boroojerdi, B., Prager, A., Muellbacher, W., & Cohen, L. G. (2000). Reduction of human visual cortex excitability using 1-Hz transcranial magnetic stimulation. *Neurology, 54*(7), 1529-1531.

Boudreau, C. E., Williford, T. H., & Maunsell, J. H. R. (2006). Effects of Task Difficulty and Target Likelihood in Area V4 of Macaque Monkeys. *J Neurophysiol, 96*(5), 2377-2387.

Brasil-Neto, J. P., McShane, L. M., Fuhr, P., Hallett, M., & Cohen, L. G. (1992). Topographic mapping of the human motor cortex with magnetic stimulation: factors affecting accuracy and reproducibility. *Electroencephalography and Clinical Neurophysiology/Evoked Potentials Section, 85*(1), 9-16.

Brazier, M. A. B. (1963). The history of the electrical activity of the brain as a method for localizing sensory function. *Medical History, 7*(3), 199-211.

Britten, K., Shadlen, M., Newsome, W., & Movshon, J. (1992). The analysis of visual motion: a comparison of neuronal and psychophysical performance. *The Journal of Neuroscience, 12*(12), 4745-4765.

Britten, K. H., Newsome, W. T., Shadlen, M. N., Celebrini, S., & Movshon, J. A. (1996). A relationship between behavioral choice and the visual responses of neurons in macaque MT. *Visual Neuroscience, 13*(01), 87-100.

Britten, K. H., Shadlen, M. N., Newsome, W. T., & Movshon, J. A. (1993). Responses of neurons in macaque MT to stochastic motion signals. *Visual Neuroscience, 10*(06), 1157-1169.

Brody, C. D., Hernández, A., Zainos, A., & Romo, R. (2003). Timing and Neural Encoding of Somatosensory Parametric Working Memory in Macaque Prefrontal Cortex. *Cerebral Cortex, 13*(11), 1196-1207.

Brovelli, A., Ding, M., Ledberg, A., Chen, Y., Nakamura, R., & Bressler, S. L. (2004). Beta oscillations in a large-scale sensorimotor cortical network: Directional influences revealed by Granger causality. *Proceedings of the National Academy of Sciences of the United States of America, 101*(26), 9849-9854.

Brown, P. (2006). Bad oscillations in Parkinson's disease. In P. Riederer, H. Reichmann, M. B. H. Youdim & M. Gerlach (Eds.), *Parkinson's Disease and Related Disorders* (Vol. 70, pp. 27-30): Springer Vienna.

Brown, S., & Heathcote, A. (2005). A Ballistic Model of Choice Response Time. *Psychological Review, 112*(1), 117-128.

Brown, S., Steyvers, M., & Wagenmakers, E.-J. (2009). Observing evidence accumulation during multi-alternative decisions. *Journal of Mathematical Psychology, 53*(6), 453-462.

Bruce, C. J., & Goldberg, M. E. (1985). Primate frontal eye fields. I. Single neurons discharging before saccades. *Journal of Neurophysiology, 53*(3), 603-635.

Bruce, C. J., Goldberg, M. E., Bushnell, M. C., & Stanton, G. B. (1985). Primate frontal eye fields. II. Physiological and anatomical correlates of electrically evoked eye movements. *Journal of Neurophysiology, 54*(3), 714-734.

Brunia, C. H. M. (1993). Waiting in readiness: Gating in attention and motor preparation. *Psychophysiology, 30*(4), 327-339.

Buffalo, E. A., Fries, P., Landman, R., Buschman, T. J., & Desimone, R. (2011). Laminar differences in gamma and alpha coherence in the ventral stream. *Proceedings of the National Academy of Sciences, 108*(27), 11262-11267.

Bullier, J. (2001). Integrated model of visual processing. *Brain Research Reviews, 36*(2-3), 96-107.

Buneo, C. A., & Andersen, R. A. (2006). The posterior parietal cortex: Sensorimotor interface for the planning and online control of visually guided movements. *Neuropsychologia, 44*(13), 2594-2606.

Buneo, C. A., Jarvis, M. R., Batista, A. P., & Andersen, R. A. (2002). Direct visuomotor transformations for reaching. *Nature, 416*(6881), 632-636.

Buneo, C. A., Jarvis, M. R., Batista, A. P., & Andersen, R. A. (2003). Properties of spike train spectra in two parietal reach areas. *Experimental Brain Research, 153*(2), 134-139.

Bunge, S. A., Hazeltine, E., Scanlon, M. D., Rosen, A. C., & Gabrieli, J. D. E. (2002). Dissociable Contributions of Prefrontal and Parietal Cortices to Response Selection. *NeuroImage, 17*(3), 1562-1571.

Burton, M. P., McKeefry, D. J., Barrett, B. T., Vakrou, C., & Morland, A. B. (2009). Disruptions to human speed perception induced by motion adaptation and transcranial magnetic stimulation. *European Journal of Neuroscience, 30*(10), 1989-1998.

Buschman, T. J., & Miller, E. K. (2007). Top-Down Versus Bottom-Up Control of Attention in the Prefrontal and Posterior Parietal Cortices. *Science, 315*(5820), 1860-1862.

Buschman, T. J., & Miller, E. K. (2009). Serial, Covert Shifts of Attention during Visual Search Are Reflected by the Frontal Eye Fields and Correlated with Population Oscillations. *Neuron, 63*(3), 386-396.

Buzsaki, G., & Draguhn, A. (2004). Neuronal Oscillations in Cortical Networks. *Science, 304*(5679), 1926-1929.

Caminiti, R., Ferraina, S., & Johnson, P. B. (1996). The Sources of Visual Information to the Primate Frontal Lobe: A Novel Role for the Superior Parietal Lobule. *Cerebral Cortex, 6*(3), 319-328.

Campana, G., Cowey, A., & Walsh, V. (2002). Priming of Motion Direction and Area V5/MT: a Test of Perceptual Memory. *Cerebral Cortex, 12*(6), 663-669.

Canolty, R. T., & Knight, R. T. (2010). The functional role of cross-frequency coupling. *Trends in Cognitive Sciences, 14*(11), 506-515.

Capotosto, P., Babiloni, C., Romani, G. L., & Corbetta, M. (2009). Frontoparietal Cortex Controls Spatial Attention through Modulation of Anticipatory Alpha Rhythms. *J. Neurosci., 29*(18), 5863-5872.

Carrasco, M., Ling, S., & Read, S. (2004). Attention alters appearance. *Nat Neurosci, 7*(3), 308-313.

Caton, R. (1875). The electric currents of the brain. *British Medical Journal, ii*, 278.

Cavada, C., & Goldman-Rakic, P. S. (1989). Posterior parietal cortex in rhesus monkey: II. Evidence for segregated corticocortical networks linking sensory and limbic areas with the frontal lobe. *The Journal of Comparative Neurology, 287*(4), 422-445.

Celebrini, S., & Newsome, W. T. (1995). Microstimulation of extrastriate area MST influences performance on a direction discrimination task. *Journal of Neurophysiology, 73*(2), 437-448.

Chakarov, V., Naranjo, J. R., Schulte-Mönting, J., Omlor, W., Huethe, F., & Kristeva, R. (2009). Beta-Range EEG-EMG Coherence With Isometric Compensation for Increasing Modulated Low-Level Forces. *Journal of Neurophysiology, 102*(2), 1115-1120.

Chambers, C. D., & Heinen, K. (2010). TMS and the functional neuroanatomy of attention. *Cortex, 46*(1), 114-117.

Chambers, C. D., Payne, J. M., & Mattingley, J. B. (2007). Parietal disruption impairs reflexive spatial attention within and between sensory modalities. *Neuropsychologia, 45*(8), 1715-1724.

Chambers, C. D., Payne, J. M., Stokes, M. G., & Mattingley, J. B. (2004a). Fast and slow parietal pathways mediate spatial attention. *Nat Neurosci, 7*(3), 217-218.

Chambers, C. D., Stokes, M. G., & Mattingley, J. B. (2004b). Modality-Specific Control of Strategic Spatial Attention in Parietal Cortex. *Neuron, 44*(6), 925-930.

Chao, C.-M., Tseng, P., Hsu, T.-Y., Su, J.-H., Tzeng, O. J. L., Hung, D. L., Muggleton, N. G., & Juan, C.-H. (2011). Predictability of saccadic behaviors is modified by transcranial magnetic stimulation over human posterior parietal cortex. *Human Brain Mapping*, n/a-n/a.

Chatrian, G. E., Lettich, E., & Nelson, P. L. (1985). Ten percent electrode system for topographic studies of spontaneous and evoked EEG activities. *American Journal of EEG Technology, 25*(2), 83-92.

Chatrian, G. E., Petersen, M. C., & Lazarte, J. A. (1959). The blocking of the rolandic wicket rhythm and some central changes related to movement. *Electroencephalography and Clinical Neurophysiology, 11*(3), 497-510.

Chawla, D., Rees, G., & Friston, K. J. (1999). The physiological basis of attentional modulation in extrastriate visual areas. *Nat Neurosci, 2*(7), 671-676.

Chelazzi, L., Miller, E. K., Duncan, J., & Desimone, R. (1993). A neural basis for visual search in inferior temporal cortex. *Nature, 363*(6427), 345-347.

Chen, R., Classen, J., Gerloff, C., Celnik, P., Wassermann, E. M., Hallett, M., & Cohen, L. G. (1997). Depression of motor cortex excitability by low,Äêfrequency transcranial magnetic stimulation. *Neurology, 48*(5), 1398-1403.

Churchland, A. K., Kiani, R., Chaudhuri, R., Wang, X.-J., Pouget, A., & Shadlen, M. N. (2011). Variance as a Signature of Neural Computations during Decision Making. *Neuron, 69*(4), 818-831.

Cisek, P. (2007). Cortical Mechanisms of Action Selection: The Affordance Competition Hypothesis. *Philosophical Transactions: Biological Sciences, 362*(1485), 1585-1599.

Cisek, P., & Kalaska, J. F. (2010). Neural Mechanisms for Interacting with a World Full of Action Choices. *Annual Review of Neuroscience, 33*(1), 269-298.

Cisek, P., Puskas, G. A., & El-Murr, S. (2009). Decisions in Changing Conditions: The Urgency-Gating Model. *The Journal of Neuroscience, 29*(37), 11560-11571.

Clark, V. P., & Hillyard, S. A. (1996). Spatial Selective Attention Affects Early Extrastriate But Not Striate Components of the Visual Evoked Potential. *Journal of Cognitive Neuroscience, 8*(5), 387-402.

Coe, B., Tomihara, K., Matsuzawa, M., & Hikosaka, O. (2002). Visual and Anticipatory Bias in Three Cortical Eye Fields of the Monkey during an Adaptive Decision-Making Task. *The Journal of Neuroscience, 22*(12), 5081-5090.

Cohen, M. R., & Maunsell, J. H. R. (2009). Attention improves performance primarily by reducing interneuronal correlations. *Nat Neurosci, 12*(12), 1594-1600.
Cohen, M. R., & Maunsell, J. H. R. (2010). A Neuronal Population Measure of Attention Predicts Behavioral Performance on Individual Trials. *J. Neurosci., 30*(45), 15241-15253.
Cohen, Y. E., & Andersen, R. A. (2002). A common reference frame for movement plans in the posterior parietal cortex. *Nat Rev Neurosci, 3*(7), 553-562.
Colby, C. L., & Duhamel, J.-R. (1991). Heterogeneity of extrastriate visual areas and multiple parietal areas in the Macaque monkey. *Neuropsychologia, 29*(6), 517-537.
Colby, C. L., Duhamel, J. R., & Goldberg, M. E. (1996). Visual, presaccadic, and cognitive activation of single neurons in monkey lateral intraparietal area. *Journal of Neurophysiology, 76*(5), 2841-2852.
Colby, C. L., & Goldberg, M. E. (1999). Space and attention in parietal cortex. *Annual Review of Neuroscience, 22*(1), 319-349.
Conway, B. A., Halliday, D. M., Farmer, S. F., Shahani, U., Maas, P., Weir, A. I., & Rosenberg, J. R. (1995). Synchronization between motor cortex and spinal motoneuronal pool during the performance of a maintained motor task in man. *The Journal of Physiology, 489*(Pt 3), 917-924.
Cook, E. P., & Maunsell, J. H. R. (2002). Dynamics of neuronal responses in macaque MT and VIP during motion detection. *Nat Neurosci, 5*(10), 985-994.
Corbetta, M., & Shulman, G. L. (2002). Control of goal-directed and stimulus-driven attention in the brain. *Nat Rev Neurosci, 3*(3), 201-215.
Cornwell, B. R., Carver, F. W., Coppola, R., Johnson, L., Alvarez, R., & Grillon, C. (2008). Evoked amygdala responses to negative faces revealed by adaptive MEG beamformers. *Brain Research, 1244*(0), 103-112.
Cotti, J., Rohenkohl, G., Stokes, M., Nobre, A. C., & Coull, J. T. (2011). Functionally dissociating temporal and motor components of response preparation in left intraparietal sulcus. *NeuroImage, 54*(2), 1221-1230.
Cowey, A., & Walsh, V. (2000). Magnetically induced phosphenes in sighted, blind and blindsighted observers. *NeuroReport, 11*(14), 3269-3273.
Craig, A. D. (2009). How do you feel [mdash] now? The anterior insula and human awareness. *Nat Rev Neurosci, 10*(1), 59-70.
Crammond, D. J., & Kalaska, J. F. (1996). Differential relation of discharge in primary motor cortex and premotor cortex to movements versus actively maintained postures during a reaching task. *Experimental Brain Research, 108*(1), 45-61.
Crick, F. (1984). Function of the thalamic reticular complex: the searchlight hypothesis. *Proceedings of the National Academy of Sciences of the United States of America, 81*(14), 4586-4590.
Crick, F., & Koch, C. (1995). Are we aware of neural activity in primary visual cortex? *Nature, 375*(6527), 121-123.
Crone, N. E., Miglioretti, D. L., Gordon, B., & Lesser, R. P. (1998a). Functional mapping of human sensorimotor cortex with electrocorticographic spectral analysis. II. Event-related synchronization in the gamma band. *Brain, 121*(12), 2301-2315.
Crone, N. E., Miglioretti, D. L., Gordon, B., Sieracki, J. M., Wilson, M. T., Uematsu, S., & Lesser, R. P. (1998b). Functional mapping of human sensorimotor cortex with electrocorticographic spectral analysis. I. Alpha and beta event-related desynchronization. *Brain, 121*(12), 2271-2299.
Cui, H., & Andersen, R. A. (2007). Posterior Parietal Cortex Encodes Autonomously Selected Motor Plans. *Neuron, 56*(3), 552-559.

Curtis, C. E., & Lee, D. (2010). Beyond working memory: the role of persistent activity in decision making. *Trends in Cognitive Sciences, 14*(5), 216-222.

Davare, M., Rothwell, J. C., & Lemon, R. N. (2010). Causal Connectivity between the Human Anterior Intraparietal Area and Premotor Cortex during Grasp. *Current Biology, 20*(2), 176-181.

Davare, M., Zénon, A., Pourtois, G., Desmurget, M., & Olivier, E. (2011). Role of the Medial Part of the Intraparietal Sulcus in Implementing Movement Direction. *Cerebral Cortex*.

de Lafuente, V., & Romo, R. (2005). Neuronal correlates of subjective sensory experience. *Nat Neurosci, 8*(12), 1698-1703.

de Lange, F. P., Hagoort, P., & Toni, I. (2005). Neural Topography and Content of Movement Representations. *Journal of Cognitive Neuroscience, 17*(1), 97-112.

de Lange, F. P., Jensen, O., Bauer, M., & Toni, I. (2008). Interactions between posterior gamma and frontal alpha/beta oscillations during imagined actions. *Frontiers in Human Neuroscience, 2*.

de Lange, F. P., Jensen, O., & Dehaene, S. (2010). Accumulation of Evidence during Sequential Decision Making: The Importance of Top-Down Factors. *J. Neurosci., 30*(2), 731-738.

Delorme, A., & Makeig, S. (2004). EEGLAB: an open source toolbox for analysis of single-trial EEG dynamics including independent component analysis. *Journal of Neuroscience Methods, 134*(1), 9-21.

Desmurget, M., Reilly, K. T., Richard, N., Szathmari, A., Mottolese, C., & Sirigu, A. (2009). Movement Intention After Parietal Cortex Stimulation in Humans. *Science, 324*(5928), 811-813.

Deubel, H., & Schneider, W. X. (1996). Saccade target selection and object recognition: Evidence for a common attentional mechanism. *Vision Research, 36*(12), 1827-1837.

Ding, L., & Gold, J. I. (2010). Caudate Encodes Multiple Computations for Perceptual Decisions. *J. Neurosci., 30*(47), 15747-15759.

Ditterich, J. (2006). Stochastic models of decisions about motion direction: Behavior and physiology. *Neural Networks, 19*(8), 981-1012.

Ditterich, J., Mazurek, M. E., & Shadlen, M. N. (2003). Microstimulation of visual cortex affects the speed of perceptual decisions. *Nat Neurosci, 6*(8), 891-898.

Dockree, P. M., Kelly, S. P., Foxe, J. J., Reilly, R. B., & Robertson, I. H. (2007). Optimal sustained attention is linked to the spectral content of background EEG activity: Greater ongoing tonic alpha (~10 Hz) power supports successful phasic goal activation. *European Journal of Neuroscience, 25*(3), 900-907.

Donders, F. C. (1969). On the speed of mental processes. *Acta Psychologica, 30*, 412-431.

Donner, T. H., & Siegel, M. (2011). A framework for local cortical oscillation patterns. *Trends in Cognitive Sciences, 15*(5), 191-199.

Donner, T. H., Siegel, M., Fries, P., & Engel, A. K. (2009). Buildup of Choice-Predictive Activity in Human Motor Cortex during Perceptual Decision Making. *Current Biology, 19*(18), 1581-1585.

Donner, T. H., Siegel, M., Oostenveld, R., Fries, P., Bauer, M., & Engel, A. K. (2007). Population Activity in the Human Dorsal Pathway Predicts the Accuracy of Visual Motion Detection. *J Neurophysiol, 98*(1), 345-359.

Doppelmayr, M., Klimesch, W., Pachinger, T., & Ripper, B. (1998). Individual differences in brain dynamics: Important implications for the calculation of event-related band power. *Biological Cybernetics, 79*(1), 49-57.

Dorris, M. C., & Glimcher, P. W. (2004). Activity in Posterior Parietal Cortex Is Correlated with the Relative Subjective Desirability of Action. *Neuron, 44*(2), 365-378.

Doyle, L. M. F., Yarrow, K., & Brown, P. (2005). Lateralization of event-related beta desynchronization in the EEG during pre-cued reaction time tasks. *Clinical Neurophysiology, 116*(8), 1879-1888.

Driver, J., Blankenburg, F., Bestmann, S., Vanduffel, W., & Ruff, C. C. (2009). Concurrent brain-stimulation and neuroimaging for studies of cognition. *Trends in Cognitive Sciences, 13*(7), 319-327.

Duhamel, Colby, C., & Goldberg, M. (1992). The updating of the representation of visual space in parietal cortex by intended eye movements. *Science, 255*(5040), 90-92.

Eckstein, M. P., Pham, B. T., & Shimozaki, S. S. (2004). The footprints of visual attention during search with 100% valid and 100% invalid cues. *Vision Research, 44*(12), 1193-1207.

Eckstein, M. P., Shimozaki, S. S., & Abbey, C. K. (2002). The footprints of visual attention in the Posner cueing paradigm revealed by classification images. *Journal of Vision, 2*(1).

Egner, T., Monti, J. M. P., Trittschuh, E. H., Wieneke, C. A., Hirsch, J., & Mesulam, M. M. (2008). Neural integration of top-down spatial and feature-based information in visual search. *Journal of Neuroscience, 28*(24), 6141-6151.

Ehrsson, H. H., Geyer, S., & Naito, E. (2003). Imagery of Voluntary Movement of Fingers, Toes, and Tongue Activates Corresponding Body-Part-Specific Motor Representations. *Journal of Neurophysiology, 90*(5), 3304-3316.

Engel, A. K., & Fries, P. (2010). Beta-band oscillations -- signalling the status quo? *Current Opinion in Neurobiology, 20*(2), 156-165.

Engel, A. K., König, P., Kreiter, A. K., & Singer, W. (1991). Interhemispheric Synchronization of Oscillatory Neuronal Responses in Cat Visual Cortex. *Science, 252*(5009), 1177-1179.

Ergenoglu, T., Demiralp, T., Bayraktaroglu, Z., Ergen, M., Beydagi, H., & Uresin, Y. (2004). Alpha rhythm of the EEG modulates visual detection performance in humans. *Cognitive Brain Research, 20*(3), 376-383.

Farmer, S. F. (1998). Rhythmicity, synchronization and binding in human and primate motor systems. *The Journal of Physiology, 509*(1), 3-14.

Fernandez-Ruiz, J., Goltz, H. C., DeSouza, J. F. X., Vilis, T., & Crawford, J. D. (2007). Human Parietal "Reach Region" Primarily Encodes Intrinsic Visual Direction, Not Extrinsic Movement Direction, in a Visual Motor Dissociation Task. *Cereb. Cortex, 17*(10), 2283-2292.

Ferrera, V. P., Yanike, M., & Cassanello, C. (2009). Frontal eye field neurons signal changes in decision criteria. *Nat Neurosci, 12*(11), 1458-1462.

Feurra, M., Bianco, G., Santarnecchi, E., Del Testa, M., Rossi, A., & Rossi, S. (2011a). Frequency-Dependent Tuning of the Human Motor System Induced by Transcranial Oscillatory Potentials. *The Journal of Neuroscience, 31*(34), 12165-12170.

Feurra, M., Paulus, W., Walsh, V., & Kanai, R. (2011b). Frequency specific modulation of human somatosensory cortex. *Frontiers in Psychology, 2*.

Filimon, F. (2010). Human Cortical Control of Hand Movements: Parietofrontal Networks for Reaching, Grasping, and Pointing. *The Neuroscientist, 16*(4), 388-407.

Fischer, T., Langner, R., Diers, K., Brocke, B., & Birbaumer, N. (2010). Temporo-Spatial Dynamics of Event-Related EEG Beta Activity during the Initial Contingent Negative Variation. *PLoS ONE, 5*(9), e12514.

Forstmann, B. U., Anwander, A., Schäfer, A., Neumann, J., Brown, S., Wagenmakers, E.-J., Bogacz, R., & Turner, R. (2010a). Cortico-striatal connections predict control over speed and accuracy in perceptual decision making. *Proceedings of the National Academy of Sciences, 107*(36), 15916-15920.

Forstmann, B. U., Brown, S., Dutilh, G., Neumann, J., & Wagenmakers, E.-J. (2010b). The neural substrate of prior information in perceptual decision making: a model-based analysis. *Frontiers in Human Neuroscience, 4*.

Foxe, J. J., Simpson, G. V., & Ahlfors, S. P. (1998). Parieto-occipital ~10 Hz activity reflects anticipatory state of visual attention mechanisms. *NeuroReport, 9*(17), 3929-3933.

Foxe, J. J., & Snyder, A. C. (2011). The role of alpha-band brain oscillations as a sensory suppression mechanism during selective attention. *Frontiers in Psychology, 2*.

Frank, M. J. (2006). Hold your horses: A dynamic computational role for the subthalamic nucleus in decision making. *Neural Networks, 19*(8), 1120-1136.

Freedman, D. J., & Assad, J. A. (2011). A proposed common neural mechanism for categorization and perceptual decisions. *Nat Neurosci, 14*(2), 143-146.

Freedman, D. J., Riesenhuber, M., Poggio, T., & Miller, E. K. (2003). A Comparison of Primate Prefrontal and Inferior Temporal Cortices during Visual Categorization. *The Journal of Neuroscience, 23*(12), 5235-5246.

Fries, P. (2009). Neuronal Gamma-band Synchronization as a Fundamental Process in Cortical Computation. *Annual Review of Neuroscience, 32*(1).

Fries, P., Reynolds, J. H., Rorie, A. E., & Desimone, R. (2001). Modulation of Oscillatory Neuronal Synchronization by Selective Visual Attention. *Science, 291*(5508), 1560-1563.

Fu, K. M. G., Foxe, J. J., Murray, M. M., Higgins, B. A., Javitt, D. C., & Schroeder, C. E. (2001). Attention-dependent suppression of distracter visual input can be cross-modally cued as indexed by anticipatory parieto-occipital alpha-band oscillations. *Cognitive Brain Research, 12*(1), 145-152.

Fuggetta, G., Fiaschi, A., & Manganotti, P. (2005). Modulation of cortical oscillatory activities induced by varying single-pulse transcranial magnetic stimulation intensity over the left primary motor area: A combined EEG and TMS study. *NeuroImage, 27*(4), 896-908.

Fuggetta, G., Pavone, E. F., Walsh, V., Kiss, M., & Eimer, M. (2006). Cortico-Cortical Interactions in Spatial Attention: A Combined ERP/TMS Study. *Journal of Neurophysiology, 95*(5), 3277-3280.

Furman, M., & Wang, X.-J. (2008). Similarity Effect and Optimal Control of Multiple-Choice Decision Making. *Neuron, 60*(6), 1153-1168.

Gail, A., & Andersen, R. A. (2006). Neural Dynamics in Monkey Parietal Reach Region Reflect Context-Specific Sensorimotor Transformations. *The Journal of Neuroscience, 26*(37), 9376-9384.

Gaynor, D., Kühn, A. A., Dileone, M., Litvak, V., Eusebio, A., Pogosyan, A., Androulidakis, A. G., Tisch, S., Limousin, P., et al. (2008). Suppression of beta oscillations in the subthalamic nucleus following cortical stimulation in humans. *European Journal of Neuroscience, 28*(8), 1686-1695.

Gillebert, C. R., Mantini, D., Thijs, V., Sunaert, S., Dupont, P., & Vandenberghe, R. (2011). Lesion evidence for the critical role of the intraparietal sulcus in spatial attention. *Brain, 134*(6), 1694-1709.

Giraud, A.-L., Kleinschmidt, A., Poeppel, D., Lund, T. E., Frackowiak, R. S. J., & Laufs, H. (2007). Endogenous Cortical Rhythms Determine Cerebral Specialization for Speech Perception and Production. *Neuron, 56*(6), 1127-1134.

Gloor, P. (1985). Neuronal Generators and the Problem of Localization in Electroencephalography: Application of Volume Conductor Theory to Electroencephalography. *Journal of Clinical Neurophysiology, 2*(4), 327-354.
Gnadt, J., & Andersen, R. (1988). Memory related motor planning activity in posterior parietal cortex of macaque. *Experimental Brain Research, 70*(1), 216-220.
Godschalk, M., Lemon, R. N., Kuypers, H. G. J. M., & Van Der Steen, J. (1985). The involvement of monkey premotor cortex neurones in preparation of visually cued arm movements. *Behavioural Brain Research, 18*(2), 143-157.
Godschalk, M., Lemon, R. N., Nijs, H. G. T., & Kuypers, H. G. J. M. (1981). Behaviour of neurons in monkey peri-arcuate and precentral cortex before and during visually guided arm and hand movements. *Experimental Brain Research, 44*(1), 113-116.
Gold, J. I., Law, C.-T., Connolly, P., & Bennur, S. (2010). Relationships Between the Threshold and Slope of Psychometric and Neurometric Functions During Perceptual Learning: Implications for Neuronal Pooling. *Journal of Neurophysiology, 103*(1), 140-154.
Gold, J. I., & Shadlen, M. N. (2003). The Influence of Behavioral Context on the Representation of a Perceptual Decision in Developing Oculomotor Commands. *The Journal of Neuroscience, 23*(2), 632-651.
Gold, J. I., & Shadlen, M. N. (2007). The Neural Basis of Decision Making. *Annual Review of Neuroscience, 30*(1), 535-574.
Goldman, R. I., Stern, J. M., Engel Jr, J., & Cohen, M. S. (2002). Simultaneous EEG and fMRI of the alpha rhythm. *NeuroReport, 13*(18), 2487-2492.
Gomez, C. M., Delinte, A., Vaquero, E., Cardoso, M. J., Vazquez, M., Crommelinck, M., & Roucoux, A. (2001). Current source density analysis of CNV during temporal Gap paradigm. *Brain Topography, 13*(3), 149-159.
Gomez, C. M., Marco, J., & Grau, C. (2003). Preparatory visuo-motor cortical network of the contingent negative variation estimated by current density. *NeuroImage, 20*(1), 216-224.
Gottlieb, J. (2007). From Thought to Action: The Parietal Cortex as a Bridge between Perception, Action, and Cognition. *Neuron, 53*(1), 9-16.
Gottlieb, J., & Balan, P. (2010). Attention as a decision in information space. *14*(6), 240-248.
Gottlieb, J., & Goldberg, M. E. (1999). Activity of neurons in the lateral intraparietal area of the monkey during an antisaccade task. *Nat Neurosci, 2*(10), 906-912.
Gottlieb, J. P., Kusunoki, M., & Goldberg, M. E. (1998). The representation of visual salience in monkey parietal cortex. *Nature, 391*(6666), 481-484.
Gould, I. C., Rushworth, M. F., & Nobre, A. C. (2011). Indexing the graded allocation of visuospatial attention using anticipatory alpha oscillations. *Journal of Neurophysiology, 105*(3), 1318-1326.
Gould, I. C., Wolfgang, B. J., & Smith, P. L. (2007). Spatial uncertainty explains exogenous and endogenous attentional cuing effects in visual signal detection. *Journal of Vision, 7*(13).
Gratton, G., Coles, M. G. H., Sirevaag, E. J., Eriksen, C. W., & Donchin, E. (1988). Pre- and poststimulus activation of response channels: A psychophysiological analysis. *Journal of Experimental Psychology: Human Perception and Performance, 14*(3), 331-344.
Green, D. M., & Swets, J. A. (1974). *Signal detection theory and psychophysics*: R. E. Krieger Pub. Co.
Grefkes, C., & Fink, G. R. (2005). REVIEW: The functional organization of the intraparietal sulcus in humans and monkeys. *Journal of Anatomy, 207*(1), 3-17.

Grefkes, C., Ritzl, A., Zilles, K., & Fink, G. R. (2004). Human medial intraparietal cortex subserves visuomotor coordinate transformation. *NeuroImage, 23*(4), 1494-1506.

Gregoriou, G. G., Gotts, S. J., Zhou, H., & Desimone, R. (2009). High-Frequency, Long-Range Coupling Between Prefrontal and Visual Cortex During Attention. *Science, 324*(5931), 1207-1210.

Grinband, J., Hirsch, J., & Ferrera, V. P. (2006). A Neural Representation of Categorization Uncertainty in the Human Brain. *Neuron, 49*(5), 757-763.

Gross, J., Schmitz, F., Schnitzler, I., Kessler, K., Shapiro, K., Hommel, B., & Schnitzler, A. (2004). Modulation of long-range neural synchrony reflects temporal limitations of visual attention in humans. *Proceedings of the National Academy of Sciences of the United States of America, 101*(35), 13050-13055.

Gu, Y., Liu, S., Fetsch, Christopher R., Yang, Y., Fok, S., Sunkara, A., DeAngelis, Gregory C., & Angelaki, Dora E. (2011). Perceptual Learning Reduces Interneuronal Correlations in Macaque Visual Cortex. *Neuron, 71*(4), 750-761.

Guillot, A., Collet, C., Nguyen, V. A., Malouin, F., Richards, C., & Doyon, J. (2009). Brain activity during visual versus kinesthetic imagery: An fMRI study. *Human Brain Mapping, 30*(7), 2157-2172.

Haegens, S., Händel, B. F., & Jensen, O. (2011a). Top-Down Controlled Alpha Band Activity in Somatosensory Areas Determines Behavioral Performance in a Discrimination Task. *The Journal of Neuroscience, 31*(14), 5197-5204.

Haegens, S., Nácher, V., Hernández, A., Luna, R., Jensen, O., & Romo, R. (2011b). Beta oscillations in the monkey sensorimotor network reflect somatosensory decision making. *Proceedings of the National Academy of Sciences*.

Hämäläinen, M., & Hari, R. (2002). Magnetoencephalographic characterization of dynamic brain activation: Basic principles and methods of data collection and source analysis. In A. W. Toga & J. C. Mazziotta (Eds.), *Brain Mapping: The methods* (pp. 227-253). San Diego: Academic Press.

Hamalainen, M., Hari, R., Ilmoniemi, R. J., Knuutila, J., & Lounasmaa, O. V. (1993). Magnetoencephalography- theory, instrumentation, and applications to noninvasive studies of the working human brain. *Reviews of Modern Physics, 65*(2), 413.

Hanes, D. P., & Schall, J. D. (1996). Neural Control of Voluntary Movement Initiation. *Science, 274*(5286), 427-430.

Hanks, T. D., Ditterich, J., & Shadlen, M. N. (2006). Microstimulation of macaque area LIP affects decision-making in a motion discrimination task. *Nature Neuroscience, 9*(5), 682-689.

Hari, R., & Salmelin, R. (1997). Human cortical oscillations: A neuromagnetic view through the skull. *Trends in Neurosciences, 20*(1), 44-49.

Hari, R., Salmelin, R., Mäkelä, J. P., Salenius, S., & Helle, M. (1997). Magnetoencephalographic cortical rhythms. *International Journal of Psychophysiology, 26*(1-3), 51-62.

Harris, J. A., Clifford, C. W. G., & Miniussi, C. (2008). The functional effect of transcranial magnetic stimulation: Signal suppression or neural noise generation? *J. Cognitive Neuroscience, 20*(4), 734-740.

Harris, J. A., Miniussi, C., Harris, I. M., & Diamond, M. E. (2002). Transient Storage of a Tactile Memory Trace in Primary Somatosensory Cortex. *The Journal of Neuroscience, 22*(19), 8720-8725.

Heekeren, H. R., Marrett, S., Bandettini, P. A., & Ungerleider, L. G. (2004). A general mechanism for perceptual decision-making in the human brain. *Nature, 431*(7010), 859-862.

Heekeren, H. R., Marrett, S., Ruff, D. A., Bandettini, P. A., & Ungerleider, L. G. (2006). Involvement of human left dorsolateral prefrontal cortex in perceptual decision making is independent of response modality. *Proceedings of the National Academy of Sciences, 103*(26), 10023-10028.

Heekeren, H. R., Marrett, S., & Ungerleider, L. G. (2008). The neural systems that mediate human perceptual decision making. *Nat Rev Neurosci, 9*(6), 467-479.

Heinen, K., Ruff, C. C., Bjoertomt, O., Schenkluhn, B., Bestmann, S., Blankenburg, F., Driver, J., & Chambers, C. D. (2011). Concurrent TMS–fMRI reveals dynamic interhemispheric influences of the right parietal cortex during exogenously cued visuospatial attention. *European Journal of Neuroscience, 33*(5), 991-1000.

Helmholtz, H. L. F. (1853). Ueber einige Gesetze der Vertheilung elektrischer Ströme in körperlichen Leitern mit Anwendung auf die thierisch-elektrischen Versuche. *Annalen der Physik und Chemie, 89*, 211-233, 353-377.

Hernández, A., Nácher, V., Luna, R., Zainos, A., Lemus, L., Alvarez, M., Vázquez, Y., Camarillo, L., & Romo, R. (2010). Decoding a Perceptual Decision Process across Cortex. *Neuron, 66*(2), 300-314.

Hernández, A., Zainos, A., & Romo, R. (2000). Neuronal correlates of sensory discrimination in the somatosensory cortex. *Proceedings of the National Academy of Sciences, 97*(11), 6191-6196.

Hernández, A., Zainos, A., & Romo, R. (2002). Temporal Evolution of a Decision-Making Process in Medial Premotor Cortex. *Neuron, 33*(6), 959-972.

Hesse, M. D., Thiel, C. M., Stephan, K. E., & Fink, G. R. (2006). The left parietal cortex and motor intention: An event-related functional magnetic resonance imaging study. *Neuroscience, 140*(4), 1209-1221.

Hillyard, S. A., & Anllo-Vento, L. (1998). Event-related brain potentials in the study of visual selective attention. *Proceedings of the National Academy of Sciences of the United States of America, 95*(3), 781-787.

Hillyard, S. A., Vogel, E. K., & Luck, S. J. (1998). Sensory gain control (amplification) as a mechanism of selective attention: Electrophysiological and neuroimaging evidence. *Philosophical Transactions of the Royal Society B: Biological Sciences, 353*(1373), 1257-1270.

Hinkley, L. B. N., Krubitzer, L. A., Padberg, J., & Disbrow, E. A. (2009). Visual-Manual Exploration and Posterior Parietal Cortex in Humans. *J Neurophysiol, 102*(6), 3433-3446.

Hipp, J. F., Engel, A. K., & Siegel, M. (2011). Oscillatory Synchronization in Large-Scale Cortical Networks Predicts Perception. *Neuron, 69*(2), 387-396.

Ho, T. C., Brown, S., & Serences, J. T. (2009). Domain General Mechanisms of Perceptual Decision Making in Human Cortex. *J. Neurosci., 29*(27), 8675-8687.

Hodsoll, J., Mevorach, C., & Humphreys, G. W. (2009). Driven to Less Distraction: rTMS of the Right Parietal Cortex Reduces Attentional Capture in Visual Search. *Cereb. Cortex, 19*(1), 106-114.

Horwitz, G. D., Batista, A. P., & Newsome, W. T. (2004). Representation of an Abstract Perceptual Decision in Macaque Superior Colliculus. *Journal of Neurophysiology, 91*(5), 2281-2296.

Horwitz, G. D., & Newsome, W. T. (1999). Separate Signals for Target Selection and Movement Specification in the Superior Colliculus. *Science, 284*(5417), 1158-1161.

Horwitz, G. D., & Newsome, W. T. (2001). Target Selection for Saccadic Eye Movements: Prelude Activity in the Superior Colliculus During a Direction-Discrimination Task. *Journal of Neurophysiology, 86*(5), 2543-2558.

Hovey, C., & Jalinous, R. (2008). *The Guide to Magnetic Stimulation*: The Magstim Company, U.K.

Huang, Y.-Z., Edwards, M. J., Rounis, E., Bhatia, K. P., & Rothwell, J. C. (2005). Theta Burst Stimulation of the Human Motor Cortex. *Neuron, 45*(2), 201-206.

Huettel, S. (2006). Behavioral, but not reward, risk modulates activation of prefrontal, parietal, and insular cortices. *Cognitive, Affective, & Behavioral Neuroscience, 6*(2), 141-151.

Huettel, S. A., Song, A. W., & McCarthy, G. (2005). Decisions under uncertainty: Probabilistic context influences activation of prefrontal and parietal cortices. *Journal of Neuroscience, 25*(13), 3304-3311.

Hughes, S. W., & Crunelli, V. (2005). Thalamic Mechanisms of EEG Alpha Rhythms and Their Pathological Implications. *Neuroscientist, 11*(4), 357-372.

Huk, A. C., & Shadlen, M. N. (2005). Neural Activity in Macaque Parietal Cortex Reflects Temporal Integration of Visual Motion Signals during Perceptual Decision Making. *The Journal of Neuroscience, 25*(45), 10420-10436.

Hung, J., Driver, J., & Walsh, V. (2005). Visual Selection and Posterior Parietal Cortex: Effects of Repetitive Transcranial Magnetic Stimulation on Partial Report Analyzed by Bundesen's Theory of Visual Attention. *The Journal of Neuroscience, 25*(42), 9602-9612.

Ikeda, T., & Hikosaka, O. (2003). Reward-Dependent Gain and Bias of Visual Responses in Primate Superior Colliculus. *Neuron, 39*(4), 693-700.

Ilmoniemi , R. J., Virtanen, J., Ruohonen, J., Karhu, J., Aronen, H. J., Naatanen, R., & Katila, T. (1997). Neuronal responses to magnetic stimulation reveal cortical reactivity and connectivity. *Neuroreport, 8*(16), 3537-3540.

Itti, L., & Koch, C. (2001). Computational modelling of visual attention. *Nature reviews. Neuroscience, 2*(3), 194-203.

Janssen, P., & Shadlen, M. N. (2005). A representation of the hazard rate of elapsed time in macaque area LIP. *Nat Neurosci, 8*(2), 234-241.

Jeannerod, M., & Frak, V. (1999). Mental imaging of motor activity in humans. *Current Opinion in Neurobiology, 9*(6), 735-739.

Jenkinson, N., & Brown, P. (2011). New insights into the relationship between dopamine, beta oscillations and motor function. *Trends in Neurosciences*.

Jensen, O., Bahramisharif, A., Oostenveld, R., Klanke, S., Hadjipapas, A., Okazaki, Y. O., & van Gerven, M. A. J. (2011). Using brain-computer interfaces and brain-state dependent stimulation as tools in cognitive neuroscience. *Frontiers in Psychology, 2*.

Jensen, O., Gelfand, J., Kounios, J., & Lisman, J. E. (2002). Oscillations in the Alpha Band (9-12 Hz) Increase with Memory Load during Retention in a Short-term Memory Task. *Cereb. Cortex, 12*(8), 877-882.

Jensen, O., & Mazaheri, A. (2010). Shaping functional architecture by oscillatory alpha activity: gating by inhibition. *Frontiers in Human Neuroscience, 4*.

Johnson, P. B., Ferraina, S., Bianchi, L., & Caminiti, R. (1996). Cortical Networks for Visual Reaching: Physiological and Anatomical Organization of Frontal and Parietal Lobe Arm Regions. *Cerebral Cortex, 6*(2), 102-119.

Jones, S. R., Kerr, C. E., Wan, Q., Pritchett, D. L., Hämäläinen, M., & Moore, C. I. (2010). Cued Spatial Attention Drives Functionally Relevant Modulation of the Mu Rhythm in Primary Somatosensory Cortex. *The Journal of Neuroscience, 30*(41), 13760-13765.

Jones, S. R., Pritchett, D. L., Sikora, M. A., Stufflebeam, S. M., Hämäläinen, M., & Moore, C. I. (2009). Quantitative Analysis and Biophysically Realistic Neural Modeling of

the MEG Mu Rhythm: Rhythmogenesis and Modulation of Sensory-Evoked Responses. *Journal of Neurophysiology, 102*(6), 3554-3572.

Jones, S. R., Pritchett, D. L., Stufflebeam, S. M., Hämäläinen, M., & Moore, C. I. (2007). Neural Correlates of Tactile Detection: A Combined Magnetoencephalography and Biophysically Based Computational Modeling Study. *The Journal of Neuroscience, 27*(40), 10751-10764.

Jonikaitis, D., & Deubel, H. (2011). Independent Allocation of Attention to Eye and Hand Targets in Coordinated Eye-Hand Movements. *Psychological Science*.

Juan, C.-H., Shorter-Jacobi, S. M., & Schall, J. D. (2004). Dissociation of spatial attention and saccade preparation. *Proceedings of the National Academy of Sciences of the United States of America, 101*(43), 15541-15544.

Jun, J. K., Miller, P., Hernández, A., Zainos, A., Lemus, L., Brody, C. D., & Romo, R. (2010). Heterogenous Population Coding of a Short-Term Memory and Decision Task. *The Journal of Neuroscience, 30*(3), 916-929.

Kable, J. W., & Glimcher, P. W. (2009). The Neurobiology of Decision: Consensus and Controversy. *63*(6), 733-745.

Kalaska, J. F., & Crammond, D. J. (1995). Deciding Not to GO: Neuronal Correlates of Response Selection in a GO/NOGO Task in Primate Premotor and Parietal Cortex. *Cerebral Cortex, 5*(5), 410-428.

Kanai, R., Chaieb, L., Antal, A., Walsh, V., & Paulus, W. (2008). Frequency-Dependent Electrical Stimulation of the Visual Cortex. *Current Biology, 18*(23), 1839-1843.

Kastner, S., Pinsk, M. A., De Weerd, P., Desimone, R., & Ungerleider, L. G. (1999). Increased Activity in Human Visual Cortex during Directed Attention in the Absence of Visual Stimulation. *22*(4), 751-761.

Kastner, S., & Ungerleider, L. G. (2000). Mechanisms of visual attention in the human cortex, *Annual Review of Neuroscience* (Vol. 23, pp. 315-341).

Kayser, A. S., Buchsbaum, B. R., Erickson, D. T., & D'Esposito, M. (2010a). The Functional Anatomy of a Perceptual Decision in the Human Brain. *J Neurophysiol, 103*(3), 1179-1194.

Kayser, A. S., Erickson, D. T., Buchsbaum, B. R., & D'Esposito, M. (2010b). Neural Representations of Relevant and Irrelevant Features in Perceptual Decision Making. *J. Neurosci., 30*(47), 15778-15789.

Kelley, T. A., Serences, J. T., Giesbrecht, B., & Yantis, S. (2008). Cortical Mechanisms for Shifting and Holding Visuospatial Attention. *Cereb. Cortex, 18*(1), 114-125.

Kelly, S. P., Gomez-Ramirez, M., & Foxe, J. J. (2009). The strength of anticipatory spatial biasing predicts target discrimination at attended locations: A high-density EEG study. *European Journal of Neuroscience, 30*(11), 2224-2234.

Kelly, S. P., Lalor, E. C., Reilly, R. B., & Foxe, J. J. (2006). Increases in Alpha Oscillatory Power Reflect an Active Retinotopic Mechanism for Distracter Suppression During Sustained Visuospatial Attention. *J Neurophysiol, 95*(6), 3844-3851.

Kiani, R., Hanks, T. D., & Shadlen, M. N. (2008). Bounded Integration in Parietal Cortex Underlies Decisions Even When Viewing Duration Is Dictated by the Environment. *J. Neurosci., 28*(12), 3017-3029.

Kiebel, S. J., Tallon-Baudry, C., & Friston, K. J. (2005). Parametric analysis of oscillatory activity as measured with EEG/MEG. *Human Brain Mapping, 26*(3), 170-177.

Kilner, J. M., Baker, S. N., Salenius, S., Hari, R., & Lemon, R. N. (2000). Human Cortical Muscle Coherence Is Directly Related to Specific Motor Parameters. *The Journal of Neuroscience, 20*(23), 8838-8845.

Kim, J.-N., & Shadlen, M. N. (1999). Neural correlates of a decision in the dorsolateral prefrontal cortex of the macaque. *Nat Neurosci, 2*(2), 176-185.

Kingstone, A. (1992). Combining Expectancies. *The Quarterly Journal of Experimental Psychology Section A: Human Experimental Psychology, 44*(1), 69 - 104.

Klimesch, W., Russegger, H., Doppelmayr, M., & Pachinger, T. (1998). A method for the calculation of induced band power: Implications for the significance of brain oscillations. *Electroencephalography and Clinical Neurophysiology, 108*(2), 123-130.

Knowlton, B. J., Mangels, J. A., & Squire, L. R. (1996). A Neostriatal Habit Learning System in Humans. *Science, 273*(5280), 1399-1402.

Knowlton, B. J., Squire, L. R., & Gluck, M. A. (1994). Probabilistic classification learning in amnesia. *Learning & Memory, 1*(2), 106-120.

Koch, G., Franca, M., Fernandez Del Olmo, M., Cheeran, B., Milton, R., Alvarez Sauco, M., & Rothwell, J. C. (2006). Time Course of Functional Connectivity between Dorsal Premotor and Contralateral Motor Cortex during Movement Selection. *J. Neurosci., 26*(28), 7452-7459.

Koch, S. P., Werner, P., Steinbrink, J., Fries, P., & Obrig, H. (2009). Stimulus-Induced and State-Dependent Sustained Gamma Activity Is Tightly Coupled to the Hemodynamic Response in Humans. *The Journal of Neuroscience, 29*(44), 13962-13970.

Kolster, H., Peeters, R., & Orban, G. A. (2010). The Retinotopic Organization of the Human Middle Temporal Area MT/V5 and Its Cortical Neighbors. *J. Neurosci., 30*(29), 9801-9820.

Kopell, N., Ermentrout, G. B., Whittington, M. A., & Traub, R. D. (2000). Gamma rhythms and beta rhythms have different synchronization properties. *Proceedings of the National Academy of Sciences, 97*(4), 1867-1872.

Kowler, E., Anderson, E., Dosher, B., & Blaser, E. (1995). The role of attention in the programming of saccades. *Vision Research, 35*(13), 1897-1916.

Krajbich, I., Armel, C., & Rangel, A. (2010). Visual fixations and the computation and comparison of value in simple choice. *Nat Neurosci, 13*(10), 1292-1298.

Krajbich, I., & Rangel, A. (2011). Multialternative drift-diffusion model predicts the relationship between visual fixations and choice in value-based decisions. *Proceedings of the National Academy of Sciences, 108*(33), 13852-13857.

Króliczak, G., & Frey, S. H. (2009). A Common Network in the Left Cerebral Hemisphere Represents Planning of Tool Use Pantomimes and Familiar Intransitive Gestures at the Hand-Independent Level. *Cerebral Cortex, 19*(10), 2396-2410.

Kurata, K., & Wise, S. P. (1988). Premotor cortex of rhesus monkeys: set-related activity during two conditional motor tasks. *Experimental Brain Research, 69*(2), 327-343.

LaBerge, D. (1997). Attention, Awareness, and the Triangular Circuit. *Consciousness and Cognition, 6*(2-3), 149-181.

Lachaux, J.-P., Fonlupt, P., Kahane, P., Minotti, L., Hoffmann, D., Bertrand, O., & Baciu, M. (2007). Relationship between task-related gamma oscillations and BOLD signal: New insights from combined fMRI and intracranial EEG. *Human Brain Mapping, 28*(12), 1368-1375.

Lakatos, P., Karmos, G., Mehta, A. D., Ulbert, I., & Schroeder, C. E. (2008). Entrainment of Neuronal Oscillations as a Mechanism of Attentional Selection. *Science, 320*(5872), 110-113.

Laming, D. R. J. (1968). *Information theory of choice-reaction times*: Academic P.

Laufs, H., Holt, J. L., Elfont, R., Krams, M., Paul, J. S., Krakow, K., & Kleinschmidt, A. (2006). Where the BOLD signal goes when alpha EEG leaves. *NeuroImage, 31*(4), 1408-1418.

Laufs, H., Kleinschmidt, A., Beyerle, A., Eger, E., Salek-Haddadi, A., Preibisch, C., & Krakow, K. (2003a). EEG-correlated fMRI of human alpha activity. *NeuroImage, 19*(4), 1463-1476.

Laufs, H., Krakow, K., Sterzer, P., Eger, E., Beyerle, A., Salek-Haddadi, A., & Kleinschmidt, A. (2003b). Electroencephalographic signatures of attentional and cognitive default modes in spontaneous brain activity fluctuations at rest. *Proceedings of the National Academy of Sciences of the United States of America, 100*(19), 11053-11058.

Law, C.-T., & Gold, J. I. (2008). Neural correlates of perceptual learning in a sensory-motor, but not a sensory, cortical area. *Nat Neurosci, 11*(4), 505-513.

Lawrence, B. M., & Snyder, L. H. (2006). Comparison of Effector-Specific Signals in Frontal and Parietal Cortices. *Journal of Neurophysiology, 96*(3), 1393-1400.

Leite, F. P., & Ratcliff, R. (2010). Modeling reaction time and accuracy of multiple-alternative decisions. *Attention, Perception, & Psychophysics, 72*(1), 246-273.

Lemus, L., Hernández, A., Luna, R., Zainos, A., Nácher, V., & Romo, R. (2007). Neural correlates of a postponed decision report. *Proceedings of the National Academy of Sciences, 104*(43), 17174-17179.

Leocani, L., Toro, C., Zhuang, P., Gerloff, C., & Hallett, M. (2001). Event-related desynchronization in reaction time paradigms: a comparison with event-related potentials and corticospinal excitability. *Clinical Neurophysiology, 112*(5), 923-930.

Leon, M. I., & Shadlen, M. N. (2003). Representation of Time by Neurons in the Posterior Parietal Cortex of the Macaque. *Neuron, 38*(2), 317-327.

Leopold, D. A., & Logothetis, N. K. (1999). Multistable phenomena: changing views in perception. *Trends in Cognitive Sciences, 3*(7), 254-264.

Leuthardt, E. C., Schalk, G., Wolpaw, J. R., Ojemann, J. G., & Moran, D. W. (2004). A brain-computer interface using electrocorticographic signals in humans. *Journal of Neural Engineering, 1*(2), 63.

Leuthold, H., Sommer, W., & Ulrich, R. (2004). Preparing for Action: Inferences from CNV and LRP. *Journal of Psychophysiology, 18*(2), 77-88.

Lewis, J. W., & Van Essen, D. C. (2000a). Corticocortical connections of visual, sensorimotor, and multimodal processing areas in the parietal lobe of the macaque monkey. *Journal of Comparative Neurology, 428*(1), 112-137.

Lewis, J. W., & Van Essen, D. C. (2000b). Mapping of architectonic subdivisions in the macaque monkey, with emphasis on parieto-occipital cortex. *Journal of Comparative Neurology, 428*(1), 79-111.

Li, C.-S. R., Mazzoni, P., & Andersen, R. A. (1999). Effect of Reversible Inactivation of Macaque Lateral Intraparietal Area on Visual and Memory Saccades. *Journal of Neurophysiology, 81*(4), 1827-1838.

Lindgren, K. A., Larson, C. L., Schaefer, S. M., Abercrombie, H. C., Ward, R. T., Oakes, T. R., Holden, J. E., Perlman, S. B., Benca, R. M., et al. (1999). Thalamic metabolic rate predicts EEG alpha power in healthy control subjects but not in depressed patients. *Biological Psychiatry, 45*(8), 943-952.

Lindner, A., Iyer, A., Kagan, I., & Andersen, R. A. (2010). Human Posterior Parietal Cortex Plans Where to Reach and What to Avoid. *J. Neurosci., 30*(35), 11715-11725.

Link, S., & Heath, R. (1975). A sequential theory of psychological discrimination. *Psychometrika, 40*(1), 77-105.

Litvak, V., Jha, A., Eusebio, A., Oostenveld, R., Foltynie, T., Limousin, P., Zrinzo, L., Hariz, M. I., Friston, K., et al. (2010). Resting oscillatory cortico-subthalamic connectivity in patients with Parkinson's disease. *Brain*.

Liu, Y., Yttri, E. A., & Snyder, L. H. (2010). Intention and attention: different functional roles for LIPd and LIPv. *Nature Neuroscience*.

Llinas, R. R., Ribary, U., Jeanmonod, D., Kronberg, E., & Mitra, P. P. (1999). Thalamocortical dysrhythmia: A neurological and neuropsychiatric syndrome characterized by magnetoencephalography. *Proceedings of the National Academy of Sciences, 96*(26), 15222-15227.

Lo, C.-C., & Wang, X.-J. (2006). Cortico-basal ganglia circuit mechanism for a decision threshold in reaction time tasks. *Nat Neurosci, 9*(7), 956-963.

Logothetis, N. K., Kayser, C., & Oeltermann, A. (2007). In Vivo Measurement of Cortical Impedance Spectrum in Monkeys: Implications for Signal Propagation. *Neuron, 55*(5), 809-823.

Logothetis, N. K., & Wandell, B. A. (2004). Interpreting the BOLD Signal. *Annual Review of Physiology, 66*(1), 735-769.

Lopes da Silva, F. (1991). Neural mechanisms underlying brain waves: from neural membranes to networks. *Electroencephalography and Clinical Neurophysiology, 79*(2), 81-93.

Lorente de No, R. L. (1947). *A study of nerve physiology*: The Rockefeller Institute for Medical Research.

Lorincz, M. L., Crunelli, V., & Hughes, S. W. (2008). Cellular Dynamics of Cholinergically Induced {alpha} (8 13 Hz) Rhythms in Sensory Thalamic Nuclei In Vitro. *J. Neurosci., 28*(3), 660-671.

Lorincz, M. L., Kékesi, K. A., Juhász, G., Crunelli, V., & Hughes, S. W. (2009). Temporal Framing of Thalamic Relay-Mode Firing by Phasic Inhibition during the Alpha Rhythm. *Neuron, 63*(5), 683-696.

Louie, K., & Glimcher, P. W. (2010). Separating Value from Choice: Delay Discounting Activity in the Lateral Intraparietal Area. *J. Neurosci., 30*(16), 5498-5507.

Louie, K., Grattan, L. E., & Glimcher, P. W. (2011). Reward Value-Based Gain Control: Divisive Normalization in Parietal Cortex. *The Journal of Neuroscience, 31*(29), 10627-10639.

Lu, Z.-L., Lesmes, L. A., & Dosher, B. A. (2002). Spatial attention excludes external noise at the target location. *Journal of Vision, 2*(4).

Luce, R. D. (1991). *Response Times: Their Role in Inferring Elementary Mental Organization*: Oxford University Press.

Luck, S. J. (2005). *An introduction to the event-related potential technique*: MIT Press.

Luck, S. J., Chelazzi, L., Hillyard, S. A., & Desimone, R. (1997). Neural mechanisms of spatial selective attention in areas V1, V2, and V4 of macaque visual cortex. *Journal of Neurophysiology, 77*(1), 24-42.

Luck, S. J., Woodman, G. F., & Vogel, E. K. (2000). Event-related potential studies of attention. *Trends in Cognitive Sciences, 4*(11), 432-440.

Lynch, J. C., Graybiel, A. M., & Lobeck, L. J. (1985). The differential projection of two cytoarchitectonic subregions of the inferior parietal lobule of macaque upon the deep layers of the superior colliculus. *The Journal of Comparative Neurology, 235*(2), 241-254.

Machens, C. K., Romo, R., & Brody, C. D. (2005). Flexible Control of Mutual Inhibition: A Neural Model of Two-Interval Discrimination. *Science, 307*(5712), 1121-1124.

MacKay, W. A., & Bonnet, M. (1990). CNV, stretch reflex and reaction time correlates of preparation for movement direction and force. *Electroencephalography and Clinical Neurophysiology, 76*(1), 47-62.

Macmillan, N. A., & Creelman, C. D. (2005). *Detection theory: a user's guide*: Lawrence Erlbaum Associates.

Maier, A., Wilke, M., Aura, C., Zhu, C., Ye, F. Q., & Leopold, D. A. (2008). Divergence of fMRI and neural signals in V1 during perceptual suppression in the awake monkey. *Nat Neurosci, 11*(10), 1193-1200.

Makela, J. P., Salmelin, R., Kotila, M., Salonen, O., Laaksonen, R., Hokkanen, L., & Hari, R. (1998). Modification of neuromagnetic cortical signals by thalamic infarctions. *Electroencephalography and Clinical Neurophysiology, 106*(5), 433-443.

Mallet, N., Pogosyan, A., Sharott, A., Csicsvari, J., Bolam, J. P., Brown, P., & Magill, P. J. (2008). Disrupted Dopamine Transmission and the Emergence of Exaggerated Beta Oscillations in Subthalamic Nucleus and Cerebral Cortex. *The Journal of Neuroscience, 28*(18), 4795-4806.

Manning, J. R., Jacobs, J., Fried, I., & Kahana, M. J. (2009). Broadband Shifts in Local Field Potential Power Spectra Are Correlated with Single-Neuron Spiking in Humans. *The Journal of Neuroscience, 29*(43), 13613-13620.

Mantini, D., Perrucci, M. G., Del Gratta, C., Romani, G. L., & Corbetta, M. (2007). Electrophysiological signatures of resting state networks in the human brain. *Proceedings of the National Academy of Sciences of the United States of America, 104*(32), 13170-13175.

Maris, E., & Oostenveld, R. (2007). Nonparametric statistical testing of EEG- and MEG-data. *Journal of Neuroscience Methods, 164*(1), 177-190.

Mars, R., Bestmann, S., Rothwell, J., & Haggard, P. (2007). Effects of motor preparation and spatial attention on corticospinal excitability in a delayed-response paradigm. *Experimental Brain Research, 182*(1), 125-129.

Mars, R. B., Coles, M. G. H., Hulstijn, W., & Toni, I. (2008a). Delay-related cerebral activity and motor preparation. *Cortex, 44*(5), 507-520.

Mars, R. B., Debener, S., Gladwin, T. E., Harrison, L. M., Haggard, P., Rothwell, J. C., & Bestmann, S. (2008b). Trial-by-Trial Fluctuations in the Event-Related Electroencephalogram Reflect Dynamic Changes in the Degree of Surprise. *The Journal of Neuroscience, 28*(47), 12539-12545.

Mars, R. B., Jbabdi, S., Sallet, J., O'Reilly, J. X., Croxson, P. L., Olivier, E., Noonan, M. P., Bergmann, C., Mitchell, A. S., et al. (2011). Diffusion-Weighted Imaging Tractography-Based Parcellation of the Human Parietal Cortex and Comparison with Human and Macaque Resting-State Functional Connectivity. *The Journal of Neuroscience, 31*(11), 4087-4100.

Mars, R. B., Klein, M. C., Neubert, F.-X., Olivier, E., Buch, E. R., Boorman, E. D., & Rushworth, M. F. S. (2009). Short-Latency Influence of Medial Frontal Cortex on Primary Motor Cortex during Action Selection under Conflict. *J. Neurosci., 29*(21), 6926-6931.

Marsden, J. F., Werhahn, K. J., Ashby, P., Rothwell, J., Noachtar, S., & Brown, P. (2000). Organization of Cortical Activities Related to Movement in Humans. *The Journal of Neuroscience, 20*(6), 2307-2314.

Martínez-García, M., Rolls, E. T., Deco, G., & Romo, R. (2011). Neural and computational mechanisms of postponed decisions. *Proceedings of the National Academy of Sciences, 108*(28), 11626-11631.

Martinez-Trujillo, J. C., & Treue, S. (2002). Attentional Modulation Strength in Cortical Area MT Depends on Stimulus Contrast. *35*(2), 365-370.

Masaki, H., Wild-wall, N., Sangals, J., & Sommer, W. (2004). The functional locus of the lateralized readiness potential. *Psychophysiology, 41*(2), 220-230.

Mathewson, K. E., Gratton, G., Fabiani, M., Beck, D. M., & Ro, T. (2009). To See or Not to See: Prestimulus α Phase Predicts Visual Awareness. *J. Neurosci., 29*(9), 2725-2732.
Mattingley, J. B., Husain, M., Rorden, C., Kennard, C., & Driver, J. (1998). Motor role of human inferior parietal lobe revealed in unilateral neglect patients. *Nature, 392*(6672), 179-182.
Maunsell, J., & van Essen, D. (1983). The connections of the middle temporal visual area (MT) and their relationship to a cortical hierarchy in the macaque monkey. *The Journal of Neuroscience, 3*(12), 2563-2586.
Mazurek, M. E., Roitman, J. D., Ditterich, J., & Shadlen, M. N. (2003). A Role for Neural Integrators in Perceptual Decision Making. *Cerebral Cortex, 13*(11), 1257-1269.
McAdams, C. J., & Maunsell, J. H. R. (1999). Effects of Attention on Orientation-Tuning Functions of Single Neurons in Macaque Cortical Area V4. *J. Neurosci., 19*(1), 431-441.
McAlonan, K., Cavanaugh, J., & Wurtz, R. H. (2008). Guarding the gateway to cortex with attention in visual thalamus. *Nature, 456*(7220), 391-394.
McFarland, D., Miner, L., Vaughan, T., & Wolpaw, J. (2000). Mu and Beta Rhythm Topographies During Motor Imagery and Actual Movements. *Brain Topography, 12*(3), 177-186.
McKeefry, D. J., Burton, M. P., Vakrou, C., Barrett, B. T., & Morland, A. B. (2008). Induced Deficits in Speed Perception by Transcranial Magnetic Stimulation of Human Cortical Areas V5/MT+ and V3A. *The Journal of Neuroscience, 28*(27), 6848-6857.
McMains, S. A., Fehd, H. M., Emmanouil, T. A., & Kastner, S. (2007). Mechanisms of feature- and space-based attention: Response modulation and baseline increases. *Journal of Neurophysiology, 98*(4), 2110-2121.
McPeek, R. M., & Keller, E. L. (2004). Deficits in saccade target selection after inactivation of superior colliculus. *Nat Neurosci, 7*(7), 757-763.
Medendorp, W. P., Beurze, S. M., Van Pelt, S., & Van Der Werf, J. (2008). Behavioral and cortical mechanisms for spatial coding and action planning. *Cortex, 44*(5), 587-597.
Medendorp, W. P., Goltz, H. C., Crawford, J. D., & Vilis, T. (2005). Integration of Target and Effector Information in Human Posterior Parietal Cortex for the Planning of Action. *Journal of Neurophysiology, 93*(2), 954-962.
Medendorp, W. P., Goltz, H. C., Vilis, T., & Crawford, J. D. (2003). Gaze-Centered Updating of Visual Space in Human Parietal Cortex. *J. Neurosci., 23*(15), 6209-6214.
Mesulam, M. M. (1981). A cortical network for directed attention and unilateral neglect. *Annals of Neurology, 10*(4), 309-325.
Meyer, K. (2011). Primary sensory cortices, top-down projections and conscious experience. *Progress in Neurobiology, 94*(4), 408-417.
Michelon, P., Vettel, J. M., & Zacks, J. M. (2006). Lateral Somatotopic Organization During Imagined and Prepared Movements. *Journal of Neurophysiology, 95*(2), 811-822.
Miller, E. K., & Cohen, J. D. (2001). An integrative theory of prefrontal cortex function. *Annual Review of Neuroscience, 24*(1), 167-202.
Miller, K. J., Schalk, G., Fetz, E. E., den Nijs, M., Ojemann, J. G., & Rao, R. P. N. (2010). Cortical activity during motor execution, motor imagery, and imagery-based online feedback. *Proceedings of the National Academy of Sciences, 107*(9), 4430-4435.
Miller, K. J., Sorensen, L. B., Ojemann, J. G., & den Nijs, M. (2009a). Power-Law Scaling in the Brain Surface Electric Potential. *PLoS Comput Biol, 5*(12), e1000609.
Miller, K. J., Zanos, S., Fetz, E. E., den Nijs, M., & Ojemann, J. G. (2009b). Decoupling the Cortical Power Spectrum Reveals Real-Time Representation of Individual Finger Movements in Humans. *The Journal of Neuroscience, 29*(10), 3132-3137.

Milosavljevic, M., Malmaud, J., Huth, A., Koch, C., & Rangel, A. (2010). The Drift Diffusion Model can account for the accuracy and reaction time of value-based choices under high and low time pressure. *Judgment and Decision Making, 5*(6), 437-449.

Miniussi, C., & Thut, G. (2010). Combining TMS and EEG Offers New Prospects in Cognitive Neuroscience. *Brain Topography, 22*(4), 249-256.

Mirpour, K., Ong, W. S., & Bisley, J. W. (2010). Microstimulation of Posterior Parietal Cortex Biases the Selection of Eye Movement Goals During Search. *Journal of Neurophysiology, 104*(6), 3021-3028.

Mitchell, J. F., Sundberg, K. A., & Reynolds, J. H. (2009). Spatial Attention Decorrelates Intrinsic Activity Fluctuations in Macaque Area V4. *63*(6), 879-888.

Mitra, P. P., & Pesaran, B. (1999). Analysis of Dynamic Brain Imaging Data. *Biophysical Journal, 76*(2), 691-708.

Mochizuki, H., Franca, M., Huang, Y.-Z., & Rothwell, J. (2005). The role of dorsal premotor area in reaction task: comparing the "virtual lesion" effect of paired pulse or theta burst transcranial magnetic stimulation. *Experimental Brain Research, 167*(3), 414-421.

Monosov, I. E., Trageser, J. C., & Thompson, K. G. (2008). Measurements of Simultaneously Recorded Spiking Activity and Local Field Potentials Suggest that Spatial Selection Emerges in the Frontal Eye Field. *Neuron, 57*(4), 614-625.

Moore, T., & Armstrong, K. M. (2003). Selective gating of visual signals by microstimulation of frontal cortex. *Nature, 421*(6921), 370-373.

Moore, T., & Fallah, M. (2001). Control of eye movements and spatial attention. *Proceedings of the National Academy of Sciences, 98*(3), 1273-1276.

Moran, J., & Desimone, R. (1985). Selective attention gates visual processing in the extrastriate cortex. *Science, 229*(4715), 782-784.

Morris, A. P., Chambers, C. D., & Mattingley, J. B. (2007). Parietal stimulation destabilizes spatial updating across saccadic eye movements. *Proceedings of the National Academy of Sciences, 104*(21), 9069-9074.

Mukamel, R., Gelbard, H., Arieli, A., Hasson, U., Fried, I., & Malach, R. (2005). Coupling Between Neuronal Firing, Field Potentials, and fMRI in Human Auditory Cortex. *Science, 309*(5736), 951-954.

Mulert, C., Leicht, G., Hepp, P., Kirsch, V., Karch, S., Pogarell, O., Reiser, M., Hegerl, U., J√§ger, L., et al. (2010). Single-trial coupling of the gamma-band response and the corresponding BOLD signal. *NeuroImage, 49*(3), 2238-2247.

Munoz, D. P., & Wurtz, R. H. (1995). Saccade-related activity in monkey superior colliculus. I. Characteristics of burst and buildup cells. *Journal of Neurophysiology, 73*(6), 2313-2333.

Müri, R., Bühler, R., Heinemann, D., Mosimann, U., Felblinger, J., Schlaepfer, T., & Hess, C. (2002). Hemispheric asymmetry in visuospatial attention assessed with transcranial magnetic stimulation. *Experimental Brain Research, 143*(4), 426-430.

Murray, M., Brunet, D., & Michel, C. (2008). Topographic ERP Analyses: A Step-by-Step Tutorial Review. *Brain Topography, 20*(4), 249-264.

Murthy, V. N., & Fetz, E. E. (1996). Oscillatory activity in sensorimotor cortex of awake monkeys: synchronization of local field potentials and relation to behavior. *Journal of Neurophysiology, 76*(6), 3949-3967.

Musallam, S., Corneil, B. D., Greger, B., Scherberger, H., & Andersen, R. A. (2004). Cognitive Control Signals for Neural Prosthetics. *Science, 305*(5681), 258-262.

Nagai, Y., Critchley, H. D., Featherstone, E., Fenwick, P. B. C., Trimble, M. R., & Dolan, R. J. (2004). Brain activity relating to the contingent negative variation: an fMRI investigation. *NeuroImage, 21*(4), 1232-1241.

Nagamine, T., Kajola, M., Salmelin, R., Shibasaki, H., & Hari, R. (1996). Movement-related slow cortical magnetic fields and changes of spontaneous MEG- and EEG-brain rhythms. *Electroencephalography and Clinical Neurophysiology, 99*(3), 274-286.

Nakamura, H., Kuroda, T., Wakita, M., Kusunoki, M., Kato, A., Mikami, A., Sakata, H., & Itoh, K. (2001). From Three-Dimensional Space Vision to Prehensile Hand Movements: The Lateral Intraparietal Area Links the Area V3A and the Anterior Intraparietal Area in Macaques. *The Journal of Neuroscience, 21*(20), 8174-8187.

Nelson, S. M., Cohen, A. L., Power, J. D., Wig, G. S., Miezin, F. M., Wheeler, M. E., Velanova, K., Donaldson, D. I., Phillips, J. S., et al. (2010). A Parcellation Scheme for Human Left Lateral Parietal Cortex. *Neuron, 67*(1), 156-170.

Neuper, C., Wörtz, M., Pfurtscheller, G., Christa, N., & Wolfgang, K. (2006). ERD/ERS patterns reflecting sensorimotor activation and deactivation *Progress in Brain Research* (Vol. Volume 159, pp. 211-222): Elsevier.

Nevado Holgado, A. J., Terry, J. R., & Bogacz, R. (2010). Conditions for the Generation of Beta Oscillations in the Subthalamic Nucleus-Globus Pallidus Network. *The Journal of Neuroscience, 30*(37), 12340-12352.

Newsome, W., & Pare, E. (1988). A selective impairment of motion perception following lesions of the middle temporal visual area (MT). *The Journal of Neuroscience, 8*(6), 2201-2211.

Newsome, W., Wurtz, R., Dursteler, M., & Mikami, A. (1985). Deficits in visual motion processing following ibotenic acid lesions of the middle temporal visual area of the macaque monkey. *The Journal of Neuroscience, 5*(3), 825-840.

Newsome, W. T., Britten, K. H., & Movshon, J. A. (1989). Neuronal correlates of a perceptual decision. *Nature, 341*(6237), 52-54.

Newsome, W. T., Wurtz, R. H., & Komatsu, H. (1988). Relation of cortical areas MT and MST to pursuit eye movements. II. Differentiation of retinal from extraretinal inputs. *Journal of Neurophysiology, 60*(2), 604-620.

Niessing, J., Ebisch, B., Schmidt, K. E., Niessing, M., Singer, W., & Galuske, R. A. W. (2005). Hemodynamic Signals Correlate Tightly with Synchronized Gamma Oscillations. *Science, 309*(5736), 948-951.

Niwa, M., & Ditterich, J. (2008). Perceptual Decisions between Multiple Directions of Visual Motion. *The Journal of Neuroscience, 28*(17), 4435-4445.

Nobre, A. C. (2001). Orienting attention to instants in time. *Neuropsychologia, 39*(12), 1317-1328.

Nobre, A. C., Sebestyen, G. N., Gitelman, D. R., Mesulam, M. M., Frackowiak, R. S., & Frith, C. D. (1997). Functional localization of the system for visuospatial attention using positron emission tomography. *Brain, 120*(3), 515-533.

Noonan, M. P., Walton, M. E., Behrens, T. E. J., Sallet, J., Buckley, M. J., & Rushworth, M. F. S. (2010). Separate value comparison and learning mechanisms in macaque medial and lateral orbitofrontal cortex. *Proceedings of the National Academy of Sciences, 107*(47), 20547-20552.

Noppeney, U., Ostwald, D., & Werner, S. (2010). Perceptual Decisions Formed by Accumulation of Audiovisual Evidence in Prefrontal Cortex. *J. Neurosci., 30*(21), 7434-7446.

Nunez, P. L. (1981). *Electric fields of the brain: the neurophysics of EEG*: Oxford University Press.

O'Connell, R. G., Dockree, P. M., Robertson, I. H., Bellgrove, M. A., Foxe, J. J., & Kelly, S. P. (2009). Uncovering the Neural Signature of Lapsing Attention: Electrophysiological Signals Predict Errors up to 20 s before They Occur. *J. Neurosci., 29*(26), 8604-8611.

O'Shea, J., Johansen-Berg, H., Trief, D., Göbel, S., & Rushworth, M. F. S. (2007a). Functionally Specific Reorganization in Human Premotor Cortex. *Neuron, 54*(3), 479-490.

O'Shea, J., Sebastian, C., Boorman, E. D., Johansen-Berg, H., & Rushworth, M. F. S. (2007b). Functional specificity of human premotor-motor cortical interactions during action selection. *European Journal of Neuroscience, 26*(7), 2085-2095.

Ohara, S., Ikeda, A., Kunieda, T., Yazawa, S., Baba, K., Nagamine, T., Taki, W., Hashimoto, N., Mihara, T., et al. (2000). Movement-related change of electrocorticographic activity in human supplementary motor area proper. *Brain, 123*(6), 1203-1215.

Oldfield, R. C. (1971). The assessment and analysis of handedness: The Edinburgh inventory. *Neuropsychologia, 9*(1), 97-113.

Oliveira, F. T. P., Diedrichsen, J., Verstynen, T., Duque, J., & Ivry, R. B. (2010). Transcranial magnetic stimulation of posterior parietal cortex affects decisions of hand choice. *Proceedings of the National Academy of Sciences, 107*(41), 17751-17756.

Oostenveld, R., Fries, P., Maris, E., & Schoffelen, J.-M. (2011). FieldTrip: Open Source Software for Advanced Analysis of MEG, EEG, and Invasive Electrophysiological Data. *Computational Intelligence and Neuroscience*.

Orban, G. A., Van Essen, D., & Vanduffel, W. (2004). Comparative mapping of higher visual areas in monkeys and humans. *Trends in Cognitive Sciences, 8*(7), 315-324.

Oristaglio, J., Schneider, D. M., Balan, P. F., & Gottlieb, J. (2006). Integration of Visuospatial and Effector Information during Symbolically Cued Limb Movements in Monkey Lateral Intraparietal Area. *The Journal of Neuroscience, 26*(32), 8310-8319.

Padoa-Schioppa, C., & Assad, J. A. (2006). Neurons in the orbitofrontal cortex encode economic value. *Nature, 441*(7090), 223-226.

Palmer, J., Ames, C. T., & Lindsey, D. T. (1993). Measuring the Effect of Attention on Simple Visual Search. *Journal of Experimental Psychology: Human Perception and Performance, 19*(1), 108-130.

Palmer, J., Huk, A. C., & Shadlen, M. N. (2005). The effect of stimulus strength on the speed and accuracy of a perceptual decision. *Journal of Vision, 5*(5).

Palva, S., & Palva, J. M. (2007). New vistas for α-frequency band oscillations. *Trends in Neurosciences, 30*(4), 150-158.

Paré, M., & Wurtz, R. H. (2001). Progression in Neuronal Processing for Saccadic Eye Movements From Parietal Cortex Area LIP to Superior Colliculus. *Journal of Neurophysiology, 85*(6), 2545-2562.

Park, J., & Zhang, J. (2010). Sensorimotor Locus of the Buildup Activity in Monkey Lateral Intraparietal Area Neurons. *J Neurophysiol, 103*(5), 2664-2674.

Pascual-Leone, A. (1999). Transcranial magnetic stimulation: studying the brain--behaviour relationship by induction of ‚Äòvirtual lesions‚Äô. *Philosophical transactions of the Royal Society of London. Series B: Biological sciences, 354*(1387), 1229-1238.

Pascual-Leone, A., & Walsh, V. (2001). Fast Backprojections from the Motion to the Primary Visual Area Necessary for Visual Awareness. *Science, 292*(5516), 510-512.

Pastor-Bernier, A., & Cisek, P. (2011). Neural Correlates of Biased Competition in Premotor Cortex. *The Journal of Neuroscience, 31*(19), 7083-7088.

Paus, T., Jech, R., Thompson, C. J., Comeau, R., Peters, T., & Evans, A. C. (1997). Transcranial Magnetic Stimulation during Positron Emission Tomography: A New Method for Studying Connectivity of the Human Cerebral Cortex. *The Journal of Neuroscience, 17*(9), 3178-3184.

Paus, T., Sipila, P. K., & Strafella, A. P. (2001). Synchronization of Neuronal Activity in the Human Primary Motor Cortex by Transcranial Magnetic Stimulation: An EEG Study. *Journal of Neurophysiology, 86*(4), 1983-1990.

Pelli, D. G. (1985). Uncertainty explains many aspects of visual contrast detection and discrimination. *Journal of the Optical Society of America a-Optics Image Science and Vision, 2*(9), 1508-1532.

Pertzov, Y., Avidan, G., & Zohary, E. (2011). Multiple Reference Frames for Saccadic Planning in the Human Parietal Cortex. *The Journal of Neuroscience, 31*(3), 1059-1068.

Pesaran, B., Nelson, M. J., & Andersen, R. A. (2008). Free choice activates a decision circuit between frontal and parietal cortex. *Nature, 453*(7193), 406-409.

Pesaran, B., Pezaris, J. S., Sahani, M., Mitra, P. P., & Andersen, R. A. (2002). Temporal structure in neuronal activity during working memory in macaque parietal cortex. *Nat Neurosci, 5*(8), 805-811.

Pessoa, L., & Padmala, S. (2005). Quantitative prediction of perceptual decisions during near-threshold fear detection. *Proceedings of the National Academy of Sciences of the United States of America, 102*(15), 5612-5617.

Pessoa, L., & Padmala, S. (2007). Decoding Near-Threshold Perception of Fear from Distributed Single-Trial Brain Activation. *Cerebral Cortex, 17*(3), 691-701.

Pezzulo, G., & Castelfranchi, C. (2009). Thinking as the control of imagination: a conceptual framework for goal-directed systems. *Psychological Research, 73*(4), 559-577.

Pfurtscheller, G. (1981). Central beta rhythm during sensorimotor activities in man. *Electroencephalography and Clinical Neurophysiology, 51*(3), 253-264.

Pfurtscheller, G., & Berghold, A. (1989). Patterns of cortical activation during planning of voluntary movement. *Electroencephalography and Clinical Neurophysiology, 72*(3), 250-258.

Pfurtscheller, G., Brunner, C., Schlogl, A., & Lopes da Silva, F. H. (2006). Mu rhythm (de)synchronization and EEG single-trial classification of different motor imagery tasks. *NeuroImage, 31*(1), 153-159.

Pfurtscheller, G., & Lopes da Silva, F. H. (1999). Event-related EEG/MEG synchronization and desynchronization: basic principles. *Clinical Neurophysiology, 110*(11), 1842-1857.

Pfurtscheller, G., Neuper, C., Andrew, C., & Edlinger, G. (1997). Foot and hand area mu rhythms. *International Journal of Psychophysiology, 26*(1-3), 121-135.

Pfurtscheller, G., Stancák, A., & Neuper, C. (1996). Event-related synchronization (ERS) in the alpha band -- an electrophysiological correlate of cortical idling: A review. *International Journal of Psychophysiology, 24*(1-2), 39-46.

Philiastides, Marios G., Auksztulewicz, R., Heekeren, Hauke R., & Blankenburg, F. (2011). Causal Role of Dorsolateral Prefrontal Cortex in Human Perceptual Decision Making. *Current Biology, 21*(11), 980-983.

Philiastides, M. G., Biele, G., & Heekeren, H. R. (2010). A mechanistic account of value computation in the human brain. *Proceedings of the National Academy of Sciences, 107*(20), 9430-9435.

Philiastides, M. G., Ratcliff, R., & Sajda, P. (2006). Neural Representation of Task Difficulty and Decision Making during Perceptual Categorization: A Timing Diagram. *J. Neurosci., 26*(35), 8965-8975.

Philiastides, M. G., & Sajda, P. (2006). Temporal Characterization of the Neural Correlates of Perceptual Decision Making in the Human Brain. *Cerebral Cortex, 16*(4), 509-518.

Philiastides, M. G., & Sajda, P. (2007). EEG-Informed fMRI Reveals Spatiotemporal Characteristics of Perceptual Decision Making. *The Journal of Neuroscience, 27*(48), 13082-13091.

Picton, T. W., Bentin, S., Berg, P., Donchin, E., Hillyard, S. A., Johnson, R., Miller, G. A., Ritter, W., Ruchkin, D. S., et al. (2000). Guidelines for using human event-related potentials to study cognition: Recording standards and publication criteria. *Psychophysiology, 37*(2), 127-152.

Pineda, J. A. (2005). The functional significance of mu rhythms: Translating "seeing" and "hearing" into "doing". *Brain Research Reviews, 50*(1), 57-68.

Platt, M. L., Dayan, P., Dehaene, S., McCabe, K., Menzel, R., Phelps, E., Plassmann, H., Ratcliff, R., Shadlen, M. N., et al. (2008). Neuronal Correlates of Decision Making. In C. Engel & W. Singer (Eds.), *Better Than Conscious? Decision Making, the Human Mind, and Implications For Institutions* (pp. 125-154): MIT Press.

Platt, M. L., & Glimcher, P. W. (1997). Responses of Intraparietal Neurons to Saccadic Targets and Visual Distractors. *Journal of Neurophysiology, 78*(3), 1574-1589.

Platt, M. L., & Glimcher, P. W. (1999). Neural correlates of decision variables in parietal cortex. *Nature, 400*(6741), 233-238.

Pleger, B., Ruff, C. C., Blankenburg, F., Bestmann, S., Wiech, K., Stephan, K. E., Capilla, A., Friston, K. J., & Dolan, R. J. (2006). Neural Coding of Tactile Decisions in the Human Prefrontal Cortex. *The Journal of Neuroscience, 26*(48), 12596-12601.

Ploran, E. J., Nelson, S. M., Velanova, K., Donaldson, D. I., Petersen, S. E., & Wheeler, M. E. (2007). Evidence Accumulation and the Moment of Recognition: Dissociating Perceptual Recognition Processes Using fMRI. *The Journal of Neuroscience, 27*(44), 11912-11924.

Pogosyan, A., Gaynor, L. D., Eusebio, A., & Brown, P. (2009). Boosting Cortical Activity at Beta-Band Frequencies Slows Movement in Humans. *Current Biology, 19*(19), 1637-1641.

Poort, J., & Roelfsema, P. R. (2009). Noise Correlations Have Little Influence on the Coding of Selective Attention in Area V1. *Cerebral Cortex, 19*(3), 543-553.

Porro, C. A., Francescato, M. P., Cettolo, V., Diamond, M. E., Baraldi, P., Zuiani, C., Bazzocchi, M., & di Prampero, P. E. (1996). Primary Motor and Sensory Cortex Activation during Motor Performance and Motor Imagery: A Functional Magnetic Resonance Imaging Study. *The Journal of Neuroscience, 16*(23), 7688-7698.

Premereur, E., Vanduffel, W., & Janssen, P. (2011). Functional Heterogeneity of Macaque Lateral Intraparietal Neurons. *The Journal of Neuroscience, 31*(34), 12307-12317.

Prins, N., & Kingdom, F. A. A. (2009). Palamedes: Matlab routines for analyzing psychophysical data. http://www.palamedestoolbox.org.

Prinzmetal, W., McCool, C., & Park, S. (2005). Attention: Reaction time and accuracy reveal different mechanisms. *Journal of Experimental Psychology: General, 134*(1), 73-92.

Prinzmetal, W., Zvinyatskovskiy, A., Gutierrez, P., & Dilem, L. (2009). Voluntary and involuntary attention have different consequences: The effect of perceptual difficulty. *Quarterly Journal of Experimental Psychology, 62*(2), 352-369.

Prut, Y., & Fetz, E. E. (1999). Primate spinal interneurons show pre-movement instructed delay activity. *Nature, 401*(6753), 590-594.

Purcell, B. A., Heitz, R. P., Cohen, J. Y., Schall, J. D., Logan, G. D., & Palmeri, T. J. (2010). Neurally constrained modeling of perceptual decision making. *Psychological Review, 117*(4), 1113-1143.

Quian Quiroga, R., Kraskov, A., Koch, C., & Fried, I. (2009). Explicit Encoding of Multimodal Percepts by Single Neurons in the Human Brain. *Current Biology, 19*(15), 1308-1313.

Quian Quiroga, R., Snyder, L. H., Batista, A. P., Cui, H., & Andersen, R. A. (2006). Movement Intention Is Better Predicted than Attention in the Posterior Parietal Cortex. *J. Neurosci., 26*(13), 3615-3620.

Quiroga, R. Q., Reddy, L., Kreiman, G., Koch, C., & Fried, I. (2005). Invariant visual representation by single neurons in the human brain. *Nature, 435*(7045), 1102-1107.

Quraan, M. A., Moses, S. N., Hung, Y., Mills, T., & Taylor, M. J. (2011). Detection and localization of hippocampal activity using beamformers with MEG: A detailed investigation using simulations and empirical data. *Human Brain Mapping, 32*(5), 812-827.

Rahnev, D., Lau, H., & de Lange, F. P. (2011). Prior Expectation Modulates the Interaction between Sensory and Prefrontal Regions in the Human Brain. *The Journal of Neuroscience, 31*(29), 10741-10748.

Raichle, M. E., MacLeod, A. M., Snyder, A. Z., Powers, W. J., Gusnard, D. A., & Shulman, G. L. (2001). A default mode of brain function. *Proceedings of the National Academy of Sciences, 98*(2), 676-682.

Raichle, M. E., & Snyder, A. Z. (2007). A default mode of brain function: A brief history of an evolving idea. *NeuroImage, 37*(4), 1083-1090.

Rasch, M. J., Gretton, A., Murayama, Y., Maass, W., & Logothetis, N. K. (2008). Inferring Spike Trains From Local Field Potentials. *Journal of Neurophysiology, 99*(3), 1461-1476.

Ratcliff, R. (1978). A theory of memory retrieval. *Psychological Review, 85*(2), 59-108.

Ratcliff, R., Cherian, A., & Segraves, M. (2003a). A Comparison of Macaque Behavior and Superior Colliculus Neuronal Activity to Predictions From Models of Two-Choice Decisions. *Journal of Neurophysiology, 90*(3), 1392-1407.

Ratcliff, R., Cherian, A., & Segraves, M. (2003b). A Comparison of Macaque Behavior and Superior Colliculus Neuronal Activity to Predictions From Models of Two-Choice Decisions. *J Neurophysiol, 90*(3), 1392-1407.

Ratcliff, R., & McKoon, G. (2008). The diffusion decision model: theory and data for two-choice decision tasks. *Neural Computation, 20*(4), 873-922.

Ratcliff, R., McKoon, G., & Gomez, P. (2004). A Diffusion Model Account of the Lexical Decision Task. *Psychological Review, 111*(1), 159-182.

Ratcliff, R., Philiastides, M. G., & Sajda, P. (2009). Quality of evidence for perceptual decision making is indexed by trial-to-trial variability of the EEG. *Proceedings of the National Academy of Sciences, 106*(16), 6539-6544.

Ratcliff, R., & Rouder, J. N. (1998). Modeling Response Times for Two-Choice Decisions. *Psychological Science, 9*(5), 347-356.

Ratcliff, R., & Smith, P. L. (2004). A Comparison of Sequential Sampling Models for Two-Choice Reaction Time. *Psychological Review, 111*(2), 333-367.

Ratcliff, R., Thapar, A., & McKoon, G. (2001). The effects of aging on reaction time in a signal detection task. *Psychology and Aging, 16*(2), 323-341.

Ratcliff, R., Thapar, A., & McKoon, G. (2003c). A diffusion model analysis of the effects of aging on brightness discrimination. *Attention, Perception, & Psychophysics, 65*(4), 523-535.

Ratcliff, R., Van Zandt, T., & McKoon, G. (1999). Connectionist and diffusion models of reaction time. *Psychological Review, 106*(2), 261-300.

Rees, G., Frith, C. D., & Lavie, N. (1997). Modulating irrelevant motion perception by varying attentional load in an unrelated task. *Science, 278*(5343), 1616-1619.

Reilly, E. L. (2005). EEG Recording and Operation of the Apparatus. In E. Niedermeyer & F. H. Lopes da Silva (Eds.), *Electroencephalography: basic principles, clinical applications, and related fields* (5th ed., pp. 139-160). Philadelphia: Lippincott Williams & Wilkins.

Ress, D., Backus, B. T., & Heeger, D. J. (2000). Activity in primary visual cortex predicts performance in a visual detection task. *Nat Neurosci, 3*(9), 940-945.

Reynolds, J. H., & Chelazzi, L. (2004). Attentional Modulation of Visual Processing. *Annual Review of Neuroscience, 27*(1), 611-647.

Reynolds, J. H., Pasternak, T., & Desimone, R. (2000). Attention Increases Sensitivity of V4 Neurons. *26*(3), 703-714.

Rihs, T. A., Michel, C. M., & Thut, G. (2007). Mechanisms of selective inhibition in visual spatial attention are indexed by alpha-band EEG synchronization. *European Journal of Neuroscience, 25*(2), 603-610.

Rihs, T. A., Michel, C. M., & Thut, G. (2009). A bias for posterior alpha-band power suppression versus enhancement during shifting versus maintenance of spatial attention. *NeuroImage, 44*(1), 190-199.

Robinson, D. A., & Fuchs, A. F. (1969). Eye movements evoked by stimulation of frontal eye fields. *Journal of Neurophysiology, 32*(5), 637-648.

Roitman, J. D., Brannon, E. M., & Platt, M. L. (2007). Monotonic Coding of Numerosity in Macaque Lateral Intraparietal Area. *PLoS Biol, 5*(8), e208.

Roitman, J. D., & Shadlen, M. N. (2002). Response of Neurons in the Lateral Intraparietal Area during a Combined Visual Discrimination Reaction Time Task. *The Journal of Neuroscience, 22*(21), 9475-9489.

Romei, V., Brodbeck, V., Michel, C., Amedi, A., Pascual-Leone, A., & Thut, G. (2008a). Spontaneous Fluctuations in Posterior alpha-Band EEG Activity Reflect Variability in Excitability of Human Visual Areas. *Cereb. Cortex, 18*(9), 2010-2018.

Romei, V., Driver, J., Schyns, P. G., & Thut, G. (2011). Rhythmic TMS over Parietal Cortex Links Distinct Brain Frequencies to Global versus Local Visual Processing. *Current biology : CB, 21*(4), 334-337.

Romei, V., Gross, J., & Thut, G. (2010). On the Role of Prestimulus Alpha Rhythms over Occipito-Parietal Areas in Visual Input Regulation: Correlation or Causation? *The Journal of Neuroscience, 30*(25), 8692-8697.

Romei, V., Rihs, T., Brodbeck, V., & Thut, G. (2008b). Resting electroencephalogram alpha-power over posterior sites indexes baseline visual cortex excitability. *NeuroReport, 19*(2), 203-208.

Romo, R., Brody, C. D., Hernandez, A., & Lemus, L. (1999). Neuronal correlates of parametric working memory in the prefrontal cortex. *Nature, 399*(6735), 470-473.

Romo, R., Hernández, A., & Zainos, A. (2004). Neuronal Correlates of a Perceptual Decision in Ventral Premotor Cortex. *Neuron, 41*(1), 165-173.

Romo, R., Hernández, A., Zainos, A., Brody, C. D., & Lemus, L. (2000). Sensing without Touching: Psychophysical Performance Based on Cortical Microstimulation. *Neuron, 26*(1), 273-278.

Romo, R., Hernandez, A., Zainos, A., Lemus, L., & Brody, C. D. (2002). Neuronal correlates of decision-making in secondary somatosensory cortex. *Nat Neurosci, 5*(11), 1217-1225.

Romo, R., Hernandez, A., Zainos, A., & Salinas, E. (1998). Somatosensory discrimination based on cortical microstimulation. *Nature, 392*(6674), 387-390.

Romo, R., & Salinas, E. (2003). Flutter Discrimination: neural codes, perception, memory and decision making. *Nat Rev Neurosci, 4*(3), 203-218.

Rorie, A. E., Gao, J., McClelland, J. L., & Newsome, W. T. (2010). Integration of Sensory and Reward Information during Perceptual Decision-Making in Lateral Intraparietal Cortex (LIP) of the Macaque Monkey. *PLoS ONE, 5*(2), e9308.

Rorie, A. E., & Newsome, W. T. (2005). A general mechanism for decision-making in the human brain? *Trends in Cognitive Sciences, 9*(2), 41-43.

Rossi, S., Hallett, M., Rossini, P. M., & Pascual-Leone, A. (2009). Safety, ethical considerations, and application guidelines for the use of transcranial magnetic stimulation in clinical practice and research. *Clinical Neurophysiology, 120*(12), 2008-2039.

Roth, M., Decety, J., Raybaudi, M., Massarelli, R., Delon-Martin, C., Segebarth, C., Morand, S. p., Gemignani, A., D√©corps, M., et al. (1996). Possible involvement of primary motor cortex in mentally simulated movement: a functional magnetic resonance imaging study. *NeuroReport, 7*(7), 1280-1284.

Ruff, C. C., Driver, J., & Bestmann, S. (2009). Combining TMS and fMRI: From `virtual lesions' to functional-network accounts of cognition. *Cortex, 45*(9), 1043-1049.

Rugg, M. D., & Coles, M. G. H. (1996). *Electrophysiology of mind: event-related brain potentials and cognition*: Oxford University Press.

Ruohonen, J., & Ilmoniemi, R. J. (1999). Modeling of the stimulating field generation in TMS. *Electroencephalography and clinical neurophysiology. Supplement, 51*, 30-40.

Rushworth, M. F. S., Ellison, A., & Walsh, V. (2001a). Complementary localization and lateralization of orienting and motor attention. *Nature Neuroscience, 4*(6), 656-661.

Rushworth, M. F. S., Johansen-Berg, H., Göbel, S. M., & Devlin, J. T. (2003). The left parietal and premotor cortices: motor attention and selection. *NeuroImage, 20*(Supplement 1), S89-S100.

Rushworth, M. F. S., Krams, M., & Passingham, R. E. (2001b). The Attentional Role of the Left Parietal Cortex: The Distinct Lateralization and Localization of Motor Attention in the Human Brain. *Journal of Cognitive Neuroscience, 13*(5), 698-710.

Rushworth, M. F. S., Nixon, P. D., Renowden, S., Wade, D. T., & Passingham, R. E. (1997). The left parietal cortex and motor attention. *Neuropsychologia, 35*(9), 1261-1273.

Rushworth, Matthew F. S., Noonan, MaryAnn P., Boorman, Erie D., Walton, Mark E., & Behrens, Timothy E. (2011). Frontal Cortex and Reward-Guided Learning and Decision-Making. *Neuron, 70*(6), 1054-1069.

Rushworth, M. F. S., Paus, T., & Sipila, P. K. (2001c). Attention Systems and the Organization of the Human Parietal Cortex. *The Journal of Neuroscience, 21*(14), 5262-5271.

Ruzzoli, M., Abrahamyan, A., Clifford, C. W. G., Marzi, C. A., Miniussi, C., & Harris, J. A. (2011). The effect of TMS on visual motion sensitivity: an increase in neural noise or a decrease in signal strength? *Journal of Neurophysiology, 106*(1), 138-143.

Ruzzoli, M., Marzi, C. A., & Miniussi, C. (2010). The Neural Mechanisms of the Effects of Transcranial Magnetic Stimulation on Perception. *J Neurophysiol, 103*(6), 2982-2989.

Sack, A. T., Kohler, A., Bestmann, S., Linden, D. E. J., Dechent, P., Goebel, R., & Baudewig, J. (2007). Imaging the brain activity changes underlying impaired visuospatial judgments: Simultaneous fMRI, TMS, and behavioral studies. *Cerebral Cortex, 17*(12), 2841-2852.

Sack, A. T., Kohler, A., Linden, D. E. J., Goebel, R., & Muckli, L. (2006). The temporal characteristics of motion processing in hMT/V5+: Combining fMRI and neuronavigated TMS. *NeuroImage, 29*(4), 1326-1335.

Salenius, S., Kajola, M., Thompson, W. L., Kosslyn, S., & Hari, R. (1995). Reactivity of magnetic parieto-occipital alpha rhythm during visual imagery. *Electroencephalography and Clinical Neurophysiology, 95*(6), 453-462.

Salenius, S., Portin, K., Kajola, M., Salmelin, R., & Hari, R. (1997). Cortical Control of Human Motoneuron Firing During Isometric Contraction. *Journal of Neurophysiology, 77*(6), 3401-3405.

Salinas, E., Hernández, A., Zainos, A., & Romo, R. (2000). Periodicity and Firing Rate As Candidate Neural Codes for the Frequency of Vibrotactile Stimuli. *The Journal of Neuroscience, 20*(14), 5503-5515.

Salinas, E., & Romo, R. (1998). Conversion of Sensory Signals into Motor Commands in Primary Motor Cortex. *The Journal of Neuroscience, 18*(1), 499-511.

Salinas, E., & Sejnowski, T. J. (2001). Correlated neuronal activity and the flow of neural information. *Nat Rev Neurosci, 2*(8), 539-550.

Salmelin, R., Hamalainen, M., Kajola, M., & Hari, R. (1995). Functional segregation of movement-related rhythmic activity in the human brain. *NeuroImage, 2*(4), 237-243.

Salmelin, R., & Hari, R. (1994a). Characterization of spontaneous MEG rhythms in healthy adults. *Electroencephalography and Clinical Neurophysiology, 91*(4), 237-248.

Salmelin, R., & Hari, R. (1994b). Spatiotemporal characteristics of sensorimotor neuromagnetic rhythms related to thumb movement. *Neuroscience, 60*(2), 537-550.

Salmelin, R., Hari, R., Lounasmaa, O. V., & Sams, M. (1994). Dynamics of brain activation during picture naming. *Nature, 368*(6470), 463-465.

Salzman, C., Murasugi, C., Britten, K., & Newsome, W. (1992). Microstimulation in visual area MT: effects on direction discrimination performance. *The Journal of Neuroscience, 12*(6), 2331-2355.

Salzman, C. D., Britten, K. H., & Newsome, W. T. (1990). Cortical microstimulation influences perceptual judgements of motion direction. *Nature, 346*(6280), 174-177.

Salzman, C. D., Paton, J. J., Belova, M. A., & Morrison, S. E. (2007). Flexible Neural Representations of Value in the Primate Brain. *Annals of the New York Academy of Sciences, 1121*(Linking affect to Action: Critical Contributions of the Orbitofrontal Cortex), 336-354.

Sanes, J. N., & Donoghue, J. P. (1993). Oscillations in local field potentials of the primate motor cortex during voluntary movement. *Proceedings of the National Academy of Sciences, 90*(10), 4470-4474.

Sasaki, R., & Uka, T. (2009). Dynamic Readout of Behaviorally Relevant Signals from Area MT during Task Switching. *62*(1), 147-157.

Sauseng, P., Klimesch, W., Gerloff, C., & Hummel, F. C. (2009). Spontaneous locally restricted EEG alpha activity determines cortical excitability in the motor cortex. *Neuropsychologia, 47*(1), 284-288.

Sauseng, P., Klimesch, W., Stadler, W., Schabus, M., Doppelmayr, M., Hanslmayr, S., Gruber, W. R., & Birbaumer, N. (2005). A shift of visual spatial attention is selectively associated with human EEG alpha activity. *European Journal of Neuroscience, 22*(11), 2917-2926.

Sawamura, H., Shima, K., & Tanji, J. (2010). Deficits in Action Selection Based on Numerical Information After Inactivation of the Posterior Parietal Cortex in Monkeys. *Journal of Neurophysiology, 104*(2), 902-910.

Schall, J., Morel, A., King, D., & Bullier, J. (1995). Topography of visual cortex connections with frontal eye field in macaque: convergence and segregation of processing streams. *The Journal of Neuroscience, 15*(6), 4464-4487.

Scheeringa, R., Fries, P., Petersson, K.-M., Oostenveld, R., Grothe, I., Norris, D. G., Hagoort, P., & Bastiaansen, M. C. M. (2011). Neuronal Dynamics Underlying High- and Low-Frequency EEG Oscillations Contribute Independently to the Human BOLD Signal. *Neuron, 69*(3), 572-583.

Scheeringa, R., Petersson, K. M., Oostenveld, R., Norris, D. G., Hagoort, P., & Bastiaansen, M. C. M. (2009). Trial-by-trial coupling between EEG and BOLD identifies networks related to alpha and theta EEG power increases during working memory maintenance. *NeuroImage, 44*(3), 1224-1238.

Scheibe, C., Schubert, R., Sommer, W., & Heekeren, H. R. (2009). Electrophysiological evidence for the effect of prior probability on response preparation. *Psychophysiology, 46*(4), 758-770.

Scheibe, C., Ullsperger, M., Sommer, W., & Heekeren, H. R. (2010). Effects of Parametrical and Trial-to-Trial Variation in Prior Probability Processing Revealed by Simultaneous Electroencephalogram/Functional Magnetic Resonance Imaging. *J. Neurosci., 30*(49), 16709-16717.

Schenkluhn, B., Ruff, C. C., Heinen, K., & Chambers, C. D. (2008). Parietal Stimulation Decouples Spatial and Feature-Based Attention. *J. Neurosci., 28*(44), 11106-11110.

Scherberger, H., & Andersen, R. A. (2007). Target Selection Signals for Arm Reaching in the Posterior Parietal Cortex. *The Journal of Neuroscience, 27*(8), 2001-2012.

Schiller, P. H., Tehovnik, E. J., V.A. Casagrande, R. W. G., & Sherman, S. M. (2005). Neural mechanisms underlying target selection with saccadic eye movements *Progress in Brain Research* (Vol. Volume 149, pp. 157-171): Elsevier.

Schluter, N. D., Krams, M., Rushworth, M. F. S., & Passingham, R. E. (2001). Cerebral dominance for action in the human brain: the selection of actions. *Neuropsychologia, 39*(2), 105-113.

Schluter, N. D., Rushworth, M. F., Passingham, R. E., & Mills, K. R. (1998). Temporary interference in human lateral premotor cortex suggests dominance for the selection of movements. A study using transcranial magnetic stimulation. *Brain, 121*(5), 785-799.

Schluter, N. D., Rushworth, M. F. S., Mills, K. R., & Passingham, R. E. (1999). Signal-, set-, and movement-related activity in the human premotor cortex. *Neuropsychologia, 37*(2), 233-243.

Schnitzler, A., Salenius, S., Salmelin, R., Jousmäki, V., & Hari, R. (1997). Involvement of Primary Motor Cortex in Motor Imagery: A Neuromagnetic Study. *NeuroImage, 6*(3), 201-208.

Schoffelen, J.-M., Oostenveld, R., & Fries, P. (2005). Neuronal Coherence as a Mechanism of Effective Corticospinal Interaction. *Science, 308*(5718), 111-113.

Schoffelen, J.-M., Oostenveld, R., & Fries, P. (2008). Imaging the human motor system's beta-band synchronization during isometric contraction. *NeuroImage, 41*(2), 437-447.

Schoffelen, J.-M., Poort, J., Oostenveld, R., & Fries, P. (2011). Selective Movement Preparation Is Subserved by Selective Increases in Corticomuscular Gamma-Band Coherence. *The Journal of Neuroscience, 31*(18), 6750-6758.

Schoppenhorst, M., Brauer, F., Freund, G., & Kubicki, S. (1980). The significance of coherence estimates in determining central alpha and mu activities. *Electroencephalography and Clinical Neurophysiology, 48*(1), 25-33.

Sehatpour, P., Molholm, S., Schwartz, T. H., Mahoney, J. R., Mehta, A. D., Javitt, D. C., Stanton, P. K., & Foxe, J. J. (2008). A human intracranial study of long-range

oscillatory coherence across a frontal–occipital–hippocampal brain network during visual object processing. *Proceedings of the National Academy of Sciences, 105*(11), 4399-4404.

Seidemann, E., Zohary, E., & Newsome, W. T. (1998). Temporal gating of neural signals during performance of a visual discrimination task. *Nature, 394*(6688), 72-75.

Seo, H., Barraclough, D. J., & Lee, D. (2009). Lateral Intraparietal Cortex and Reinforcement Learning during a Mixed-Strategy Game. *J. Neurosci., 29*(22), 7278-7289.

Sereno, A. B., & Maunsell, J. H. R. (1998). Shape selectivity in primate lateral intraparietal cortex. *Nature, 395*(6701), 500-503.

Sereno, M. I., Pitzalis, S., & Martinez, A. (2001). Mapping of Contralateral Space in Retinotopic Coordinates by a Parietal Cortical Area in Humans. *Science, 294*(5545), 1350-1354.

Shadlen, M. N., Kiani, R., Hanks, T. D., & Churchland, A. K. (2008). Neurobiology of Decision Making - An Intentional Framework. In C. Engel & W. Singer (Eds.), *Better Than Conscious? Decision Making, the Human Mind, and Implications For Institutions* (pp. 71-101): MIT Press.

Shadlen, M. N., & Newsome, W. T. (1996). Motion perception: seeing and deciding. *Proceedings of the National Academy of Sciences, 93*(2), 628-633.

Shadlen, M. N., & Newsome, W. T. (1998). The Variable Discharge of Cortical Neurons: Implications for Connectivity, Computation, and Information Coding. *J. Neurosci., 18*(10), 3870-3896.

Shadlen, M. N., & Newsome, W. T. (2001). Neural basis of a perceptual decision in the parietal cortex (area LIP) of the rhesus monkey. *Journal of Neurophysiology, 86*(4), 1916-1936.

Shiu, L., & Pashler, H. (1994). Negligible effect of spatial precuing on identification of single digits. *Journal of Experimental Psychology: Human Perception and Performance, 20*(5), 1037-1054.

Shulman, G. L., Fiez, J. A., Corbetta, M., Buckner, R. L., Miezin, F. M., Raichle, M. E., & Petersen, S. E. (1997). Common Blood Flow Changes across Visual Tasks: II. Decreases in Cerebral Cortex. *Journal of Cognitive Neuroscience, 9*(5), 648-663.

Siebner, H. R., Bergmann, T. O., Bestmann, S., Massimini, M., Johansen-Berg, H., Mochizuki, H., Bohning, D. E., Boorman, E. D., Groppa, S., et al. (2009). Consensus paper: Combining transcranial stimulation with neuroimaging. *Brain Stimulation, 2*(2), 58-80.

Siegel, M., Donner, T. H., Oostenveld, R., Fries, P., & Engel, A. K. (2007). High-Frequency Activity in Human Visual Cortex Is Modulated by Visual Motion Strength. *Cerebral Cortex, 17*(3), 732-741.

Siegel, M., Engel, A. K., & Donner, T. H. (2011). Cortical Network Dynamics of Perceptual Decision-Making in the Human Brain. *Frontiers in Human Neuroscience, 5*.

Silvanto, J., Cattaneo, Z., Battelli, L., & Pascual-Leone, A. (2008). Baseline Cortical Excitability Determines Whether TMS Disrupts or Facilitates Behavior. *Journal of Neurophysiology, 99*(5), 2725-2730.

Silvanto, J., Lavie, N., & Walsh, V. (2005). Double Dissociation of V1 and V5/MT activity in Visual Awareness. *Cerebral Cortex, 15*(11), 1736-1741.

Singer, W. (1993). Synchronization of Cortical Activity and its Putative Role in Information Processing and Learning. *Annual Review of Physiology, 55*(1), 349-374.

Sirotin, Y. B., & Das, A. (2009). Anticipatory haemodynamic signals in sensory cortex not predicted by local neuronal activity. *Nature, 457*(7228), 475-479.

Smith, P. L. (2000). Attention and luminance detection: Effects of cues, masks, and pedestals. *Journal of Experimental Psychology-Human Perception and Performance, 26*(4), 1401-1420.

Smith, P. L. (2010). From Poisson shot noise to the integrated Ornstein-Uhlenbeck process: Neurally principled models of information accumulation in decision-making and response time. *Journal of Mathematical Psychology, 54*(2), 266-283.

Smith, P. L., & Ratcliff, R. (2004). Psychology and neurobiology of simple decisions. *Trends in Neurosciences, 27*(3), 161-168.

Smith, P. L., & Ratcliff, R. (2009). An Integrated Theory of Attention and Decision Making in Visual Signal Detection. *Psychological Review, 116*(2), 283-317.

Smith, P. L., Ratcliff, R., & Wolfgang, B. J. (2004). Attention orienting and the time course of perceptual decisions: response time distributions with masked and unmasked displays. *Vision Research, 44*(12), 1297-1320.

Snyder, A. C., & Foxe, J. J. (2010). Anticipatory Attentional Suppression of Visual Features Indexed by Oscillatory Alpha-Band Power Increases:A High-Density Electrical Mapping Study. *J. Neurosci., 30*(11), 4024-4032.

Snyder, L. H., Batista, A. P., & Andersen, R. A. (1997). Coding of intention in the posterior parietal cortex. *Nature, 386*(6621), 167-170.

Snyder, L. H., Dickinson, A. R., & Calton, J. L. (2006). Preparatory Delay Activity in the Monkey Parietal Reach Region Predicts Reach Reaction Times. *The Journal of Neuroscience, 26*(40), 10091-10099.

Soltani, A., & Wang, X.-J. (2010). Synaptic computation underlying probabilistic inference. *Nat Neurosci, 13*(1), 112-119.

Soteropoulos, D. S., Edgley, S. A., & Baker, S. N. (2011). Lack of Evidence for Direct Corticospinal Contributions to Control of the Ipsilateral Forelimb in Monkey. *The Journal of Neuroscience, 31*(31), 11208-11219.

Spitzer, B., Wacker, E., & Blankenburg, F. (2010). Oscillatory Correlates of Vibrotactile Frequency Processing in Human Working Memory. *The Journal of Neuroscience, 30*(12), 4496-4502.

Spivey, M. J., Grosjean, M., & Knoblich, G. (2005). Continuous attraction toward phonological competitors. *Proceedings of the National Academy of Sciences of the United States of America, 102*(29), 10393-10398.

Stanford, T. R., Shankar, S., Massoglia, D. P., Costello, M. G., & Salinas, E. (2010). Perceptual decision making in less than 30 milliseconds. *Nat Neurosci, 13*(3), 379-385.

Stern, E. R., Gonzalez, R., Welsh, R. C., & Taylor, S. F. (2010). Updating Beliefs for a Decision: Neural Correlates of Uncertainty and Underconfidence. *J. Neurosci., 30*(23), 8032-8041.

Sternberg, S. (1969). The discovery of processing stages: Extensions of Donders' method. *Acta Psychologica, 30*, 276-315.

Stevens, L. K., McGraw, P. V., Ledgeway, T., & Schluppeck, D. (2009). Temporal characteristics of global motion processing revealed by transcranial magnetic stimulation. *European Journal of Neuroscience, 30*(12), 2415-2426.

Stevenson, C. M., Brookes, M. J., & Morris, P. G. (2011). β-Band correlates of the fMRI BOLD response. *Human Brain Mapping, 32*(2), 182-197.

Stokes, M., Thompson, R., Nobre, A. C., & Duncan, J. (2009). Shape-specific preparatory activity mediates attention to targets in human visual cortex. *Proceedings of the National Academy of Sciences, 106*(46), 19569-19574.

Stokes, M. G., Chambers, C. D., Gould, I. C., English, T., McNaught, E., McDonald, O., & Mattingley, J. B. (2007). Distance-adjusted motor threshold for transcranial magnetic stimulation. *Clinical Neurophysiology, 118*(7), 1617-1625.

Stokes, M. G., Chambers, C. D., Gould, I. C., Henderson, T. R., Janko, N. E., Allen, N. B., & Mattingley, J. B. (2005). Simple metric for scaling motor threshold based on scalp-cortex distance: Application to studies using transcranial magnetic stimulation. *Journal of Neurophysiology, 94*(6), 4520-4527.

Stone, M. (1960). Models for choice-reaction time. *Psychometrika, 25*(3), 251-260.

Striemer, C. L., Chouinard, P. A., & Goodale, M. A. (2011). Programs for action in superior parietal cortex: A triple-pulse TMS investigation. *Neuropsychologia, 49*(9), 2391-2399.

Sugrue, L. P., Corrado, G. S., & Newsome, W. T. (2004). Matching Behavior and the Representation of Value in the Parietal Cortex. *Science, 304*(5678), 1782-1787.

Sugrue, L. P., Corrado, G. S., & Newsome, W. T. (2005). Choosing the greater of two goods: neural currencies for valuation and decision making. *Nat Rev Neurosci, 6*(5), 363-375.

Sylvester, C. M., Jack, A. I., Corbetta, M., & Shulman, G. L. (2008). Anticipatory suppression of nonattended locations in visual cortex marks target location and predicts perception. *Journal of Neuroscience, 28*(26), 6549-6556.

Tadin, D., Silvanto, J., Pascual-Leone, A., & Battelli, L. (2011). Improved Motion Perception and Impaired Spatial Suppression following Disruption of Cortical Area MT/V5. *The Journal of Neuroscience, 31*(4), 1279-1283.

Tanné-Gariépy, J., Rouiller, E., & Boussaoud, D. (2002). Parietal inputs to dorsal versus ventral premotor areas in the macaque monkey: evidence for largely segregated visuomotor pathways. *Experimental Brain Research, 145*(1), 91-103.

Taylor, P. C. J., Nobre, A. C., & Rushworth, M. F. S. (2007). FEF TMS affects visual cortical activity. *Cerebral Cortex, 17*(2), 391-399.

Taylor, P. C. J., Walsh, V., & Eimer, M. (2008). Combining TMS and EEG to study cognitive function and cortico-cortico interactions. *Behavioural Brain Research, 191*(2), 141-147.

Tegenthoff, M., Ragert, P., Pleger, B., Schwenkreis, P., Förster, A.-F., Nicolas, V., & Dinse, H. R. (2005). Improvement of Tactile Discrimination Performance and Enlargement of Cortical Somatosensory Maps after 5 Hz rTMS. *PLoS Biol, 3*(11), e362.

Tesche, C. D., & Karhu, J. (1999). MEG Study of Hippocampal Theta During a Working Memory Task. *Biomedizinische Technik/Biomedical Engineering, 44*(s2), 74-78.

Thakral, P. P., & Slotnick, S. D. (2011). Disruption of MT impairs motion processing. *Neuroscience Letters, 490*(3), 226-230.

Thielscher, A., & Pessoa, L. (2007). Neural Correlates of Perceptual Choice and Decision Making during Fear–Disgust Discrimination. *The Journal of Neuroscience, 27*(11), 2908-2917.

Thomson, D. J. (1982). Spectrum estimation and harmonic analysis. *Proceedings of the IEEE, 70*(9), 1055-1096.

Thut, G., & Miniussi, C. (2009). New insights into rhythmic brain activity from TMS-EEG studies. *Trends in Cognitive Sciences, 13*(4), 182-189.

Thut, G., Nietzel, A., Brandt, S. A., & Pascual-Leone, A. (2006). α-Band Electroencephalographic Activity over Occipital Cortex Indexes Visuospatial Attention Bias and Predicts Visual Target Detection. *J. Neurosci., 26*(37), 9494-9502.

Thut, G., Northoff, G., Ives, J. R., Kamitani, Y., Pfennig, A., Kampmann, F., Schomer, D. L., & Pascual-Leone, A. (2003). Effects of single-pulse transcranial magnetic stimulation (TMS) on functional brain activity: a combined event-related TMS and evoked

potential study. *Clinical neurophysiology : official journal of the International Federation of Clinical Neurophysiology, 114*(11), 2071-2080.
Thut, G., & Pascual-Leone, A. (2010a). Integrating TMS with EEG: How and What For? *Brain Topography, 22*(4), 215-218.
Thut, G., & Pascual-Leone, A. (2010b). A Review of Combined TMS-EEG Studies to Characterize Lasting Effects of Repetitive TMS and Assess Their Usefulness in Cognitive and Clinical Neuroscience. *Brain Topography, 22*(4), 219-232.
Thut, G., Veniero, D., Romei, V., Miniussi, C., Schyns, P., & Gross, J. (2011). Rhythmic TMS Causes Local Entrainment of Natural Oscillatory Signatures. *Current biology : CB*.
Tiitinen, H. T., Sinkkonen, J., Reinikainen, K., Alho, K., Lavikainen, J., & Naatanen, R. (1993). Selective attention enhances the auditory 40-Hz transient response in humans. *Nature, 364*(6432), 59-60.
Tomasino, B., Skrap, M., & Rumiati, R. I. (2010). Causal Role of the Sensorimotor Cortex in Action Simulation: Neuropsychological Evidence. *Journal of Cognitive Neuroscience, 23*(8), 2068-2078.
Tong, F. (2003). Primary Visual Cortex and Visual Awareness. *Nature Reviews | Neuroscience*.
Torrence, C., & Compo, G. (1998). A Practical Guide to Wavelet Analysis. *Bulletin of the American Meteorological Society, 79*(1), 61-78.
Tosoni, A., Galati, G., Romani, G. L., & Corbetta, M. (2008). Sensory-motor mechanisms in human parietal cortex underlie arbitrary visual decisions. *Nat Neurosci, 11*(12), 1446-1453.
Toth, L. J., & Assad, J. A. (2002). Dynamic coding of behaviourally relevant stimuli in parietal cortex. *Nature, 415*(6868), 165-168.
Townsend, J. T., & Ashby, F. G. (1983). *The stochastic modeling of elementary psychological processes*: Cambridge University Press.
Treue, S., & Trujillo, J. C. M. (1999). Feature-based attention influences motion processing gain in macaque visual cortex. *Nature, 399*(6736), 575-579.
Tsetsos, K., Usher, M., & McClelland, J. L. (2011). Testing multi-alternative decision models with non-stationary evidence. *Frontiers in Neuroscience, 5*.
Tuladhar, A. M., Huurne, N. t., Schoffelen, J.-M., Maris, E., Oostenveld, R., & Jensen, O. (2007). Parieto-occipital sources account for the increase in alpha activity with working memory load. *Human Brain Mapping, 28*(8), 785-792.
Tzagarakis, C., Ince, N. F., Leuthold, A. C., & Pellizzer, G. (2010a). Beta-band activity during motor planning reflects response uncertainty. *J Neurosci, 30*(34), 11270-11277.
Tzagarakis, C., Ince, N. F., Leuthold, A. C., & Pellizzer, G. (2010b). Beta-Band Activity during Motor Planning Reflects Response Uncertainty. *J. Neurosci., 30*(34), 11270-11277.
Ueno, S., Tashiro, T., & Harada, K. (1988). *Localized stimulation of neural tissues in the brain by means of a paired configuration of time?varying magnetic fields* (Vol. 64): AIP.
Uhlhaas, P. J., & Singer, W. (2006). Neural Synchrony in Brain Disorders: Relevance for Cognitive Dysfunctions and Pathophysiology. *Neuron, 52*(1), 155-168.
Uhlhaas, P. J., & Singer, W. (2010). Abnormal neural oscillations and synchrony in schizophrenia. *Nat Rev Neurosci, 11*(2), 100-113.
Ulrich, R., Leuthold, H., & Sommer, W. (1998). Motor programming of response force and movement direction. *Psychophysiology, 35*(6), 721-728.

Usher, M., & McClelland, J. L. (2001). The Time Course of Perceptual Choice: The Leaky, Competing Accumulator Model. *Psychological Review, 108*(3), 550-592.

Vallar, G., & Perani, D. (1986). The anatomy of unilateral neglect after right-hemisphere stroke lesions. A clinical/CT-scan correlation study in man. *Neuropsychologia, 24*(5), 609-622.

Vallbo, A. B., & Wessberg, J. (1993). Organization of motor output in slow finger movements in man. *The Journal of Physiology, 469*(1), 673-691.

van den Hurk, P., Mars, R. B., van Elswijk, G., Hegeman, J., Pasman, J. W., Bloem, B. R., & Toni, I. (2007). Online Maintenance of Sensory and Motor Representations: Effects on Corticospinal Excitability. *Journal of Neurophysiology, 97*(2), 1642-1648.

Van Der Werf, J., Buchholz, V. N., Jensen, O., & Medendorp, W. P. (2009). Neuronal synchronization in human parietal cortex during saccade planning. *Behavioural Brain Research, 205*(2), 329-335.

Van Der Werf, J., Jensen, O., Fries, P., & Medendorp, W. P. (2008). Gamma-Band Activity in Human Posterior Parietal Cortex Encodes the Motor Goal during Delayed Prosaccades and Antisaccades. *J. Neurosci., 28*(34), 8397-8405.

Van Der Werf, J., Jensen, O., Fries, P., & Medendorp, W. P. (2010). Neuronal Synchronization in Human Posterior Parietal Cortex during Reach Planning. *The Journal of Neuroscience, 30*(4), 1402-1412.

Van Der Werf, Y., & Paus, T. (2006). The neural response to transcranial magnetic stimulation of the human motor cortex. I. Intracortical and cortico-cortical contributions. *Experimental Brain Research, 175*(2), 231-245.

Van Der Werf, Y., Sadikot, A., Strafella, A., & Paus, T. (2006). The neural response to transcranial magnetic stimulation of the human motor cortex. II. Thalamocortical contributions. *Experimental Brain Research, 175*(2), 246-255.

Van Dijk, H., Schoffelen, J. M., Oostenveld, R., & Jensen, O. (2008). Prestimulus oscillatory activity in the alpha band predicts visual discrimination ability. *Journal of Neuroscience, 28*(8), 1816-1823.

van Ede, F., de Lange, F., Jensen, O., & Maris, E. (2011). Orienting Attention to an Upcoming Tactile Event Involves a Spatially and Temporally Specific Modulation of Sensorimotor Alpha- and Beta-Band Oscillations. *The Journal of Neuroscience, 31*(6), 2016-2024.

van Ede, F., Jensen, O., & Maris, E. (2010). Tactile expectation modulates pre-stimulus [beta]-band oscillations in human sensorimotor cortex. *NeuroImage, 51*(2), 867-876.

van Elswijk, G., Kleine, B. U., Overeem, S., & Stegeman, D. F. (2007). Expectancy Induces Dynamic Modulation of Corticospinal Excitability. *Journal of Cognitive Neuroscience, 19*(1), 121-131.

van Elswijk, G., Maij, F., Schoffelen, J.-M., Overeem, S., Stegeman, D. F., & Fries, P. (2010). Corticospinal Beta-Band Synchronization Entails Rhythmic Gain Modulation. *The Journal of Neuroscience, 30*(12), 4481-4488.

Van Essen, D. C., Lewis, J. W., Drury, H. A., Hadjikhani, N., Tootell, R. B. H., Bakircioglu, M., & Miller, M. I. (2001). Mapping visual cortex in monkeys and humans using surface-based atlases. *Vision Research, 41*(10-11), 1359-1378.

van Wijk, B. C. M., Daffertshofer, A., Roach, N., & Praamstra, P. (2009). A Role of Beta Oscillatory Synchrony in Biasing Response Competition? *Cereb. Cortex, 19*(6), 1294-1302.

Vandenberghe, R., Gitelman, D. R., Parrish, T. B., & Mesulam, M. M. (2001). Functional Specificity of Superior Parietal Mediation of Spatial Shifting. *NeuroImage, 14*(3), 661-673.

Vanni, S., Revonsuo, A., & Hari, R. (1997). Modulation of the Parieto-Occipital Alpha Rhythm during Object Detection. *J. Neurosci., 17*(18), 7141-7147.

Vaughan, T. M., Miner, L. A., McFarland, D. J., & Wolpaw, J. R. (1998). EEG-based communication: analysis of concurrent EMG activity. *Electroencephalography and Clinical Neurophysiology, 107*(6), 428-433.

Veniero, D., Bortoletto, M., & Miniussi, C. (2009). TMS-EEG co-registration: On TMS-induced artifact. *Clinical Neurophysiology, 120*(7), 1392-1399.

Veniero, D., Brignani, D., Thut, G., & Miniussi, C. (2011). Alpha-generation as basic response-signature to transcranial magnetic stimulation (TMS) targeting the human resting motor cortex: A TMS/EEG co-registration study. *Psychophysiology*, no-no.

Verbruggen, F., & Logan, G. D. (2009). Proactive adjustments of response strategies in the stop-signal paradigm. *Journal of Experimental Psychology: Human Perception and Performance, 35*(3), 835-854.

Vesia, M., Prime, S. L., Yan, X., Sergio, L. E., & Crawford, J. D. (2010). Specificity of Human Parietal Saccade and Reach Regions during Transcranial Magnetic Stimulation. *The Journal of Neuroscience, 30*(39), 13053-13065.

Vesia, M., Yan, X., Henriques, D. Y., Sergio, L. E., & Crawford, J. D. (2008). Transcranial Magnetic Stimulation Over Human Dorsal–Lateral Posterior Parietal Cortex Disrupts Integration of Hand Position Signals Into the Reach Plan. *Journal of Neurophysiology, 100*(4), 2005-2014.

Vickers, D. (1979). *Decision processes in visual perception*: Academic Press.

Vidal, F., Bonnet, M., & Macar, F. o. (1995). Programming the duration of a motor sequence: role of the primary and supplementary motor areas in man. *Experimental Brain Research, 106*(2), 339-350.

Volz, K. G., Schubotz, R. I., & von Cramon, D. Y. (2004). Why am I unsure? Internal and external attributions of uncertainty dissociated by fMRI. *NeuroImage, 21*(3), 848-857.

von Stein, A., Rappelsberger, P., Sarnthein, J., & Petsche, H. (1999). Synchronization Between Temporal and Parietal Cortex During Multimodal Object Processing in Man. *Cerebral Cortex, 9*(2), 137-150.

Wagner, T. A., Zahn, M., Grodzinsky, A. J., & Pascual-Leone, A. (2004). Three-dimensional head model Simulation of transcranial magnetic stimulation. *Biomedical Engineering, IEEE Transactions on, 51*(9), 1586-1598.

Waldert, S., Preissl, H., Demandt, E., Braun, C., Birbaumer, N., Aertsen, A., & Mehring, C. (2008). Hand Movement Direction Decoded from MEG and EEG. *The Journal of Neuroscience, 28*(4), 1000-1008.

Wallis, J. D., Anderson, K. C., & Miller, E. K. (2001). Single neurons in prefrontal cortex encode abstract rules. *Nature, 411*(6840), 953-956.

Wallis, J. D., & Kennerley, S. W. (2010). Heterogeneous reward signals in prefrontal cortex. *Current Opinion in Neurobiology, 20*(2), 191-198.

Walsh, V., & Cowey, A. (2000). Transcranial magnetic stimulation and cognitive neuroscience. *Nat Rev Neurosci, 1*(1), 73-80.

Walsh, V., & Pascual-Leone, A. (2003). *Transcranial Magnetic Stimulation: A Neurochronometrics of Mind*: MIT Press.

Walsh, V., Pascual-Leone, A., & Kosslyn, S. M. (2005). *Transcranial Magnetic Stimulation: A Neurochronometrics of Mind*: MIT Press.

Walter, W. G., Cooper, R., Aldridge, V. J., McCallum, W. C., & Winter, A. L. (1964). Contingent Negative Variation : An Electric Sign of Sensori-Motor Association and Expectancy in the Human Brain. *Nature, 203*(4943), 380-384.

Wang, X.-J. (2002). Probabilistic Decision Making by Slow Reverberation in Cortical Circuits. *Neuron, 36*(5), 955-968.
Wang, X.-J. (2010). Neurophysiological and Computational Principles of Cortical Rhythms in Cognition. *Physiological Reviews, 90*(3), 1195-1268.
Wardak, C., Olivier, E., & Duhamel, J.-R. (2011). The relationship between spatial attention and saccades in the frontoparietal network of the monkey. *European Journal of Neuroscience, 33*(11), 1973-1981.
Wassermann, E. M. (1998). Risk and safety of repetitive transcranial magnetic stimulation: report and suggested guidelines from the International Workshop on the Safety of Repetitive Transcranial Magnetic Stimulation, June 5-7, 1996. *Electroencephalography and Clinical Neurophysiology/Evoked Potentials Section, 108*(1), 1-16.
Wassermann, E. M., Wang, B., Zeffiro, T. A., Sadato, N., Pascual-Leone, A., Toro, C., & Hallett, M. (1996). Locating the Motor Cortex on the MRI with Transcranial Magnetic Stimulation and PET. *NeuroImage, 3*(1), 1-9.
Westendorff, S., Klaes, C., & Gail, A. (2010). The Cortical Timeline for Deciding on Reach Motor Goals. *J. Neurosci., 30*(15), 5426-5436.
White, C. N., Ratcliff, R., Vasey, M. W., & McKoon, G. (2010). Using diffusion models to understand clinical disorders. *Journal of Mathematical Psychology, 54*(1), 39-52.
Whittingstall, K., & Logothetis, N. K. (2009). Frequency-Band Coupling in Surface EEG Reflects Spiking Activity in Monkey Visual Cortex. *Neuron, 64*(2), 281-289.
Wilke, M., Mueller, K. M., & Leopold, D. A. (2009). Neural activity in the visual thalamus reflects perceptual suppression. *Proceedings of the National Academy of Sciences of the United States of America, 106*(23), 9465-9470.
Wise, S. P., & Murray, E. A. (2000). Arbitrary associations between antecedents and actions. *Trends in Neurosciences, 23*(6), 271-276.
Witham, C. L., Wang, M., & Baker, S. N. (2007). Cells in somatosensory areas show synchrony with beta oscillations in monkey motor cortex. *European Journal of Neuroscience, 26*(9), 2677-2686.
Wolbers, T., Weiller, C., & Büchel, C. (2003). Contralateral Coding of Imagined Body Parts in the Superior Parietal Lobe. *Cerebral Cortex, 13*(4), 392-399.
Wolpaw, J. R., Birbaumer, N., McFarland, D. J., Pfurtscheller, G., & Vaughan, T. M. (2002). Brain-computer interfaces for communication and control. *Clinical Neurophysiology, 113*(6), 767-791.
Wolpaw, J. R., & McFarland, D. J. (2004). Control of a two-dimensional movement signal by a noninvasive brain-computer interface in humans. *Proceedings of the National Academy of Sciences of the United States of America, 101*(51), 17849-17854.
Wong, K.-F., Huk, A. C., Shadlen, M. N., & Wang, X.-J. (2007). Neural circuit dynamics underlying accumulation of time-varying evidence during perceptual decision making. *Frontiers in Computational Neuroscience, 1*.
Wong, K. F., & Wang, X. J. (2006). A recurrent network mechanism of time integration in perceptual decisions. *The Journal of neuroscience : the official journal of the Society for Neuroscience, 26*(4), 1314-1328.
Worden, M. S., Foxe, J. J., Wang, N., & Simpson, G. V. (2000). Anticipatory biasing of visuospatial attention indexed by retinotopically specific alpha-band electroencephalography increases over occipital cortex. *The Journal of neuroscience : the official journal of the Society for Neuroscience, 20*(6).

Wunderlich, K., Rangel, A., & O'Doherty, J. P. (2009). Neural computations underlying action-based decision making in the human brain. *Proceedings of the National Academy of Sciences, 106*(40), 17199-17204.

Wyart, V., & Tallon-Baudry, C. (2008). Neural Dissociation between Visual Awareness and Spatial Attention. *The Journal of Neuroscience, 28*(10), 2667-2679.

Yamagishi, N., Callan, D. E., Anderson, S. J., & Kawato, M. (2008). Attentional changes in pre-stimulus oscillatory activity within early visual cortex are predictive of human visual performance. *Brain Research, 1197*(C), 115-122.

Yang, T., & Shadlen, M. N. (2007). Probabilistic reasoning by neurons. *Nature, 447*(7148), 1075-1080.

Yantis, S., & Jonides, J. (1990). Abrupt Visual Onsets and Selective Attention: Voluntary Versus Automatic Allocation. *Journal of Experimental Psychology: Human Perception and Performance, 16*(1), 121-134.

Yantis, S., Schwarzbach, J., Serences, J. T., Carlson, R. L., Steinmetz, M. A., Pekar, J. J., & Courtney, S. M. (2002). Transient neural activity in human parietal cortex during spatial attention shifts. *Nat Neurosci, 5*(10), 995-1002.

Yuan, H., Liu, T., Szarkowski, R., Rios, C., Ashe, J., & He, B. (2010). Negative covariation between task-related responses in alpha/beta-band activity and BOLD in human sensorimotor cortex: An EEG and fMRI study of motor imagery and movements. *NeuroImage, 49*(3), 2596-2606.

Zaehle, T., Frund, I., Schadow, J., Tharig, S., Schoenfeld, M. A., & Herrmann, C. S. (2009). Inter- and intra-individual covariations of hemodynamic and oscillatory gamma responses in the human cortex. *Frontiers in Human Neuroscience, 3*.

Zanto, T. P., Rubens, M. T., Thangavel, A., & Gazzaley, A. (2011). Causal role of the prefrontal cortex in top-down modulation of visual processing and working memory. *Nat Neurosci, 14*(5), 656-661.